Innate sensing of bacterial flagellin in acute and chronic intestinal inflammation

Sofia Nordlander
Wolfson College, University of Oxford

A thesis submitted in partial fulfilment of the requirements for degree of Doctor of Philosophy, Trinity Term 2013

Abstract

Flagellin is a highly immunogenic, bacterial protein considered to be abundant in the intestinal lumen. It has been reported to be an immunodominant antigen in patients with inflammatory bowel disease (IBD). In the work presented in this thesis several complementary murine models of IBD were employed to elucidate the role of innate immune sensing of flagellin in the development of intestinal inflammation. Pattern recognition receptors (PRRs) enable mammals to discriminate self from non-self through the recognition of microbial signatures, such as bacterial flagellin. Flagellin is detected by at least two distinct PRRs, NOD-like receptor 4 (NLRC4) and Toll-like receptor 5 (TLR5). Our experiments revealed that NLRC4 promoted protective effects during acute intestinal inflammation mediated by infection with *Citrobacter rodentium*, a close relative of enteropathogenic *E. coli*. Following infection with *C. rodentium, Nlrc4*$^{-/-}$ mice developed more severe weight loss, increased bacterial colonisation levels and exacerbated intestinal inflammation compared to WT counterparts. Bone marrow chimera experiments revealed that NLRC4 expression in non-hematopoietic cells provided protection and intestinal epithelial cells expressed high NLRC4 mRNA levels. These results suggest that NLRC4 inflammasome activation in the intestinal epithelium provides potent, protective effects during infection with a mucosal pathogen. In contrast, TLR5 was shown to promote protective effects during chronic, T-cell mediated intestinal inflammation driven by adoptive transfer of naïve CD4^{+} T-cells into lymphopenic Rag$^{-/-}$ hosts. The absence of TLR5 in Rag$^{-/-}$ recipients resulted in accelerated and exacerbated IBD. Furthermore, chronic T-cell dependent colitis driven by *Helicobacter hepaticus*, a flagellated, enteric bacterium, was more severe in mice deficient in TLR5. Finally, construction of a *H.hepaticus* Type 6 secretion system deletion mutant revealed delayed pathogenicity in an innate model of intestinal inflammation, most likely due to reduced initial colonisation of mutant *H. hepaticus*.

Acknowledgements

I would like to start by thanking my supervisor Dr. Kevin Maloy for giving me the opportunity to work in the lab and for supporting my DPhil studies. I am very grateful for all the discussions over the years, the advice and for the freedom to pursue research.

I have had the privilege to work with a number of talented, friendly and entertaining people. Thank you Mark for all your help, your kindness and sense of humour. Thank you Philip, Sofia B, Ana, Sophie and Marie for being simply brilliant. Rose – thank you for everything. I enjoyed seeing the Mediterranean with you!

I was very fortunate to be able to discuss my work with Margherita and Johanna. Thank you so much for all your sound advice. Also, thank you Johanna for really helping out in any way you could and being great.

A warm thank you to Claire, Julia, Corinne, Tessa, Carolina, Emily W and Emily T. Thank you for all the support before and during the thesis writing, including table tennis and discovering beautiful parts of Britain. Thank you Aga, Abhi, George, Naren, Ollie and Sarah – you made the lab entertaining and inspiring to work in! I would also like to thank past and present members of the Dunn School and the Powrie/Maloy lab who turned this into a nice experience: Alessandra, Thibault, Annette, Stefanie, Rut, Andrew, Michael, Stephanie, Ricardo, Eleanor, Dina, Richard, Takeshi and Marie-Laure.

Finally I would like to thank my family. Mum, Dad, Bodil and Åsa – thank you for your endless support. I could not have done this without you.

Abbreviations

Abx	Antibiotics
AMP	Antimicrobial peptide
AOM	Azoxymethane
ASC	Apoptosis-associated speck-like protein
BIR	Baculovirus inhibitor domain
CARD	Caspase recruitment domain
CD	Crohn's disease
DC	Dendritic cell
DSS	Dextran sodium sulphate
EAE	Experimental autoimmune encephalomyelitis
EDTA	Ethylenediaminetetraacetic acid
EHEC	Enterohemorrhagic *E. coli*
EPEC	Enteropathogenic *E. coli*
FACS	Fluorescence activated cell sorting
FCS	Fetal calf serum
GALT	Gut associated lymphoid tissue
GF	Germ free
GM-CSF	Granulocyte macrophage colony-stimulating factor
GWAS	Genome wide association studies
Hcp	Hemolysin coregulated protein
Hh	*Helicobacter hepaticus*
IBD	Inflammatory bowel disease
IEC	Intestinal epithelial cell
IEL	Intraepithelial lymphocyte
IHC	Immunohistochemsitry
IL-1RA	IL-1 receptor antagonist
ILC	Innate lymphoid cell
ILF	Isolated lymphoid follicle
i.p.	Intraperitoneal

i.v.	Intravenous
LEE	Locus of enterocyte effacement
LP	Lamina propria
LPL	Lamina propria leukocyte
LPS	Lipopolysaccharide
LRR	Leucine rich repeat
LTi	Lymphoid tissue inducer cell
M cell	Microfold cell
MLN	Mesenteric lymph node
MyD88	Myeloid differentiation primary response gene (88)
NLR	NOD-like receptor
NOD	Nucleotide binding and oligomerization domain
PAI	Pathogenicity island
PBS	Phosphate buffered saline
PP	Peyer's patches
PRR	Pattern recognition receptor
PYD	Pyrin domain
RA	Retinoic acid
RAG	Recombinase activating gene
SPI	*Salmonella* pathogenicity island
SPF	Specific pathogen free
STAT	Signal transducer and activation of transcription
T3SS	Type 3 secretion system
T6SS	Type 6 secretion system
TCR	T-cell receptor
Tfh	T follicular helper cell
TLR	Toll like receptor
Treg	Regulatory T-cell
UC	Ulcerative colitis
VgrG	Valine-glycine-repeat proteins

Contents

Chapter 1 General Introduction 1
1.1 The intestinal immune system 1
1.2 Cells of the intestinal immune system 2
1.2.1 Intestinal epithelial cells 2
1.2.2. Intestinal stromal cells 3
1.2.3 Mononuclear phagocytes 3
1.2.4 Eosinophils 4
1.2.5 Innate lymphoid cells 5
1.2.6 Intraepithelial lymphocytes 6
1.2.7 $CD4^+$ T-cells 7
1.3 Pattern recognition receptors 13
1.3.1 TLRs 13
1.3.2 TLR5 14
1.3.3 NLRs 15
1.3.4 Inflammasomes 18
1.3.5 NLRC4 22
1.3.6 Inflammasome associated IL-1 family cytokines 26
1.3.7 Pyroptosis 27
1.3.8 Negative regulation of the inflammasome 28
1.4 Inflammatory bowel disease 29
1.5 Models of intestinal inflammation employed in this thesis 31
1.5.1 *Citrobacter rodentium* infection – a model of acute intestinal inflammation 31
1.5.2 T-cell transfer colitis – a model of T-cell dependent chronic intestinal inflammation 34
1.5.3 *Helicobacter hepaticus* infection and αIL-10R blockade – a model of bacterially triggered T-cell dependent chronic inflammation 35
1.5.4. *Helicobacter hepaticus* infection of $Rag^{-/-}$ mice – a model of bacterially triggered innate chronic inflammation 37
1.5.5 Dextran sodium sulphate (DSS) colitis – a model of acute intestinal inflammation 38
1.6 Aims 41
Chapter 2 Materials and methods 43
2.1 Materials 43
2.1.1 Mice 43
2.1.2 Antibodies 44
2.2 Assessment of intestinal inflammation 45
2.3 Cell isolation and fluorescent-activated cell sorting (FACS) 48

2.3.1 Enrichment of $CD4^+$ T-cells 48
2.3.2 FACS purification of naïve T-cells 48
2.3.3 Isolation of lamina propria leukocytes (LPL) 49
2.3.4 Isolation of splenocytes 50
2.3.5 Cell staining for FACS analysis 50
2.4 Bacterial culture 51
2.4.1 *C. rodentium* growth conditions 51
2.4.2 *Helicobacter hepaticus* growth conditions 51
2.4.3 *Helicobacter hepaticus* screening 52
2.5 Induction of intestinal inflammation 52
2.5.1 *Citrobacter rodentium* infection 52
2.5.2 Quantification of *C. rodentium* colonisation 53
2.5.3 *Helicobacter hepaticus* infection 53
2.5.4 Quantification of *Helicobacter hepaticus* colonisation 53
2.5.5 T-cell transfer colitis 54
2.5.6 Generation of bone marrow chimeric mice 55
2.6 Cytokine analysis 55
2.6.1 Cytokine detection in tissue explant supernatants 55
2.6.2 Detection of IL-1β, IL-α and IL-18 55
2.7 Analysis of antibody responses 56
2.7.1 *C. rodentium* IgG ELISA 56
2.7.2 *C. rodentium* secretory IgA ELISA 57
2.7.3 Preparation of soluble *Helicobacter hepaticus* antigen (sHelAg) 57
2.7.4 *H. hepaticus* specific IgG and sIgA ELISA 58
2.8 Analysis of mRNA expression by qPCR 58
2.8.1 RNA extraction from tissues and cell isolates 58
2.8.2 Quantitative PCR (qPCR) 59
2.9 Western blot 60
2.9.1 Sample preparation 60
2.9.2 Western blot 61
2.10 *In vivo* treatment 61
2.10.1 Treatment with recombinant IL-18 61
2.10.2 Treatment with antibiotics 62
2.11 Isolation of tissue subsets 62
2.11.1 Isolation of intestinal crypts 62
2.11.2 Isolation of intestinal stromal cells 63

2.12 Immunohistochemistry (IHC) 63
2.13 Microarray analysis 63
2.14 Generation of an *IcmF*-deficient *Helicobacter hepaticus* deletion mutant 64
2.14.1 Cloning 64
2.14.2 Electroporation of *Helicobacter hepaticus* 65
2.15 Statistical analysis 67
Chapter 3: Role of the cytosolic sensor NLRC4 in acute bacterially triggered intestinal inflammation 68
3.1 Introduction 68
3.2 Results 70
3.2.1 NLRC4 deficiency results in elevated systemic immune responses to infection with the enteric pathogen *Citrobacter rodentium* 70
3.2.2 NLRC4 deficiency results in the development of severe intestinal pathology during infection with *C. rodentium* 74
3.2.3 NLRC4 limits bacterial colonisation of the intestinal mucosa 77
3.2.4 NLRC4 deficiency results in exaggerated cytokine responses following *C. rodentium* infection 79
3.2.5 NLRC4 deficiency primarily affects the innate immune axis 87
3.2.6 NLRC4 deficiency does not impair protective innate IL-22/AMP responses. 91
3.2.7 NLRC4 deficiency is not associated with reduced IL-1 levels or impaired neutrophil recruitment during *C. rodentium* infection 93
3.2.8 NLRC4 contributes to steady state IL-18 production in the large intestine 96
3.2.9 NLRC4 mediates steady state caspase-1 activation in the cecum. 99
3.2.10 Broad spectrum antibiotic treatment exacerbates *C. rodentium* induced inflammation in WT mice 101
3.2.11 Broad spectrum antibiotic treatment equalises *C. rodentium* colonisation levels in WT and *Nlrc4*$^{-/-}$ mice 104
3.2.12 NLRC4 expression in non-hematopoietic cells is protective during *C. rodentium* infection 108
3.2.13 NLRC4 is highly expressed in intestinal crypts 113
3.2.14 Microarray analysis of transcriptional changes during *C. rodentium* infection 115
3.2.15 WT and *Nlrc4*$^{-/-}$ mice harbour equivalent eosinophil frequencies in the lamina propria 121
3.3 Discussion 123
Chapter 4: Role of NLRC4 in chronic bacterially triggered intestinal inflammation 132
4.1 Introduction 132
4.2 Results 134
4.2.1 NLRC4 is dispensable for the development of *Helicobacter hepaticus*-induced T-cell dependent intestinal inflammation 134

4.2.2 NLRC4 is dispensable for the development of Th1 and Th17 responses in the intestine 136

4.2.3 NLRC4 limits *H. hepaticus* colonisation during T-cell dependent intestinal inflammation 138

4.2.4 NLRC4 expression during the onset of *H. hepaticus* driven T-cell dependent colitis is dispensable for the development of intestinal inflammation 140

4.2.5 NLRC4 restrains systemic and local granulocyte accumulation during the onset of *H. hepaticus* mediated T-cell dependent colitis 142

4.2.6 NLRC4 expression does not affect long-term *H. hepaticus* colonisation 144

4.2.7 NLRC4 is dispensable for the development of *H. hepaticus* triggered T-cell independent intestinal inflammation 146

4.2.8 NLRC4 is dispensable for systemic immune responses during *H. hepaticus* -induced T-cell independent intestinal inflammation 148

4.2.9 NLRC4 does not regulate to the onset of *H. hepaticus*-induced T-cell independent intestinal inflammation 150

4.3 Discussion 152

Chapter 5 156

Role of Toll-like receptor 5 in chronic intestinal inflammation 156

5.1 Introduction 156

5.2 Results 158

5.2.1 TLR5 deficiency results in accelerated and exacerbated T cell transfer colitis 158

5.2.2 Exacerbated pathology in *Tlr5*$^{-/-}$*Rag1*$^{-/-}$ mice is not associated with increased Th1 or Th17 responses 161

5.2.3 Exacerbated pathology in *Tlr5*$^{-/-}$*Rag1*$^{-/-}$ mice is not associated with increased local pro-inflammatory responses 164

5.2.4 TLR5 deficiency in both non-hematopoietic and hematopoietic cells contributes to systemic disease 167

5.2.5 TLR5 signalling in hematopoietic cells protects from severe intestinal inflammation 169

5.2.6 TLR5 is dispensable for T-cell independent innate intestinal inflammation 171

5.2.7 TLR5 deficiency results in accelerated and exacerbated *Helicobacter hepaticus* triggered T-cell dependent intestinal inflammation 177

5.2.8 TLR5 deficiency is not associated with increased Th1 or Th17 responses during *Helicobacter hepaticus* triggered T-cell dependent intestinal inflammation 180

5.3 Discussion 184

Chapter 6 Effects of the *Helicobacter hepaticus* Type 6 secretion system in infection and inflammation 191

6.1 Introduction 191

6.2 Results 194

6.2.1 Generation of a *H. hepaticus IcmF* deletion mutant 194

6.2.2 Intestinal inflammation is delayed during infection with a *H. hepaticus* T6SS deletion mutant 196
6.2.3 Local and systemic immune responses are delayed during infection with a *H. hepaticus*T6SS deletion mutant 198
6.2.4 The *H. hepaticus* T6SS deletion mutant exhibits a colonisation defect 200
6.2.5 Impaired IL-10^{+} Foxp3^{+} Treg cell induction during infection with a *H. hepaticus* T6SS deletion mutant 202
6.3 Discussion 205
Chapter 7 General discussion 208
7.1 Innate sensing of flagellin contributes to tissue protection in the intestine 208
7.2 Inflammasomes and the intestinal epithelium 209
7.3 Inflammasomes and cell death 214
7.4 Inflammasomes and NLR redundancy 216
7.5 Inflammasomes and immune evasion 217
7.6 Endogenous flagellin and the intestinal immune system 218
7.7 Concluding remarks 219
References 220

Chapter 1 General Introduction

1.1 The intestinal immune system

The intestinal mucosa constitutes the interface between the outside world and the inside milieu. Separating the intestinal lumen, with its abundance of microorganisms and antigens, from host tissues is a single layer of epithelial cells and associated with them the largest immune cell network in the body. The intestinal immune system faces the difficult task of preserving homeostasis at a site of large microbial burdens while still mounting protective responses to invading pathogens.

The innate immune system contributes to intestinal homeostasis and mediates essential protection during the early stages of infection. It is active in a wide range of different cell types and provides cues for barrier fortification and immune cell activation. Modulatory factors derived from innate immune circuits have important effects on subsequent adaptive immune responses and tissue function. However, potent innate immune activation also has the capacity to inflict great damage on the host. Indeed, innate immune dysregulation and chronically active adaptive immune responses are integral components of the severe condition termed inflammatory bowel disease (IBD).[1]

1.2 Cells of the intestinal immune system

1.2.1 Intestinal epithelial cells

The intestinal epithelium is a one-cell layer barrier that separates the intestinal lumen from the inside environment. Intestinal epithelial cells (IECs) consist of several different types mediating absorption, secretion and antigen translocation.[2] The absorptive enterocytes are the most abundant and carry microvilli which increase the surface area.[2] There are three types of secretory cells; the enteroendocrine cells, the Paneth cells and the goblet cells. The enteroendocrine cells constitute approximately 1% of total IEC and produce a number of hormones.[3] The Paneth cells are only present in the small intestine and are important producers of antimicrobial peptides (AMPs), which modulate the commensal flora and provide protection from pathogens.[4-7] Goblet cells are located throughout the intestine and produce mucus. The intestinal mucus layer is stratified, with a dense, sterile inner layer and a looser outer layer. Mucus is essential for intestinal homeostasis and provides a barrier between IECs and the luminal contents, as well as nutrients for commensal intestinal bacteria and a matrix for retention of host-protective AMPs and IgA antibodies close to the epithelium.[8-11] Microfold cells (M cells) are highly specialised IECs that are part of the gut associated lymphoid tissue (GALT). These cells are situated in the epithelium covering Peyer's patches (PP) in the small intestine and isolated lymphoid follicles (ILFs) in the colon. They mediate the delivery of antigens to the basolateral membrane and have highly increased endocytosis and transcytosis. M cells are covered by a mucus layer of reduced thickness and can serve as entry routes for bacterial pathogens.[12-14]

All different types of IEC are derived from the same type of intestinal stem cells, which are located in the base of the intestinal crypts. The epithelial barrier is highly self-

renewing and IECs are replaced after 4-5 days[15] The exception is the Paneth cell which remains in the crypt base and has a life-span of up to 3 weeks.[5] During IEC proliferation and differentiation cells gradually move toward the tip of the villi in the small intestine and the end of the invagination in the colon.[15] IECs express pattern recognition receptors (PRRs) and actively contribute to immune responses.[16, 17] Among these responses are the promotion of IgA production and delivery of secretory IgA to the lumen via the polymeric Ig receptor, which is expressed on the basolateral surface. Furthermore IECs mediate the release of chemokines with effects on leukocyte recruitment.[18-20] The continuous barrier is dependent on tight junctions, which firmly connect the IECs. The actin cytoskeleton of IECs can be modified by bacterial pathogens, altering barrier functions.[21, 22]

1.2.2. Intestinal stromal cells

IECs are supported by conjunctive lamina propria (LP), composed of stromal cells. Stromal cells consist of myofibroblasts, fibroblasts, pericytes, smooth muscle cells and endothelial cells.[23-25] The most abundant stromal cells in the intestine are the subepithelial myofibroblasts (stroma), which are in direct contact with the IECs.[25] Stroma interact with IECs and affect IEC proliferation and differentiation.[25, 26] Stromal cells produce a wide array of cytokines, chemokines, growth factors and other mediators.[25, 27] They express TLRs and NLRs and promote recruitment of inflammatory cells upon infection.[28, 29]

1.2.3 Mononuclear phagocytes

Intestinal mononuclear phagocytes are essential for bridging innate and adaptive immune responses. Although ontology and subset relationships of intestinal mononuclear phagocytes are not completely understood, two main categories can be

discerned, based on the expression of surface markers, function and phenotype.[30-32] Intestinal dendritic cells (DCs) migrate from the mucosa through the afferent lymphatic vessels to the PP and ILFs of the GALT and to the mesenteric lymph nodes (MLN).[30, 33, 34] Expression of the gut homing receptor CCR7 is necessary for migration and the majority of trafficking DCs are positive for the integrin receptor CD103.[33, 35] In the lymph nodes DCs induce activation and differentiation of $CD4^+$ T-cells that traffic back to the intestine by inducing expression of gut homing receptors α4β7 and CCR9.[36] As a result of distinct TLR signalling and cytokine production, DC populations of the small intestine have been shown to promote induction of Th1, Th17, regulatory T-cells (Treg) and production of IgA.[31, 37-39] In the large intestine, tissue resident macrophages expressing the CX3CR1 surface marker constitute the largest group of mononuclear phagocytes.[31] Tissue resident macrophages produce IL-10 in response to TLR ligands *in vitro* and support Treg in the tissue.[31, 37, 40] Subsequently Th17 cells are more frequent in the small intestine than in the large intestine and the colon harbours large populations of regulatory T-cells (Treg).[31, 37] The proliferation rate of intestinal macrophages is low compared with DCs. They have been shown to be phagocytic but not to migrate and they are less efficient at activating T-cells *in vitro* compared with DCs.[31, 41] During inflammation, inflammatory mononuclear phagocytes derived from a blood monocyte precursor expand in the tissue. Pro-inflammatory signalling within this accumulating myeloid population promotes intestinal inflammation.[31, 40, 42]

1.2.4 Eosinophils

The gastrointestinal tract harbours a large population of eosinophils.[43] It is difficult to establish the exact proportion, since cell isolation protocols could favour eosinophil survival over other cells, but the use of cell specific surface markers shows that up to 1/3 of cells expressing the hematopoietic marker CD45 are eosinophils.[44-46] The

recruitment to the intestine starts during gestation and is dependent on eotaxin but independent of intestinal flora.[47] Eosinophils harbour granules containing proteins with cytotoxic effects and have traditionally been known to accumulate and mediate protective functions during parasite invasion.[48] However, the activities of eosinophils in the intestinal tract may be more extensive than previously thought. Eosinophil frequencies are increased during IBD and correlate with disease severity.[49, 50] Supporting a pathogenic role, IECs and macrophages produce eotaxin during acute, experimental colitis and mediate eosinophil recruitment and subsequent exacerbated disease.[51] However, accumulation of eosinophils also occurs during IBD remission, suggesting that they may have effects on tissue repair.[50]

Eosinophils isolated from human blood express a number of TLRs and can produce multiple cytokines.[48, 52, 53] Lipopolysaccharide (LPS) stimulation of eosinophils that have been primed with IFN-γ or IL-5 can result in catapult like expulsion of mitochondrial DNA. These extracellular structures with bactericidal function are similar to neutrophil extracellular traps (NETs).[54, 55] Strengthening an antibacterial effect, eosinophilia limits bacterial colonisation in the peritoneal cavity in a murine model of bacterial infection.[56] However, mice deficient in eosinophils do not exhibit a spontaneous gut phenotype and it remains to be seen what role these innate cells play in the intestinal immune responses.[57]

1.2.5 Innate lymphoid cells

Innate lymphoid cells (ILCs) have the morphology of lymphocytes and produce cytokines normally associated with effector T-cells, but lack a rearranged TCR.[58] ILCs are enriched in the intestinal mucosa, where they are important producers of IL-22 and IL-17A.[59, 60] These cells belong to a heterogeneous population which consists of several

branches. One group can be characterized by expression of the nuclear hormone receptor Rorγt and responds to the cytokine IL-23.[61] ILCs are the main producers of IL-22 in the intestine during homeostatic conditions and serve as an important first line of defence during acute bacterial infection.[59, 60, 62] However, ILCs can also promote chronic intestinal inflammation by producing IL-17A and IFN-γ.[63] Furthermore, ILCs are needed for the development of cryptopatches, precursors of organised lymphoid structures that consist of stromal cells, DCs and a particular group of ILCs, the lymphoid tissue inducer cells (LTis).[64, 65] Cryptopatches can develop into more organised ILF structures and are a site of T-cell independent IgA production in the LP.[64, 65]

1.2.6 Intraepithelial lymphocytes

Intraepithelial lymphocytes (IELs) are interspersed among the IEC in the intestinal mucosa and contribute to host defence. There are two main categories; the natural IEL and the induced IEL.[66] Natural IELs have γδ or αβ TCR and are mainly $CD8\alpha\alpha^{+}$ in the small intestine and $CD4^{-}CD8^{-}$ in the colon. Some natural IELs are activated by self-peptides in the thymus and migrate to the intestine.[66] The microbiota has an impact on overall IEL development and mice reared in germ-free (GF) conditions harbour significantly reduced numbers of IELs, with the exception of γδ IELs.[67] These cells are able to sense small, non-protein antigens derived from bacteria without the requirement of antigen processing and can develop in the absence of self-peptides.[68-70] γδ IELs modulate barrier function and provide protection during infection with parasites and bacteria, preventing a leaky epithelium.[71, 72] γδ IEL also promote IEC proliferation in homeostasis and during healing.[73, 74] Over the life-time natural IEL numbers decline and the proportion of induced IELs increases.[66] Induced IELs, which are the progeny of

conventional T-cells, mainly have αβ TCR and are $CD8\alpha\beta^+$ in the small intestine while $CD4^+$ cells dominate in the colon.[66]

1.2.7 $CD4^+$ T-cells

There are four main lineages of $CD4^+$ T helper cells: T helper 1 (Th1), T helper 2 (Th2), T helper 17 (Th17) and induced Treg (iTreg). After activation in the lymph nodes, $CD4^+$ T-cells undergo differentiation and clonal expansion. Several differentiation programmes can be initiated, depending on cytokine cues.[75] Cytokines produced by antigen-presenting cells (APCs) bind surface receptors on naïve $CD4^+$ T-cells. Differentiation is mediated by specific signal transducer and activation of transcription (STAT) transcription factors, which promote cell fate determination by inducing expression of master transcription factors. These master transcription factors determine the overall adherence to a differentiation program by activating specific gene expression.[76]

The first $CD4^+$ T-cell lineages to be described were the Th1 and Th2 subsets.[77] Th1 commitment is induced by IFN-γ activation of STAT1 and expression of the master transcription factor T-bet.[78] IL-12 activation of STAT4 together with T-bet promote production of IFN-γ, the key Th1 cytokine, and thus the lineage is sustained through a positive feedback loop.[78] IL-18, an IL-1 family cytokine, potentiates IFN-γ production by Th1 cells.[79] One key activity of IFN-γ is macrophage activation, and thus Th1 cells are classically known to mediate defence against intracellular pathogens.[80, 81] However, IFN-γ can also promote IgG2a class switching in B cells.[82] Excessive Th1 activation can mediate deleterious effects and is associated with intestinal inflammation in Crohn's disease, a type of IBD.[83, 84]

The intestinal mucosa harbours a homeostatic population of Th17 cells, particularly in the small intestine. In terms of differentiation, Th17 lineage commitment is determined by TGF-β and IL-6 induction of STAT3 signalling and the subsequent expression of the Rorγt transcription factor.[75] Th17 cells express both IL-17A and IL-17F.[85] Out of the IL-17 family of cytokines, which consists of IL-17A, B, C, D, E and F, IL-17A and IL-17F are the most closely related with regards to sequence homology.[86] In addition to being produced by lymphocytes, IL-17F is also expressed by intestinal epithelial cells.[87] Although IL-17F has been shown to mediate pathological effects in the DSS model of colitis,[88] IL-17A remains vastly more studied in the context of intestinal Th17 cells.

The presence of intestinal flora, and possibly of specific bacteria such as segmented filamentous bacteria (SFB), is essential for Th17 induction.[89] Th17 cells are associated with protective effects against extracellular bacterial and fungal pathogens. [90] However, depending on the cytokine context, Th17 cells also have the capacity to produce different cytokines and thus constitute a fine tuned component of the adaptive immune system.[90]

During infection and inflammation, Th17 cells are associated with both pathogenic and protective properties. Stimulation with IL-1β, IL-6 and IL-23 favours the development of Th17 cells that can drive disease in experimental autoimmune encephalomyelitis (EAE), which is a chronic inflammatory condition of the CNS. By contrast, $CD4^+$ T-cells exposed to IL-1β, IL-6 and TGF-β become non-pathogenic Th17 cells, unable to promote disease.[91] The pathogenicity of Th17 cells during EAE has been contributed to the expression of Rorγt and the production of granulocyte macrophage colony-stimulating factor (GM-CSF), while IL-17A itself was dispensable.[92] In addition, the plasticity of Th17 cells has been confirmed using fate-mapping of cells expressing the IL-17A gene, which revealed that IL-$17A^+$ cells develop into IFN-γ producers during

EAE.[93] In the intestinal tract, the occurrence of cells producing both IL-17A and IFN-γ has been correlated with chronic inflammation and there is similar evidence of Th17 to Th1 conversion.[94, 95] So far, there is no evidence of Th1 cells adopting a Th17 phenotype and it has been suggested that Th17 cells represent cells with increased longevity which retain the ability to differentiate into other effector types.[75, 96]

Ligation of the aryl hydrocarbon receptor, which is exclusively expressed by Th17 cells in mice, promotes IL-17A, IL-17F and IL-22 production by Th17 cells.[97] Increasing levels of IL-6 during Th17 differentiation promotes production of IL-22, converting Th17 cells into what has been labelled T helper 22 cells (Th22). These cells are protective during infection with an extracellular gastrointestinal pathogen.[98] However, serum levels of IL-22 are increased in IBD patients and correlate with disease activity.[99]

Regulatory T-cells (Treg) are $CD4^+$ T lymphocytes that promote tolerance by suppressing immune responses. Tregs can broadly be divided into two categories; natural Treg, which are induced in the thymus, and induced Treg, iTreg, which are more abundant in the intestine.[100]

Natural Treg bind self-peptides of moderate affinity and respond to IL-2 and IL-15 by STAT5 signalling. This results in expression of the master regulator Foxp3.[100] In the MLN, increasing levels of TGF-β early during T helper cell differentiation favour extrathymic generation of iTreg from $Foxp3^-$ $CD4^+$ T-cells. Further conditioning with retinoic acid (RA), which is produced in the intestine, steers the lineage development to iTreg.[75, 101] Figure 1.1. shows an overview of $CD4^+$ T-cell differentiation in the MLN. TGF-β and IL-10 are key suppressive cytokines in the gut.[102] More than half of colonic Treg express IL-10 [103] and polymorphisms in the IL-10R gene are associated with early

onset IBD.[104] Furthermore, mutations in the FOXP3 gene result in IPEX syndrome, a lethal autoimmune condition.[105]

In the colon Tregs contribute to homeostasis by producing IL-10 and by promoting IgA producing plasma B-cells in the lamina propria.[106, 107] Secretory IgA is essential for limiting systemic T-cell recognition of antigens. The generation of secretory IgA specific for the microflora maintains a situation in which the systemic immune system remains unaware of commensal gut microorganisms.[108]

iTreg and Th17 share the dependency on TGF-β for differentiation.[75] By the use of a system in which all cells expressing *Foxp3* at any time during their development acquired fluorescence, cells previously, but not currently, expressing *Foxp3* were shown to develop effector $CD4^+$ T-cell characteristics.[109] In the GALT, a Th17 phenotype dominated. This suggested conversion of Treg to Th17 in the gut.[109] However, studies based on different tracking systems revealed that $CD4^+$ T-cells expressing transient *Foxp3* did not display suppressive functions and might not qualify as true Treg.[110] Additionally, $CD4^+$ T-cells exhibiting stable *Foxp3* expression remained $Foxp3^+$ during inflammatory conditions, contradicting Treg to Th17 conversion.[111]

T follicular helper cells (Tfh) are considered to be a separate subset of $CD4^+$ T-cells.[112, 113] Tfh express specific surface molecules and cytokines, such as CD40L, OX40, IL-21 and IL-10. These factors support the Tfh phenotype and, together with cognate T-cell help, serve to promote B-cell survival, expansion and differentiation, resulting in the generation of plasma cells and memory B-cells.[112, 113] Tfh express low levels of transcription factors and cytokines traditionally associated with other $CD4^+$ T-helper subsets. The development of Tfh is thought to occur through interactions with DCs and B-cells, leading to the localisation of Tfh to the B-cell follicles in the lymph node, the

generation of germinal centres and the repression of pathways promoting Th1, Th2 and Th17 differentiation.[113] Although Tfh express specific transcription factors linked with their occurrence and function, evidence suggest that other $CD4^+$ T-helper subsets can develop similar phenotype and functions.[112, 113] For example, adoptive transfer of Th17 cells revealed homing to the small intestine and the expression of Tfh markers and promotion of IgA production in PP.[93]

Figure 1.1

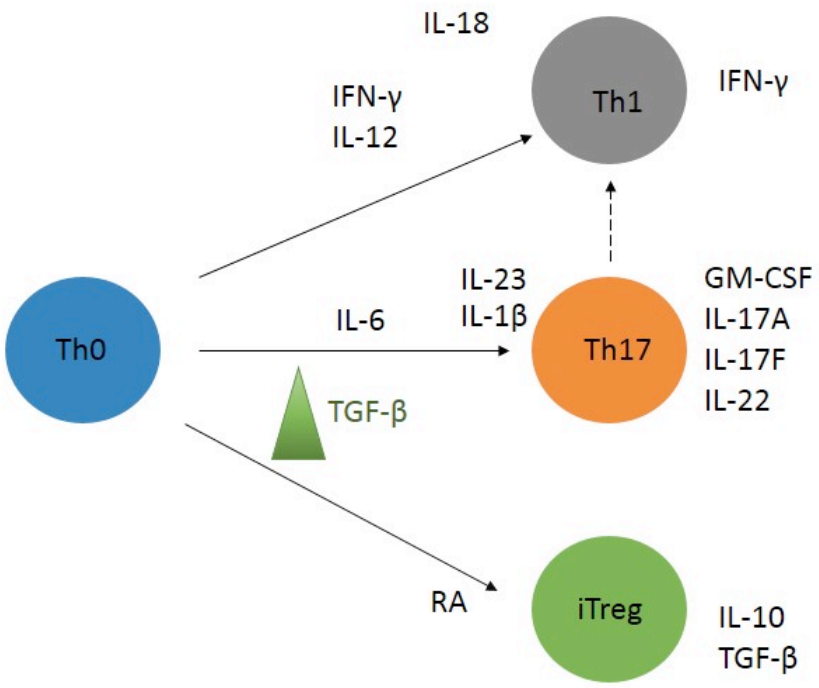


Figure 1.1 $CD4^+$ T-cell differentiation

Th1 cell differentiation is mediated by sequential stimulation of IFN-γ and IL-12. IL-18 enhances production of IFN-γ. IL-6, IL-1β and IL-23 promote pathogenic Th17 cells which are associated with production of GM-CSF. IL-6, IL-1β and TGF-β promote the generation of non-pathogenic Th17 cells. High levels of IL-6 results in the development of Th22 cells. Development of iTreg is promoted by high levels of TGF-β and is enhanced by RA.

During intestinal inflammation $IFN\text{-}\gamma^+IL\text{-}17A^+$ cells occur, suggesting Th17 to Th1 conversion.

1.3 Pattern recognition receptors

Pattern recognition receptors (PRRs) recognise conserved structures of components derived from the external or internal milieu. PRR agonists of microbial origin are referred to as microbial associated molecular patterns (MAMPs) while agonists derived from host constituents are named danger associated molecular patterns (DAMPs).[114, 115] There are several categories of PRRs depending on structure and target molecules. Toll-like receptors (TLRs) and C-type lectin receptors (CLRs) are membrane bound. Cytosolic PRRs comprise several categories: RIG I like receptors (RLR), cytosolic DNA sensors and NOD-like receptors (NLRs)[16]

1.3.1 TLRs

TLR localisation and ligands

Mice express 12 functional TLRs, which are divided into two groups depending on their subcellular localisation. TLR1, 2, 4, 5, 6 and 11 are present in the plasma membrane and predominantly recognise bacterial products.[116] TLR2 senses a wide range of bacterial lipopeptides and forms heterodimers with either TLR1 or TLR6. TLR4 forms homodimers and binds the Gram negative bacterial outer membrane component lipopolysaccharide (LPS). TLR5 forms homodimers and binds bacterial flagellin, while TLR10 is non-functional in mice.[116] TLR11 and TLR12 detect components from the parasite *Toxoplasma gondii*.[117, 118]. In addition, TLR11 has recently been found to detect flagellin derived from *Salmonella*.[119] TLR 3, 7, 8, 9 and 13 are expressed in intracellular vesicles and detect foreign nucleic acids. [116, 118]

The ligand-binding domain of TLRs is composed of leucine rich repeats. The intracellular signalling region consists of a Toll-interleukin 1 receptor (TIR) domain, which associates with different adaptor molecules. The TLR2/1 and TLR2/6

heterodimers interact with the adaptor molecules TIRAP and myeloid differentiation primary response gene (88) (MyD88), initiating the NF-κB transcription programme.[116] Upon stimulation, the TLR2/1 or TLR2/6 complexes accumulate in phagosomes. Depending on the bacterium, phagocytosis might be required for TLR2 activation, presumably for breakdown and sampling.[120] TLR4 forms a complex with the LPS co-receptor CD14 and MD-2, a secreted glycoprotein. This complex cycles between the Golgi and the plasma membrane.[120] After binding of LPS, the complex interacts with the adaptors TIRAP and MyD88 and NF-κB is activated. The complex is also internalised and translocated to an endosome.[120] From this position, the TLR4 complex associates with the adaptor molecules TRAM and TRIF, which will induce both the activation of NF-κB and the interferon regulatory factor 3. Thus, TLR4 signalling is sequential, resulting in early and late activation of NF-κB and the generation of interferons.[116, 120] The cycling of TLR4 is well described in macrophages. In the case of intestinal epithelial cells, *in vitro* studies support intracellular localisation and activation of TLR4.[121]

1.3.2 TLR5

After binding flagellin, a homodimer forms from two flagellin-TLR5 complexes.[122] Activated TLR5 signals via MyD88, resulting in NF-κB activation.[123] Similarly to TLR2 and TLR4, TLR5 has been suggested to function as an endocytic receptor.[124] The use of TCR restricted $CD4^+$ T-cells has shown that TLR5 promotes MHCII presentation of flagellin and OVA-antigen linked to flagellin.[124, 125] TLR5 ligation is known to promote DC activation and the clustering of antigen-specific $CD4^+$ T-cells and DCs in lymph nodes, suggesting that TLR5 expression favours adaptive immune responses to flagellin.[124, 125] Furthermore, flagellin and TLR5 ligation are associated with the induction of adaptive IFN-γ and innate IL-17A production. Flagellin stimulation of DCs

and subsequent co-culture with $CD4^+$ T-cells results in IL-12 production and the promotion of Th1 cell development *in vitro*.[126] Consistent with these adjuvant effects of TLR5 stimulation, flagellin is an immunodominant antigen in IBD patients.[127] Systemic administration of flagellin induces transient IL-22 and IL-17A production by innate cells, possibly ILC. [128] Systemic injection of flagellin has also been reported to mediate cytoprotective effects in IEC by negative regulation of the JNK pathway and reduced apoptosis.[129] Similarly, systemic administration of flagellin before induction of dextran sodium sulphate (DSS) colitis, or infection with pathogenic *Enterococcus,* reduced both the development of pathology and the colonisation levels.[130, 131] However, whether flagellin-mediated contribution to mucosal defence would be beneficial during chronic intestinal inflammation is unclear.

1.3.3 NLRs

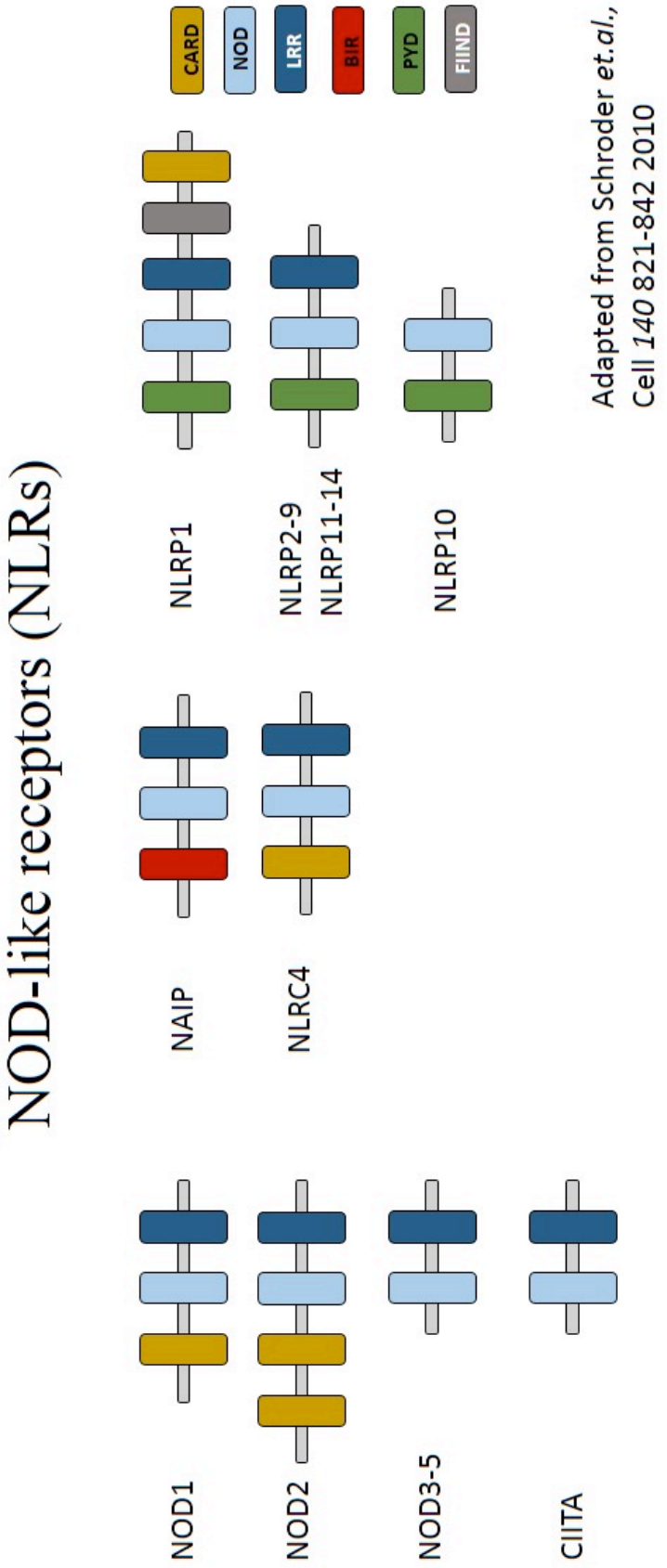
NLRs have a tripartite structure of C-terminal leucine rich repeat domains (LRR), a central nucleotide binding and oligomerisation domain (NOD) and an N-terminal domain of variable structure.[132] The central domain is needed for homotypic oligomerisation and has dNTPase activity. The N-terminal end can be a caspase recruitment domain (CARD), a pyrin domain (PYD) or a baculovirus inhibitor domain (BIR).[132] Humans have 22 NLR genes and mice have more than 30.[133]

NLRs are highly conserved and proteins with NOD and LRR domains exist in plants, although CARD, PYD and BIR regions are unique for animal NLR.[134] Plant NLRs detect endogenous components that have been altered by translocated factors or stress, as well as the effector proteins themselves. NLR activation in plants is often associated with localised cell death.[134] NLRs in animal cells are known for the sensing of invading pathogens and environmental stress. However, certain NLRs, namely NLRC5 and class II transactivator (CIITA), mediate important functions in regulating MHC class I and

class 2 gene expression.[135] NOD-like receptor 1 and 2 (NOD1, NOD2) are two relatively well characterised members of the NLR family which sense derivatives of peptidoglycan from bacterial cell walls.[136, 137] Sensing results in forming of signalling complexes, which can contain other NLRs, and NF-κB mediated pro-inflammatory signalling. Mutated alleles of *NOD2*, thought to encode for loss-of-function versions of the protein, are more prevalent in patients with Crohn's disease, a type of inflammatory bowel disease (IBD), than in healthy controls.[137, 138] However, despite extensive studies there is no consensus as to how the NOD2 polymorphisms predispose to IBD. Several theories exist; NF-κB activation upon NOD2 activation could be reduced. Alternatively mutated NOD2 could fail to inhibit TLR2 signalling resulting in increased NF-κB activation and elevated Th1 responses, or, in the case of a NOD2 frame-shift mutation, transcription of IL-10 could be repressed.[139, 140]

A number of NLRs form large, multi-protein complexes known as inflammasomes in response to infection and stress, and these are discussed in more detail below. An overview of the NLRs is presented in figure 1.2.

Figure 1.2


NOD-like receptors (NLRs)
CARD
NOD
LRR
BIR
PYD
FIIND
NLRP1
NLRP2-9
NLRP11-14
NLRP10
NAIP
NLRC4
NOD1
NOD2
NOD3-5
CIITA
Adapted from Schroder et.al.,
Cell 140 821-842 2010

1.3.4 Inflammasomes

The term inflammasome was coined for a cytosolic, multi-protein scaffold that processed the inactive pro-form of IL-1β into the active, mature form.[141] The first described inflammasome comprised the cytosolic NOD-like receptor NLRP1, the adaptor protein apoptosis-associated speck-like protein (ASC) and caspase-1 and caspase-5. The processed forms of the caspases coincided with the generation and secretion of mature IL-1β.[141]

Inflammasome activation is considered a two-signal system. The first signal is the initial priming. This occurs through TLR signalling, subsequent NF-κB activation and the production of pro-forms of two key inflammatory cytokines, pro-IL-1β and pro-IL-18. The second signal is the activation of the sensor molecule, usually a NLR, which triggers assembly of the multi-protein inflammasome complex.[133] The complex formation occurs when an activated sensor molecule associates with the adaptor molecule ASC, which contains a CARD domain and a PYD domain.[142] These domains are able to interact homotypically and are prone to aggregation. Inflammasome activation *in vitro* can under certain conditions be seen by microscopy as clusters, or ASC specks.[143] Pro-caspase-1, a cysteine protease, contains a CARD region that allows it to associate with ASC.[142, 144] The recruitment of pro-caspase-1 monomers to the scaffold results in auto-proteolysis and the generation of active caspase-1. [144] Caspase-1 cleaves the pro-IL-1β and pro-IL-18, leading to the release of mature cytokines, although the precise mechanism of secretion remains to be determined.[133] The CARD and PYD domains are so-called death-fold domains[144] and inflammasome activation is also associated with a type of inflammatory cell death termed pyroptosis.[145]

Seven distinct inflammasomes have been described to date. Five inflammasomes - those triggered by NLRP1, NLRP3, NLRP6, NLRP7 and NLRP12 - are formed with NOD-

like receptors containing C-terminal LRR domains, a central NOD domain and an N-terminal pyrin domain. NLRP7 is not expressed in mice.[146] Since these sensors do not express a CARD region, the ASC adaptor protein is necessary for homotypic interaction and oligomerisation with pro-caspase-1.

NLRP1 was the first NLR to be described in the context of the inflammasome. The structure of NLRP1 is unique in that it not only contains an N-terminal PYD-domain, a central NOD-domain, LRR sequences, the function to find domain (FIIND) but also a C-terminal CARD domain.[147] Three mouse orthologs of human NLRP1 are expressed: *Nlrp1a*, *Nlrp1b* and *Nlrp1c*. Mouse strains with a functional *Nlrp1b* gene are sensitive to lethal toxin, a pathogenicity factor of *Bacillus antracis*.[148] Deletion of *Nlrp1b* results in abrogated IL-1β production and reduced susceptibility to lung injury in mice treated intratracheally with LPS and lethal toxin.[149] In contrast, mice with constitutively active *Nlrp1a* exhibit neutrophil infiltration and inflammatory conditions in multiple organs, among them the gut and liver.[150] The importance of NLRP1 in steady-state conditions remains to be investigated.

NLRP3 senses a wide variety of stimuli, although no direct binding of ligands has been shown. Triggering occurs following manipulation of the intracellular environment, indicating a state of pathogen invasion, stress or cell death.[132] One major cause of NLRP3 activation is reduced intracellular potassium levels. Stimulation of plasma membrane P2X7 ion channels by extracellular ATP, or by pore-forming toxins, results in potassium efflux and NLRP3 inflammasome activation.[151, 152] Lysosomal rupture following uptake of particulate matter and alteration of mitochondrial function are also known to induce activation, indicating a situation of stress and pathology.[153] Furthermore, release of oxidised mitochondrial DNA into the cytosol and the generation of reactive oxygen species (ROS) following mitochondrial dysfunction also triggers the

NLRP3 inflammasome.[154, 155] NLRP3 mRNA expression is induced by TLR signalling and thus the NLRP3 inflammasome can be rapidly upregulated at the onset of stress and invasion.[156] NLRP3 contributes to tissue protection and *Nlrp3*$^{-/-}$ mice develop severe intestinal pathology in response to DSS treatment.[157] Furthermore, NLRP3 also contributes to protection during bacterial infection with *Salmonella typhimurium* and *Citrobacter rodentium*.[143, 158]

NLRP6 is highly expressed in the liver and the intestine. In the gut, expression appears to be particularly high in IECs and myofibroblasts.[159, 160] No stimulatory ligands have been identified, but co-transfection of NLRP6, pro-caspase-1 and ASC in a cell line resulted in production of mature IL-1β, which is highly suggestive of a functional inflammasome.[161] In a model of DSS-induced intestinal inflammation and tumorigenesis *Nlrp6*$^{-/-}$ mice exhibited increased pathological changes.[159, 160] In addition, *Nlrp6*$^{-/-}$ mice were reported to exhibit dysbiosis of the intestinal microbiota, characterized by outgrowth of the bacterial genus *Prevotella*, and they displayed signs of mild intestinal inflammation, suggesting that NLRP6 modulated host responses against bacteria in the mucosa.[162] Furthermore, the hyper-susceptibility to DSS could be transferred to WT mice by co-housing with *Nlrp6*$^{-/-}$ mice.[162] A recent study reported that during systemic infection with bacterial pathogens, NLRP6 expression in both hematopoietic and non-hematopoietic cells restrained inflammatory responses in the tissue.[163] Bone marrow derived macrophages deficient in NLRP6 exhibited increased NF-κB activation following stimulation with *Listeria monocytogenes*, suggesting that NLRP6 limits innate immune responses in this cell type.[163]

The NLRP12 inflammasome was first identified through bioinformatics studies linking proteins containing PYRIN domains to ASC clustering and caspase-1 dependent cytokine processing.[161] Inflammasome potential was shown *in vitro* by transfection of a

cell line with NLRP12, ASC and pro-caspase 1, which resulted in secretion of IL-1β. [161] NLRP12 has known protective effects both during bacterial infection and chronic inflammation.[164-166] NLRP12 mediates protective effects against *Yersinia pestis* by the generation of IL-18 and by promoting survival, limiting bacterial colonisation and regulating IFN-γ induction.[164] In models of DSS-induced intestinal inflammation and colon carcinogenesis, *Nlrp12*$^{-/-}$ mice exhibited increased and prolonged pro-inflammatory signalling and developed exacerbated pathology and increased numbers of tumours.[166] Hematopoietic cells express the highest levels of NLRP12 and also mediated protection from increased inflammation and tumour formation.[166] *In vitro* studies using bone marrow derived macrophages revealed that NLRP12 deficient macrophages displayed enhanced NF-κB activation and STAT3 signalling in response to TLR ligands. [161, 166] This evidence suggests that NLRP12 dampens pro-inflammatory signalling, but whether NLRP12 contributes to intestinal homeostasis remains to be investigated.

Absent in melanoma 2 (AIM2) is a member of the HIN-200 family and is composed of an N-terminal PYD domain and a C-terminal oligonucleotide/oligosaccharide-binding domain.[167] A screen of human tissues showed that AIM2 is expressed in spleen, small intestine and peripheral leukocytes.[168] AIM2 binds cytosolic, double-stranded DNA via the oligonucleotide/oligosaccharide-binding domain and forms inflammasomes with ASC.[169, 170] *Aim2*$^{-/-}$ mice displayed reduced resistance to infection with mouse cytomegalovirus and produced lower levels of IL-18, harboured increased bacterial burdens and exhibited increased mortality when infected with *Francisella tularensis*. [171, 172] Whether AIM2 plays a role in intestinal homeostasis, or modulates gut inflammation and carcinogenesis remains to be determined.

1.3.5 NLRC4

NOD-like receptor 4 (NLRC4) consists of a C-terminal LRR region, a central NOD region and an N-terminal CARD region.[133] In the inactivated state, the LRR domain conformation blocks interactions between the NOD regions, thereby preventing inflammasome formation.[173] Upon ligand sensing, the conformation is changed and NOD regions are exposed, allowing clustering.[173] Since aggregation with pro-caspase-1 is dependent on CARD-CARD association, NLRC4 inflammasome activation theoretically could take place independently of ASC. This has been reported to occur during pyroptosis, but in the case of cytokine production the presence of ASC highly increases the efficacy of cytokine maturation.[174, 175] One theory is that ASC associates with NLRC4 via CARD-CARD interactions and forms an inner layer surrounding NLRC4.[144] In this way ASC would serve as an amplifier and facilitate pro-caspase-1 recruitment and activation.

Flagellin and components of the bacterial T3SS are the only known ligands for NLRC4.[176-178] NLRC4 does not bind these bacterial molecules directly. However, flagellin and T3SS proteins have been shown to be present in protein complexes containing NAIP proteins and NLRC4.[179, 180] NAIP proteins are NLRs similar to NLRC4, containing BIR domains instead of CARD regions. The proposed theory of NLRC4 activation is that NAIP proteins determine the specificity of the inflammasome and that NLRC4 could be viewed as an adaptor for NAIP proteins.[181] NAIP5 and NAIP6 interact with flagellin and NAIP2 associates with T3SS components, possibly by direct binding.[179, 180] This theory has been challenged by the fact that humans only express one NAIP gene. However, human NAIP recognises T3SS proteins, further supporting the NAIP dependent model of NLRC4 inflammasome activation.[180, 182] A recent study provided evidence that NLRC4 inflammasome formation was dependent

on phosphorylation of a specific serine residue in NLRC4 by protein kinase C delta (PKC δ).[183] However, it remains to be determined if this mechanism is essential *in vivo*. An overview of NLRC4 inflammasome activation is displayed in figure 1.3.

Initial studies in human tissue revealed that NLRC4 is widely expressed in various tissues, for example bone marrow, lymph node, spleen, brain and intestine.[184, 185] However, NLRC4 expression patterns in different cell types, and cues for induction, such as age and conditions of stress, are largely unknown. In humans, several splice forms exist for the *Nlrc4* gene, while mice only express one transcript.[185, 186]

The NLRC4 inflammasome is activated in response to flagellated intracellular pathogens. NLRC4 mediates processing of pro-IL-1β in response to *Salmonella typhimurium* infection.[186] The *S. typhimurium* genome contains several different pathogenicity islands (SPI). SPI1 and SPI2 encode for two different T3SS.[187] In addition to flagellin, NLRC4 also detects the *S. typhimurium* PrgJ rod protein of the SPI1 T3SS.[178] The SPI2 system is activated when the bacteria have invaded epithelial cells and macrophages. Expression of the SPI2 T3SS repressed production of flagellin, thus the ligands activating NLRC4 are removed and *S. typhimurium* actively evades inflammasome activation.[187]

The invasive bacterium *Shigella flexneri* also activates the NLRC4 inflammasome in macrophages and triggers cell death and production of active IL-1β.[188] In this case, inflammasome activation was independent of flagellin, but was dependent on the T3SS. Cell death was partially dependent on NLRC4 and caspase-1, but did not require ASC, although cytokine production was augmented by the presence of ASC.[188] Furthermore, the opportunistic pathogen *Pseudomonas aeruginosa* triggers NLRC4 dependent cell death and IL-1β production in infected macrophages. Similarly to *S. flexneri*, the

process of pyroptosis required NLRC4 and caspase-1, while ASC was needed for IL-1β production. [189] Inflammasome activation by *P. aeruginosa* required a functional T3SS, but not flagellin, again indicating that a T3SS product could trigger NLRC4. NLRC4 deficient mice exhibited elevated bacterial numbers in the spleen and had reduced serum levels of IL-1β following systemic challenge with *P. aeruginosa*.[189] The effect of NLRC4 during *in vivo* infection with *S. typhimurium* is unclear. NLRC4 was shown to be redundant during gastrointestinal inflammation when mice had been treated with antibiotics prior to infection.[190, 191] During oral inoculation in the absence of antibiotic treatment, which results in systemic infection, NLRC4 was shown to be either redundant for protection or to promote survival.[143, 190, 192] The mode of infection and genetic background of the mice most likely affected the outcome. Finally, NLRC4 limits intracellular replication of *Legionella pneumophila* in macrophages.[193] In macrophages, NLRC4 inflammasome activation and processing of caspase-1 resulted in activation of caspase-7, which was essential for limiting bacterial replication.[194] This effect was dependent on the presence of flagellin and Naip5 and the importance for protection was confirmed by *in vivo* findings as caspase-7 deficient mice harboured higher levels of *L. pneumophila* in the lung tissue.[194]

In addition to mediating responses to specific pathogens, a broader role of NLRC4 has been investigated in the DSS model of intestinal damage and colitis. Results were contradictory, suggesting that NLRC4 was either redundant or that NLRC4 deficency was associated with exacerbated intestinal pathology.[190, 195] In conclusion, the NLRC4 inflammasome is activated by a number of bacterial pathogens *in vitro* and has been shown to play a role in protection during *in vivo* infection. However, the role of the NLRC4 inflammasome in intestinal inflammation is not well characterised.

Figure 1.3

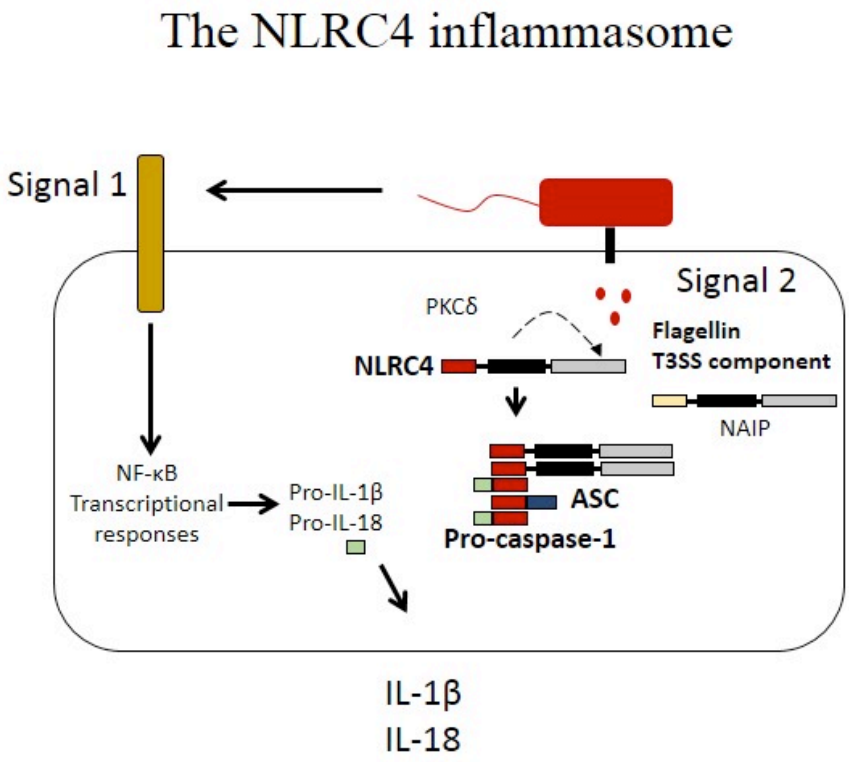


Figure 1.3 The NLRC4 inflammasome

Inflammasome activation is a 2 signal system. Signal 1 constitutes TLR signalling, pro-inflammatory signalling and the generation of pro-forms of IL-1β and IL-18. The presence of flagellin or proteins from bacterial T3SS in the cytosol constitutes signal 2. NLRC4 undergoes conformational changes, exposing the central NOD-region, resulting in NLRC4 oligomers. Phosporylation by PKCδ is required for activation. NAIP proteins might bind ligands directly and interact with NLRC4. ASC amplifies the response and recruits pro-caspase-1. The active caspase-1 cleaves pro-IL-1β and pro-IL-18.

1.3.6 Inflammasome associated IL-1 family cytokines

The IL-1 family of cytokines consists of 11 members, divided into the three subfamilies IL-1 cytokines, IL-18 cytokines and IL-36 cytokines.[196] These proteins are synthesised as precursors without signal peptides and cannot be secreted via normal ER-mediated mechanisms.[197] IL-1β and IL-1α both signal via the IL-1R1 and the IL-1RAcP co-receptor. IL-1β requires processing in order to bind, while IL-1α is a ligand for the receptor both as full-length and as cleaved species.[196] IL-1α is processed by the cytosolic, calcium dependent enzyme calpain. IL-1α is often co-secreted with IL-1β following inflammasome activation, but the exact contribution of either cytokine to IL-1R mediated processes remains to be determined.[198] IL-1β is associated with a multitude of cellular functions and potentiates a range of innate and adaptive immune responses. [197] IL-1β has important co-stimulatory effects on $CD4^+$ T-cells, for example, the development of Th17 cells in the intestine is dependent on IL-1R expression in $CD4^+$ T-cells, IL-1β and the intestinal microflora.[199] Overall IL-1β induces pro-inflammatory responses through IL-1R/MyD88 signalling and subsequent NF-κB gene expression. Although pro-IL-1β is usually processed by active caspase-1, other enzymes, including elastase, matrix metalloprotease 9, granzyme A and proteinase 3 have been reported to cleave IL-1β.[196]

IL-1β has been shown to promote protective effects in response to intestinal pathogens, while contributing to pathogenesis in conditions of chronic inflammation.[158, 200] IL-1 receptor antagonist (IL-1RA) inhibits IL-1 receptor signalling by binding to the IL-1R. Mice that overproduce IL-1RA are protected against endotoxin shock, but display reduced resistance to systemic bacterial infection.[201] Increased production of IL-1β is associated with IBD. Levels of active IL-1β were significantly elevated in tissue from patients suffering from IBD and markedly increased in active lesions.[202, 203]

IL-18 is a ligand for the IL-18Rα and similarly to IL-1β requires a co-receptor, termed IL-18Rβ or IL-18RaP, for signalling. Binding to the receptor complex results in MyD88 recruitment and NF-κB signalling.[204] IL-18 was originally identified as a factor that potentiated IFN-γ production by Th1 cells.[79] IL-18 binding protein (IL-18BP) is a soluble factor that abrogates IL-18 mediated IFN-γ production by splenocytes.[205] IFN-γ itself induces production of IL-18BP, subsequently resulting in a negative feedback loop.[206] IL-18 is implicated in both protective and pathogenic effects during intestinal inflammation. During DSS colitis both protective and deleterious effects of IL-18 have been reported.[157, 207] One potential explanation proposed to account for these conflicting observations is that in an acute inflammatory setting where the tissue is allowed to recover after DSS administration, IL-18 secreted from intestinal epithelial cells may enhance barrier function in the epithelium. During sustained, chronic DSS treatment however, IL-18 may be released by, and act upon, leukocytes in the lamina propria, resulting in exacerbated pathogenic responses.[208] Similarly to IL-1β, IL-18 protein levels are increased in intestinal tissues and serum isolated from IBD patients. [209, 210]

It is unclear how processed IL-1 cytokines are released from cells. One way could be through the loss of membrane integrity and leakage of cytosolic contents that takes place during inflammasome mediated cell death, pyroptosis.

1.3.7 Pyroptosis

Pyroptosis is a type of lytic, inflammatory cell death associated with inflammasome activation. The phenomenon is characterised by DNA damage, the formation of membrane pores, cell swelling and plasma membrane rupture. It requires the presence of caspase-1, actin rearrangement and, when induced by *S. typhimurium*, a functional bacterial T3SS.[211] Pyroptosis is normally quantified by measuring lactate dehydrate (LDH) release into the cell medium as a readout for loss of membrane integrity.[186] The

importance of pyroptosis during *in vivo* infection and in cell types other than macrophages is unclear. Systemic infection with *S. typhimurium* in which flagellin expression was engineered to be either constant or induced, triggered NLRC4 dependent pyroptosis of infected macrophages and resulted in rapid clearance of bacteria by neutrophils.[175] Pyroptosis might be an important mechanism for limiting bacterial burdens and is most likely a target of immune evasion.[175]

1.3.8 Negative regulation of the inflammasome

Several mechanisms of inflammasome regulation exist. Humans express decoy proteins in which only the CARD or PYD domains are present, although there are no mouse homologues for these COP and POP proteins.[212] Caspase-12 is a negative regulator of caspase-1. Caspase-12 likely associates with caspase-1 and prevents processing of pro-IL-1β.[213] Mice deficient in caspase-12 have increased resistance to sepsis and display reduced bacterial burdens during systemic infection with *L. monocytogenes*. The resistance to sepsis is partially dependent on increased production of IFN-γ.[213] Caspase-12 deficient mice display increased resistance to chemically induced DSS colitis but are more prone to developing intestinal tumours in the DSS and AOM model of colon carcinogenesis.[214] In the absence of caspase-12, cellular proliferation in tumour tissue was increased, as was the expression of anti-apoptotic factor Bcl-xl.[214]

The adaptive immune system can also suppress inflammasome activation. *In vitro* experiments showed that memory $CD4^+$ T-cells were able to inhibit both caspase-1 activation and reduce subsequent production of IL-1β and IL-18 by stimulated macrophages. The inhibitory effect abrogated NLRP3 and NLRP1 inflammasome activation, but did not prevent NLRC4 inflammasome induction by *S. typhimurium*. The effect was dependent on concurrent CD3 stimulation of the $CD4^+$ T-cells and was mediated by TNF family members, for example CD40L.[215]

Finally, the cellular process of autophagy has an inhibitory effect on inflammasome function. Activation of NLRP3 and AIM2 inflammasomes in monocytes also induced autophagy.[216] Inflammasome complexes could be detected in the autophagosome compartment and this process was increased if autophagy was further induced by starvation.[216] Supporting the inhibitory effect of autophagy on inflammasome function was the finding that the NLRP3 inflammasome was hyperactivated in macrophages expressing a truncated form of the autophagy protein Atg16L1.[217] Inflammatory stimuli do not only induce inflammasome formation, but also trigger mechanisms to aid with their removal from the cytosol. In addition, changes in cellular status, such as starvation, could affect inflammasome efficacy.

1.4 Inflammatory bowel disease

Inflammatory bowel disease (IBD) can be defined as a chronic and relapsing inflammatory state of the digestive tract.[1] The aetiology is unknown, but intestinal immune responses to the gut microbial flora are highly implicated. Two main branches of the disease exist: Crohn's disease (CD) and ulcerative colitis (UC).[1] CD can affect all parts of the gastrointestinal tract, although the terminal ileum and the colon are the most common sites. CD pathology is transmural, encompassing all cell layers of the gut wall and is often seen as discrete lesions, with normal tissue adjacent to inflamed sections. By contrast, UC involves only the rectum and colon, the inflammation is restricted to the mucosa and is present as continuous inflammation.[1] Both CD and UC are characterised by cellular infiltration and the development of ulceration. The inflammation results in diarrhoea and loss of normal tissue function.[1] Animal models of IBD have revealed that chronic, intestinal inflammation can be induced or caused by genetic mutations, the presence of intestinal flora, barrier defects, excessive T-cell responses, lack of immune regulation and deficiencies in innate immunity.[218]

Genome-wide association studies (GWAS) have identified more than 90 genetic risk loci for IBD, with more than 50% of these loci also implicated in other inflammatory conditions.[219] These genes are functionally linked to diverse processes that have impact on intestinal homeostasis, including; the maintenance of the epithelial barrier; innate immune sensors and effector pathways; IL-10 signalling and negative regulation of T-cells; the Th17 program; B-cells and G-protein coupled receptors.[219] The genetic studies highlight heterogeneity in IBD and suggest that genetic factors act in concert with environmental triggers to cause disease.

The intestine holds up to 10^{11} - 10^{12} bacteria per ml of luminal contents.[220] Intestinal flora is crucial for IBD pathogenesis and mice that spontaneously develop colitis are resistant to the development of intestinal inflammation when reared in germfree conditions.[221] No specific causative agent has been identified, but the increased presence of adherent-invasive *E. coli* in the terminal ileum has been associated with IBD, suggesting that location of bacteria could influence pathogenesis.[222] However, the increased bacterial association with the epithelium could be a result of reduced or altered production of mucus, which are known traits of IBD patients.[219]

Current treatment for IBD includes anti-inflammatory 5-aminosalicylic acid formulations, which can be given by the systemic, oral or rectal route. Patients that do not respond to this treatment may be given immunosuppressive corticosteroids. Monoclonal antibodies to TNF-α can be used for both CD and UC, both as early treatment and as maintenance therapy.[223] However, despite treatment patients often relapse and surgery is required, especially in the case of CD patients.[223] A better understanding of the disease pathophysiology would facilitate the development of new and improved treatment.

CD and UC are characterised by strong T-helper cell mediated responses. Traditionally, UC has been viewed as dominated by Th2 responses with increased production of IL-13. CD patients develop elevated Th1 responses and display increased production of IFN-γ.[224] Furthermore, CD patients exhibit increased levels of IL-17A.[225] IL-17A production and Th17 responses are augmented by IL-23.[226] Consistent with a pathogenic role of the IL-23/Th17 axis, CD susceptibility is linked to polymorphisms in the IL-23R and IL-23 mediates crucial protective or pathogenic effects in a number of different animal models of intestinal inflammation.[227]

1.5 Models of intestinal inflammation employed in this thesis

1.5.1 *Citrobacter rodentium* infection – a model of acute intestinal inflammation

C. rodentium infection of mice provides an acute model of bacterially-triggered intestinal inflammation. *C. rodentium* is a gram negative attaching and effacing (A/E) bacterial pathogen. It shares many features with the human pathogens enterohemorrhagic *E. coli* (EHEC) and enteropathogenic E. coli (EPEC).[228] These bacteria adhere to IECs and cause cytoskeletal changes, resulting in altered cellular structure and the destruction of the cell surface.[229] *C. rodentium* expresses a locus of enterocyte effacement (LEE) which encodes for a T3SS and a number of effector proteins.[230] Translocation of the intimin receptor (Tir) to the host cell and the expression of intimin, an outer membrane protein, anchors *C. rodentium* to the intestinal epithelium.[231] Subsequent rearrangement of the host actin cytoskeleton results in pedestal-shaped formations to which the bacteria localise.[228]

Infection of WT mice results in diarrhoea and inflammatory responses mainly in the distal part of the colon.[228] The use of bioluminescent luciferase expressing *C. rodentium*

established that colonisation of the large intestine is sequential.[232] Initial colonisation takes place in the cecum, with a tropism for the cecal patch, a site of lymphoid follicles and associated epithelium rich in M-cells.[233] The distal colon is the second site of infection and remains a reservoir for the bacterium throughout the infection.[232]

The infection is rapidly transmitted between animals and *C. rodentium* is known to cause outbreaks of diarrhoea in animal facilities.[229, 234] *C. rodentium* that have been conditioned by passage through the mouse intestine exhibit increased virulence, most likely caused by increased production of the LEE associated proteins.[234, 235]

C. rodentium infection remains local and is cleared within 3-4 weeks by specific IgG mediated responses.[236, 237] Although WT mice do not develop severe symptoms, suckling mice are extremely susceptible and exhibit high mortality.[238] Despite the mild pathology observed in WT mice, a number of potent, protective innate and adaptive immune responses are triggered. Among innate immune signalling, MyD88 and IL-1R expression are essential for survival.[239-241] Furthermore, TLR2 deficiency results in a high rate of lethality while TLR4 expression contributes to pathology.[242, 243] The pro-inflammatory cytokine IL-23 is essential for mucosal defence and survival.[244] ILCs respond to IL-23 and produce IL-22, a cytokine of the IL-10 family, which is required for early protection and survival during *C. rodentium* infection.[59, 60, 245] Although ILCs are the initial producers of IL-22, at a later stage IL-22 producing $CD4^+$ cells, Th22 cells, contribute to protection in an IL-6 dependent manner.[98] IL-22 acts on IECs and induces production of AMPs, including the c-type lectin RegIIIγ, which has known protective functions during *C. rodentium* infection.[60]

$CD4^+$ T-cell orchestrated adaptive immune defences are crucial for *C. rodentium* eradication and host survival. B-and T-cell deficient $Rag^{-/-}$ mice initially exhibit milder

pathology, but eventually develop severe disease, due to their inability to clear the infection.[236, 246, 247] IFN-γ and Th1 cells promote protective effects but also drive the hyperplastic response which is a key feature of the pathology.[237, 248, 249]

Considering the highly localised niche and the non-invasive nature of the bacterium, *C. rodentium* infection of the intestinal tract offers the possibility to investigate several different aspects of mucosal immunity. The expression of specific virulence factors and subsequent secretory responses makes *C. rodentium* infection of mice an excellent model of diarrhoea and also allows for the specific study of A/E pathogens and their effector proteins. These studies provide valuable input to the understanding of the human pathogens EPEC and EHEC. In a more general sense, *C. rodentium* infection illuminates key aspects of mucosal immune mechanisms activated during acute intestinal inflammation. In the context of IBD, *C. rodentium* infection elicits several shared pathological features, such as hyperplasia, cellular infiltration and T-helper cell responses.[249] Finally, the fact that *C. rodentium* interacts with IECs and remains extracellular makes it an ideal model to study immune mechanisms of the intestinal epithelium itself.

In our studies, we used a time course infection model in order to assess different properties of immune responses. Histological changes and colonisation levels were evaluated after 3, 8 and 14 days of infection. Day 3 represents a time point of early colonisation[228] but little pathology, when the infection is inducing initial innate immune responses. Day 8 represents peak colonisation[228] and a stage at which protective responses have been launched and when pathological features of disease are evident. After 14 days of infection, eradication of bacteria has begun[228] and adaptive immune responses are fully formed. An outline of the infection protocol is shown in Fig.1.4 A.

1.5.2 T-cell transfer colitis – a model of T-cell dependent chronic intestinal inflammation

Adoptive transfer of naïve $CD4^+CD25^-CD45RB^{hi}$ T-cells into a lymphopenic (*Rag*$^{-/-}$ or *Scid*) mouse results in a progressively exacerbated condition of severe intestinal inflammation and wasting disease.[250] After transfer, naïve T-cells reconstitute the lymphopenic hosts and are exposed to microbial antigens derived from the intestinal microbiota, driving their differentiation into effector Th1 and Th17 $CD4^+$ cells.[251] The systemic and intestinal pathology is driven by effector Th1 cells and IFN-γ, while IL-17A derived from the transferred T-cells is dispensable.[252-254]

The intestinal inflammation that develops during T cell transfer colitis displays traits typical of both UC and CD. The major features are epithelial hyperplasia, mucin depletion, epithelial ulceration and cellular infiltrates.[255] Similar to CD, the pathology can also be transmural, although it is typically multifocal and does not encompass the entire circumference of the intestinal wall. Despite the high epithelial cell turnover, formation of tumours does not occur.[255]

The development of T-cell transfer colitis is dependent on the interplay of pro-inflammatory signalling and the absence of regulation. Pro-inflammatory signalling is dependent on IL-23 expression in the *Rag*$^{-/-}$ mouse and on IL-23 responsiveness by the transferred naïve T-cells.[94, 251] IL-23 potentiates the development of Th1 and Th17 responses and the disease is associated with the emergence of a population of IFN-γ^+IL-$17A^+$ double positive $CD4^+$ T cells within the intestinal lamina propria.[94] Similarly, IFN-γ^+IL-$17A^+$ double positive $CD4^+$ T cells have been isolated from the inflamed intestines of CD patients.[256] In addition, in experimental autoimmune encephalomyelitis (EAE) IL-$17A^+$ $CD4^+$ T-cells were shown to transform into IFN-γ producing cells,

indicating Th17 to Th1 conversion in a pro-inflammtory environment[93] IL-23 also promotes disease by inhibiting the development of suppressive Treg cell populations and, if regulatory cytokines such as IL-10 or TGF-β are blocked, disease develops in IL-23 deficient Rag mice.[252]

T-cell transfer colitis can be prevented by the co-transfer of $CD4^+CD25^+$ Treg and 'cured' by transfer of $CD4^+CD25^+$ Treg into animals with established colitis.[250, 257] It thus provides an excellent model to study Treg cell functional activities and has been extensively employed to identify key factors involved in suppression of intestinal pathology by $CD4^+CD25^+$ Treg cells *in vivo*.[258] T-cell transfer colitis is devoid of bacterial pathogens and the disease develops as a result of dysregulated $CD4^+$ T-cell responses to the commensal microflora. Thus, it is a model that allows for the study of disrupted homeostasis and the development of chronic, intestinal inflammation. The kinetics of T cell transfer colitis depend on the composition of the intestinal microflora and vary in different animal facilities. However, in most SPF facilities, the end point, which is reached when mice have developed chronic diarrhoea and/or lost more than 20% of their initial body weight, occurs around 6-8 weeks after adoptive transfer. An overview of the experimental design is presented in figure 1.4 B.

1.5.3 *Helicobacter hepaticus* infection and αIL-10R blockade – a model of bacterially triggered T-cell dependent chronic inflammation

Infection with the gram negative bacterium *Helicobacter hepaticus* and treatment with blocking αIL-10 receptor antibody (αIL-10R) results in the development of intestinal inflammation in the cecum and colon, as well as systemic immune responses.[259] *H. hepaticus* can be considered a normal constituent of the murine flora. The bacterium is flagellated, is situated in the mucus layer on the epithelial surface, and penetrates deep

into the colonic crypts.[260] It causes life-long colonisation but does not induce inflammatory changes in normal, WT mice.[261] However, *H. hepaticus* is not treated as benign commensal by the host, as potent *H. hepaticus*-specific systemic $CD4^+$T-cell and antibody responses are elicited.[262] Despite these responses, pathology does not ensue because *H. hepaticus* infection also drives the development of potent Treg cell responses that effectively suppress pathogenic effector responses.[263, 264] Thus, when these regulatory responses are blocked in *H. hepaticus*-infected mice, either by administering an anti-IL-10R mAb to WT mice or by genetic ablation of IL-10, colitogenic $CD4^+$ T cell responses towards *H. hepaticus* are revealed and drive severe intestinal inflammation.[259, 262] The pathological changes during *H. hepaticus* infection and αIL-10R treatment of WT mice are dependent on innate MyD88 signalling and IL-23 expression.[259, 265]

Histological changes observed during *H. hepaticus* infection and αIL-10R treatment of WT mice are reminiscent of IBD and are characterised by epithelial hyperplasia, goblet cell depletion, oedema and cellular infiltration.[259] Even in the presence of elevated *H. hepaticus* specific Th1 and IgG responses, the infection is not cleared.[262] It is unknown how *H. hepaticus* evades eradication in a context of constant inflammation, but the mainly luminal, extracellular localisation[260] could favour persistence. *H. hepaticus* most likely displays immune evasive traits such as non-reactivity to TLR5. This is supported by the fact that some bacterial species belonging to α and ε proteobacteria, among them *Helicobacter pylori*, have been shown to express flagellins of altered sequence that are not ligands for TLR5.[266]

The combination of a bacterial infection and dysregulated immune regulation provides the possibility to study mucosal immune responses mimicking a number of features

typical of human IBD. A schematic illustration of the experimental protocol is shown in figure 1.4 C.

1.5.4. *Helicobacter hepaticus* infection of Rag$^{-/-}$ mice – a model of bacterially triggered innate chronic inflammation

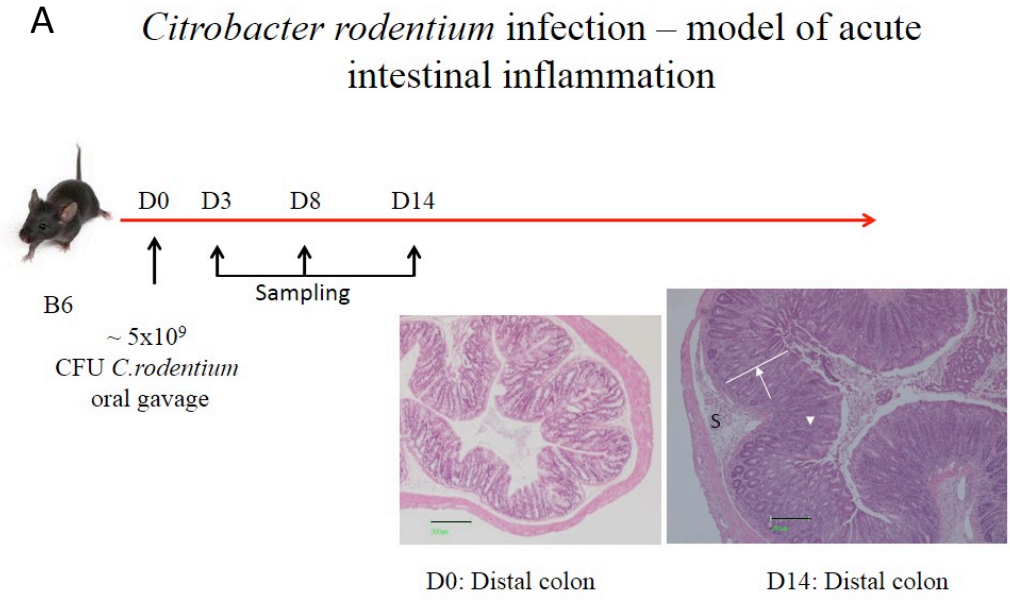
Infection of 129SvEv*Rag2*$^{-/-}$ mice with *H. hepaticus* results in persistent infection, chronic, intestinal inflammation and systemic immune responses.[267] The susceptibility is strain dependent, since B6*Rag1*$^{-/-}$ mice only develop mild colitis following infection.[268, 269] As in T-cell dependent *H. hepaticus* colitis, IL-23 expression is necessary for pathogenesis.[251] In the absence of CD4^{+} T-cells, IL-23 responsive ILCs mediate inflammatory responses and produce IFN-γ and IL-17A that are pathogenic in this setting.[63] Furthermore, innate immune signalling via MyD88 in hematopoietic cells is essential for pathogenesis in *H. hepaticus*-infected 129SvEv*Rag2*$^{-/-}$ mice.[265] This suggests that the detection of *H. hepaticus* by myeloid cells, in the absence of Treg, promotes disease.

The pathology is characterised by epithelial hyperplasia, cellular infiltration and systemic immune responses, such as splenomegaly.[267] The innate model of colitis provides the means to study innate immune pathways during chronic inflammation. It is also a reductionist model in which innate immune sensing of *H. hepaticus* is pathogenic, facilitating the investigation of bacterial products involved in virulence and colonisation. In addition, if used in conjunction with the carcinogen AOM, it can be used to study colitis-associated colon carcinogenesis.[270] An overview of the model is presented in figure 1.4 D.

1.5.5 Dextran sodium sulphate (DSS) colitis – a model of acute intestinal inflammation

DSS colitis is commonly used as a model of intestinal inflammation and it is frequently referred to throughout this thesis, although no data derived from this model will be presented. DSS is a polymer that is added to the drinking water and concentrated in the colon, which mainly is where disease occurs.[271] DSS is considered to be toxic to intestinal epithelial cells and causes intestinal damage, characterised by ulceration, granulocyte infiltration and bloody diarrhoea.[271] DSS induced colitis displays similarities to human IBD in that Th1 responses are induced, colon carcinogenesis can occur and disruption of epithelial cell barrier function results in pathology.[272] $Rag^{-/-}$ mice are slightly protected compared with WT mice, indicating a contribution of T-cell mediated immunopathology.[273] However, considering the acute nature of the inflammation, innate immune signalling is essential for the outcome. A number of innate immune components confer protection, for example MyD88, TLR2, TLR4 and TLR5.[274-277] During DSS colitis inflammation is promoted by translocation of bacteria across the epithelium and robust innate immune sensing and responsiveness is required for protection. The role of IL-23 in DSS colitis is not well studied, but IL-23 appears to drive pathogenic responses in adaptive settings and protective mechanisms in innate settings.[278]

Figure 1.4


A
Citrobacter rodentium infection – model of acute intestinal inflammation
D0
D3
D8
D14
Sampling
B6
~ 5x10⁹
CFU *C.rodentium*
oral gavage
S
D0: Distal colon
D14: Distal colon

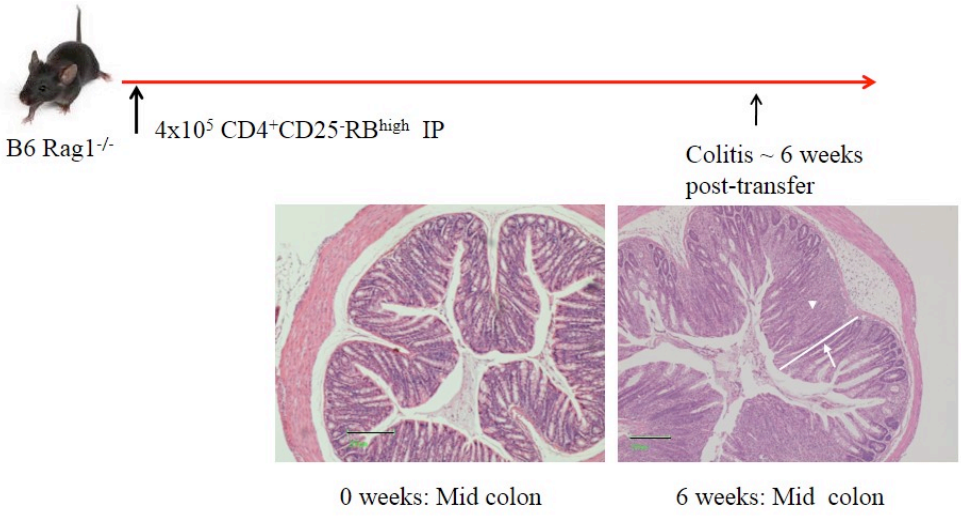

B
T-cell transfer colitis – model of T-cell dependent chronic intestinal inflammation
B6 Rag1-/-
4x10⁵ CD4+CD25-RBhigh IP
Colitis ~ 6 weeks post-transfer
0 weeks: Mid colon
6 weeks: Mid colon

Figure 1.4 Part 2

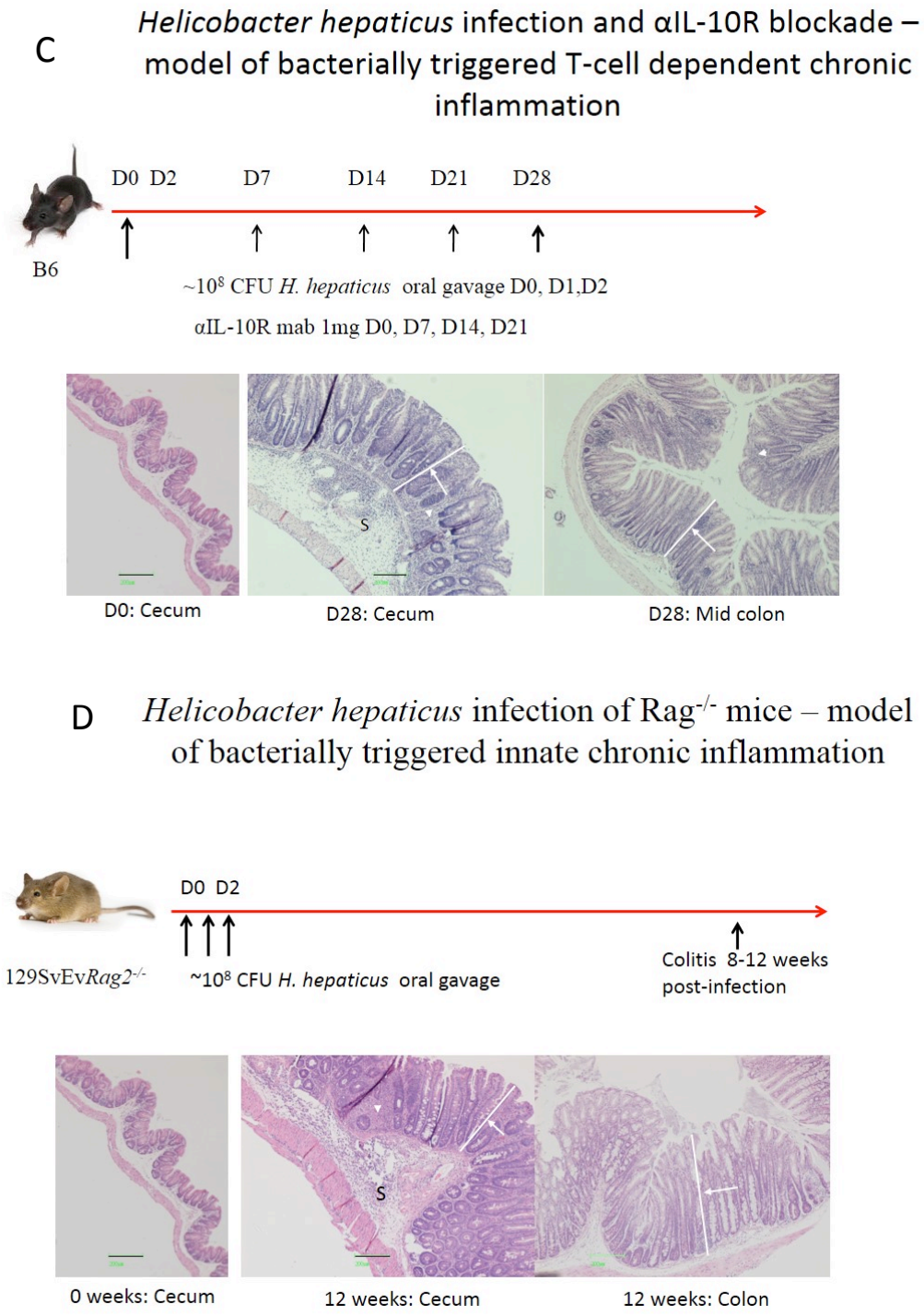


Figure 1.4 Models of intestinal inflammation

Four complementary models of colitis were used to characterise the role of flagellin sensing in intestinal inflammation. (A) *Citrobacter rodentium* infection (B) $CD4^{+}CD25^{-}CD45RB^{hi}$ cell transfer into lymphopenic hosts (C) *Helicobacter hepaticus* infection and αIL-10R blockade (D) *H. hepaticus* infection of 129SvEv*Rag2*$^{-/-}$ mice. White arrows indicate hyperplasia, white arrowheads denote cellular infiltration and the letter S marks submucosal inflammation.

1.6 Aims

The aim of this thesis was to investigate the role of innate immune sensing of flagellin and flagellated bacteria in the development of intestinal inflammation. The innate immune sensors for flagellin were interesting targets, considering the abundance of bacteria in the intestinal tract, the immunogenic properties of bacterial flagellin and the reported pro-and anti-inflammatory effects of flagellin. By using mice deficient in two different innate sensors of flagellin, NLRC4 and TLR5, the effects of flagellin could be studied in the context of intestinal bacteria. Two different scenarios of innate flagellin sensing were envisioned: (a) Sensing of specific flagellated bacteria used to induce intestinal inflammation and (b) Sensing of commensal bacteria. In this sense responses to flagellin could either be a direct result of bacterial invasion and host-pathogen interactions or a constant signal from the commensal flora, possibly contributing to homeostasis. By using knockout mice I could analyse the effects of flagellin mediated signalling in chronic, inflammatory settings.

In the laboratory several well characterised models of intestinal inflammation were available. In the first part I investigated the contribution of NLRC4 to host defence in a model of acute intestinal inflammation, based on infection with *C. rodentium*. These findings are presented in chapter 3. In order to evaluate NLRC4 in chronic colitis I utilised two complementary models of chronic intestinal inflammation. To explore the effects of NLRC4 in T cell-dependent IBD I used the *H. hepaticus* α-IL-10R model of colitis. To investigate the effects of NLRC4 in innate responses further, the *H. hepaticus* innate model of colitis was employed. These results are presented in chapter 4.

As a separate project the impact of TLR5 in chronic colitis was investigated. To assess the role of TLR5 during disruption of intestinal homeostasis, the T-cell transfer model of colitis was used. To elucidate the importance of TLR5 in T-cell dependent IBD, the *H .hepaticus* α-IL-10R model of colitis was employed. Finally, the *H. hepaticus* innate model served to investigate TLR5 dependent circuits in an innate setting. These results are displayed in chapter 5. Lastly, as part of a smaller side project in which virulence factors of *H. hepaticus* were investigated, I generated a *Helicobacter hepaticus* type 6 secretion system mutant and performed the initial characterisation with regards to *in vivo* effects on development of intestinal inflammation. This constitutes chapter 6.

Chapter 2 Materials and methods

2.1 Materials

2.1.1 Mice

C57/BL6 (B6), B6 *Nlrc4*$^{-/-}$, B6 *Tlr5*$^{-/-}$, B6 *Rag1*$^{-/-}$, B6 *Nlrc4*$^{-/-}$*Rag1*$^{-/-}$, B6 *Tlr5*$^{-/-}$*Rag1*$^{-/-}$, 129SvEv *Rag2*$^{-/-}$, 129SvEv *Nlrc4*$^{-/-}$*Rag2*$^{-/-}$,129SvEv *Tlr5*$^{-/-}$*Rag2*$^{-/-}$ and B6 *Il10*$^{gfp/gfp}$ FOXP3 'knockin' hCD2/CD52 were housed in specific pathogen free conditions in accredited animal facilities at the University of Oxford. B6 *Nlrc4*$^{-/-}$ were provided courtesy of Professor Vishva Dixit (Genentech Inc., USA).[186] B6 *Tlr5*$^{-/-}$ mice were a gift from Professor Shizuo Akira (Osaka University, Japan).[279] B6IL-10 GFP reporter mice crossed to B6FOXP3 knockin fusion hCD2/CD52 mice were provided by Professor Richard Flavell (Yale University, USA) and Professor Herman Waldmann (University of Oxford) respectively.[280, 281]

B6 *Nlrc4*$^{-/-}$ mice were back-crossed onto the 129SvEV*Rag2*$^{-/-}$ background using a speed congenic approach based on microsatellite markers.[282] Each generation of backcrossed mice was screened for a total of 63 microsatellite markers, which were designed to be distributed over the 129SvEv genome. Mice from the F8 generation were intercrossed to generate 129SvEv*Nlrc4*$^{-/-}$*Rag2*$^{-/-}$ mice.

B6 *Nlrc4*$^{-/-}$ mice were crossed with B6 *Rag1*$^{-/-}$ mice to generate B6 *Nlrc4*$^{-/-}$*Rag1*$^{-/-}$ mice. The crossing of B6 *Tlr5*$^{-/-}$ mice to B6 *Rag1*$^{-/-}$ mice to generate B6 *Tlr5*$^{-/-}$*Rag1*$^{-/-}$ mice and the backcrossing of B6 *Tlr5*$^{-/-}$ mice to the 129SvEv*Rag2*$^{-/-}$ background was performed by Mark Asquith.[268]

To generate FOXP3 IL-10 reporter mice, B6 *Il10*$^{gfp/gfp}$ *Foxp3*$^{hCD2//hCD2}$ were crossed with B6 *Foxp3*$^{hCD2/hCD2}$ mice for each experiment.

2.1.2 Antibodies

A summary of antibodies used for cell sorting, FACS staining, immunohistochemistry (IHC), ELISA and *in vivo* experiments are displayed in Table 2.1

Specificity	Clone	Source	Fluorochrome	Concentration
CD4 enrichment				
αB220	RA36B2	In-house	N/A	~10μg/mL
αMac-1	M1/70	In-house	N/A	~10μg/mL
αCD8	YTS 169	In-house	N/A	~10μg/mL
αMHCII	TIB120	In-house	N/A	~10μg/mL
Cell sorting and FACS				
CD45RB	16A	BD	FITC	5 μg/mL
CD25	PC61.5	eBioscience	PE	2 μg/mL
CD4	RM4.5	eBioscience	APC	2 μg/mL
CD4	GK1.5	eBioscience	PeCy7	2.5-5 μg/mL
TCRβ	H57-597	eBioscience	PerCp	2.5-5 μg/mL
CD11b	M1/70	eBioscience	PE	0.25-0.5 μg/mL
CD11b	M1/70	BD	PerCp	1 μg/mL
Gr1	R86-8C5	eBioscience	PerCP	0.5 μg/mL
CD45	30-F11	eBioscience	e450	0.7 μg/mL
CD45	104	eBioscience	FITC	2.5 μg/mL
F4/80	BM8	eBioscience	APC	1-4 μg/mL
Ly6G	1A8	Biolegend	PeCy7	0.5-1 μg/mL
MHCII	M5/114.15.2	eBioscience	e450	1 μg/mL
Siglec-F	E50-2440	BD	PE	1 μg/mL
CD16/32 (FC block)	93	Biolegend	N/A	5 μg/mL
Human CD2	RPA-2.10	eBioscience	PE	Dilution 1/50
Intracellular FACS staining				
IL-17A	eBio17B7	eBioscience	Alexa 647 (APC)	2 μg/mL
IL-17A	eBio17B7	eBioscience	PE	2 μg/mL
IFN-γ	XMG1.2	eBioscience	e450	2 μg/mL
IFN-γ	XMG1.2	eBioscience	APC	2 μg/mL
Isotype Controls				
IgG2A	eBR2a	eBioscience	Alexa 647 (APC)	2 μg/mL
IgG2A	eBR2a	BD	PE	2 μg/mL
IgG1	eBRG1	eBioscience	e450	2 μg/mL
IgG1	eBRG1	BD	APC	2 μg/mL
IHC				
Rabbit-α-mouse Ki67	SP6	Abcam	N/A	Dilution 1/200

Mouse α-E-cadherin	36/E-Cadherin	BD	N/A	1.25 µg/mL
Rabbit α-*C. rodentium* serum	N/A	Kind gift from Prof. G. Frankel Imperial College	N/A	Dilution 1/200
Goat- α-mouse	N/A	Invitrogen	Alexa 488	4 µg/mL
Goat- α -rabbit	N/A	Invitrogen	Alexa 555	4 µg/mL
α*C. rodentium* and *H. hepaticus* ELISA				
Biotinylated Goat-α-mouse IgG	N/A	Vector Labs	N/A	3µg/mL
HRP-Goat α-mouse IgA	N/A	Invitrogen	N/A	Dilution 1/500
In vivo				
IL-10R (blocking)	1B1.2	In-house	N/A	1mg/week

Table 2.1 Summary of antibodies

2.2 Assessment of intestinal inflammation

At necropsy colon and cecum were collected and rinsed in PBS/0.1%BSA. Samples were fixed in PBS/3.6% PFA. 4µm sections were cut and stained with hematoxylin and eosin. Sections were scored in a blinded fashion. For T-cell transfer and *H. hepaticus* infection a scoring system (0-12) previously developed in the laboratory was used (Table 2.2).[200] An average score for each colon was generated by calculating the mean value of the separate proximal-, mid- and distal colon scores.

For *C. rodentium* infection, an amended version (0-15) of the histopathology scoring system was used, as shown in Table 2.3. For the colon only the distal part was scored.

Epithelium	Hyperplasia and/or	goblet cell depletion
0	None	None
1	Mild (1.5x)	Mild (25%)
2	Moderate (2-3x)	Marked (25-50%)
3	Severe (>3x)	Substantial (>50%)

Inflammation in lamina propria

0	None – few leukocytes
1	Mild – some increases in leukocytes at the tips of crypts **or** many lymphoid follicles
2	Moderate – marked infiltrate (notable broadening of crypts)
3	Severe – dense infiltrate throughout

Area affected (% of section)

0	None
1	up to 25%
2	25-50%
3	>50%

Markers of severe inflammation

0	None
1	Submucosal inflammation **or** few crypt abscesses (<5)
2	Submucosal inflammation **and** few crypt abscesses (<5)
2	Many crypt abscesses (>5) **or** extensive submucosal inflammation **or** crypt branching
3	Many crypt abscesses (>5) **and** extensive submucosal inflammation/crypt branching
3	Ulceration or extensive fibrosis

Table 2.2 Categories for assessment of intestinal inflammation

Epithelium	Hyperplasia and/or	goblet cell depletion and/or	damage
0	None	None	None
1	Mild (1.5x)	Mild (25%)	Mild
2	Moderate (2-3x)	Marked (25-50%)	Marked
3	Severe (>3x)	Substantial (>50%)	Substantial

Inflammation in lamina propria

0	None – few leukocytes
1	Mild – some increases in leukocytes at the tips of crypts **or** many lymphoid follicles
2	Moderate – marked infiltrate (notable broadening of crypts)
3	Severe – dense infiltrate throughout

Submucosa	Edema	Infiltration	Follicle
0	None	None	None
1	Mild	Mild	Enlarged
2	Marked	Marked	**-**
3	Both marked edema and marked infiltration		**-**

Area affected (% of section)

0	None
1	up to 25%
2	25-50%
3	>50%

Markers of severe inflammation

	Bleeding and/or	Crypt abscesses and/or	Necrosis/Ulcers
0	None	None	None
1	Some	Few	-
2	Marked	Many	Few/Small
3	**-**	**-**	Large/Many

Table 2.3 Categories for assessment of intestinal inflammation- amended version for *C. rodentium* infection

2.3 Cell isolation and fluorescent-activated cell sorting (FACS)

2.3.1 Enrichment of $CD4^+$ T-cells

Spleens were collected and cell suspensions prepared in PBS/0.1%BSA by passing through a 100µm cell strainer (BD Falcon). Red blood cells were lysed with ACK lysis buffer (150mM NH_4Cl, 10mM $KHCO_3$, 0.1mM Na_2EDTA, pH 7.2-7.4), for 3 min at room temperature. Cells were washed in PBS/0.1%BSA and incubated with rat monoclonal antibodies against B220, Mac-1, CD8 and MHCII, as indicated in table 2.1. Cells were incubated with antibodies for 15 min on ice. Cells were then washed and resuspended in PBS/0.1%BSA at 10^8 cells/mL. Sheep-anti-rat coated magnetic beads (Dynal) were washed and resuspended in PBS/0.1%BSA and added to the splenocytes at a concentration of 10^8 beads/mL. The suspension was placed on a rotator at 4°C for 20 min. The suspensions were placed next to a magnet (Dynal) and beads and ligated cells were removed. The cleared suspension was transferred to a fresh tube and placed next to the magnet a second time. Cells were washed in PBS/0.1%BSA and resuspended for a final concentration of 10^8 cells/mL.

2.3.2 FACS purification of naïve T-cells

Spleen suspensions enriched for $CD4^+$ T-cells were stained for CD45RB, CD25 and CD4 (table 2.1) in PBS/0.1% BSA. Cells were incubated with antibodies for 15 min on ice, washed, resuspended at 2-5x10^7 cells/mL and filtered through a cell strainer prior to sorting. Sorting was performed with a MoFlo cell sorter (Dakocytomation). Naïve $CD4^+$ T-cells were considered to be $CD4^+CD25^-CD45RB^{hi}$.

2.3.3 Isolation of lamina propria leukocytes (LPL)

LPLs were isolated from colonic or cecal tissue. Tissues were cut open, washed in PBS/0.1% BSA, cut in 0.5cm-1cm pieces and kept on ice in PBS/0.1% BSA. Tissues were incubated in pre-warmed RPMI 1640 (PAA) containing FCS (5%) and EDTA (5 mM) at 37°C, 200rpm, for 15-20 min in order to release IEC. This procedure was repeated twice. Samples were then incubated with RPMI containing FCS (5%), and HEPES (15mM, PAA) for 10 min at room temperature. The supernatants were aspirated and tissues were digested with collagenase Type VIII (100U/mL, Sigma) in RPMI containing FCS (5%), and HEPES (15mM) for 1h at 37°C, 200rpm. Cell suspensions were collected into RPMI with FCS (5%) and EDTA (5mM) and kept at 4°C. The remaining tissues were subjected to a second collagenase digest and the resulting first and second cell suspensions were pooled. Alternatively, after the 10 min incubation with RPMI containing FCS and HEPES, tissues were digested with collagenase Type VIII (300U/mL) and DNase1 (40µg/mL) in RPMI containing FCS (5%) and HEPES (15mM) for 1h, at 37°C, 200rpm. For isolation of LPL from FOXP3 IL-10 reporter mice, tissues were incubated with collagenase Type II (10mg/sample, Sigma) for 1h at 37°C, 200rpm. The cell suspensions were collected and washed. Samples were resuspended in 3mL of 30% buffered percoll (GE). Samples were loaded on a discontinuous percoll gradient, consisting of 3 mL of 75% buffered percoll and 4 mL of overlaying 40% buffered percoll. Gradients were centrifuged for 20min at approximately 900g (1800rpm) with no brake. After centrifugation, the p30 and p30/40 interface were discarded. The remaining p40 layer and p40/p75 interface were collected into PBS/0.1% BSA, washed and kept on ice.

2.3.4 Isolation of splenocytes

Spleens were collected into ice-cold PBS/0.1% BSA, passed through a 100µm cell strainer (BD Falcon) and centrifuged. The pellets were resuspended in ACK lysis buffer as described in 2.3.1. Splenocytes were washed and resuspended in ice-cold PBS/0.1% BSA.

2.3.5 Cell staining for FACS analysis

Cell suspensions of spleen and LPL were prepared as previously described. Cell numbers were determined by the use of a hemocytometer. Cells were stained in a 96 well round bottom plate. Cells were preincubated with FC block in 100µL PBS/0.1% BSA for 15min, 4°C and then stained for innate surface markers CD11b, Gr1, Ly6G, F4/80 and Siglec-F (Table 2.1). Cells were centrifuged and incubated with 50µL PBS/0.1% BSA with appropriate antibodies for 15min, at 4°C. Cells were washed twice and fixed in 200µL PBS with PFA (2%, Electron Microscopy Sciences). Prior to flow cytometry analysis, cells were washed once and resuspended in PBS/0.1% BSA. 1-2x10^6 splenocytes and < 1x10^6 LPLs were used for each stain.

For intracellular stains, LPLs were restimulated for 3h at 37°C with 0.1 µg/mL PMA (Sigma), 1 µg/mL ionomycin (Sigma), and 10 µg/mL Brefeldin A (Biolegend) in 200µL RPMI complete, which was composed of RPMI 1640 with FCS (10%), penicillin streptomycin (100U/mL, PAA), L-glutamin (2mM, PAA) and β-mercaptoethanol (0.05M, VWR). After restimulation, cells were washed and stained for surface markers PeCy7 anti-CD4 and PerCP anti-TCRβ for 15 min at 4°C, protected from light. Cells were washed twice and fixed overnight in 100µL Fix/Perm buffer (eBioscience). Cells were then centrifuged and resuspended in 100µL perm buffer (eBioscience) with normal rat serum (2%, in-house) for 1h on ice. Cells were

centrifuged and resuspended in 50μL of permeabilization buffer with αIL-17A and αIFN-γ conjugated antibodies and normal rat serum (2%) (Table 2.1). Samples incubated with appropriate isotype controls were also included. Cells were incubated for 30 min on ice and were washed 2-3 times with perm buffer. Before flow cytometry analysis, cells were resuspended in PBS/0.1% BSA.

2.4 Bacterial culture

2.4.1 *C. rodentium* growth conditions

A nalidixic acid resistant strain of *Citrobacter rodentium* (ICC169, a kind gift from Professor Gad Frankel, Imperial College, UK)[228] was cultured at 37°C, over-night on Luria broth (LB) plates supplemented with nalidixic acid (Nal, 50 μg/mL, Sigma Aldrich). 1 colony was picked and grown in LB supplemented with Nal (50 μg/mL) at 37°C, 200rpm.

2.4.2 *Helicobacter hepaticus* growth conditions

H. hepaticus, NCI-Frederick isolate 1A[262] was grown on blood agar plates supplemented with trimethoprim, vancomycin and polymixin B (TVP, Oxoid) for two days at 37°C in a microaerophilic environment (10% H_2, 10% CO_2, balance N_2) as previously described.[267] Bacteria were harvested into tryptone soya broth (TSB) and cultures were stained with Live/Dead BacLight (Invitrogen). *H. hepaticus* cultures were deemed pure by morphology, as assessed at 100x magnification using fluorescence microscopy. Cultures were expanded in TSB broth supplemented with TVP and FCS (10%), grown at 37°C, 150rpm, in vented Erlenmeyer flasks at microaerophilic conditions.

2.4.3 *Helicobacter hepaticus* screening

Screening for *H. hepaticus* infection was performed before infection with *H. hepaticus* and αIL-10R treatment. Fresh fecal samples were collected and DNA extracted using the QIAamp DNA Stool Mini Kit (QIAGEN). Two PCR reactions were performed, one specific for *H. hepaticus*[283] and one for the *Helicobacter* genus.[284]

H. hepaticus : p25F 5'ATG GGT AAG AAA ATA GCA AAA AGA TTG CAA3' p25R 5'CTA TTT CAT ATC CAT AAG CTC TTG AGA ATC3' Amplicon: 705bp
Pan-*Helicobacter*: F 5' GCT ATG ACG GGT ATC C 3' R 5' GAT TTT ACC CCT ACA CCA 3' Amplicon: 422bp

2.5 Induction of intestinal inflammation

2.5.1 *Citrobacter rodentium* infection

C. rodentium was cultured as previously described. The over-night bacterial suspension was centrifuged at 7000rpm for 15min the following day and diluted 1/10 in PBS. Mice were inoculated with 200µL bacterial suspension by oral gavage (22G feeding needle, Popper and Sons). In order to quantify the given dose, the suspension was serially diluted, cultured on LB plates supplemented with Nal (50 µg/mL) at 37°C over-night and colony forming units (CFU) were enumerated. Mice were fed on average $5x10^9$ CFU of *C. rodentium*. At necropsy, sections of cecum and distal colon were collected for histological analysis.

2.5.2 Quantification of *C. rodentium* colonisation

Pieces of cecum and distal colon were rinsed in PBS/BSA 0.1% and kept in PBS on ice. Tissues were homogenised in PBS using homogeniser tubes (MP Biomedicals) and a homogeniser (FastPrep 24, MP Biomedicals) at 6.5m/s for 40s. Samples were serially diluted in PBS and cultured on LB plates supplemented with Nal (50 µg/mL) at 37°C overnight. CFUs were quantified, total numbers calculated and normalised to tissue weights. For quantification of CFU in spleen, the tissue was homogenised as described above and undiluted suspension plated and cultured on selective plates overnight. For fecal samples, fresh fecal pellets were collected into pre-weighed tubes. Samples were diluted in PBS to a final concentration of 100µg/µL, homogenised by vortexing and centrifuged at 1000rpm for 1 min. Supernatants were serially diluted and cultured as described above. Numbers were expressed as total CFU/g feces.

2.5.3 *Helicobacter hepaticus* infection

H. hepaticus was grown in liquid cultures as previously described. Cultures were centrifuged at 7000rpm for 15 min and pellets were resuspended at a concentration of 5OD/mL. Mice were gavaged with 200µL (1OD) per day on 3 consecutive days. For T-cell dependent *H. hepaticus* mediated IBD, mice were treated with blocking αIL-10R ab (1mg, i.p.) on day 0, in conjunction with the first bacterial inoculation, and then on day 7, day 14 and day 21.[259] At necropsy, sections of cecum and proximal-, mid- and distal colon were collected for histological analysis.

2.5.4 Quantification of *Helicobacter hepaticus* colonisation

At necropsy cecal contents were collected into 1 mL of ice-cold PBS and kept at -20°C. Cecal DNA was extracted using a commercial stool kit (QIAamp DNA Stool Mini Kit, QIAGEN) according to the manufacturer's instructions. For tissue samples, pieces of

cecal tissue were snap frozen at necropsy. Tissue DNA was isolated using the DNeasy Blood and Tissue Kit (QIAGEN). Levels of Hh DNA were quantified by q-PCR based on the *cdtB* gene, as described previously.[285] *H. hepaticus* genomic DNA was isolated using the DNeasy Blood and Tissue Kit and a standard curve of serially diluted amounts of *H. hepaticus* DNA was generated. 20ng of isolated cecal DNA or 100ng of isolated cecal tissue DNA, in a volume of 4µL, were added to each sample reaction mix for a final volume of 25µL. Colonisation levels were expressed as total *H. hepaticus* DNA/20ng of total cecal DNA. The following *H. hepaticus* specific primers were used, as previously published:

cdtB Forward: 5'CCG CAA ATT GCA GCA ATA CTT3'
cdtB Reverse: 5'TCG TCC AAA ATG CAC AGG TG3'
cdtB Probe: 5'AAT ATA CGC GCA CAC CTC TCA TCT GAC CAT3

2.5.5 T-cell transfer colitis

Naïve $CD4^+$ T-cells were purified as described in section 2.3.1 and 2.3.2. T-cell transfer colitis was induced by adoptive transfer of $4x10^5$ $CD4^+CD25^-CD45RB^{hi}$ T-cells into B6 *Rag1*$^{-/-}$ or B6 *Tlr5*$^{-/-}$*Rag1*$^{-/-}$ mice by i.p. injection. Mice were monitored weekly for weight loss, signs of colitis such as loose stool and their general appearance and behaviour. Experiments were terminated when mice displayed signs of colitis or developed severe weight loss (>20% loss of body weight from the start of the experiment). At necropsy, sections of cecum, proximal-, mid- and distal colon were collected for histological analysis.

2.5.6 Generation of bone marrow chimeric mice

Bone marrow was isolated from B6 or *Nlrc4*$^{-/-}$ mice by flushing the femur and tibia with PBS. 5x10^6 cells were injected intravenously into B6 or *Nlrc4*$^{-/-}$ recipients which had been lethally irradiated (2x 5.5 Gy, given 4h apart). Chimeric mice were allowed to reconstitute for at least 10 weeks.

Similarly, bone marrow was isolated from B6 *Rag1*$^{-/-}$ or B6 *Rag1*$^{-/-}$*Tlr5*$^{-/-}$ and 10x10^6 cells were injected intravenously into lethally irradiated (2x 5.5 Gy, given 4h apart) B6 *Rag1*$^{-/-}$ or B6 *Rag1*$^{-/-}$*Tlr5*$^{-/-}$ mice. Chimeric mice were left to reconstitute for 12 weeks.

2.6 Cytokine analysis

2.6.1 Cytokine detection in tissue explant supernatants

Pieces of cecum and distal colon were collected from mice infected with *C. rodentium*. Mid colon was collected from mice with T-cell transfer induced colitis. Tissues were cut open and washed in ice-cold PBS/0.1% BSA, weighed and cultured overnight in 400µL RPMI complete in 24 well plates at 37°C. Supernatants were collected, centrifuged at 1200rpm and the cleared supernatant stored at -20°C. Cytokines were measured with the Mouse Flowcytomix multiplex system (eBioscience) according to the manufacturer's instructions. Simplex kits were used for mouse IL-17A, IFN-γ, IL-22, TNF-α, IL-6 and IL-12p70. Samples were analysed using a FACSCalibur (BD Biosciences).

2.6.2 Detection of IL-1β, IL-α and IL-18

Tissue explants were cultured and supernatants collected as described in 2.6.1. IL-1β was quantified using a sandwich ELISA with matched coating and detection antibodies (14-7012-85 and 13-7112-85 respectively, both eBioscience). Recombinant IL-1β (211-11b, PeproTech) was used to construct a standard curve and TMB (eBioscience) was

used as substrate. The reaction was stopped with 2M H_2SO_4. IL-1α and IL-18 were quantified using Mouse IL-1α Ready-Set-Go ELISA (eBioscience) and Mouse IL-18 Platinum ELISA (eBioscience) respectively, according to protocols provided by the manufacturer.

2.7 Analysis of antibody responses

2.7.1 *C. rodentium* IgG ELISA

Heat-killed *C. rodentium* was prepared as described previously.[286] In brief, an overnight culture of *C. rodentium* was resuspended at 1 OD/mL in PBS with protease inhibitor (1 tablet/10mL Complete mini, Roche). The suspension was heated at 60°C for 1h and then frozen at -80°C. Nunc maxisorp plates (eBioscience) were coated with 50µL of bacterial suspension diluted 1/50 in PBS. Plates were incubated at 4°C overnight. After 3 washes in PBS/0.05%Tween20 (Sigma), plates were blocked with 150µL 5%BSA/PBS for 2h at room temperature. After discarding the blocking buffer, plates were incubated with serially diluted mouse sera. The initial dilution was 1/100 in PBS/0.05%Tween, 100µL per well in duplicate. Uninfected mice and sample free wells were included as controls. Plates were incubated with samples for 3h at room temperature. After 3 washes with PBS/0.05%Tween20, plates were incubated with 100µL of detection antibody (Table 2.1) in PBS/0.05%Tween for 1h at room temperature (Table 2.1). Plates were washed 4 times with PBS/0.05%Tween. 100µL of avidinD-HRP (Vector) diluted 1/1000 in PBS/0.05%Tween were added to each well. Plates were incubated for 1h at room temperature. Plates were washed 6 times with PBS/0.05%Tween. 100µL TMB substrate (eBioscience) was added per well and the reaction was stopped with 2M H_2SO_4 after approximately 3-5 min. Plates were read at 450nm (Molecular Devices).

2.7.2 *C. rodentium* secretory IgA ELISA

At necropsy the small intestine was removed and flushed with 6mL of PBS with EDTA (50mM) and protease inhibitor (1 tablet/ 7mL, Complete mini, Roche). The resulting small intestinal lavage was centrifuged at 3000rpm (~700g) for 10 min at 4°C and 3mL of cleared supernatant were collected from each individual mouse. 60µL of PMSF (100mM, Pierce) was added to each sample. Supernatants were centrifuged at 13000 rpm (~14000g) for 15 min at 4°C. 2 mL of clarified supernatant were collected from each sample. 20µL of PMSF (100mM), 100µL FCS and 20µL sodium azide (1%, in PBS) were added per sample, which was stored at -20°C. For *C. rodentium* specific sIgA ELISA, the same protocol described in 2.7.1 was used, with the following adjustments: Samples were loaded in duplicates, starting with neat samples and serial dilutions in PBS/0.05%Tween of 1/3 and 1/9. Instead of incubating plates with a biotinylated Goat-α-mouse IgG detection antibody, a HRP-conjugated Goat-α-mouse IgA antibody was used (Table 2.1).

2.7.3 Preparation of soluble *Helicobacter hepaticus* antigen (sHelAg)

Soluble *Helicobacter hepaticus* antigen (sHelAg) was prepared, according to a previously published protocol.[262] *H. hepaticus* was grown in liquid culture. Up to 500mL of liquid culture was harvested and the bacterial pellet washed twice in PBS. The pellet was resuspended in PBS with EDTA (2mM) at a concentration of 5OD/mL. The suspension was subjected to 5 freeze thaw cycles, with mixing by vortexing in between each cycle. The suspension was then sonicated for 7 pulses of 30s at 10µm. In between pulses samples were kept on ice. Sonicates were then centrifuged at 13000 rpm at 4°C for 10 min and resuspended in PBS. After sterile filtration through a 22µm filter, protein concentrations in samples were measured by the Bradford assay. Samples were kept at -80°C.

2.7.4 *H. hepaticus* specific IgG and sIgA ELISA

Nunc maxisorp plates were coated with 50µL of sHelAg at 10µg/mL in 0.1M carbonate buffer (0.1M Na_2CO_3, 0.1M $NaHCO_3$, pH9.5). Plates were incubated at 4°C overnight and then washed 3 times with PBS/0.05%Tween. Plates were blocked with 200µL of 5%BSA/PBS for 2h at room temperature. Serum samples and small intestinal lavage fluids were assayed in duplicate. The initial dilution was 1/300 for serum and non-diluted for small intestinal lavage, with sequential 1/3 dilutions. Plates were incubated with samples for 3h at room temperature Plates were then washed, incubated with detection antibody (Table 2.1) and avidinD-HRP or HRP conjugated detection antibody according to the same protocol as 2.7.1. After incubation with avidinD-HRP plates were washed 6 times and incubated with ABTS substrate (2,29-azinobis(3-ethylbenzthiazolinesulfonicacid) Sigma). A colour reaction developed after 5-10 min, the reaction was stopped with 2M H_2SO_4 and plates were read at 405nm.

2.8 Analysis of mRNA expression by qPCR

2.8.1 RNA extraction from tissues and cell isolates

Tissues were snap-frozen at necropsy and stored at -80°C. For RNA isolation, tissues were homogenised in 600µL RLT (QIAGEN) with 2-mercaptoethanol, using homogeniser tubes (MP Biomedicals) and a FastPrep 24 homogeniser (MP Biomedicals) at 6.5m/s for 40s. Lysates were centrifuged at 13000rpm for 3min. Supernatants were mixed with ethanol (70%) and loaded onto a RNeasy mini column (QIAGEN). RNA was isolated according to the manufacturer's instructions, including a DNase digest. RNA was eluted in water and amounts were quantified using a NanoDrop (Thermo Scientific). RNA was stored at -80°C. Cell isolates were resuspended in RLT with 2-mercaptoethanol and stored at -80°C. RNA isolation was

performed using the same protocol as for tissues. cDNA was synthesized through reverse transcription, using SuperscriptIII (Invitrogen).

2.8.2 Quantitative PCR (qPCR)

Quantitative PCR analysis was performed using the Taqman and SYBRGreen systems (Table 2.4). 4µL of cDNA were used for a final reaction volume of 20µL. Samples were assayed in triplicates, primers were when possible designed to span introns and a non-reverse transcribed sample was run as a control. For Taqman assays 300nmol of unlabelled primers and 100nmol of labelled probe (FAM/TAMRA or VIC/TAMRA) were used. SYBRgreen assays and Taqman assays were performed according to the manufacturer's instructions and detected using a Chromo4 detection system (MJ Research). Gene expression was normalised to HPRT expression and gene expression levels were calculated using the 2^Δ-Ct method.[287]

Taqman assays (ABI Life technologies)	
Hprt1	N/A
Reg3g	N/A
Reg3b	N/A
S100a8	N/A
S100a9	N/A
Ptprc	N/A
Villin1	N/A
Itgae	N/A
Retnla	N/A
Ear1/2	N/A
Taqman assays (published)	
Hprt1	F: 5'GAC CGG TCC CGT CAT GC 3' R: 5'TCA AAC CTG GTT CAT CAT CGC 3' P: 5' ACC CGC AGT CCC AGC GTC GTC 3'
Il23a	F: 5'AGC GGG ACA TAT GAA TCT ACT AAG AGA 3'

	R: 5'GTC CTA GTA GGG AGG TGT GAA GTT G 3' P: 5'GCC AGT TCT GCT TGC AAA GGA TCC GC 3'	
Ifng	F: 5'GGA TGC ATT CAT GAG TAT TGC 3' R: 5' GCT TCC TGA GGC TGG ATT C 3' P: 5' TTT GAG GTC AAC AAC CCA CAG GTC CA 3'	
Il17a	F: 5'GCT CCA GAA GGC CT CAG 3' R: 5' CTT TCC CTC CGC ATT GAC A 3' P: 5' GAC CTC AAC CGT TCC ACG TCA CCC TG 3'	
SYBRgreen assays		
Hprt1	N/A	QIAGEN
Nlrc4	F: 5' CGG CCT GCA ACC TCT TTC TT 3'	In-house
	R: 5' TGG GCC AAA ACA TTC AGG TCT 3'	In-house

Table 2.4 qPCR primers and assays

2.9 Western blot

2.9.1 Sample preparation

Tissue samples were snap-frozen at necropsy and kept at -80°C. Samples were homogenised in ice-cold RIPA buffer (50mM Tris HCL pH 8, 150mM NaCl, 1% Igepal, 0.5% sodium deoxycholate, 0,1% SDS) as described in 2.5.2. Homogenates were centrifuged at 13000rpm, 4°C, for 5 min. Protein concentrations were determined in supernatants by the BCA protein assay kit (Thermo scientific) according to manufacturer's instructions. Sample concentrations were normalised and sample buffer (0.25% bromophenol blue, 0.25% Xylen Cyanol Ff, 30% glycerol, β-mercaptoethanol) was added. Samples were boiled at 95°C for 10 min and stored at -80°C.

2.9.2 Western blot

Samples were loaded on a 15% SDS-PAGE gel and transferred onto a PVDF membrane, which had been pre-activated in methanol. Membranes were fixed in PFA (0.5% PFA in PBS) for 20 min and blocked (5% milk, PBS 0.5% Tween-20) for 45 min at room temperature. Membranes were then incubated with primary antibody (0.1µg/mL, rabbit α-mouse caspase-1 p10, M-20, Santa Cruz) at 4°C overnight. After thorough washing (PBS 0.5% Tween-20) membranes were incubated with peroxidase conjugated secondary antibody (1/7000, goat α-rabbit IgG HRP linked, 7074, Cell Signaling) for 1h at room temperature. After extensive washing samples were incubated with SuperSignal West Femto (Thermo Scientific) according to the manufacturers's instructions. Membranes were developed using medical X-ray film (Fuji) and a XOGraph (XOGraph healthcare). Membranes were incubated in stripping buffer (0.2M glycine, 1% SDS, 10% Tween-20, β-mercaptoethanol) for 10 min. After repeating this step once, membranes were washed twice in PBS for 10 min and twice in PBS/0.5% Tween-20 for 5 min. Membranes were then blocked as described above and incubated with loading control antibody (1/2000, rabbit α-mouse α-tubulin, Cell Signaling) at 4°C overnight. Membranes were washed and incubated with secondary antibody as described above. Finally, membranes were developed with ECL Western blotting substrate (Thermo Scientific).

2.10 *In vivo* treatment

2.10.1 Treatment with recombinant IL-18

Mice were injected i.p. with 0.5µg recombinant Mouse IL-18 (Carrier-free, B005-5, MBL International Corporation) one time per day. The treatment was started 2 days

prior to infection and continued for 6 days following infection. Mice received a total of 9 injections.

2.10.2 Treatment with antibiotics

A cocktail of antibiotics consisting of vancomycin (Acros Organics), neomycin (Sigma), metronidazole (Acros Organics), gentamycin (Fisher Scientific) and ampicillin (Sigma) was prepared.[277] A dose of 50mg/kg of vancomycin and 100mg/kg of the remaining compounds was used.[288] A standard dose for a mouse of 22g was used. Mice of at least 8 weeks of age were orally gavaged with 200µL of freshly prepared antibiotic mixture twice daily for 10 days. Fecal samples were collected prior to and during the treatment and DNA extracted as described in 2.4.3. DNA levels were normalised and SYBRgreen PCR for eubacterial 16s rRNA (Eub338F 5' ACT CCT ACG GGA GGC AGC AG 3', Eub338F 5'ATT ACC GCG GCT GCT GG 3')[289] was performed.

2.11 Isolation of tissue subsets

2.11.1 Isolation of intestinal crypts

Intestinal crypts were isolated following a published procedure, with some alterations.[290] Cecal and colonic tissues were collected, cut open longitudinally and divided into 5mm pieces. The tissues were washed with ice-cold PBS several times using a pipettor. Tissues were then incubated in PBS with EDTA (25mM) and kept with at 4°C, with gentle agitation, for 1 hour. Tissues were washed as before and supernatants were collected. The collected fractions were enriched for intestinal crypts, which was confirmed by examination under an inverted microscope (Leitz labovert, Leica Microsystems). Crypts were resuspended in RLT buffer (QIAGEN) and stored at -20°C. Purity was tested by quantifying mRNA levels of *Villin1* and *Ptprc*.

2.11.2 Isolation of intestinal stromal cells

Intestinal stromal cells were isolated from the 30/40% Percoll interface during LPL isolation, as described in 2.3.3. Isolates were cultured in R10 media (RPMI 1640, 10% FCS, HEPES 10mM, penicillin, streptomycin and amphotericin B). Cells were cultured for > 14 days and were passaged several times until a homogenous fibroblast-like cell population remained.

2.12 Immunohistochemistry (IHC)

For immunohistochemistry 5µm paraffin tissue sections were deparaffinised and rehydrated with xylene and ethanol. Sections were immersed in citrate buffer (10mM, pH6) and boiled using a pressure cooker for antigen retrieval and blocked in BSA (5%) and normal goat serum (10%) in a moist chamber at room temperature for 1h. Sections were then stained with primary antibodies (Table 2.1) in PBS with BSA (5%) and normal goat serum (5%) at 4°C overnight. After 2 washes in PBS, sections were stained with secondary antibodies (Table 2.1) in PBS with BSA (5%) and normal goat serum (5%) for 1h at room temperature. Samples were washed and mounted with Vectashield mounting media, containing DAPI (Vector laboratories). An Inverted Olympus FV1000 Confocal system (Olympus) was used to view the staining.

2.13 Microarray analysis

Cecal tissue was collected into RNAlater (Ambion) and kept at 4°C. RNA was isolated using the RiboPure kit (Ambion). The following procedures and analyses were performed by Dr Dilair Baban, The Wellcome Trust Centre for Human Genetics, University of Oxford. RNA quantity and quality were measured using a NanoDrop ND1000 and BioAnalyzer 2100 (Agilent Technologies) respectively. Samples were hybridized with the Illumina Single Colour Mouse WG-6_V2_0_R0_11278593

BeadChip with direct hybridization assay (Illumina) and biotinylated cRNA was prepared by using the Illumina TotalPrep-96 RNA Amplification Kit (Ambion). Following streptavidin-Cy3 staining the iScan system was used to analyse fluorescent emission. Data was generated using the GenomStudio 2011 software (Illumina) and analysed using GeneSpring GX 12 (Agilent).

2.14 Generation of an *IcmF*-deficient *Helicobacter hepaticus* deletion mutant

2.14.1 Cloning

The *H. hepaticus* HH0252 gene, encoding the IcmF protein, was replaced with a chloramphenicol resistance cassette by homologous recombination. Primers amplifying the 609bp sequence upstream of HH0252, were designed containing Xba1, Mfe1 and Xho1 restriction enzyme sites (Table 2.5). The 760bp sequence downstream of HH0252, including the stop codon, was amplified with primers containing Mfe1 and Kpn1 restriction sites. The amplification reaction mix contained genomic *H. hepaticus* DNA (10ng), dNTP (200µM, Sigma), primers (0.5µM of each) and Finnzyme Phusion DNA polymerase (0.5U, Thermo Scientific) in Hf buffer. The PCR amplification conditions were 2 min at 98°C, 35 cycles of 10s at 98°C, 30s at 47°C and 1min at 72°C followed by a final extension step of 10 min at 72°C. PCR products were separated by gel electrophoresis and purified using the QiaQuick gel extraction kit (QIAGEN). First the upstream segment was digested with Xba1 and Xho1, ligated into a pBluescriptSK+ vector, transferred into NovaBlue cells (EMD Millipore) and single colonies grown overnight on agarose plates supplemented with ampicillin (100µg/mL). Plasmids were isolated with QiaPrep Spin Miniprep kit (QIAGEN). Then the downstream region was digested with Mfe1 and Kpn1 and ligated into the

pBluescriptSK+ vector containing the upstream region. The plasmid was transferred into NovaBlue cells, cultured for single colonies overnight and plasmids were isolated. Finally the plasmid was digested with EcoR1, which targets the Mfe1 restriction site, and a chloramphenicol resistance cassette was inserted between the upstream and downstream regions. The chloramphenicol cassette was obtained from the pMOD-2Cm plasmid, which had been digested with EcoR1.[291] The final construct was propagated in *E. coli* 1793 (New England Biolabs). Constructs were sequenced after each sequential step.

2.14.2 Electroporation of *Helicobacter hepaticus*

40 mL of *H. hepaticus* liquid culture was harvested by centrifugation at 7000 rpm, at 4°C for 15min. The pellet was washed twice in ice-cold wash buffer (15%w/v glycerol, 7% w/v sucrose, sterile- filtered). The pellet was resuspended in 1mL of wash buffer and centrifuged at 13000rpm, 5min, at 4°C. The resulting pellet was resuspended in 160µL ice-cold wash buffer and 40µL of suspension and 2µL of plasmid (1.6µg) were transferred into prechilled electroporation cuvettes and electroporated at 12.5 kV/cm in an *E. coli* pulser (Bio-Rad). The cuvette was immediately placed on ice and 160µL SOC medium (New England Biolabs) was added. The suspension was plated onto blood agar plates supplemented with TVP (as in section 2.4.2) and cultured at 37°C in microaerophilic conditions. After 2 days, the bacterial lawn was harvested and transferred onto blood agar plates containing chloramphenicol (50µg/mL) and were cultured for an additional 7 days. Round, bacterial aggregates were harvested into tryptone soya broth (50µL) and plated for single colonies on selective blood agar plates. After approximately 7 days of culture, colonies were picked and cultured for single colonies. This was repeated 3 times in order to obtain pure cultures. The resulting clones were expanded, genomic DNA extracted and assayed by PCR to investigate if

the correct replacement had occurred. Primers C1 and C2, which anneal to regions outside of the deleted region, were used (Table 2.4). Finally, C1 and C2 primers were used to amplify the deleted area. The PCR product was gel purified and sequenced, using C1, C2, USF seq, USR seq, DSF seq, DSR seq, CatF and CatR primers (Table 4.2). Primers labelled seq annealed to regions outside of the cloned area but within the amplified segment. The HH0252 gene was further confirmed to be deleted in Hh0252 mutant *H. hepaticus* using HH0252 specific primers.

Primer	Sequence 5'-3'
USF	GACGAC**TCTAGA**CTATCGGAAGCAATCTCAATGC
USR	GATGAT **CTCGAGCAATTG**GCCAAATTACATTTCCTTAATC
DSF	GATGAT**CAATTG**CACTCAACAATAAGGAACGC
DSR	GATGAT**GGTACC**GGTATTATGCAGGATAGAATC
C1	CAG GCA TAC TTG ATG ATA GC
C2	GCT AAT AAG GGC TAG TAT GAG
USF seq	GGA AGC AAT CTC AAT GCT TTG C
USR seq	CTC ATG TGG AGA TAC CTT GAA G
DSF seq	GAA CGC AAA TGG AGC AAA TAG C
DSR seq	CTT GTG TGT CAA GTA TGT GCT C
CatF	CGT GAT ATA GAT TGA AAA GTG G
CatR	AAC AGA TCT GCA GGA CGC
Hh0252Fw	CAT ATA CTC GCC CTT ATT TGC
Hh0252Rv	GGC TTA AAT GTA AAA GTT CTA GC

Table 2.4 Primers used for *H. hepaticus* cloning. Restriction enzyme sites are indicated in bold.

2.15 Statistical analysis

Statistical analysis was performed using Prism (GraphPad software, La Jolla CA USA). The nonparametric Mann–Whitney test was used for all statistical comparisons except weight curves, which were analysed using Two-Way ANOVA. Differences were considered statistically significant at a *p*-value of less than 0.05.

Chapter 3: Role of the cytosolic sensor NLRC4 in acute bacterially triggered intestinal inflammation

3.1 Introduction

The intestinal tract is colonised by vast numbers of bacteria, many of which are flagellated.[292, 293] Flagellin is an immunodominant antigen in the gut[127] and a known agonist for NOD-like receptor 4, NLRC4.[176, 177] Sensing of flagellin by NLRC4 results in inflammasome activation and the generation of active caspase-1 and subsequent cleavage and production of mature Il-1β and IL-18.[294] In order for the NLRC4 inflammasome to assemble, flagellin needs to be translocated into the cytosol.[176, 177] This is associated with the presence of bacterial Type 3 or Type 4 secretion systems (T3SS or T4SS), a feature of many pathogenic bacteria. Although flagellin is the most well characterised agonist, NLRC4 is also known to detect components of the bacterial T3SS, which share some structural homology with flagellin.[178]

The impact of NLRC4 in mucosal inflammation and immunity has been investigated in several recent studies. A murine model of infection of the lung with the bacterial pathogen *Burkholderia pseudomallei* revealed protective effects of NLRC4.[295] NLRC4 expression provided a limiting effect on systemic dissemination of the bacterium and promoted survival, in part by preventing excessive recruitment of neutrophils to the tissue.[295] In the intestine, NLRC4 was described in one study to limit tumour development in a model of colitis-associated colon carcinogenesis induced by administration of DSS and the carcinogen AOM.[296] However, another study in which a slightly different protocol was used found that NLRC4 expression did not confer protection from colon tumours.[297] In bacterial infection NLRC4 was shown to be dispensable in the sensing of the intracellular, enteric pathogen *S. typhimurium*, whereas

mice deficient in both NLRC4 and NLRP3 displayed increased susceptibility, suggesting redundant roles for different NLR in host protective inflammasome activation.[143] Conversely, an independent study reported increased susceptibility of NLRC4-deficient mice to *Salmonella* infection, possibly reflecting differences in infection protocols.[190] Thus, the precise roles of NLRC4 in protection and inflammation in the gut is still under debate.

We aimed to characterise the role of NLRC4 in the development of acute intestinal inflammation in the gut mucosa. For this purpose, we used bacterially driven models based on infection with *Citrobacter rodentium*. This bacterium colonises the large intestine of mice and although it adheres to the intestinal epithelium, it remains extracellular.[228] *C. rodentium* is a non-motile enteric pathogen that expresses a T3SS, which is required for *in vivo* virulence.[230] We hypothesised that the *C. rodentium* T3SS might provide an agonist for NLRC4 and that this could implicate a role for direct sensing of *C. rodentium* by NLRC4. However, we did not exclude potentially activating effects of the commensal microflora and luminal flagellin. The use of the *C. rodentium* model of intestinal inflammation would allow for analysis of the contribution of the NLRC4 inflammasome to host responses during acute infection and inflammation in the gut mucosa.

3.2 Results

3.2.1 NLRC4 deficiency results in elevated systemic immune responses to infection with the enteric pathogen *Citrobacter rodentium*

Innate immune signalling has been shown to be required for protection against *C. rodentium*,[239, 240] but a comprehensive study of the contribution of the NLRC4 inflammasome to immune responses during infection with an extracellular, enteric pathogen had not been performed. In order to investigate the role of NLRC4 in this context wild type C57BL/6 (WT) and *Nlrc4*$^{-/-}$ mice were infected with *C. rodentium*. Susceptibility to *C. rodentium* can be affected by the intestinal microbiota[298] and NLRP6 inflammasome deficient animals have recently been reported to harbour altered intestinal flora that could confer susceptibility to DSS colitis.[162] In order to correct for any potential differences in intestinal microbiota, we co-housed WT and *Nlrc4*$^{-/-}$ mice for several weeks before infecting with *C. rodentium*. In addition, WT and *Nlrc4*$^{-/-}$ mice that had been housed separately were infected, resulting in identical responses to those of co-housed mice. Results shown are pooled from experiments of both protocols.

Following *C. rodentium* infection, WT mice developed diarrhoea from approximately day 6 p.i., but did not lose any weight (Fig.3.1 A). *Nlrc4*$^{-/-}$ mice also developed diarrhoea but suffered significant weight loss during the infection, starting approximately 8 days p.i. and persisting until around d14 p.i. (Fig.3.1A). However, *Nlrc4*$^{-/-}$ animals eventually recovered the lost weight by around three weeks p.i. and all mice survived the infection.

C. rodentium clearance is dependent on IgG responses.[299] In order to gauge the humoral response, sera and small intestinal lavage fluid were collected from WT and *Nlrc4*$^{-/-}$ animals that had been infected for 3 weeks. Although WT and *Nlrc4*$^{-/-}$ mice developed strong *C. rodentium*-specific serum IgG responses, *Nlrc4*$^{-/-}$ animals exhibited significantly increased titres, indicating elevated adaptive immune responses (Fig.3.1B). However, levels of intestinal IgA directed at *C. rodentium* were equivalent in WT and *Nlrc4*$^{-/-}$ animals (Fig.3.1C), suggesting that the increased response was limited to the systemic immune axis. Consistent with this hypothesis, *Nlrc4*$^{-/-}$ animals also exhibited potent systemic immune activation, revealed as both significantly increased splenomegaly (Fig.3.1D) and spleen granulocyte numbers (Fig. 3.1E).

Figure 3.1

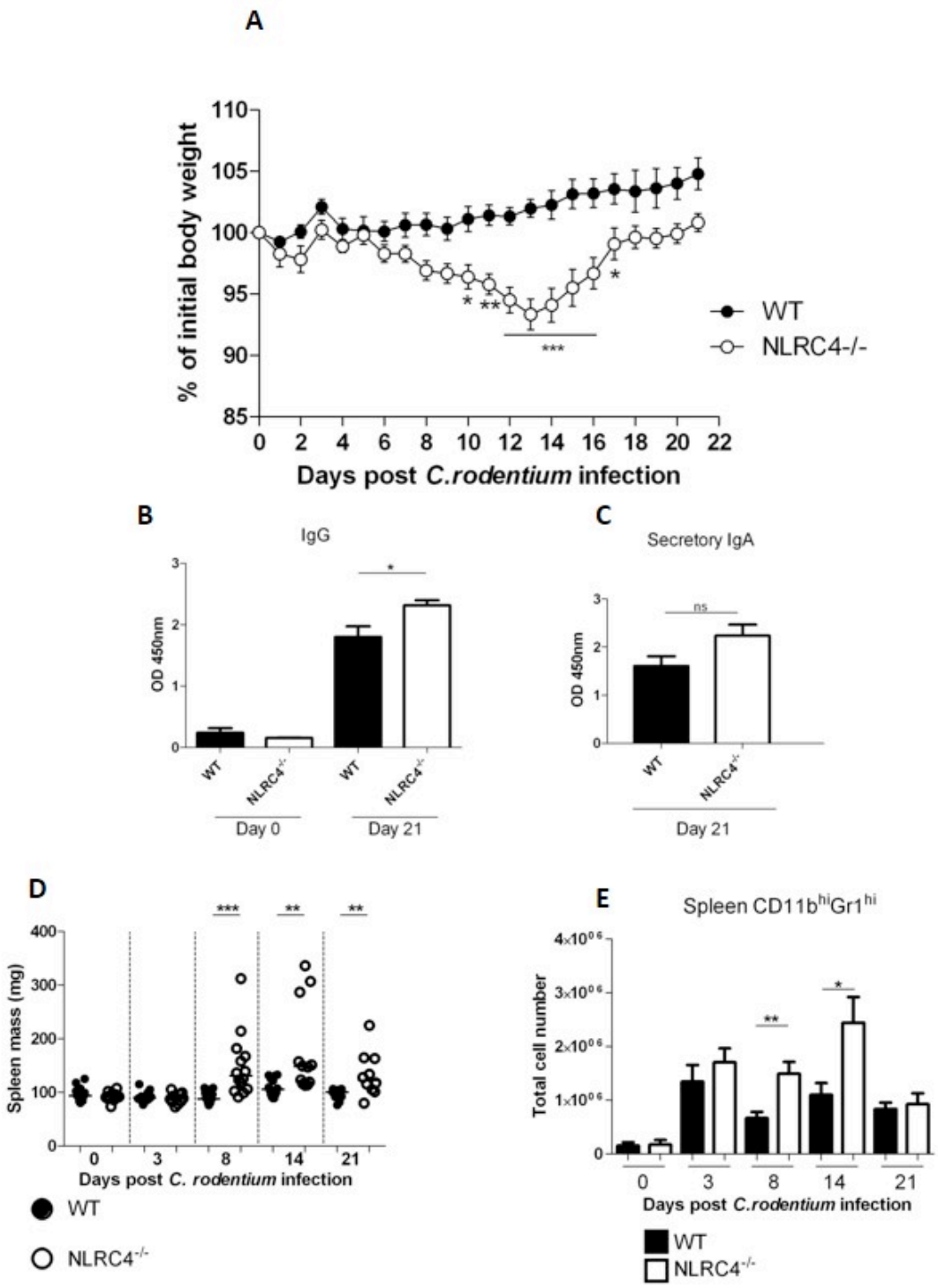

A
% of initial body weight
Days post C.rodentium infection
WT
NLRC4-/-
B
IgG
OD 450nm
Day 0
Day 21
C
Secretory IgA
ns
D
Spleen mass (mg)
Days post C. rodentium infection
E
Spleen CD11b^hiGr1^hi
Total cell number
Days post C.rodentium infection

Figure 3.1 Systemic immune responses are elevated in *Nlrc4*$^{-/-}$ mice during infection with the enteric pathogen *Citrobacter rodentium*.

WT and *Nlrc4*$^{-/-}$ mice were orally inoculated with enteropathogenic *C. rodentium*. (A) Representative weight curves of WT and *Nlrc4*$^{-/-}$ mice during 3 weeks of infection, shown as a percentage of the initial weight ± SEM at Day 0. Data are pooled from 2 independent experiments and represent n=10 per genotype. Two-way ANOVA was used for statistical analysis, *P<0.05,**P<0.01, ***P<0.001. (B) *C. rodentium* specific total IgG was measured in sera from mice that had been infected for 3 weeks. Bar graphs represent pooled data from 2 independent experiments (n=10 per genotype infected and n=6 per genotype uninfected, ±SEM). (C) *C. rodentium* specific IgA responses in small intestinal lavage fluid. Data are pooled from 2 independent experiments, n=10 per genotype ±SEM. For data in (A), (B) and (C) data were pooled from 2 independent experiments, in which animals were infected for 21 days. (D and E) Spleen mass (D) and spleen granulocyte numbers (E) were quantified. Data were pooled from 2 independent experiments for d3 and d21, and 3 independent experiments for d8 and d14 (uninfected n=11-12 for (D), n=5-6 (E), infected n=10-14 for (D) and (E)). Horizontal lines represent group medians. The non-parametric Mann-Whitney test was used for statistical analysis. * P<0.05, ** P<0.01 , ***P<0.001.

3.2.2 NLRC4 deficiency results in the development of severe intestinal pathology during infection with *C. rodentium*

Consistent with published findings,[249] we observed that WT mice developed transient intestinal inflammation during *C. rodentium* infection, as evidenced by mild inflammation of the cecum and moderate colitis on day 8 and day 14 p.i. (Fig.3.2A-C).

Increased weight loss in susceptible mice during *C. rodentium* infection is linked to aggravated intestinal pathology.[300] Evaluation of histological changes in *Nlrc4*$^{-/-}$ mice revealed severe intestinal inflammation in the large intestine. Cecal pathology, characterised by hyperplasia, cellular infiltration and edema, was significantly exacerbated in *Nlrc4*$^{-/-}$ mice on both day 8 and day 14 p.i. (Fig.3.2A,C). Similarly, *Nlrc4*$^{-/-}$ mice also displayed significantly increased pathology in the distal colon, at these time points (Fig.3.2B,C).

C. rodentium infection induces hyper-proliferation of epithelial cells in the colon.[239] In order to evaluate IEC turnover during infection, cecal sections were stained for Ki67, a marker of cell proliferation. In WT mice, proliferating Ki67^{+} IEC were restricted to the basal region of the crypts, regardless of *C. rodentium* infection status (Fig.3.2.D). In contrast, *C. rodentium*-infected *Nlrc4*$^{-/-}$ mice displayed significantly increased IEC proliferation and the proliferative zone was extended along the entire length of the crypt (Fig.3.2D), correlating with the observed inflammation-induced hyperplasia.

Figure 3.2

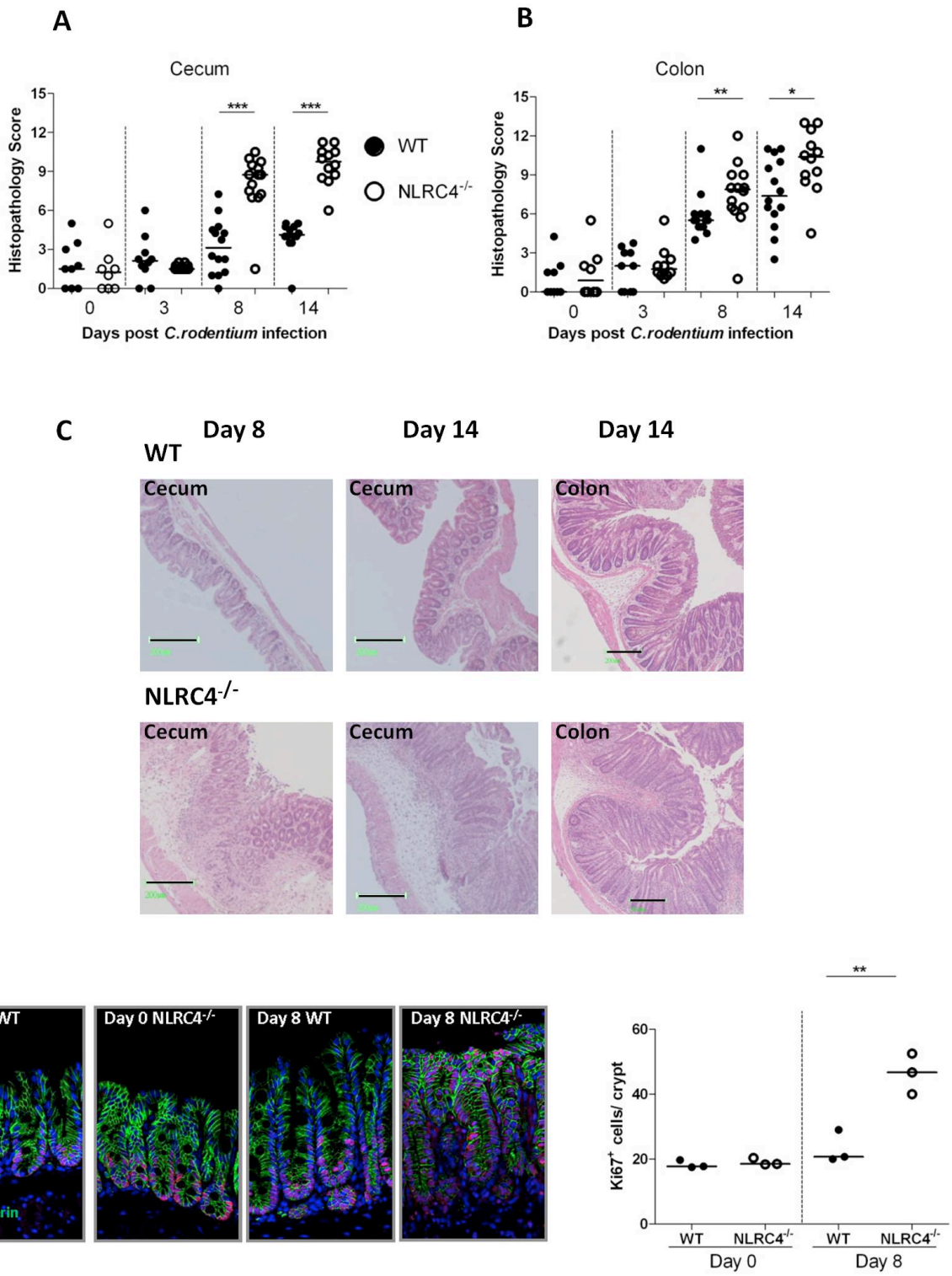

A
Cecum
Histopathology Score
Days post C.rodentium infection
WT
NLRC4-/-
***
***
B
Colon
**
*
C
Day 8
Day 14
Day 14
WT
Cecum
Cecum
Colon
NLRC4-/-
Cecum
Cecum
Colon
D
Day 0 WT
Day 0 NLRC4-/-
Day 8 WT
Day 8 NLRC4-/-
Ki67
E-Cadherin
DAPI
Ki67+ cells/ crypt
WT
NLRC4-/-
WT
NLRC4-/-
Day 0
Day 8

Figure 3.2 NLRC4 deficiency results in the development of severe intestinal pathology during infection with the enteric pathogen *Citrobacter rodentium*.

WT and *Nlrc4*$^{-/-}$ mice were orally inoculated with *C. rodentium*. Pathology was assessed in the cecum (A) and in the distal colon (B) after 0, 3, 8 and 14 days of infection. (C) Representative micrographs of cecum and distal colon. Black bars correspond to 200µm. (D) Representative images of cecal sections stained for Ki67 to evaluate epithelial cell proliferation (magnification 20x) and co-stained for E-cadherin and 4',6-diamidino-2-phenylindole (DAPI). Cells positive for Ki67 were enumerated in on average 20 crypts per section to generate an average score for each animal. Each symbol represents a single animal and for (A) and (B) data were pooled from 4 independent experiments (uninfected n = 8-9, infected n=12-14). Horizontal lines represent group medians. All statistical analysis was performed using the non-parametric Mann-Whitney test, *P<0.05, **P<0.01, ***P<0.001.

3.2.3 NLRC4 limits bacterial colonisation of the intestinal mucosa

C. rodentium has been shown to colonise the large intestine in sequential manner, with early colonisation of the cecum and subsequent infection of the distal colon.[232] Previous work had linked increased colonisation levels with exacerbated pathology[301, 302] and we therefore assessed levels of tissue-adherent *C. rodentium*. We found that, relative to WT mice, *Nlrc4*$^{-/-}$ mice harboured significantly elevated loads of tissue-adherent *C. rodentium* in the cecum at day 3 and day 8 p.i. (Fig.3.3A). However, by day 14 and day 21 p.i., colonisation levels had been reduced similarly in both WT and *Nlrc4*$^{-/-}$ mice, indicating that *Nlrc4*$^{-/-}$ mice did not have a defect in eradicating the bacterium (Fig.3.3A). By contrast, peak colonisation of the distal colon was observed at day 8 p.i. and, although *Nlrc4*$^{-/-}$ mice exhibited a trend towards higher bacterial burdens at this time point, by day 14 p.i. levels were reduced to a similar level in WT and *Nlrc4*$^{-/-}$ mice, confirming that bacterial clearance had been initiated (Fig.3.3B). Despite exhibiting more severe intestinal inflammation and harbouring higher cecal bacterial burdens, only a minority of *Nlrc4*$^{-/-}$ mice (~10% of total number of infected animals) had detectable systemic translocation of *C. rodentium* to the spleen, which was equivalent to what was observed in WT animals (Fig.3.3C). These results indicated that NLRC4 limited early cecal colonisation by *C. rodentium*, suggesting that it primarily participates in innate defense of the epithelium during the initial stages of infection.

Figure 3.3

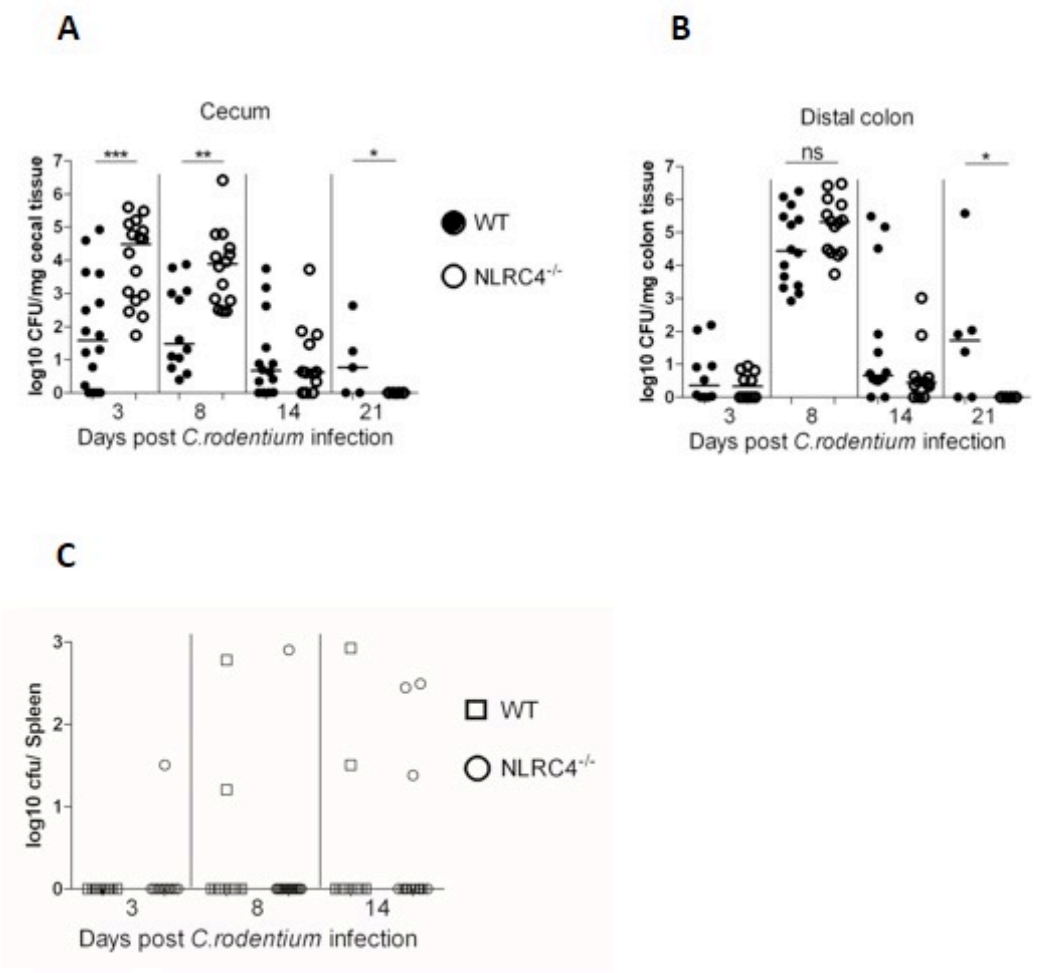


Figure 3.3 NL RC4 deficiency results in elevated bacterial colonisation levels.

WT and *Nlrc4*$^{-/-}$ mice were orally inoculated with *C. rodentium*. (A) Cecal tissue was collected 3, 8 and 14 days post infection, homogenized and cultured on selective media. CFU were determined and normalized to tissue weight. (B) Distal colon tissue was obtained after 3, 8 and 14 days of infection, homogenized and cultured on selective media. CFU were determined and normalized to tissue weight. (C) Spleens were collected at necropsy after 3, 8 and 14 days of infection, homogenized and plated on selective media. CFU were enumerated. Data are pooled from 3 independent experiments (n= 12 – 16 animals per group) for D3, D8 and D14, and from 1 experiment (n=5-6) for D21 in (A) and from at least 2 independent experiments (n=10-16) for D3, D8 and D14, and from 1 experiment (n=5-6) for D21 in (B) and (C). Each symbol represents an individual animal and horizontal bars represent median values. The non-parametric Mann-Whitney test was used for statistical analysis. *P<0.05, **P<0.01, ***P<0.001.

3.2.4 NLRC4 deficiency results in exaggerated cytokine responses following *C. rodentium* infection

Effector $CD4^+$ T-cells and cytokines, including IL-17A and IFN-γ, are known to be induced and to contribute to protection during *C. rodentium* infection.[87, 237, 244] In order to assess cytokine production, intestinal tissue explants were cultured overnight and levels of IFN-γ and IL-17A were assayed in culture supernatants. There were no baseline differences in IL-17A or IFN- γ between WT and *Nlrc4*$^{-/-}$ mice, but on day 8 and day 14 p.i. *Nlrc4*$^{-/-}$ animals had significantly increased levels of both IFN-γ and IL-17A in the cecum (Fig.3.4A). In contrast, a preliminary assessment of cytokine production in the distal colon showed that *C. rodentium* infection resulted in equivalent induction of IFN-γ and IL-17A in both WT and *Nlrc4*$^{-/-}$ mice (Fig.3.4 B).

Figure 3.4

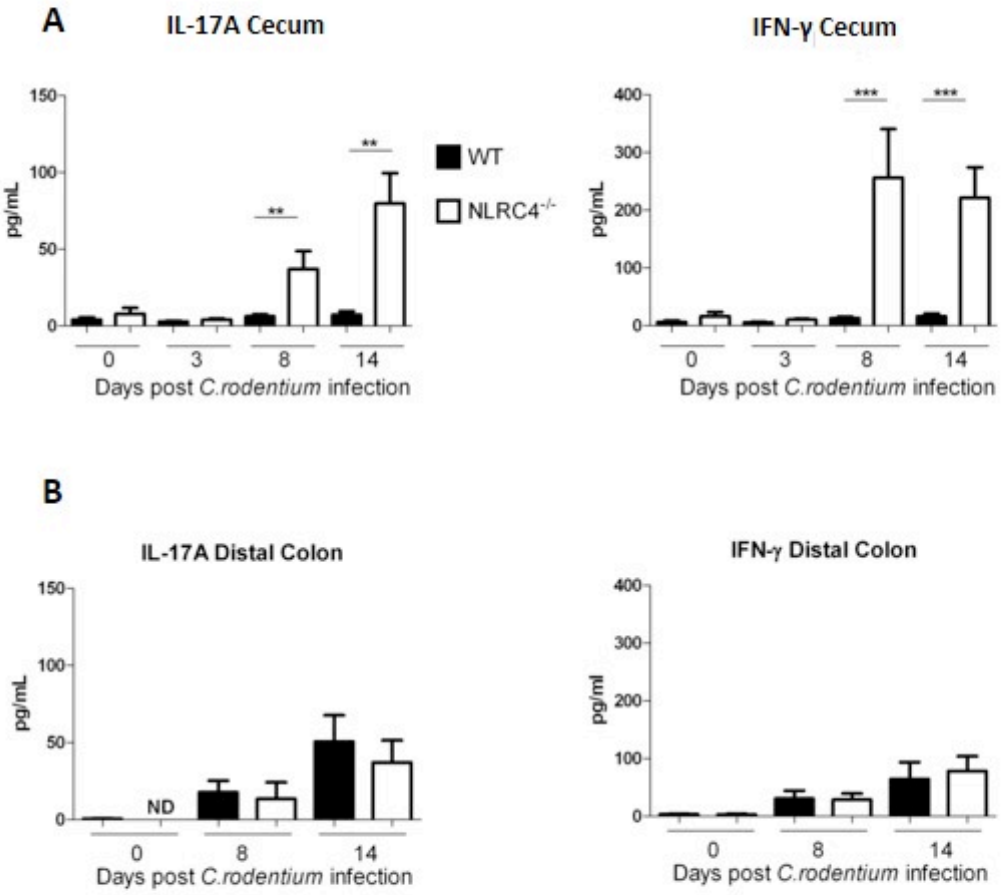


Figure 3.4 NLRC4 deficiency results in increased cytokine responses.

WT and *Nlrc4*$^{-/-}$ mice were orally inoculated with *C. rodentium* and tissue collected at 0, 3, 8 and 14 days p.i. As controls uninfected animals were used. Tissue explants were cultured overnight and supernatants harvested and assayed for Th1 and Th17 cytokines by a bead based assay and flow cytometry. Levels were normalised to tissue weights. (A and B) IFN-γ and IL-17A production derived from cecal explants (A) and distal colon explants (B). Bar graphs display data pooled from 2 independent experiments for the cecum (n=7-8/group mean ±SEM) and 1 single experiment for the distal colon (n= 3 for infected, n=2 for controls, mean ±SEM). Statistical analysis was performed using the non-parametric Mann-Whitney test, **P<0.01, ***P<0.001, ND = not detected.

In order to further characterise $CD4^+$ T cell responses during infection, we isolated LPL from the intestine and performed intracellular stains for IL-17A and IFN-γ. We observed significantly increased $CD4^+$ T-cell frequencies in the cecal lamina propria in *Nlrc4*$^{-/-}$ mice at day 14 p.i. compared with WT mice (Fig.3.5A). In WT mice *C. rodentium* infection did not lead to increased frequencies of Th1 cells, but there was a trend of increased Th17 cells and significantly increased IL-$17A^+$IFN-γ^+ cells (double producers) during infection (Fig.3.5B,C,D). In contrast, infection of *Nlrc4*$^{-/-}$ mice resulted in significantly increased proportions of Th1 cells compared with WT mice, at 8 and 14 days p.i. (Fig.3.5B). Similarly to WT mice there was a trend of increased Th17 cells and IL-$17A^+$IFN-γ^+ cells in *Nlrc4*$^{-/-}$ mice after infection (Fig.3.5B,C,D), but we could not detect any differences in frequencies of Th17 or double producers between WT and *Nlrc4*$^{-/-}$ mice (Fig.3.5C,D). Representative FACS plots of Th1 and Th17 responses among cecal LPL isolated from WT and *Nlrc4*$^{-/-}$ mice are shown for day 8 and day 14 p.i. (Fig. 3.5E,F).

We also assessed Th1 and Th17 responses in LPL isolated from the colon, which is an overtly inflamed site in WT mice during infection. In the colon, there was recruitment of $CD4^+$T-cells to the lamina propria after 14 days of *C. rodentium* infection in WT animals (Fig.3.6A), although the increase was not statistically significant. The limited sample number for uninfected mice prevented a similar analysis of *Nlrc4*$^{-/-}$ mice. Contrary to what was observed in the cecum, in WT mice there was a small trend of Th1 induction cells by day 14 p.i. (Fig.3.6B, F). Similarly, *Nlrc4*$^{-/-}$ animals displayed a trend of increased Th1 frequencies during infection, although the induction was not significantly greater than WT mice. (Fig.3.6B). There was a significant increase in Th17 cells at day 8 p.i., although the proportions of IL-$17A^+$ and IL-$17A^+$ IFN- γ^+ cells were reduced in *Nlrc4*$^{-/-}$ mice compared with WT mice at 14 days p.i. (Fig.3.6C,D).

This could correspond to a more robust shift from a Th17 dominated response at day 8 p.i. to a Th1 steered response at day 14 p.i. in the NLRC4-deficient animals (Fig.3.6 D, F). Th1 and Th17 cells are gated as $TCR\beta^{+}CD4^{+}IFN\text{-}\gamma^{+}IL\text{-}17A^{-}$ and $TCR\beta^{+}CD4^{+}IFN^{-}\gamma^{-}IL\text{-}17A^{+}$ respectively (Fig.3.6.G).

Figure 3.5

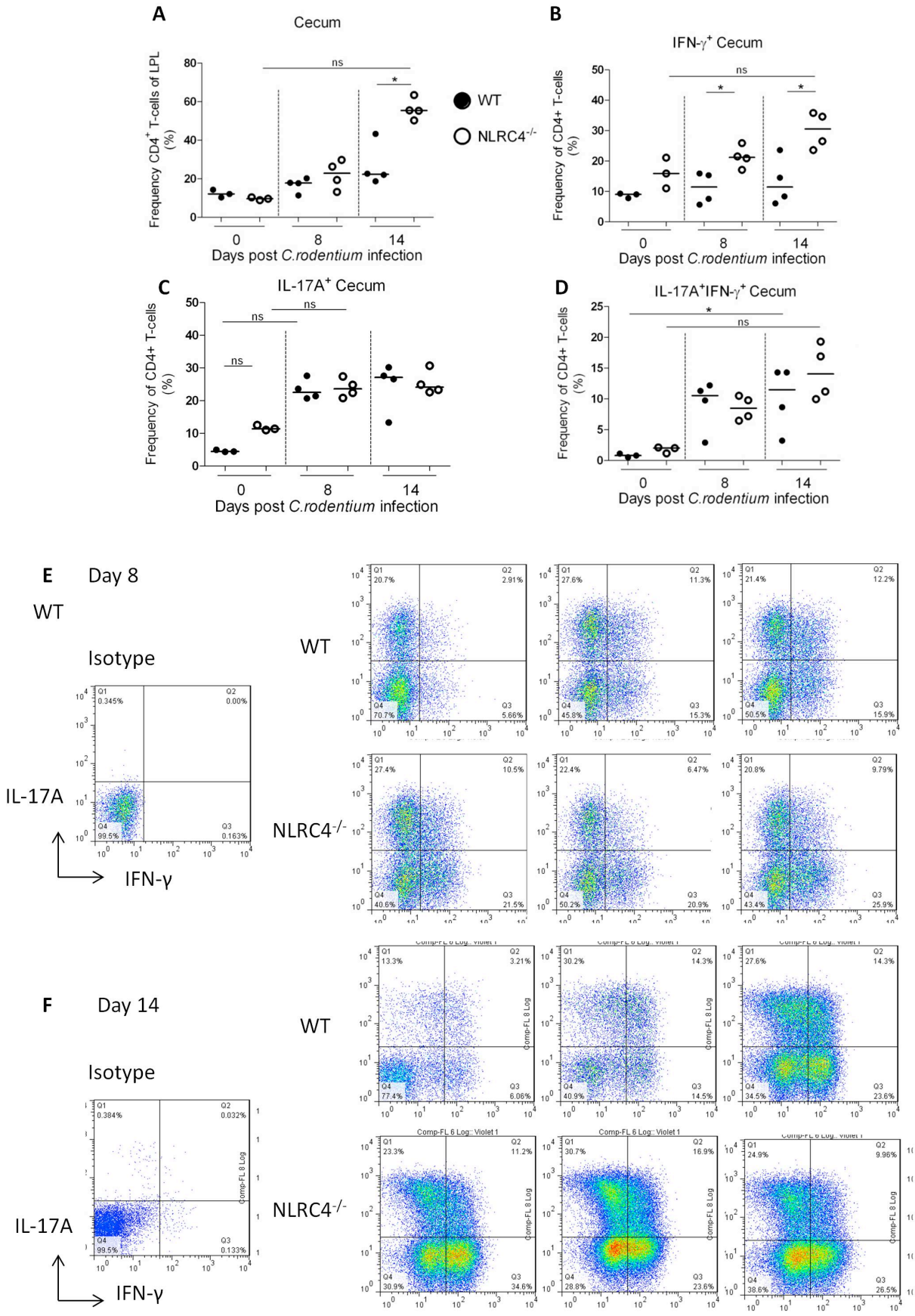

A
Cecum
Frequency CD4+ T-cells of LPL (%)
Days post C.rodentium infection
WT
NLRC4-/-
B
IFN-γ+ Cecum
Frequency of CD4+ T-cells (%)
C
IL-17A+ Cecum
D
IL-17A+IFN-γ+ Cecum
ns
E Day 8
WT
Isotype
IL-17A
IFN-γ
NLRC4-/-
F Day 14

Figure 3.5 continued

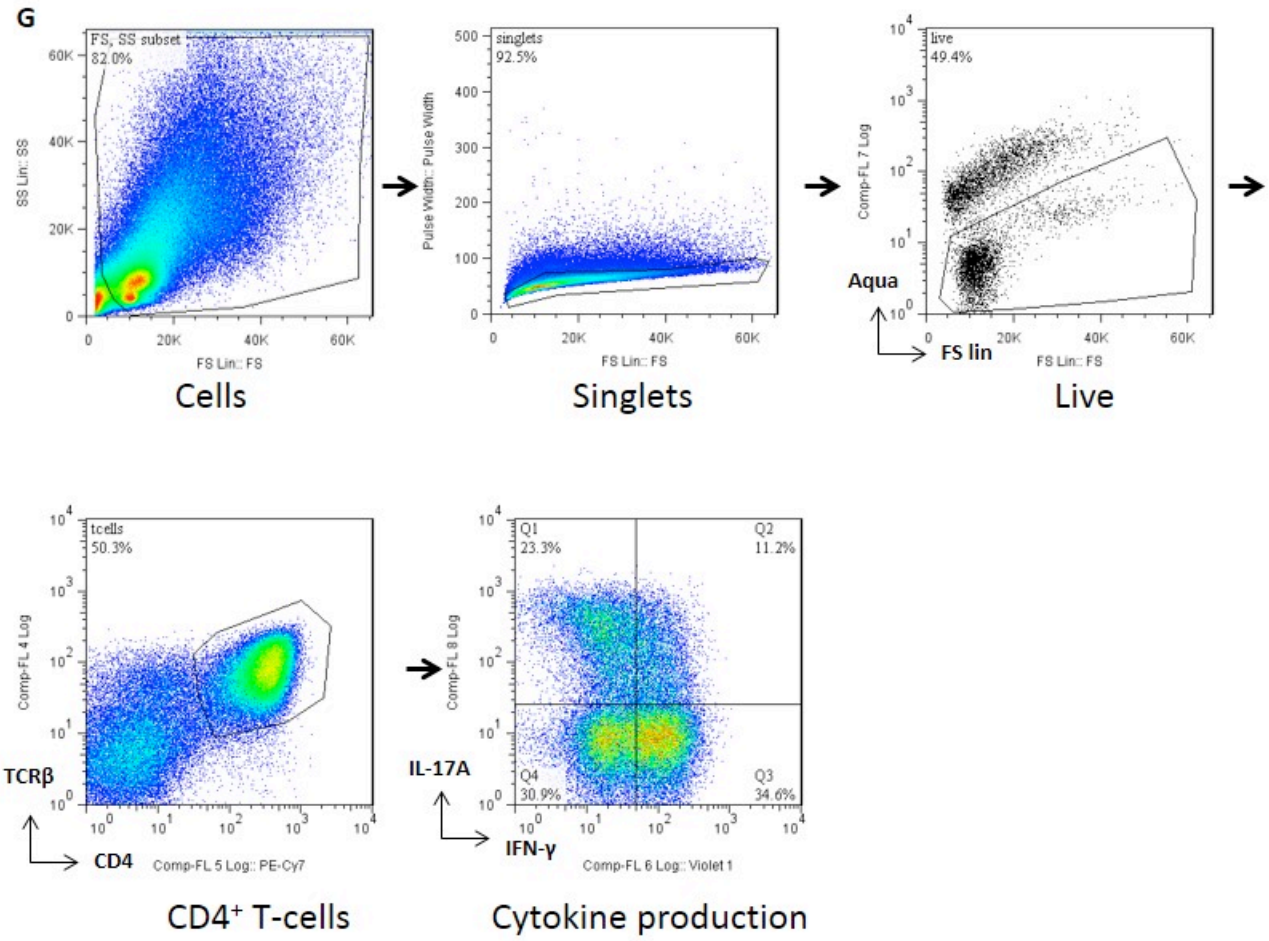


Figure 3.5 NLRC4 deficiency results in increased Th1 responses in the cecum during *C. rodentium* infection.

LPL were isolated from the cecum of WT and *Nlrc4*$^{-/-}$ mice that were either uninfected (Day 0) or had been infected with *C. rodentium* for 8 or 14 days. LPL were restimulated with PMA (0.1µg/ml), ionomycin (1µg/ml) and Brefeldin A (10µg/ml) for 3h. LPL were surfaced stained for CD4 and TCRβ. Cells were permeabilized and stained for intracellular cytokines IL-17A and IFN-γ. Non-specific labelled IgG isotype were used as controls for cytokine antibodies. (A) CD4^{+} T-lymphocyte frequencies in cecal lamina propria. (B-D) Frequencies of IFN-γ^{+} CD4^{+}T-cells (B), IL-17A^{+} CD4^{+}T-cells (C) and IL-17A^{+}IFN-γ^{+} CD4^{+}T-cells (D). Representative FACS plots are shown for Day 8 p.i. (E) and Day 14 p.i. (F). Full gating strategy is shown in (G). Cell clusters were excluded from analysis by assessment of pulse width, live cells were determined by the use of Live/Dead Aqua dead stain, which labels dead cells, and CD4^{+} T-cells were identified by positive CD4 and TCRβ staining. Displayed data are from 1 experiment, each symbol represents an individual animal (n=3-4/group) and horizontal bars denote group median values. For statistical analysis the non-parametric Mann-Whitney test was employed, *P<0.05.

Figure 3.6

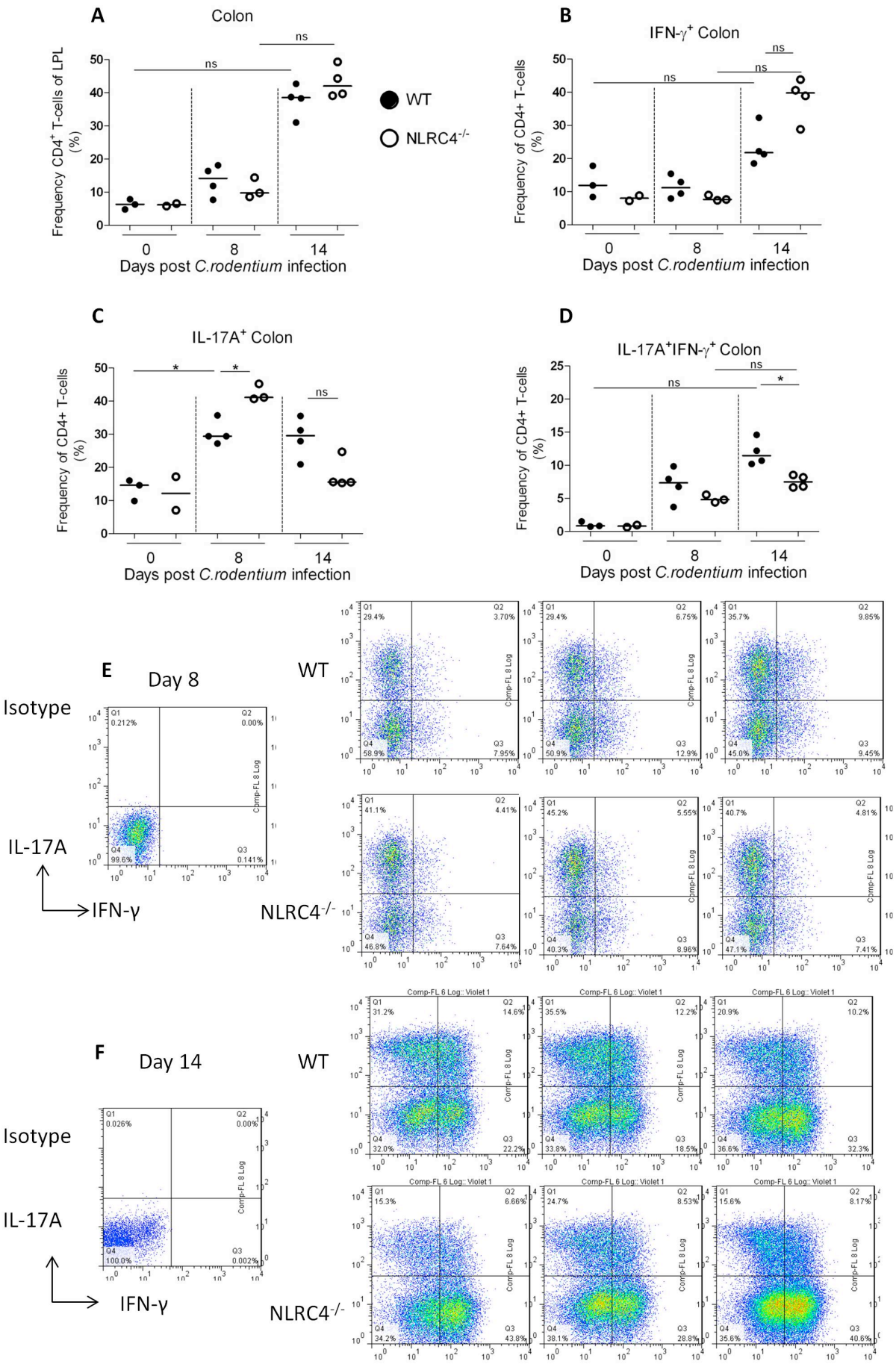

A
Colon
Frequency CD4+ T-cells of LPL (%)
Days post C.rodentium infection
WT
NLRC4-/-
ns
B
IFN-γ+ Colon
Frequency of CD4+ T-cells (%)
C
IL-17A+ Colon
D
IL-17A+IFN-γ+ Colon
E
Day 8
WT
Isotype
IL-17A
IFN-γ
NLRC4-/-
F
Day 14

Figure 3.6 Th1 and Th17 responses are induced in the colon in both WT and *Nlrc4*$^{-/-}$ mice during *C.rodentium* infection.

LPL were isolated from whole colon of WT and *Nlrc4*$^{-/-}$ mice that were either uninfected (Day 0) or had been infected with *C. rodentium* for 8 or 14 days. LPL were restimulated with PMA (0.1µg/ml), ionomycin (1µg/ml) and Brefeldin A (10µg/ml) for 3h. LPL were surfaced stained for CD4 and TCRβ. Cells were permeabilized and stained for intracellular cytokines IL-17A and IFN-γ. Non-specific labelled IgG isotype were used as controls for cytokine antibodies. Isotype controls were included for confirming specificity. (A) $CD4^+$T-cell frequencies in the whole colon. (B-D) Frequencies of IFN-γ^+ $CD4^+$T-lymphocytes (B), IL-$17A^+$ $CD4^+$T-lymphocytes (C) and double-producing IL-$17A^+$IFN-γ^+ $CD4^+$T-lymphocytes (D). Representative FACS stains are shown for Day 8 p.i. (E) and Day 14 p.i. (F). Results are from 1 experiment, n=3-4/group and horizontal bars represent group median values. The non-parametrical Mann-Whitney test was used for statistical analysis, *$P<0.05$.

3.2.5 NLRC4 deficiency primarily affects the innate immune axis

During *Listeria monocytogenes* infection robust inflammasome activation and killing of the bacteria resulted in reduced adaptive immune responses.[303, 304] We hypothesised that the excessive adaptive immune responses observed in *Nlrc4*$^{-/-}$ mice following *C. rodentium* infection might correspond to an initial defect in innate immunity. In order to investigate the role of NLRC4 in innate immunity to *C. rodentium,* T and B cell-deficient *Rag1*$^{-/-}$ or *Nlrc4*$^{-/-}$*Rag1*$^{-/-}$ mice were infected. *Nlrc4*$^{-/-}$*Rag1*$^{-/-}$ mice developed significantly exacerbated cecal inflammation at day 8 p.i compared with NLRC4-sufficient *Rag1*$^{-/-}$ mice (Fig.3.7A,C). However, the colitis was equivalent in both groups (Fig.3.7B) and the overall intestinal inflammatory response in *Rag1*$^{-/-}$ mice was less severe than in lymphocyte sufficient animals. Furthermore, although *Rag1*$^{-/-}$ or *Nlrc4*$^{-/-}$ *Rag1*$^{-/-}$ animals did not display any weight loss during the 8 day infection period (Fig.3.7D), *Nlrc4*$^{-/-}$*Rag1*$^{-/-}$mice developed marked splenomegaly compared with *Rag1*$^{-/-}$ mice, although this difference did not reach statistical significance (Fig.3.7E). Measurement of cytokines in cecal explant culture supernatants from infected mice revealed significantly increased IFN-γ production in *Nlrc4*$^{-/-}$*Rag1*$^{-/-}$ mice (Fig.3.7F), while IL-17A levels were negligible (data not shown), suggesting that both innate and adaptive sources may contribute to the exacerbated IFN-γ response observed in *Nlrc4*$^{-/-}$ animals .

The colonisation levels in cecum and distal colon were similarly high in both *Rag1*$^{-/-}$ and *Nlrc4*$^{-/-}$*Rag1*$^{-/-}$ mice (Fig.3.8A,B). In addition, the majority (80%) of both *Rag1*$^{-/-}$ and *Nlrc4*$^{-/-}$*Rag1*$^{-/-}$ mice displayed bacterial translocation to the spleen (Fig.3.8C), consistent with previous reports that *Rag1*$^{-/-}$ mice harbour increased *C. rodentium* burdens and are unable to clear the infection.[236] Taken together, these results suggest that NLRC4-deficiency primarily impacts on innate immune responses to *C. rodentium*.

Figure 3.7

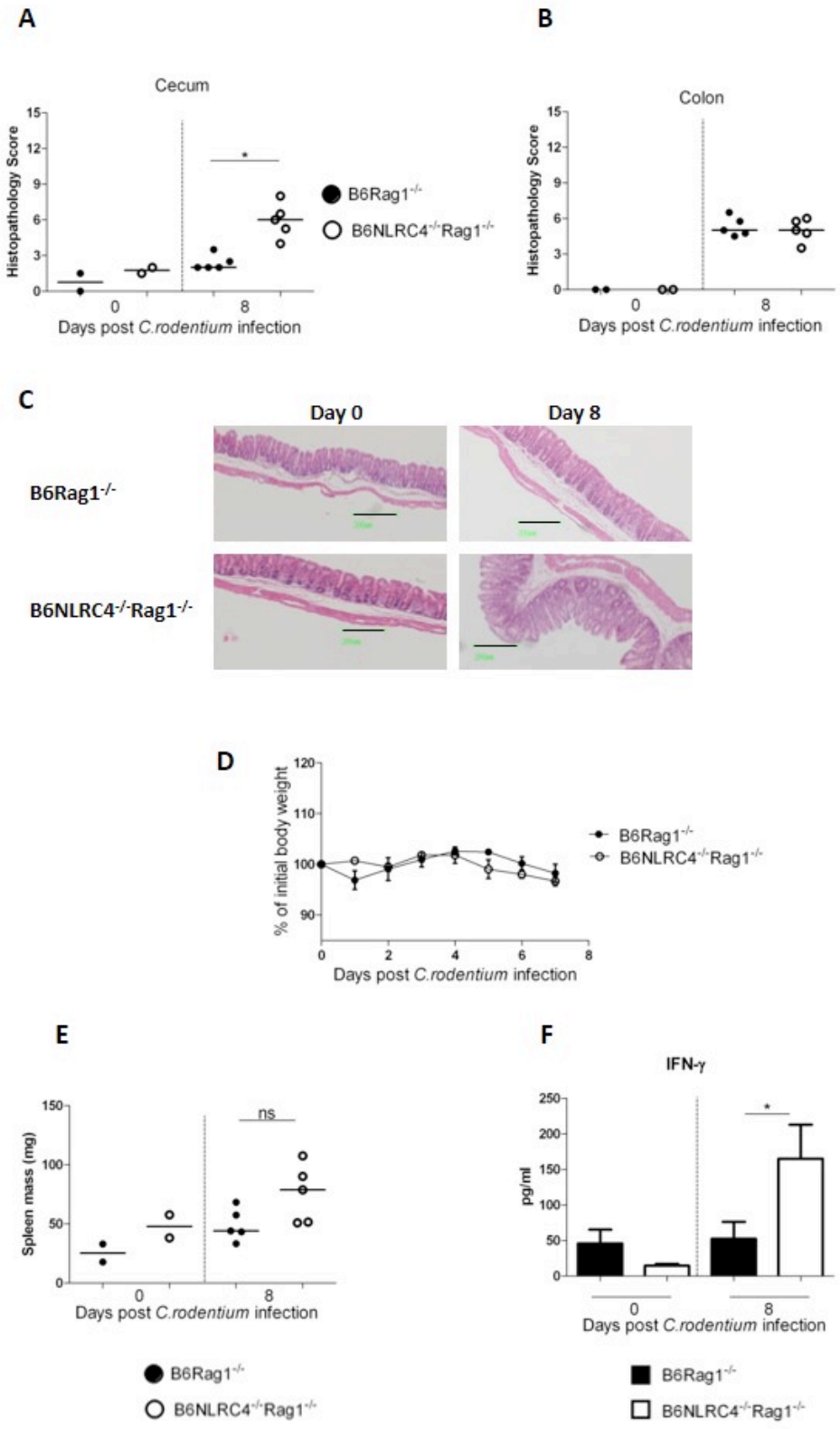

A
Cecum
Histopathology Score
15
12
9
6
3
0
*
0
8
Days post C.rodentium infection
B6Rag1-/-
B6NLRC4-/-Rag1-/-
B
Colon
Histopathology Score
15
12
9
6
3
0
0
8
Days post C.rodentium infection
C
Day 0
Day 8
B6Rag1-/-
B6NLRC4-/-Rag1-/-
D
% of initial body weight
120
110
100
90
0
2
4
6
8
Days post C.rodentium infection
B6Rag1-/-
B6NLRC4-/-Rag1-/-
E
Spleen mass (mg)
150
100
50
0
ns
0
8
Days post C.rodentium infection
B6Rag1-/-
B6NLRC4-/-Rag1-/-
F
IFN-γ
pg/ml
250
200
150
100
50
0
*
0
8
Days post C.rodentium infection
B6Rag1-/-
B6NLRC4-/-Rag1-/-

Figure 3.7 NLRC4 limits innate inflammatory responses to *C. rodentium*. *Rag1*$^{-/-}$ and *Nlrc4*$^{-/-}$*Rag1*$^{-/-}$ mice were infected with *C. rodentium* for 8 days. (A) Typhlitis scores and (B) Pathology in distal colon. (C) Representative histopathology images of cecum. Black bars are equivalent to 200μm. (D) Weight curves of infected mice; values are displayed as a percentage of the original weight mean ± SEM. (E) Spleen weights. For A, B, D and E each symbol represents an individual mouse (n=5 per group) and horizontal bars denote group medians. (F) Cecal explants were cultured overnight and IFN-γ production was assessed in supernatants and normalised to tissue weights. Bar graphs represent mean values with SEM (n=5 per group for infected mice and n=2 per group for uninfected controls). Data are from 1 experiment and were analysed statistically by using the non-parametric Mann-Whitney test, *P<0.05.

Figure 3.8

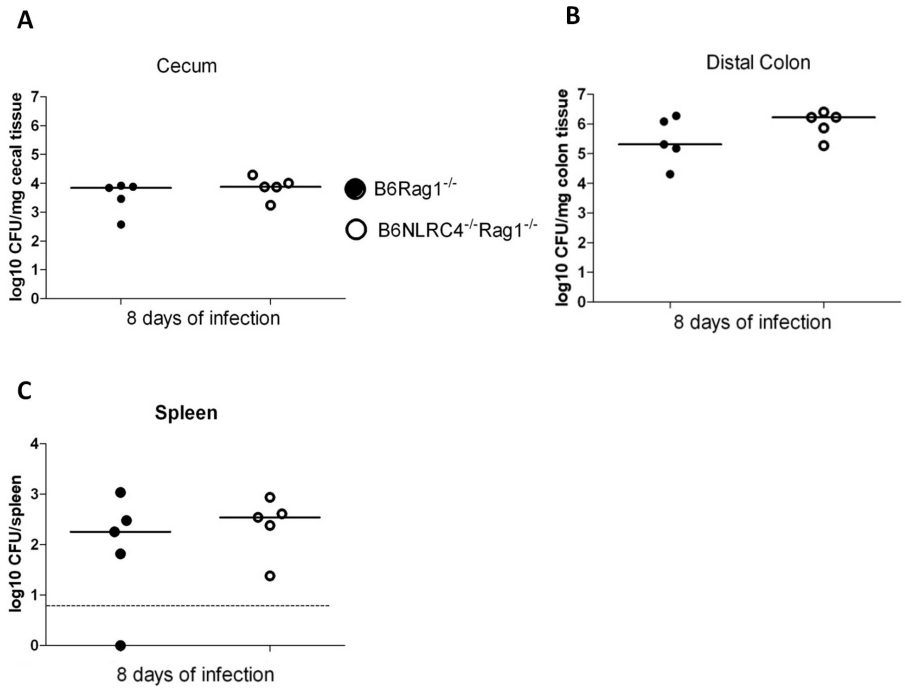


Figure 3.8 Similar intestinal and systemic *C. rodentium* burdens in *Rag1*$^{-/-}$ and *Nlrc4*$^{-/-}$ *Rag1*$^{-/-}$ mice.

C. rodentium colonisation levels were assessed in *Rag1*$^{-/-}$ and *Nlrc4*$^{-/-}$ *Rag1*$^{-/-}$ animals that had been infected for 8 days. (A) Colonisation levels in cecal tissue. (B) Bacterial burden in distal colon tissue. (C) Systemic translocation of *C. rodentium* to the spleen. Dashed line indicates the detection limit. Data are from 1 experiment (n=5 per group).

3.2.6 NLRC4 deficiency does not impair protective innate IL-22/AMP responses.

The cytokine IL-22 has recently been shown to mediate critical, early protective responses to *C. rodentium* infection.[60] Early IL-22 is mainly produced by innate lymphoid cells (ILC) and promotes anti-bacterial responses, including the production of antimicrobial peptides (AMPs) Reg3γ, Reg3β, and s100A9 and s100A8.[59, 60, 305] To investigate whether this protective IL-22/AMP axis was compromised in *Nlrc4*$^{-/-}$ mice, we assayed levels of IL-22 and mRNA expression of AMPs in cecal tissue at various time points during *C. rodentium* infection. We found that, compared to WT mice, *Nlrc4*$^{-/-}$ mice produced similar or increased amounts of IL-22, both during steady state and throughout *C. rodentium* infection (Fig.3.9A). Similarly, Q-PCR analyses of AMP expression in cecal tissue showed that *Nlrc4*$^{-/-}$ and WT mice expressed similar levels of AMPs in steady state, and that AMP expression was significantly increased in *Nlrc4*$^{-/-}$ mice at day 8 and day 14 p.i. (Fig.3.9B). Together, these results indicate that *Nlrc4*$^{-/-}$ mice do not have any defect in baseline or *C. rodentium*-induced IL-22 and AMP expression.

Figure 3.9

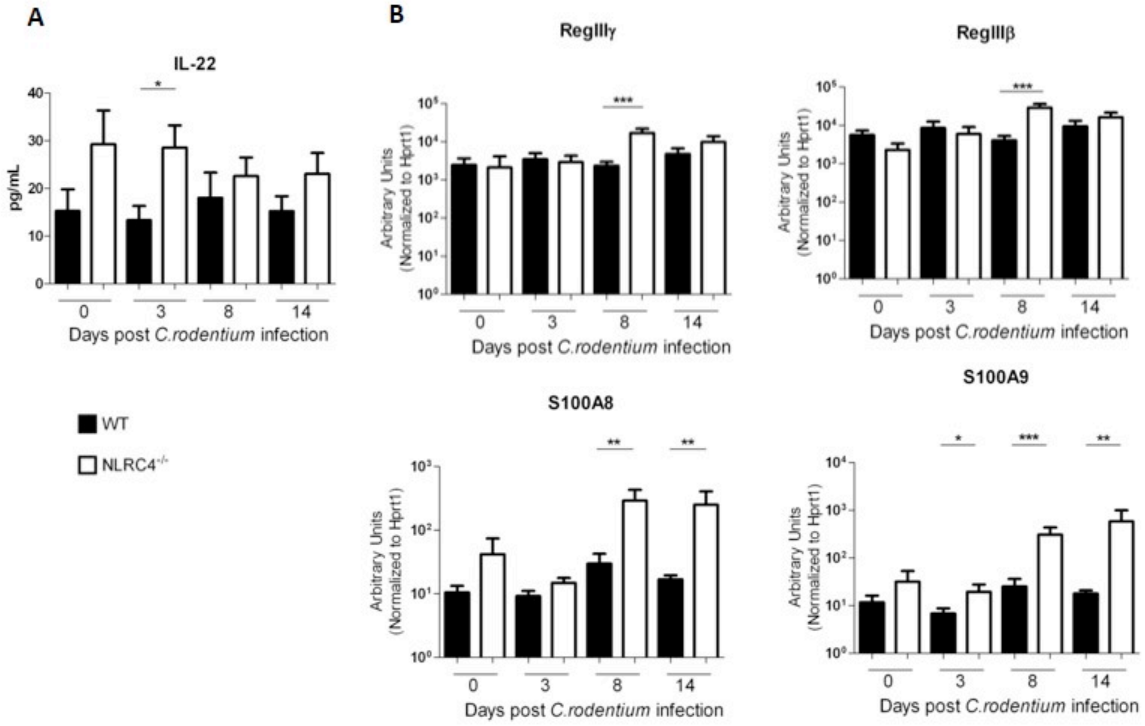


Figure 3.9 NLRC4 deficiency does not result in reduced IL-22 or AMP production during *C. rodentium* infection.

Cohorts of WT and *Nlrc4*$^{-/-}$ mice were infected with *C. rodentium* for 3, 8 and 14 days. (A) Cecal explants were cultured overnight and culture supernatants were assayed for IL-22 by a bead based assay and flow cytometry. Bar graphs represent group means ±SEM (pooled data from 2 independent experiments, n=7-8 per group). (B) Cecal tissues from uninfected and infected animals were snap-frozen at necropsy and RNA extracted. qPCR analyses for RegIIIγ, RegIIIβ, s100A8 and s100A9 were performed and normalised to Hprt1. Data represent group means ±SEM, pooled from 3 independent experiments for RegIIIγ (n=13-16 per group for d0 and d3) and 2 independent experiments for the remaining time points and AMPs (n=7-10 per group). Statistical analysis was performed using the non-parametric Mann-Whitney test, *P<0.05, **P<0.01, ***P<0.001

3.2.7 NLRC4 deficiency is not associated with reduced IL-1 levels or impaired neutrophil recruitment during *C. rodentium* infection

IL-1R signalling is essential for surviving *C. rodentium* infection and for preventing severe intestinal damage.[241] We therefore assayed supernatants from organ explants of cecum and distal colon of *C. rodentium*-infected WT and *Nlrc4*$^{-/-}$ mice for the IL-1R ligands IL-1β and IL-1α. We found that while IL-1β levels in the cecum did not fluctuate during infection (Fig.3.10A), there was significant induction of IL-1β in the distal colon during the later stage of infection (Fig.3.10B). However, intestinal levels of IL-1β were similar in WT and *Nlrc4*$^{-/-}$ mice throughout the infection, in both cecum and colon. In addition, levels of IL-1α in the cecum explant supernatants of *C. rodentium*-infected mice remained very low and were equivalent WT and *Nlrc4*$^{-/-}$ mice during the first 8 days of infection, with *Nlrc4*$^{-/-}$ mice releasing significantly more IL-1α 14 days p.i. (Fig.3.10C).

NLRC4 deficiency has been associated with reduced neutrophil recruitment during infection with mucosal pathogens.[306, 307] Furthermore, we have previously shown that blockade of IL-1β resulted in reduced granulocyte recruitment to the colon during innate intestinal inflammation, and neutrophils are linked with protective effects during *C. rodentium* infection.[200, 308] However, LPL isolation from intestinal tissue from *C. rodentium*-infected WT and *Nlrc4*$^{-/-}$ mice, revealed that neutrophil recruitment was significantly enhanced in the cecum of *Nlrc4*$^{-/-}$ mice (Fig.3.11A,C) and was equivalent in the colonic lamina propria in WT and *Nlrc4*$^{-/-}$ mice (Fig.3.11B) on day 3 and day 8 p.i.. Thus, *Nlrc4*$^{-/-}$ mice showed increased neutrophil recruitment to the cecum at early time points after *C. rodentium* infection.

Figure 3.10

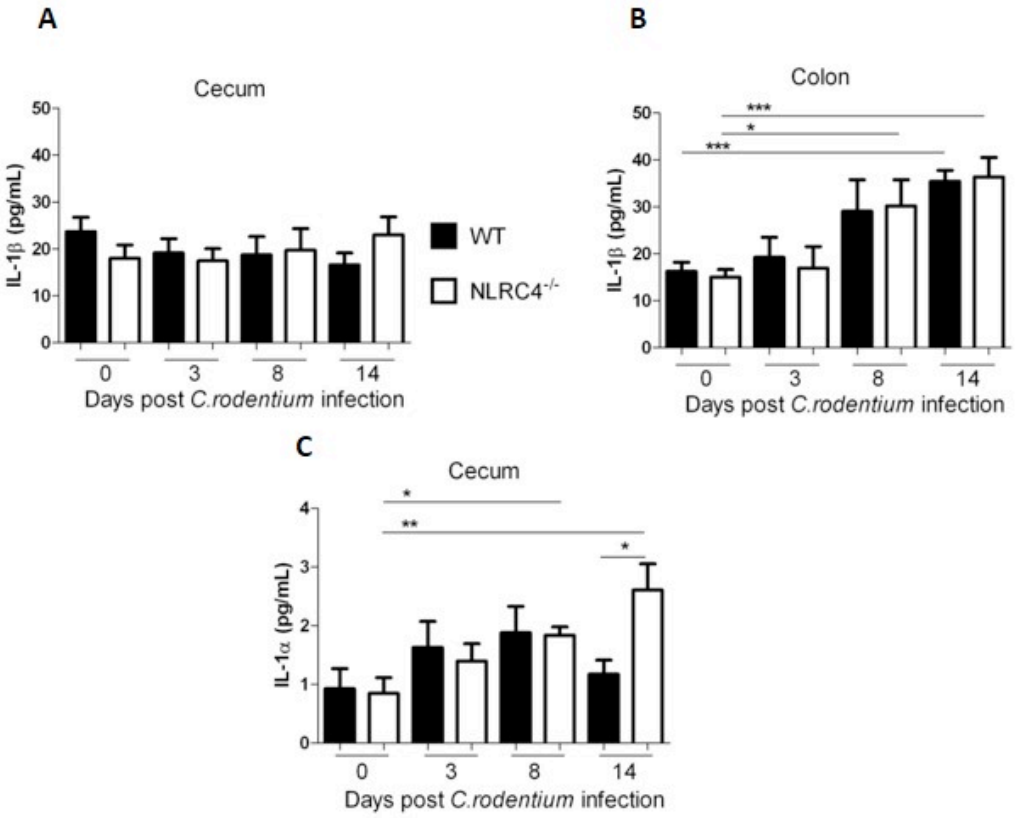


Figure 3.10 NLRC4 deficiency is not associated with reduced IL-1 secretion during *C. rodentium* infection.

WT and *Nlrc4*$^{-/-}$ mice were orally inoculated with *C. rodentium*. Tissues from cecum and distal colon were collected after 0, 3, 8 and 14 days of infection and cultured in complete media overnight. Supernatants were assayed for IL-1β and IL-1α by ELISA. Levels of IL-1β in cecum (A) and distal colon (B) and IL-1α levels in cecum (C). Levels were normalised to tissue weight. Data represent means and SEM pooled from 3 independent experiments, n=11-13 per group (A, B) or from 2 independent experiments, n=7-9 per group (C). The non-parametric Mann-Whitney test was used for statistical analysis, *P<0.05, **P<0.01, ***P<0.001.

Figure 3.11

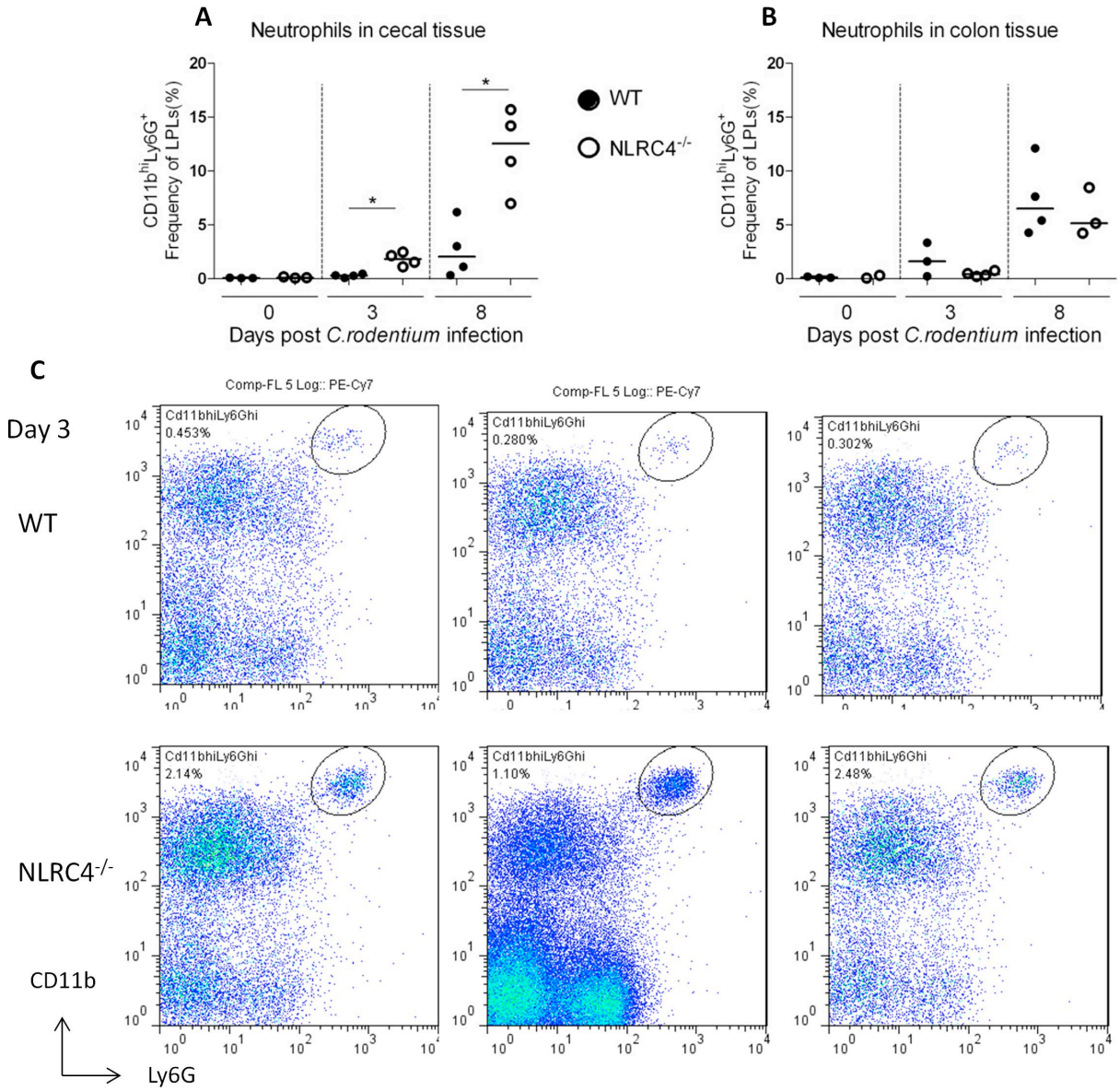


Figure 3.11 NLRC4 deficiency is associated with increased early neutrophil recruitment to the cecum during *C. rodentium* infection. WT and *Nlrc4*$^{-/-}$ mice were infected with *C. rodentium* and LPLs were isolated from cecum and whole colon after 0, 3 and 8 days of infection. Total neutrophil frequencies ($CD45^{+}CD11b^{hi}Ly6G^{hi}$) in cecum (A) and colon (B). Each symbol represents an individual mouse and horizontal bars are median values (n=3-4 per group). One of two representative experiments is shown. The non-parametric Mann-Whitney test was used to analyse the data, *P<0.05. Representative FACS plots for cecum day 3 post-infection show gating used to define neutrophils (C).

3.2.8 NLRC4 contributes to steady state IL-18 production in the large intestine

As IL-18 is also processed by inflammasomes, we also analysed the levels of IL-18 in intestinal explant supernatants from uninfected and *C. rodentium*-infected WT and *Nlrc4*$^{-/-}$ mice. There were no significant changes in intestinal IL-18 levels in WT mice during *C. rodentium* infection in either cecum or colon (Fig.3.12A,B). However, steady state IL-18 levels were significantly lower in both cecum and colon explant supernatants from *Nlrc4*$^{-/-}$ mice compared with WT mice (Fig.3.12A,B). Nevertheless, IL-18 levels were comparable in WT and *Nlrc4*$^{-/-}$ mice following infection with C. *rodentium* (Fig.3.12A,B).

We hypothesized that the reduced levels of IL-18 at steady state might contribute to the early susceptibility of *Nlrc4*$^{-/-}$ mice to *C. rodentium* infection. To investigate this, *Nlrc4*$^{-/-}$ mice were injected with recombinant mouse IL-18 (rIL18) on a daily basis, beginning 2 days before infection and continuing until day 6 p.i., before sacrifice at day 8 p.i. We found that treatment with rIL-18 did not affect *C. rodentium* colonisation levels in the cecum (Fig.3.13A) or colon (Fig.3.13B). In addition, following *C. rodentium*-infection, rIL-18-treated *Nlrc4*$^{-/-}$ mice also developed equivalent typhlitis and colitis to untreated *Nlrc4*$^{-/-}$ controls (Fig.3.13C,D). Furthermore, neither rIL-18-treated nor untreated *Nlrc4*$^{-/-}$ controls lost weight during the infection (Fig.3.13E) and both groups exhibited similar spleen weights (Fig.3.13F). These results suggest that the increased susceptibility of *Nlrc4*$^{-/-}$ mice to *C. rodentium* infection cannot be explained by reduced baseline production of IL-18.

Figure 3.12

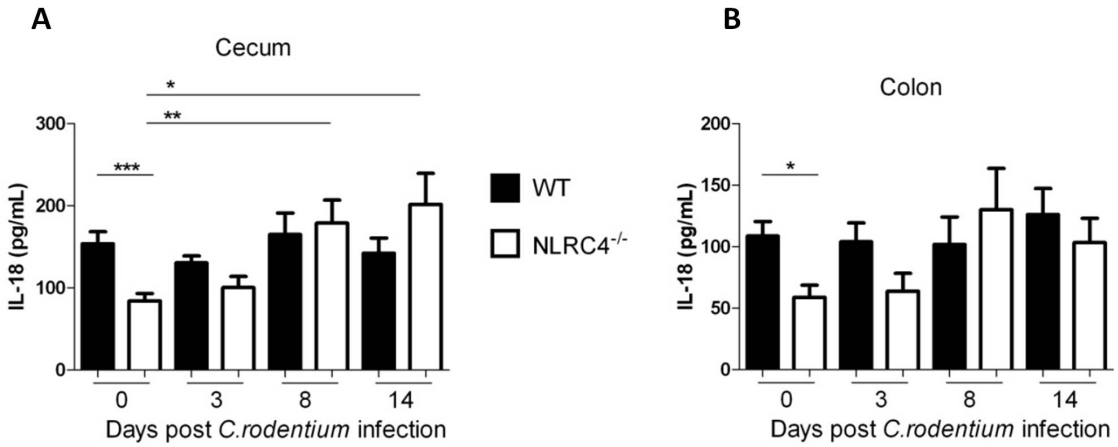


Figure 3.12 NLRC4 contributes to steady-state IL-18 production in the large intestine. WT and *Nlrc4*$^{-/-}$ mice were orally inoculated with *C. rodentium*. Tissues from cecum and distal colon were collected after 3, 8 and 14 days of infection and cultured in complete media overnight. Supernatants were assayed for IL-18 by ELISA. (A) IL-18 levels in cecum and (B) distal colon. Data represent means±SEM pooled from 2 independent experiments (n=7-9 per group). For statistical analysis the non-parametric Mann-Whitney test was used, *P<0.05, **P<0.01, ***P<0.001.

Figure 3.13

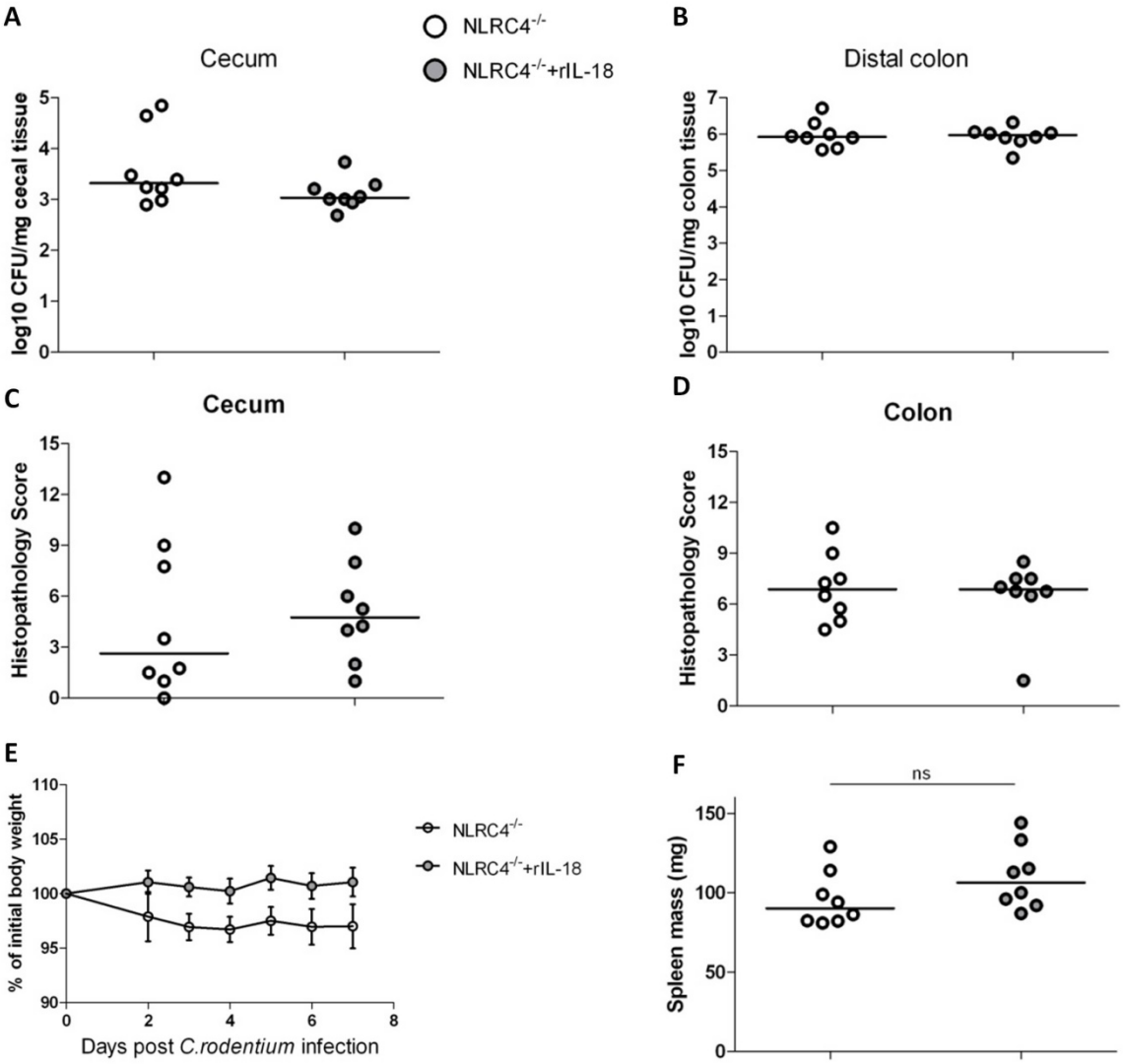


Figure 3.13 Treatment with rIL-18 does not ameliorate disease in *Nlrc4*$^{-/-}$ mice.

Nlrc4$^{-/-}$ mice were i.p. injected daily with recombinant IL-18 (0.5µg) for 2 days prior to infection with *C. rodentium* and for 6 days p.i., before sacrifice on day 8 p.i. As controls untreated *Nlrc4*$^{-/-}$ mice were infected in parallel. (A) Cecal and (B) colon tissues were homogenised and *C. rodentium* CFU enumerated. (C) Typhlitis scores. (D) Pathology in distal colon. (E) Weight curves. Values are displayed as a percentage of the original weight ± SEM. (F) Spleen weights. Data are pooled from 2 independent experiments (n=8 per group). Horizontal bars are group median values.

3.2.9 NLRC4 mediates steady state caspase-1 activation in the cecum.

Although we did not observe differences in IL-1 cytokines, baseline IL-18 production was clearly reduced in *Nlrc4*$^{-/-}$ mice compared with WT mice, suggesting that inflammasome activation was impaired in the cecum at steady state in the absence of NLRC4. We therefore characterised inflammasome activation in the intestine by immunoblotting for active caspase-1 p10 in snap-frozen cecal tissue from uninfected and *C. rodentium*-infected WT and *Nlrc4*$^{-/-}$ mice. We observed caspase-1 activation in WT cecal tissue both at the steady state and after 3 days of *C. rodentium* infection (Fig.3.14A). In contrast, caspase-1 activation was abrogated in NLRC4-deficient cecal tissue at these time points (Fig.3.14A). The differences were quantified using image analysis software and although there were no significant differences, there was a strong trend of reduced caspase-1 activation in NLRC4 deficient cecal tissue at day 0 and day 3 p.i. (Fig.3.14B). In contrast, by day 8 p.i. and day 14 p.i. equivalent levels of caspase-1 p10 subunit was detected in cecal tissues from both WT and *Nlrc4*$^{-/-}$ mice (Fig.3.14.A,B). These results suggest that NLRC4 expression drives caspase-1 activation in the cecum both at steady state and early during infection with an attaching and effacing pathogen.

Figure 3.14

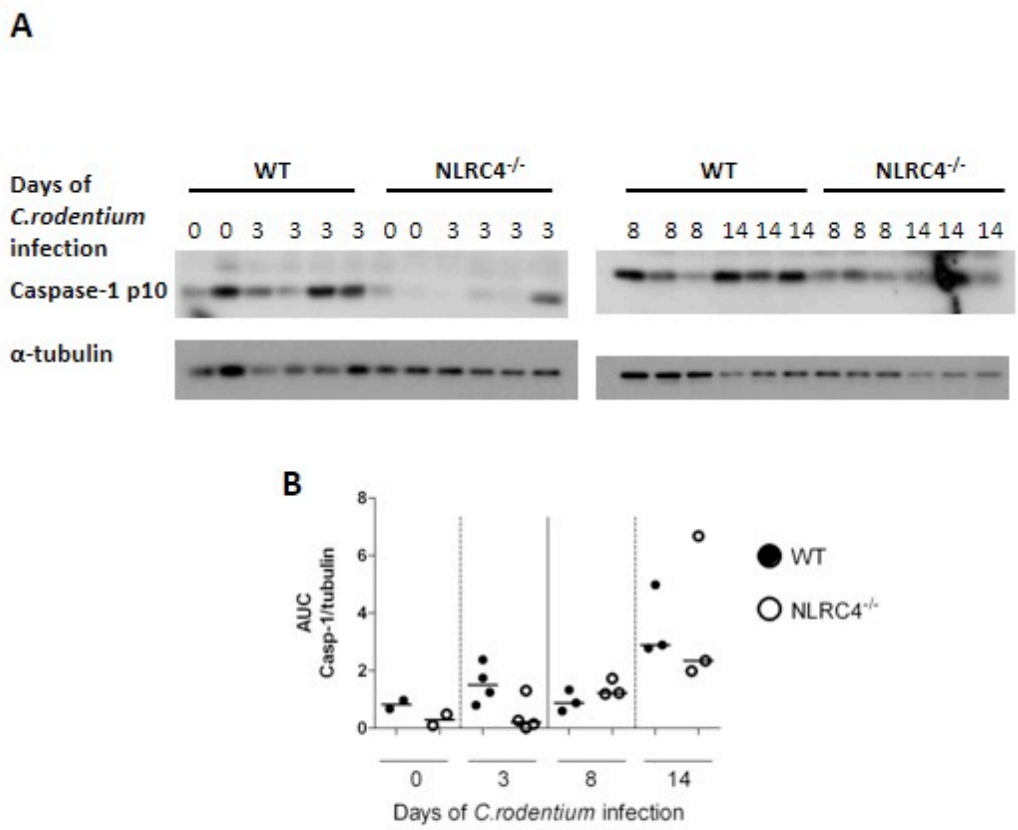


Figure 3.14 NLRC4 mediates steady state caspase-1 activation in the cecum.

WT and *Nlrc4*$^{-/-}$ mice were infected with *C. rodentium* and cecal tissue was snap-frozen after 3 (n=4 per group), 8 (n=3 per group) and 14 (n=3 per group) days of infection. As controls uninfected mice (n=2 per genotype) were sacrificed and cecal tissue frozen. (A) Tissue samples were homogenized and equivalent amounts were loaded on a SDS-PAGE gel and blotted for active caspase-1 p10. For loading control α-tubulin reactivity was measured. Results are from 1 experiment and each lane corresponds to an individual mouse. (B) Quantification of caspase-1 p10 using image analysis software. Results are from 1 time-course experiment.

3.2.10 Broad spectrum antibiotic treatment exacerbates *C. rodentium* induced inflammation in WT mice

In order to investigate the impact of *C. rodentium* colonisation levels on disease development, we treated WT and *Nlrc4*$^{-/-}$ mice with broad spectrum antibiotics (Abx) prior to infection. Previous studies had revealed deleterious effects of Abx treatment prior to infection with enteric pathogens,[309, 310] while infection of germ-free mice with *C. rodentium* resulted in long-term infection but little disease.[311] Selective depletion of anaerobes was shown to promote increased *C. rodentium* colonisation, suggesting that an intestinal niche was provided.[310] We treated mice with a combination of ampicillin, metronidazol, vancomycin, neomycin and gentamicin. This cocktail was adapted from previously published protocols with the aim to deplete the intestinal flora across phyla.[277, 288] Before the start of the treatment (D0) and after 7 and 10 days of Abx treatment fecal pellets were collected, total fecal DNA extracted and qPCR for the eubacteria 16s rRNA gene performed (Fig.3.15A). We found that the DNA yield from fecal pellets was much reduced after Abx treatment, resulting in that 5-fold less fecal DNA could be used in the Q-PCR reaction. Nevertheless, the signal from general 16s rRNA was detected 10 cycles later than at D0, representing approximately a 1000 fold reduction (Fig.3.15A). As a control, an equivalent amount of fecal DNA from an untreated animal was assayed, showing that the bacterial signal was only slightly reduced, corresponding to the reduced amount of DNA template added (Fig.3.15A) Thus, Abx-treatment effectively depleted intestinal microbiota in both WT and *Nlrc4*$^{-/-}$ mice.

After 10 days of Abx treatment, mice were infected with *C. rodentium* and were sacrificed after 8 days of infection. Assessment of intestinal pathology revealed severe typhlitis in WT mice (Fig.3.15B,D) while development of colitis in the distal colon was

relatively mild (Fig.3.15C). Interestingly, following Abx treatment and *C. rodentium* infection, WT mice developed typhlitis and colitis that were equivalent to *Nlrc4*$^{-/-}$ mice (Fig.3.15B-D).

Figure 3.15

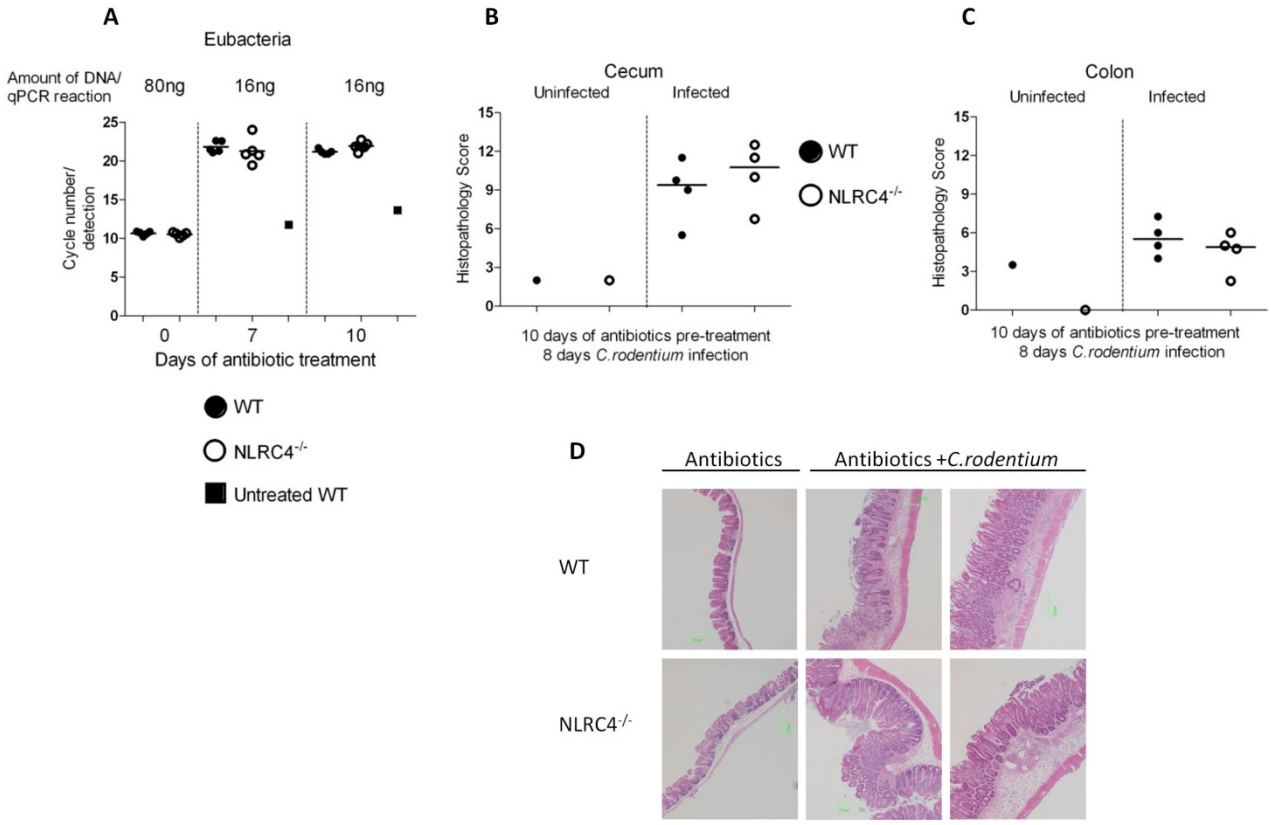


Figure 3.15 Broad spectrum antibiotic treatment prior to *C. rodentium* infection leads to exacerbated disease in WT mice.

WT and *Nlrc4*$^{-/-}$ mice were treated with broad spectrum antibiotics (Abx) twice daily by oral gavage for a total of 10 days. Mice were then infected with *C. rodentium* for 8 days. (A) Assessment of bacterial depletion: Fecal pellets were collected after 0, 7 and 10 days of Abx treatment, DNA extracted and presence of eubacterial 16s rRNA assayed by qPCR. A fecal pellet from an untreated mouse was processed and assayed in parallel. Results are displayed as detection threshold cycle number. (B) Cecal pathology scores and (C) Distal colon pathology scores. One Abx-treated mouse of each genotype remained uninfected as a control. (D) Representative micrographs of cecum. Magnification 5x. Results are from one experiment; (A) Abx-treated n=5 per group, (B) Abx-treated and *C. rodentium*-infected n=4 per group. Horizontal bars represent median values.

3.2.11 Broad spectrum antibiotic treatment equalises *C. rodentium* colonisation levels in WT and *Nlrc4*$^{-/-}$ mice

At necropsy, cecal contents were collected, total DNA extracted and qPCR for eubacterial 16s rRNA was performed. Bacterial levels in control mice, which had been Abx-treated but not infected, were very low and the detection threshold cycle numbers were high (Fig.3.16A). In contrast, cecal contents from Abx-treated mice that were subsequently infected with *C. rodentium* contained similar total eubacterial DNA levels as observed in fecal pellets isolated prior to Abx treatment (Fig.3.16A and Fig.3.15A). Colonisation levels of *C. rodentium* were monitored throughout the infection by enumerating colonies in fecal samples and comparable *C. rodentium* numbers were detectable by day 2 p.i. and throughout the infection in WT and *Nlrc4*$^{-/-}$ mice (Fig.3.16B). We also assessed the *C. rodentium* burdens in intestinal tissues at sacrifice and could confirm comparable, high colonisation by *C. rodentium* of the cecum and distal colon of both WT and *Nlrc4*$^{-/-}$ mice (Fig.3.16C,D).

Our initial experiments had shown that NLRC4 deficiency during *C. rodentium* infection resulted in increased weight loss and systemic immune activation. We did not observe significant weight loss after initiation of the Abx regimen or any additional weight loss during the 8 days of *C. rodentium* infection (Fig.3.16E). Furthermore, Abx-treated and *C. rodentium*-infected WT and *Nlrc4*$^{-/-}$ mice exhibited similar spleen weights, which were equivalent to untreated WT mice that were infected with *C. rodentium* (Fig.3.16F and Fig.3.1D). We also measured IFN-γ and IL-17A in cecal explant culture supernatants. Despite markedly exacerbated cecal pathology, little IFN-γ and IL-17A were detected in cecal tissues from Abx-treated and *C. rodentium*-infected WT mice (Fig.3.16G). Cytokine levels in cecal tissues from Abx-treated and *C. rodentium*-infected *Nlrc4*$^{-/-}$ mice were variable and, although they tended to be slightly

higher to those found in similarly treated WT mice, they were not significantly increased, suggesting that the increased pathology associated with Abx-treatment was not dependent on exacerbated adaptive immune responses. (Fig.3.16G).

Thus, Abx-mediated depletion of the microbiota leads to increased *C. rodentium* colonisation and intestinal pathology in WT mice, supporting a link between high bacterial colonisation of the tissue and the development of severe intestinal pathology.

Figure 3.16

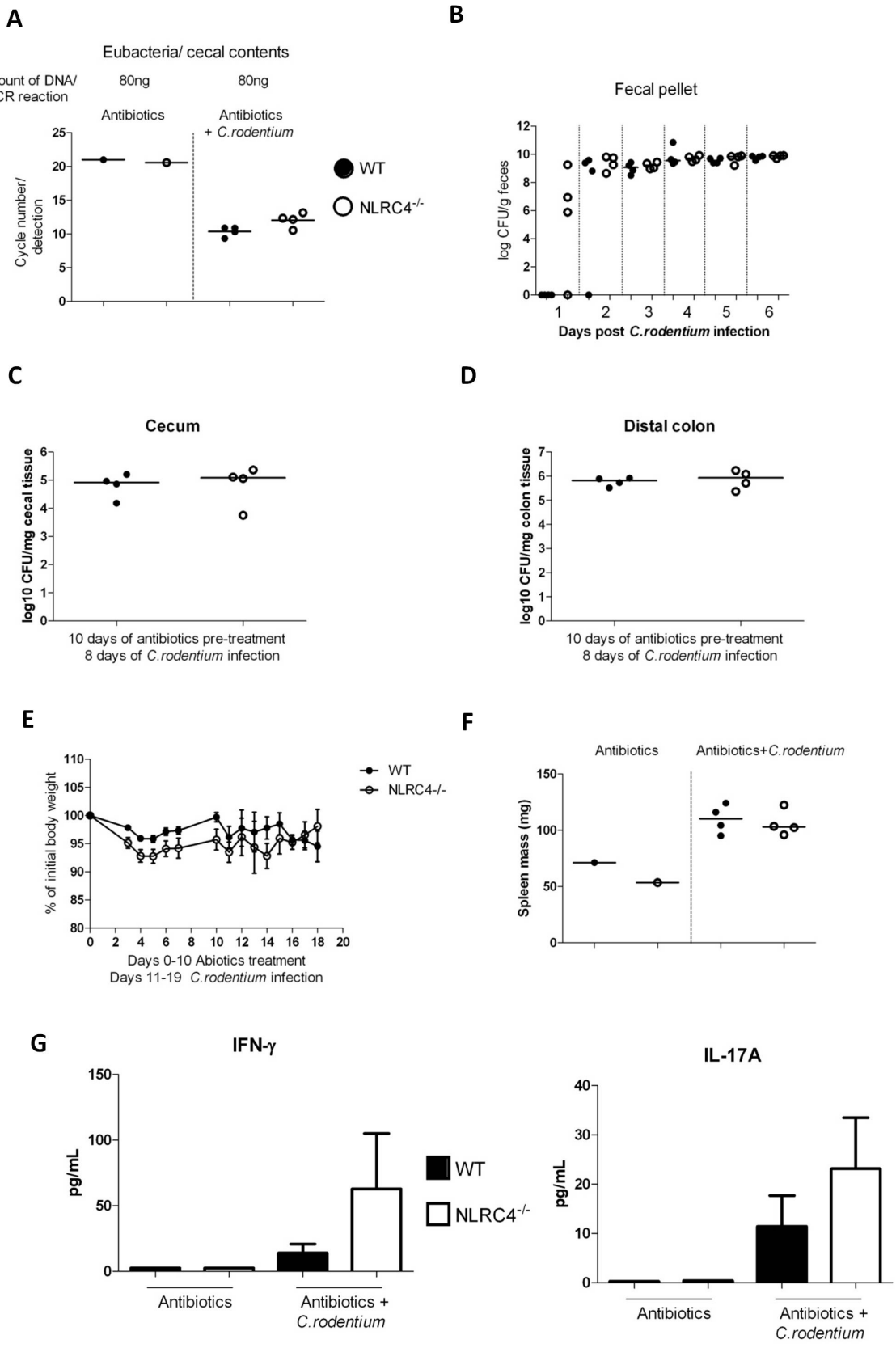

A
Eubacteria/ cecal contents
Amount of DNA/ qPCR reaction
80ng
80ng
Antibiotics
Antibiotics + C.rodentium
Cycle number/ detection
WT
NLRC4-/-
B
Fecal pellet
log CFU/g feces
Days post C.rodentium infection
C
Cecum
log10 CFU/mg cecal tissue
10 days of antibiotics pre-treatment
8 days of C.rodentium infection
D
Distal colon
log10 CFU/mg colon tissue
10 days of antibiotics pre-treatment
8 days of C.rodentium infection
E
% of initial body weight
WT
NLRC4-/-
Days 0-10 Abiotics treatment
Days 11-19 C.rodentium infection
F
Antibiotics
Antibiotics+C.rodentium
Spleen mass (mg)
G
IFN-γ
pg/mL
WT
NLRC4-/-
Antibiotics
Antibiotics + C.rodentium
IL-17A
pg/mL
Antibiotics
Antibiotics + C.rodentium

Figure 3.16 Broad spectrum antibiotic treatment leads to increased *C. rodentium* colonisation in WT mice

WT and *Nlrc4*$^{-/-}$ mice were treated with broad spectrum antibiotics (Abx) twice daily by oral gavage for a total of 10 days. Mice were then infected with *C. rodentium* for 8 days. (A) Assessment of bacterial colonisation: Cecal contents were collected, DNA extracted and presence of eubacterial 16s rRNA assayed by qPCR. Results are displayed as detection threshold cycle number. (B) Tracking of *C. rodentium* colonisation by enumerating CFU in fecal pellets. Fecal pellets were homogenised, cultured on selective media and *C. rodentium* CFU were enumerated. (C,D) Cecal and distal colon tissue were homogenised, cultured on selective media and *C. rodentium* CFU enumerated. (E) Weight curves. Weights are displayed as a percentage of the original weight (n=5/group ±SEM) at the start of the treatment (day 0) and (n=4/group ±SEM) from infection (day 11). (F) Spleen weights. Results are from one experiment; (A) Abx-treated n=5 per group, (B) Abx-treated and *C. rodentium*-infected n=4 per group. (G) Levels of IFN-γ and IL-17A were measured in cecal tissue culture supernatants by bead based assay and flow cytometry. Values were normalised to tissue weight. Bar graphs represent n=4 mean ±SEM and n=1 for infected and uninfected groups respectively.

3.2.12 NLRC4 expression in non-hematopoietic cells is protective during *C. rodentium* infection

Intestinal epithelial cells are known to express inflammasome components[157, 312] and considering the close contact between *C. rodentium* and the epithelium, inflammasome activation in these barrier cells may be important for initial immune activation. To further investigate in which cell types NLRC4 expression conveyed protective effects against *C. rodentium*, bone marrow (BM) chimeras were generated. WT or *Nlrc4*$^{-/-}$ recipient mice were subjected to lethal irradiation and subsequently injected intravenously with 5x10^6 BM cells from WT or *Nlrc4*$^{-/-}$ donor mice. The mice were left to reconstitute for 10 weeks, after which BM chimeras were infected with *C. rodentium* (Fig.3.17). We found that mice with selective NLRC4 deficiency in the non-hematopoietic cells (WT→NLRC4$^{-/-}$) exhibited significant weight loss very similar to that observed in chimeras with complete NLRC4 deficiency (NLRC4$^{-/-}$→NLRC4$^{-/-}$) (Fig.3.18A). Conversely, selective NLRC4 expression in non-hematopoietic cells (NLRC4$^{-/-}$→WT) conferred resistance to weight loss, similar to complete WT chimeras (WT→WT) (Fig.3.18A).

The resulting weight loss results were mirrored by the development of typhlitis. Thus, BM chimeras with selective NLRC4 deficiency in the non-hematopoietic cells (WT→NLRC4$^{-/-}$) developed severe inflammation in the cecum, equivalent to that observed in complete NLRC4 deficient control chimeras (NLRC4$^{-/-}$→NLRC4$^{-/-}$) (Fig.3.18B,D). Conversely, BM chimeras with NLRC4 sufficient non-hematopoietic cells (NLRC4$^{-/-}$→WT) exhibited only mild cecal pathology and were as protected as complete WT chimeras (WT→WT) (Fig.3.18B,D). As in previous experiments, *C. rodentium* induced typhlitis was characterised by epithelial hyperplasia, oedema and marked leukocytic infiltration (Fig.3.18D). In contrast, there was no clear protective

effect of NLRC4 expression against colitis, although BM chimeras with NLRC4 sufficient non-hematopoietic cells (NLRC4$^{-/-}$→WT and WT→WT) showed a trend towards less severe disease in the distal colon on day 8 p.i., there were no statistically significant differences and the majority of mice in all BM chimera groups developed severe colitis by day 14 (Fig.3.18C).

We then quantified C. *rodentium* colonisation levels in the cecal tissue. BM chimeras with NLRC4 deficient non-hematopoietic cells (NLRC4$^{-/-}$→NLRC4$^{-/-}$ and WT→NLRC4$^{-/-}$) harboured significantly increased bacterial burdens on day 8 p.i. compared to those with NLRC4 sufficient non-hematopoietic compartments (WT→WT and NLRC4$^{-/-}$→WT) (Fig.3.19A). Immunohistochemical staining confirmed the increased bacterial presence and *C. rodentium* was observed further into the crypts in BM chimeras with NLRC4 deficient non-hematopoietic cells (NLRC4$^{-/-}$→NLRC4$^{-/-}$ and WT→NLRC4$^{-/-}$) (Fig.3.19B).

Figure 3.17

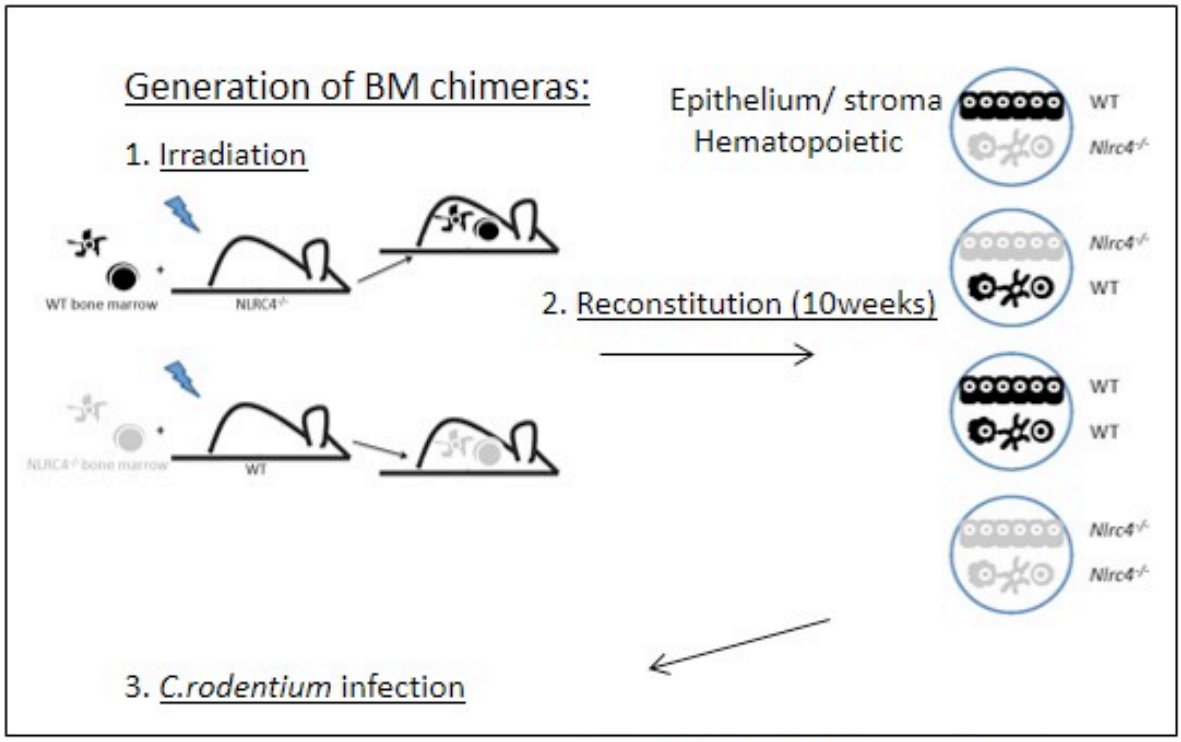


Figure 3.17 Generation of bone marrow (BM) chimeras

WT and *Nlrc4*$^{-/-}$ mice were lethally γ-irradiated and reconstituted with 5x10^{6} BM cells isolated from WT or *Nlrc4*$^{-/-}$ mice. Mice were co-housed and left to reconstitute for 10 weeks. 4 different types of chimeras were generated: Mice with selective NLRC4 expression in the non-hematopoietic compartment (NLRC4$^{-/-}$ → WT), mice with selective expression of NLRC4 in the hematopoietic compartment (WT → NLRC4$^{-/-}$), complete WT mice (WT→WT) and complete NLRC4 deficient mice (NLRC4$^{-/-}$ → NLRC4$^{-/-}$). The chimeras were subsequently infected with *Citrobacter rodentium*.

Figure 3.18

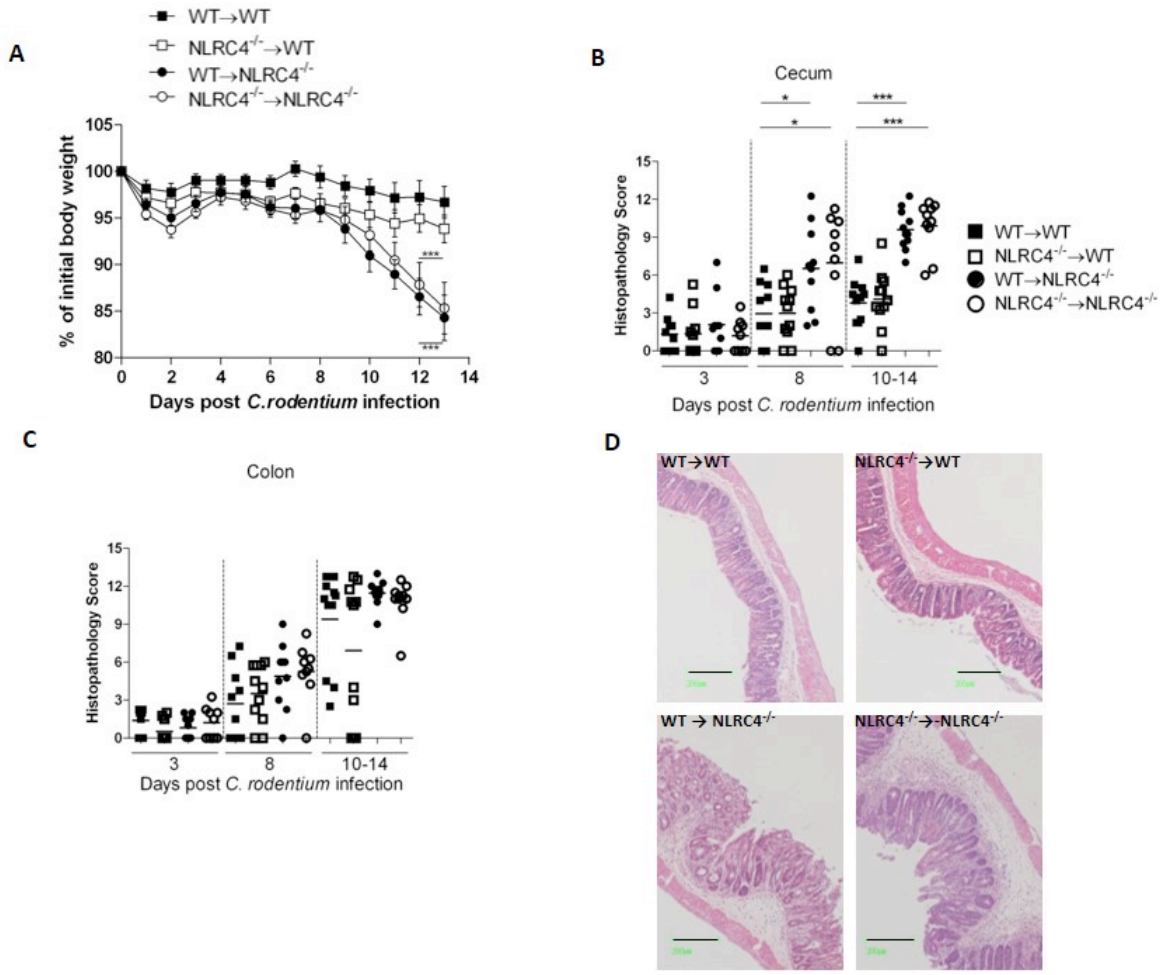


Figure 3.18 NLRC4 expression in non-hematopoietic cells is protective during *C. rodentium* infection.

WT or *Nlrc4*$^{-/-}$ mice were γ-irradiated (2X 5.5 Gy) and reconstituted with 5x10^{6} bone marrow (BM) cells isolated from either *Nlrc4*$^{-/-}$ or WT donors, resulting in 4 groups: Complete NLRC4 sufficient mice (WT→WT); mice deficient in NLRC4 in the hematopoietic compartment (NLRC4$^{-/-}$ →WT); mice deficient in NLRC4 in the non-hematopoietic compartment (WT→NLRC4$^{-/-}$); and complete NLRC4 deficient animals (NLRC4$^{-/-}$→NLRC4$^{-/-}$). BM chimeric mice were co-housed and allowed to reconstitute for 10 weeks before *C. rodentium* infection. Weight curves are shown in (A). A number of mice (NLRC4$^{-/-}$→NLRC4$^{-/-}$, n=3) and WT→NLRC4$^{-/-}$, n=5) developed severe weight loss and had to be sacrificed earlier than 14 days post-infection. Data are shown as mean ± SEM; n = 31-32 per group at Day 0 and n = 8-11 per group at Day 13 post-infection. Data are pooled from 2 independent experiments. Horizontal bars denote the time during which weight loss was significant. Two-way ANOVA was used for analysis, ***P<0.001. Cecum and colon pathology scores at d3, d8 and d14 post-infection are shown in (B) and (C) respectively. Representative micrographs of cecum at d14 are shown in (D). Black bars are equivalent to 200μm. The non-parametric Mann-Whitney test was used for statistical analysis. * P<0.05, ***P<0.001.

Figure 3.19

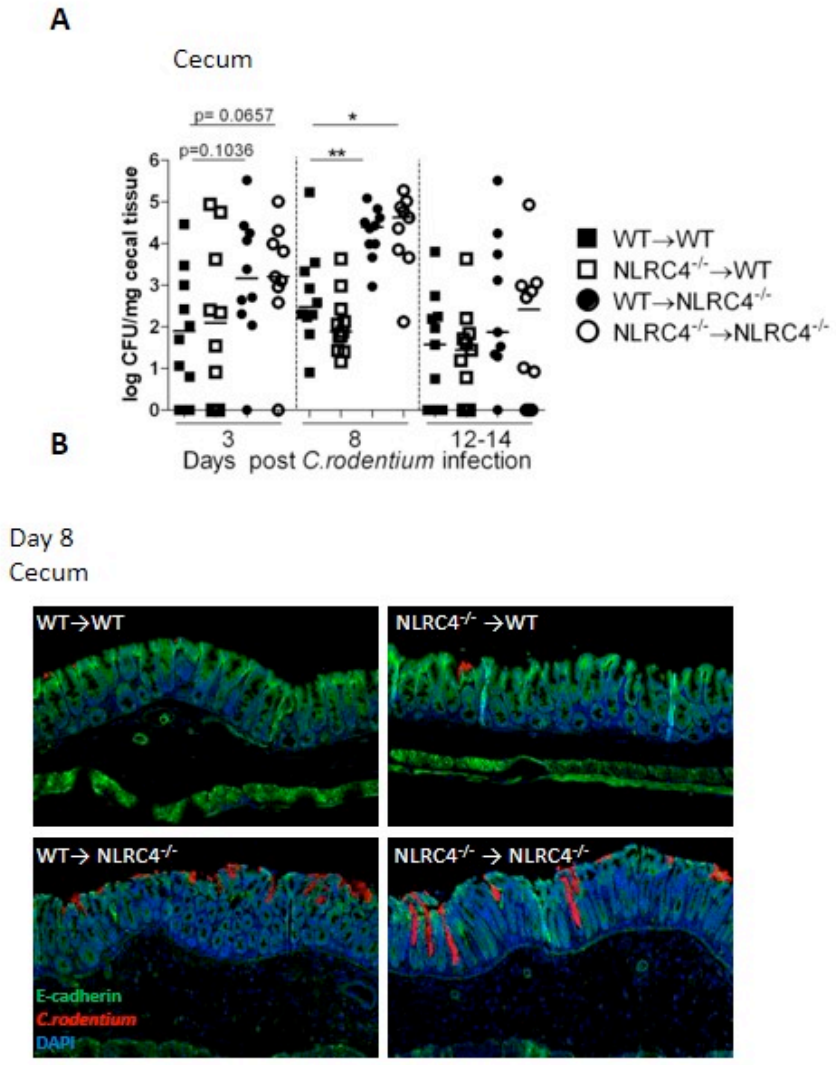


Figure 3.19 NLRC4 expression in non-hematopoietic cells limits *C. rodentium* colonisation.

WT or *Nlrc4*$^{-/-}$ mice were γ-irradiated (2X 5.5 Gy) and reconstituted with 5x10^{6} bone marrow (BM) cells isolated from either *Nlrc4*$^{-/-}$ or WT donors to generate 4 groups: Complete NLRC4 sufficient mice (WT→WT); mice deficient in NLRC4 in the hematopoietic compartment (NLRC4$^{-/-}$ →WT); mice deficient in NLRC4 in the non-hematopoietic compartment (WT→NLRC4$^{-/-}$); and complete NLRC4 deficient animals (NLRC4$^{-/-}$→NLRC4$^{-/-}$). BM chimeric mice were allowed to reconstitute for 10 weeks before *C. rodentium* infection. Cecal tissues were homogenised and cultured on selective media to assess *C. rodentium* colonisation (A). Each symbol represents an individual animal, n= 9-10 per group, pooled from 2 independent experiments. Horizontal lines represent group median values. (B) *C. rodentium* specific staining of cecum d8 p.i..*C. rodentium* specific stain (red), E-cadherin (green) and DAPI (blue). Magnification 10x. The non-parametric Mann-Whitney test was used for statistical analysis, *P<0.05, **P<0.01.

3.2.13 NLRC4 is highly expressed in intestinal crypts

To further evaluate NLRC4 expression in different mucosal cell populations several cellular compartments of the intestinal tissue were isolated. Large intestinal isolates enriched for IECs (Crypts) were isolated from normal WT mice and intestinal stromal cells (Stroma) were prepared.[313] In addition, lamina propria leukocytes (LPLs) were isolated. RNA was isolated from these distinct compartments and NLRC4 expression was measured by qPCR. We found that IEC crypts in both cecum and colon displayed significantly greater expression of NLRC4 compared with LPLs (Fig.3.20A). However, intestinal stromal cells did not express detectable levels of NLRC4 (Fig.3.20A). To assess purity in the IEC crypts and LPLs fractions, expression of the epithelial marker villin 1 and the hematopoietic marker CD45 were quantified by qPCR. Intestinal crypts were shown to express > 100-fold more villin 1 than CD45, confirming the high purity of IECs and the relatively small hematopoietic contamination (Fig.3.20B). Although LPL isolates were enriched for CD45 expressing cells compared with crypt isolates, an IEC (villin 1) signal was also detected, suggesting that the NLRC4 expression in LPL preparations may be derived from contaminating IEC (Fig.3.20C). These results strongly suggest that IECs represent the cellular compartment responsible for NLRC4-mediated protection from *C. rodentium*.

Figure 3.20

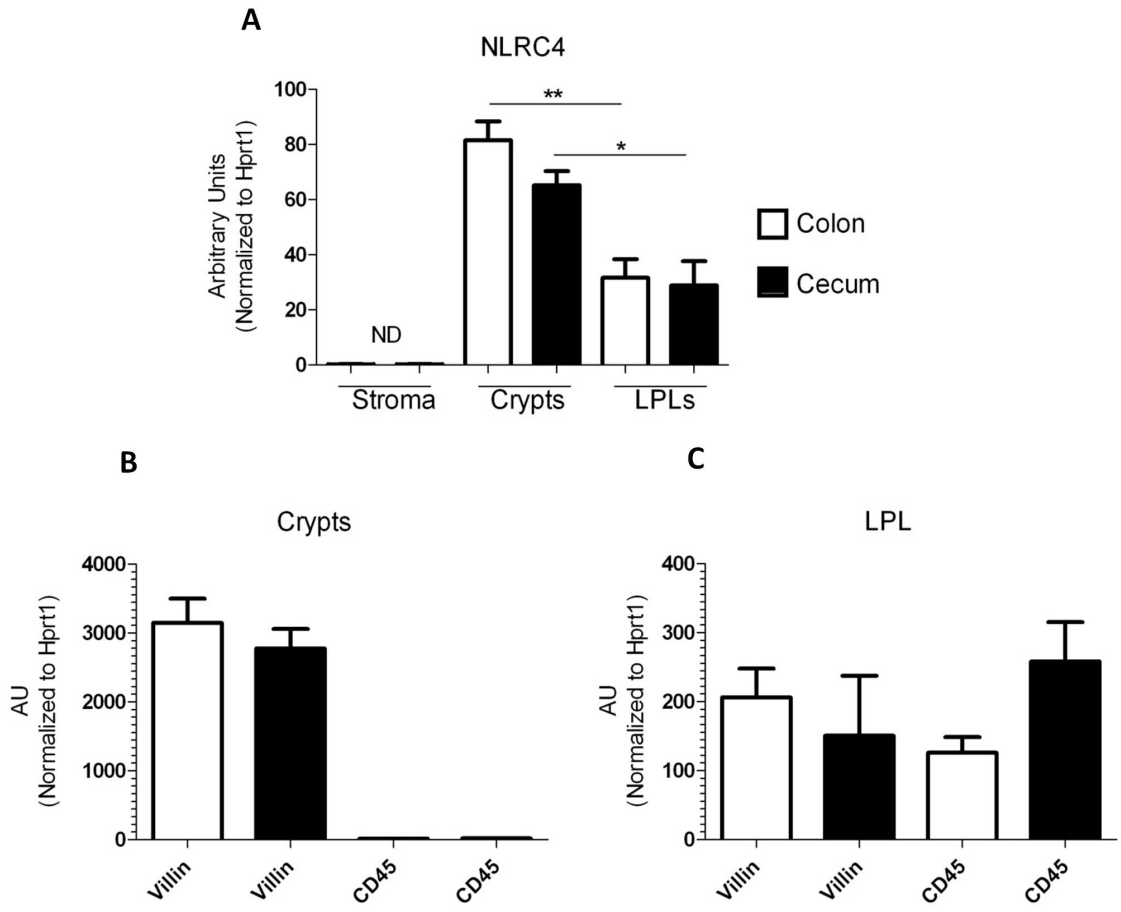


Figure. 3.20 NLRC4 is highly expressed in intestinal crypts.

Messenger RNA was isolated from preparations of intestinal stroma, intestinal epithelial crypts and LPLs from WT cecum and colon. Q-PCR analyses were used to quantify expression of NLRC4 (A), Villin 1 and CD45 (B). Data represent mean expression levels and SEM normalised to Hprt (n = 4-6 individual isolates per group). The non-parametric Mann-Whitney test was performed for statistical analysis, *P<0.05, **<0.0. ND = not detected.

3.2.14 Microarray analysis of transcriptional changes during *C. rodentium* infection

In order to gain a more comprehensive view of infection induced changes in the tissue, we decided to analyse the transcriptional responses by microarray analysis. WT and *Nlrc4*$^{-/-}$ mice were infected with *C. rodentium* and sacrificed after 3 days of infection. At day 3 p.i. bacterial burdens are highly elevated in *Nlrc4*$^{-/-}$ cecal tissue in the absence of apparent pathology. By choosing this time point we aimed to avoid a potentially strong inflammatory signature that might be occlusive. RNA from cecal tissue was isolated and transcribed into cDNA. Each cDNA sample was based on pooled mRNA from two individual mice and a total of 3 replicates were used for uninfected controls and infected animals respectively. For the microarray the Illumina Single Colour Mouse BeadChip with direct hybridization was used. Data were generated with the GenomeStudio 2011 software and analyzed with GeneSpring GX 12.

We first evaluated which genes were upregulated in WT and *Nlrc4*$^{-/-}$ mice during *C. rodentium* infection. A Venn diagram based on expression differences of at least 1.5 fold change (FC) for each gene shows the induced genes in the two genotypes (Fig.3.21). A Venn diagram of repressed genes of expression differences of at least 1.5 FC is shown in Appendix 1. Interestingly, at day 3 p.i. more than 200 genes were selectively upregulated in *Nlrc4*$^{-/-}$ mice; 21 genes were upregulated in both WT and *Nlrc4*$^{-/-}$ mice; whereas only 5 genes were selectively induced in WT mice (Fig.3.21). Among the latter 5 genes, *Ccl5*, chemokine ligand 5, is known to be chemotactic for leukocytes.[314] However, the induction of *Ccl5*, which had an FC value of 1.50 in WT mice during infection, could not be validated by qPCR (data not shown). Further validation was not performed for the remaining 4 genes selectively upregulated in WT

mice. Instead we widened our analysis to comprise responses that were either reduced or increased in *Nlrc4*$^{-/-}$ mice compared with WT mice.

Gene expression differences between *Nlrc4*$^{-/-}$ mice and WT mice at steady state and after 3 days of infection are displayed as a heat map (Fig.3.22). A FC >2 was set as a threshold.The analysis revealed that a group of genes associated with innate immunity was downregulated in *Nlrc4*$^{-/-}$ mice both at steady state and at 3 days p.i. The genes were *Itgae*, *Retnla*, *Ang4* and several *Ear* genes, which encode a group of eosinophil-associated ribonucleases.[315] qPCR validation of these genes confirmed significantly reduced expression of *Itgae* in infected *Nlrc4*$^{-/-}$ mice and of *Retnla* in both uninfected and infected *Nlrc4*$^{-/-}$ mice compared with WT mice (Fig.3.23). Upregulation of *Ang4* could not be validated. However, the most striking differences were observed for *Ear1/2* expression, which were significantly reduced in *Nlrc4*$^{-/-}$ mice compared with WT mice at both steady state and on day 3 p.i. (Fig.3.23).

Figure 3.21

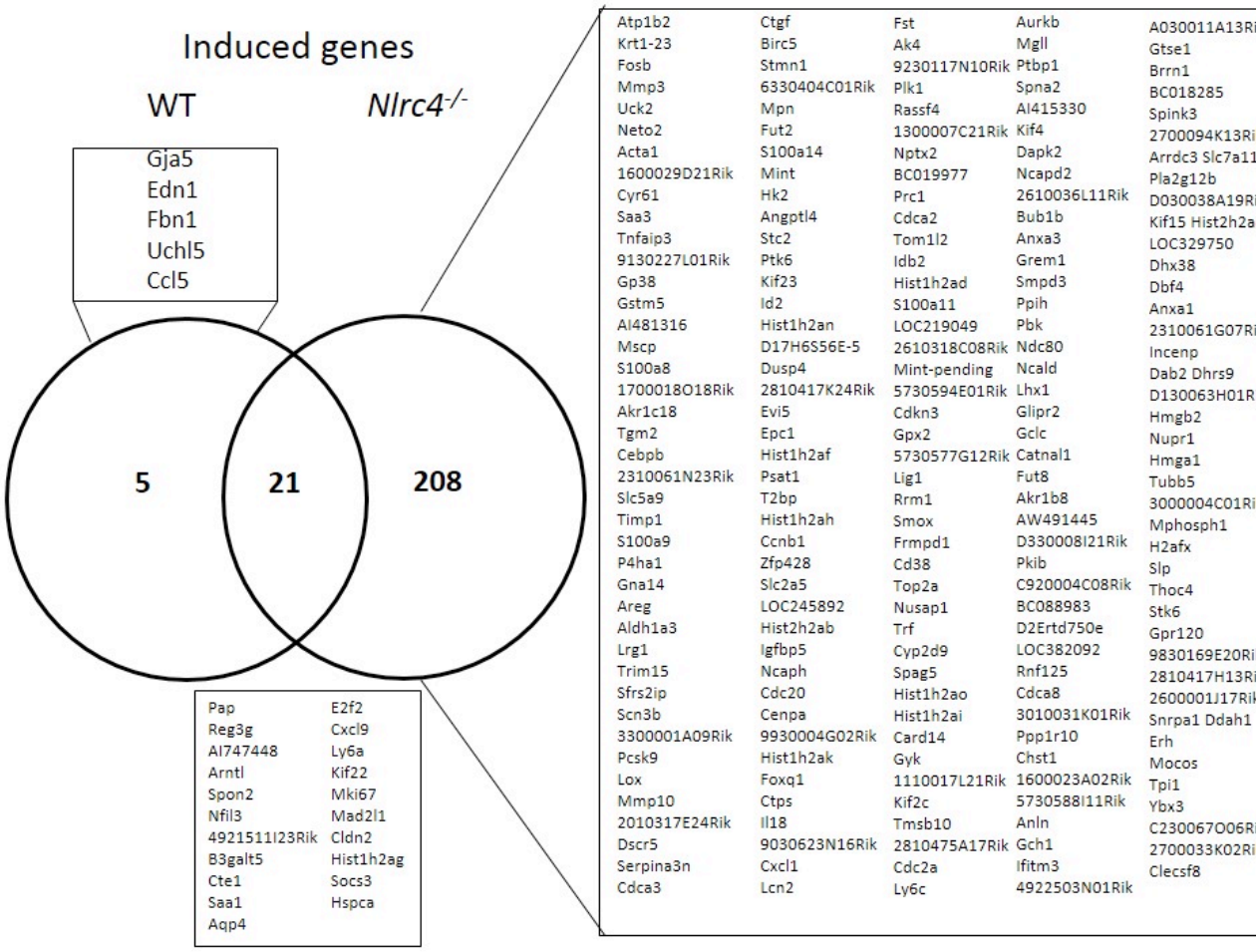


Figure 3.21 Induced genes in the cecum of WT and *Nlrc4*$^{-/-}$ mice after 3 days of *C. rodentium* infection.

WT and *Nlrc4*$^{-/-}$ mice were infected with *C. rodentium*. At day 3 p.i., cecal tissue was snap-frozen, RNA extracted and a microarray performed. Uninfected mice were included as controls. Genes displaying significant upregulation of a fold change value ≥ 1.5 are shown as a Venn diagram in order to display genes upregulated in WT mice (5 genes), *Nlrc4*$^{-/-}$ mice (208 genes) and in both genotypes (21 genes). The genes are as listed in boxes. Each cDNA sample was based on pooled mRNA from two individual mice and a total of 3 replicates for uninfected controls and infected animals respectively.

Figure 3.22

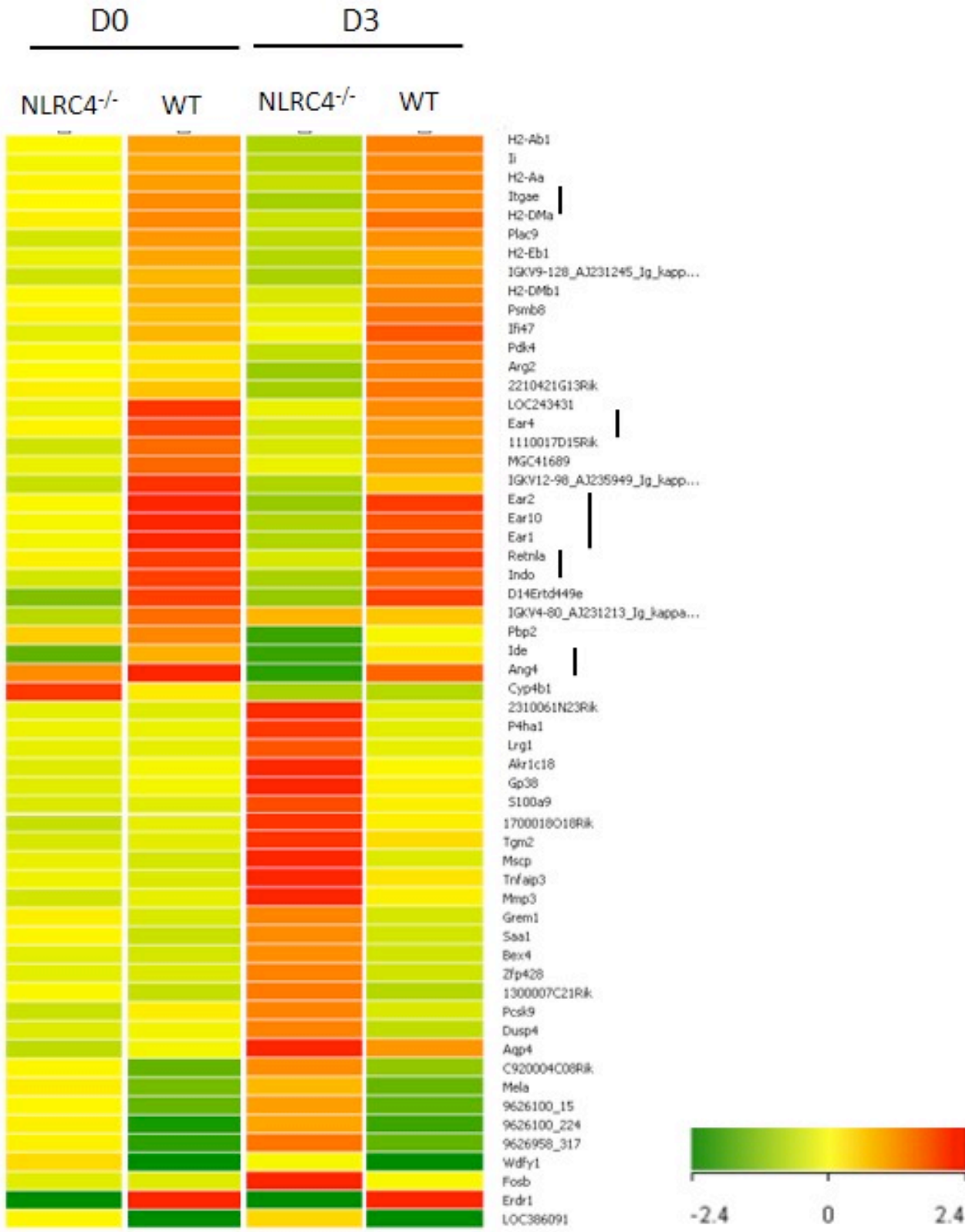

D0
D3
NLRC4-/-
WT
NLRC4-/-
WT
H2-Ab1
Ii
H2-Aa
Itgae
H2-DMa
Plac9
H2-Eb1
IGKV9-128_AJ231245_Jg_kapp...
H2-DMb1
Psmb8
Ifi47
Pdk4
Arg2
2210421G13Rik
LOC243431
Ear4
1110017D15Rik
MGC41689
IGKV12-98_AJ235949_Jg_kapp...
Ear2
Ear10
Ear1
Retnla
Indo
D14Ertd449e
IGKV4-80_AJ231213_Jg_kappa...
Pbp2
Ide
Ang4
Cyp4b1
2310061N23Rik
P4ha1
Lrg1
Akr1c18
Gp38
S100a9
1700018O18Rik
Tgm2
Mscp
Tnfaip3
Mmp3
Grem1
Saa1
Bex4
Zfp428
1300007C21Rik
Pcsk9
Dusp4
Aqp4
C920004C08Rik
Mela
9626100_15
9626100_224
9626958_317
WdFy1
Fosb
Erdr1
LOC386091
-2.4
0
2.4

Figure 3.22 Heat map of differentially expressed genes between WT and *Nlrc4*$^{-/-}$ mice in the cecum at steady state and after 3 days of *C. rodentium* infection.

WT and *Nlrc4*$^{-/-}$ mice were infected with *C. rodentium*. At day 3 (D3) p.i. cecal tissue was snap-frozen, RNA extracted and a microarray performed. The heat map represents genes that were expressed significantly lower or higher, of a fold change value of ≥2, in *Nlrc4*$^{-/-}$ mice compared with WT mice. Uninfected (D0) mice were included in the analysis. The colours ranging from green to red are equivalent to log transformed normalised intensity values.

Figure 3.23

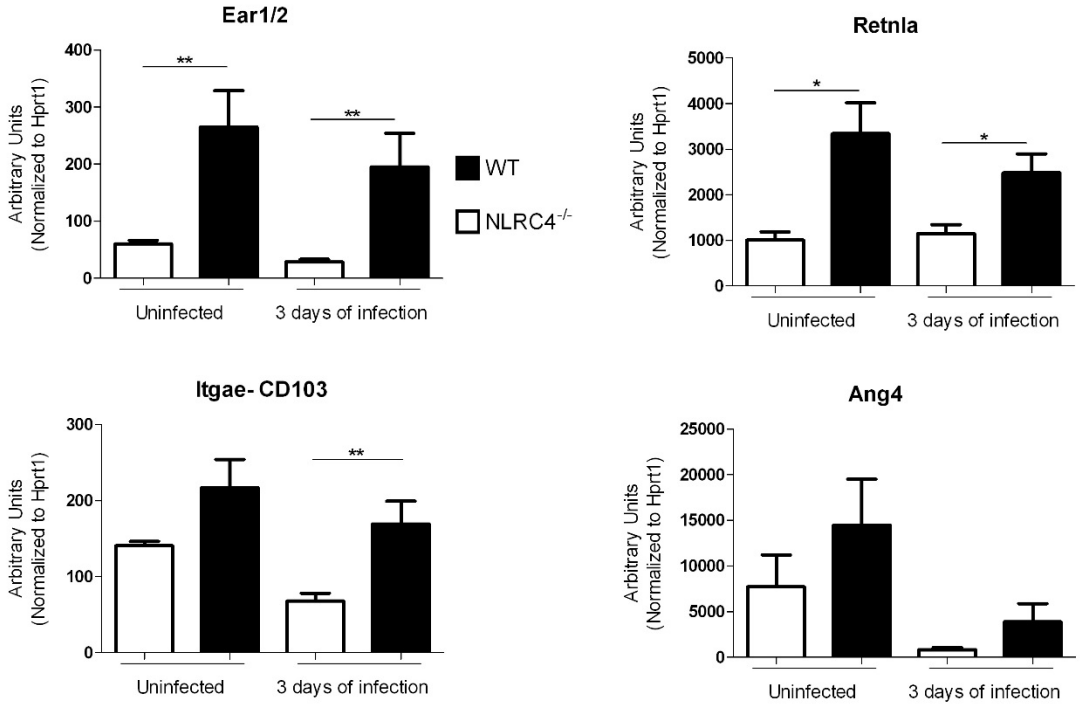


Figure 3.23 Validation of differentially expressed genes in the cecum of WT and *Nlrc4*$^{-/-}$ mice at steady state and after 3 days of *C. rodentium* infection.

WT and *Nlrc4*$^{-/-}$ mice were infected with *C. rodentium*. At day 3 p.i. cecal tissue was snap-frozen, RNA extracted and a microarray performed. qPCR analysis was performed for selected genes. Data represent mean relative expression levels ± SEM normalised to Hprt (n=6 per group). For statistical evaluation the non-parametric Mann-Whitney test was used, *P<0.05, **P<0.01.

3.2.15 WT and *Nlrc4*$^{-/-}$ mice harbour equivalent eosinophil frequencies in the lamina propria

The reduced *Ear* expression in *Nlrc4*$^{-/-}$ mice on day 3 p.i. was confirmed in samples from an independent experiment, although by day 8 p.i. WT and *Nlrc4*$^{-/-}$ mice expressed similar levels of *Ear1* and *Ear2* (Fig.3.24A). Cecal LPL from uninfected and infected animals were stained for eosinophil markers and, although eosinophil frequencies were variable, there were no statistically significant differences in eosinophil proportions in the cecal LPL between the two genotypes at any time point during *C .rodentium* infection (Fig.3.23B). We also assessed *Ear1/2* expression levels in cecal tissues from BM chimeras that had been infected with *C. rodentium* for 3 days. However, we did not detect any statistically significant differences between complete WT mice (WT→WT) and complete NLRC4 deficient animals (NLRC4$^{-/-}$→NLRC4$^{-/-}$) (Fig.3.23C). In addition, the susceptible BM chimeras in which NLRC4 was specifically ablated in the epithelium (WT→NLRC4$^{-/-}$) expressed significantly more *Ear1/2* than both complete WT and complete NLRC4 deficient animals at d3 p.i. (Fig.3.23C), suggesting that the reduced *Ear* expression levels were not associated with NLRC4 deficiency in the epithelium. It is possible that eosinophil functions in NLRC4-deficient animals are altered at steady state, but this is most likely not associated with the severe phenotype induced by *C. rodentium*

Figure 3.24

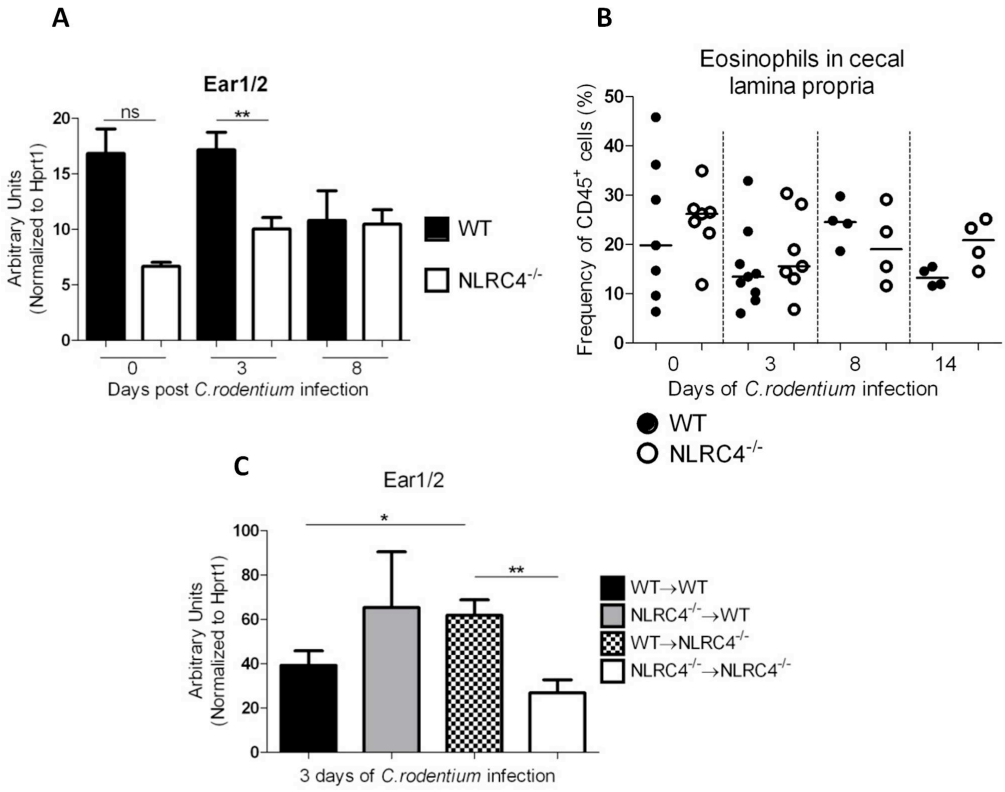


Figure 3.24 WT and *Nlrc4*$^{-/-}$ mice harbour equivalent eosinophil frequencies in the cecal lamina propria.

WT and *Nlrc4*$^{-/-}$ mice were infected for 0, 3, 8, or 14 days with *C. rodentium. (*A) *Ear1/2* mRNA expression was assayed in whole cecal tissue. Data represent mean expression levels ±SEM, normalised to *Hprt* (n=3 for D0, n=5 for D3 and D8). (B) LPL were isolated from cecal tissue and stained with a panel of cell surface markers. Cells were gated on CD45^{+}F4/80^{+}MHCII^{-}CD11b^{+}Siglec-F^{+}. Each symbol represents an individual mouse and horizontal bars indicate group median values. Values for day 0 and day 3 p.i. are pooled from 2 independent experiments and values for day 8 p.i. and day 14 p.i. are from a single experiment (n=4-9 per group). (C) *Ear1/2* mRNA expression was measured in cecal samples from chimeric mice that had been infected for 3 days with *C. rodentium*. Data represent mean expression levels ±SEM normalised to *Hprt* from 2 pooled experiments (n=8-10 per group). The non-parametric Mann-Whitney test was used for statistical analysis, *P<0.05, **P<0.01.

3.3 Discussion

In this study we have shown protective effects of the NLRC4 inflammasome during acute colitis induced by enteropathogenic *C. rodentium.* We found that *Nlrc4*$^{-/-}$ mice developed severe intestinal inflammation during *C. rodentium* infection and that this was correlated with highly increased bacterial colonisation of the tissue. Supporting this hypothesis was our finding that treatment of WT mice with broad-spectrum antibiotics resulted in increased *C. rodentium* colonisation of the cecal tissue concomitant with exacerbated damage of the epithelium.

A recent report showed that *Nlrc4*$^{-/-}$ mice harboured increased *C. rodentium* burdens in the stool after 17 and 21 days of infection.[158] However, we found that *Nlrc4*$^{-/-}$ mice displayed around 1000-fold increased tissue adherent bacteria compared with WT mice in the cecum as early as day 3 p.i. and that this persisted at least until day 8 p.i.. By this time *Nlrc4*$^{-/-}$ mice had developed severe cecal inflammation, suggesting that defective early innate host protective responses led to increased colonisation that precipitated immunopathology.

Robust Th17 responses are induced during acute *C. rodentium* infection.[244] *Nlrc4*$^{-/-}$ mice developed similar Th17 responses to WT mice, but the overall CD4^{+}T-cell recruitment to the cecum was increased by day 14 p.i.and total tissue IL-17A was elevated d8 and d14 p.i., indicating additional sources of IL-17A, such as γδ T-cells.[316] Th17 cells have been associated with protective effects during *C. rodentium* infection. Although *in vitro* stimulation of macrophages and an intestinal epithelial cell line with IL-17A was shown to induce IL-1β and GM-CSF,[87] transfer of *in vitro* polarised Th17 cells only marginally increased survival of IL-22 deficient mice during *C. rodentium* infection.[98] Furthermore, IL-23 deficient mice, which developed severe disease during

C. rodentium infection, displayed similar Th17 induction as WT mice 8 days p.i., suggesting that early accumulation of Th17 cells is largely redundant for protective or pathogenic effects during *C. rodentium* infection.[244] However, IL-17A deficient mice were shown to develop moderately increased pathology and harbour elevated bacterial burdens in the colon tissue after 14 days of *C. rodentium* infection, revealing a contribution of the cytokine IL-17A to host defence.[87]

Nlrc4$^{-/-}$ mice developed strong Th1 responses in the cecum and highly increased tissue production of IFN-γ. Both WT and *Nlrc4*$^{-/-}$ mice exhibited Th1 induction in the colon, correlating with inflammation and probably associated with immunopathology. *C. rodentium* infection is known to induce the production of IFN-γ and accumulation of Th1 cells.[237] IFN-γ$^{-/-}$ mice were shown to develop exacerbated disease and transfer of WT, but not of IFN-γ deficient, antigen-specific T-cells resulted in reduced pathology, reduced colonisation levels and increased IgG production.[237] Adaptive immune responses have also been reported to mediate depletion of goblet cells in the intestinal barrier, thereby reducing *C. rodentium* colonisation levels.[246] Lymphocyte deficient *Rag*$^{-/-}$*Nlrc4*$^{-/-}$ mice developed less severe intestinal inflammation compared with their lymphocyte replete counterparts, but displayed systemic translocation of the bacteria. This is consistent with a host protective effect of Th1 cells, which in the context of innate immune deficiency was amplified and manifested as immunopathology in *Nlrc4*$^{-/-}$ mice.

IL-23 has been shown to be essential for protection during *C. rodentium* infection as IL-23-deficient mice failed to mount inflammatory responses in the tissue and mortality reached 100% by around day 10.[244] During the early stages of *C. rodentium* infection IL-23 is necessary for IL-22 production by ILCs and subsequent IL-22 mediated protective effects, such as the secretion of AMPs by intestinal epithelial cells.[59, 60]

However, we could show that *Nlrc4*$^{-/-}$ mice did not have a baseline deficiency in either IL-22 or IL-22 induced protective AMP responses. In fact, the induction of Reg-proteins was increased during infection, suggesting elevated IL-22 responses. Thus, susceptibility in *Nlrc4*$^{-/-}$ mice did not appear to be due to impaired early IL-22/AMP responses.

We also observed increased systemic immune responses in that *Nlrc4*$^{-/-}$ mice infected with *C. rodentium* developed exacerbated weight loss and mounted increased *C. rodentium* specific serum IgG antibodies compared with WT mice. Similarly caspase-1 deficient mice, which exhibited increased colonisation and pathology during *C. rodentium* infection, developed elevated serum IgG and IgM responses.[158] Antibody production serves to eradicate *C. rodentium* [247, 299]and it is plausible that NLRC4 activation mediates important innate immune responses early during infection, which will limit *C. rodentium* colonisation and reduce the exposure of *C. rodentium* antigens to the systemic immune system. However, little systemic translocation of *C. rodentium* occurred, implicating that the increased systemic responses mainly are due to a mucosal defect.

NLRC4 inflammasome activation results in the production and release of IL-1β and although IL-1α is not directly cleaved by caspase-1, the two IL-1 cytokines are often co-secreted.[198] IL-1 receptor expression is necessary for surviving *C. rodentium* infection.[241] However, during *C. rodentium* infection, we could not detect any reduction in IL-1β or IL-1α production in the intestines of *Nlrc4*$^{-/-}$ mice compared with WT mice. If anything, IL-1α production was slightly increased in *Nlrc4*$^{-/-}$ mice during later stage infection. NLRC4 dependent production of IL-1β has been shown to mediate accumulation of neutrophils during infection in the lung with the extracellular pathogen *Klebsiella pneumonia* and NLRC4 deficient mice developed reduced disease and

suffered from increased mortality.[306] NLRC4 deficiency was also associated with reduced neutrophil recruitment and increased pathology during oral infection with *Candida albicans*.[307] In contrast, we observed increased granulocyte recruitment to the cecal tissue as early as day 3 post-infection, a time point when there is no apparent pathology. A caveat of measuring IL-1β in explant culture supernatant by ELISA is the inability to distinguish between the inactive pro-form and the active subunit. Analysis by western blotting would be preferable. Furthermore, investigating the presence of inhibitory IL-1RA[196] would more fully illuminate a potential contribution of IL-1 cytokines by the NLRC4 inflammasome.

During *Klebsiella pneumoniae* infection,[306] the protective effect of NLRC4 was indicated to be dependent on hematopoietic NLRC4 expression. In contrast, our findings showed that the protective effect of NLRC4 during *C. rodentium* infection was dependent on expression in non-hematopoietic cells. In the mouse model of oral Candidiasis, non-hematopoietic expression of NLRC4 was identified as the dominant protective moiety, with effects on colonisation, systemic translocation and pathology.[307] However, in the Candidiasis study, complete *Nlrc4*$^{-/-}$ mice displayed reduced expression of AMPs, which do not correspond with our observations in the context of *C. rodentium* infection.

We further evaluated NLRC4 expression in mucosal cells by isolating several cellular compartments of the intestinal tissue. NLRC4 mRNA expression was high in isolated intestinal epithelial crypts, while intestinal stromal cells did not express NLRC4; indicating that NLRC4 expression in non-hematopoietic cells in the large intestine was limited to IEC. Innate immune signalling by TLRs in IEC is known to contribute to maintenance of epithelial barrier function and to protection from microbial-induced pathology.[7, 265] Expression of NLRC4 and NLRP6 in colonic IECs has been reported.[162,

[296] Our results suggest that the cytosolic sensor NLRC4 mediates detection of bacterial infection in IECs, which is previously undescribed. Infection with the intestinal pathogen *Salmonella typhimurium* revealed that NLRC4 was redundant for host protection, although *Nlrc4*$^{-/-}$ mice of a different genetic background were reported to exhibit increased susceptibility.[143, 190, 192] A recent study showed that *Asc*$^{-/-}$ and *Nlrp3*$^{-/-}$ mice were hypersusceptible to *C. rodentium* infection.[158] In accordance with the latter study, our data clearly show that in the case of sensing of an extracellular bacterial pathogen in the epithelium, NLR redundancy is not applicable.

There are no reports directly describing inflammasome activation in epithelial cells, but non-hematopoietic expression of NLRP3 has been shown to mediate protection during DSS colitis, possibly by promoting IL-18 secretion by IEC.[157] Furthermore, NLRP6 was found to be highly expressed in intestinal epithelial cells.[162] *Nlrp6*$^{-/-}$ mice produced less IL-18 in the colon at steady state and developed increased inflammation during DSS administration.[162] The importance of non-hematopoietic NLR expression for protective functions during intestinal inflammation, together with our data, support a new paradigm of epithelial inflammasome activation, which appears to contribute both to intestinal homeostasis and host defence.

However, IL-18 was not induced in WT mice during *C. rodentium* infection and levels were comparable between WT and *Nlrc4*$^{-/-}$ mice throughout the infection. *Nlrc4*$^{-/-}$ mice displayed reduced IL-18 levels at steady state, both in the cecum and in the colon, suggesting that the NLRC4 inflammasome is constitutively active in the gut, possibly sensing the commensal flora. Further supporting this hypothesis was our finding that caspase-1 activation was reduced in steady state in NLRC4 deficient cecal tissue. The level of IL-18 production and caspase-1 activation in mice treated with antibiotics or kept in germfree facilities would be interesting to analyse in order to address the impact

of microflora on NLRC4 mediated caspase-1 activation and IL-18 production. IL-18 deficient mice have been reported to develop exacerbated pathology during *C. rodentium* infection and harboured increased bacterial burdens after 2 weeks of colonisation.[158, 241] Furthermore, treatment of hyper-susceptible caspase-1 deficient mice with recombinant IL-18 ameliorated intestinal damage caused by DSS.[157] We hypothesised that baseline IL-18 reduction could influence early immune responses and subsequent disease in *Nlrc4*$^{-/-}$ mice. However, treatment with recombinant IL-18 did not reduce initial colonisation or development of disease in *Nlrc4*$^{-/-}$ animals, arguing against a major role of baseline IL-18 in NLRC4-mediated innate immune defences to acute bacterial infection in the gut.

C. rodentium is known to induce cell death in the intestinal epithelium upon infection.[301] NLRC4 inflammasome activation is also associated with pyroptosis, a type of rapid, lytic cell death.[175] It is possible that this inflammasome triggered type of cell death, a phenomenon little studied *in vivo*, could be an NLRC4 mediated process in IEC, with effects on colonisation and disease. Pyroptosis has mainly been measured by quantifying lactate dehydrogenase (LDH) release using *in vitro* systems.[317] Enterocytes are very challenging to culture *ex vivo*. An alternative to a complex, *in vivo* setting could be to establish organoid *ex vivo* cultures,[318] in which stem cell derived intestinal crypts could be manipulated and the effects of *C. rodentium* infection studied.

The precise mechanism of how cytosolic NLR such as NLRC4 detect ligands is unknown. The NLRC4 inflammasome is activated after sensing cytosolic flagellin or components of bacterial type 3 secretion systems. Although *C. rodentium* is immotile,[319] it expresses a T3SS and it is possible that a T3SS component could be translocated into the cytosol and provide the activating ligand. However, a recent study showed that NLRC4 and the T3SS were dispensable for inflammasome activation

following *C. rodentium* infection of macrophages *in vitro*.[158] A non-canonical inflammasome, dependent on caspase-11 and NLRP3, was described to be activated in macrophages infected with *C. rodentium*.[320] Caspase-11 had been known to mediate caspase-1 processing of IL-1β and *Caspase-11*$^{-/-}$ mice are resistant to septic shock[321] but recent publications have shown that interaction between caspase-11 and caspase-1 is a prerequisite for NLRP3 inflammasome formation and production of active IL-1β in macrophages in response to certain gram-negative bacteria.[320, 322] NLRC4 expression was shown to be dispensable in this context. However, cell death in response to *S. typhimurium* infection of macrophages was dependent on sensing of flagellin and did not require caspase-11,[174] further supporting that the non-canonical inflammasome did not include NLRC4. Caspase-11 has been reported to be constitutively expressed in the intestine,[323] but it is not clear whether IEC express caspase-11. There is some evidence that caspase-11 is activated by intracellular LPS and the lipid A motif,[324] but whether *C. rodentium* LPS is translocated into IEC is unknown. Generation of *C. rodentium* with mutated LPS could illuminate the requirement of NLRC4 and NLRP3 for host protection.

A microarray was performed on cecal tissue 3 days p.i. Reduced expression of eosinophil associated proteins was detected and further investigated, but intestinal eosinophil frequencies were not altered in *Nlrc4*$^{-/-}$ mice compared with WT mice. This does not exclude possible altered function of these cells. Although the protective effect of NLRC4 was dependent on expression in non-hematopoietic cells, we reasoned that perturbations in IEC could affect the recruitment and maintenance of hematopoietic cells in the intestine in the steady state. Considering that eosinophils constitute approximately 30% of the hematopoietic cells in the large intestine,[44] altered recruitment or function of these cells could result in effects secondary to the initial

epithelial defect. A microarray performed on isolated intestinal crypts instead of whole tissue could be instrumental in separating the initial epithelial responses from any subsequent modulation of the endothelium and accumulation of hematopoietic cells.

An overview of our findings is presented in figure 3.25. In conclusion, our data reveal non-redundant protective effects of NLRC4 activation in non-hematopoietic cells, most likely IEC, for limiting colonisation by an extracellular pathogen and reducing subsequent intestinal damage.

Figure 3.25

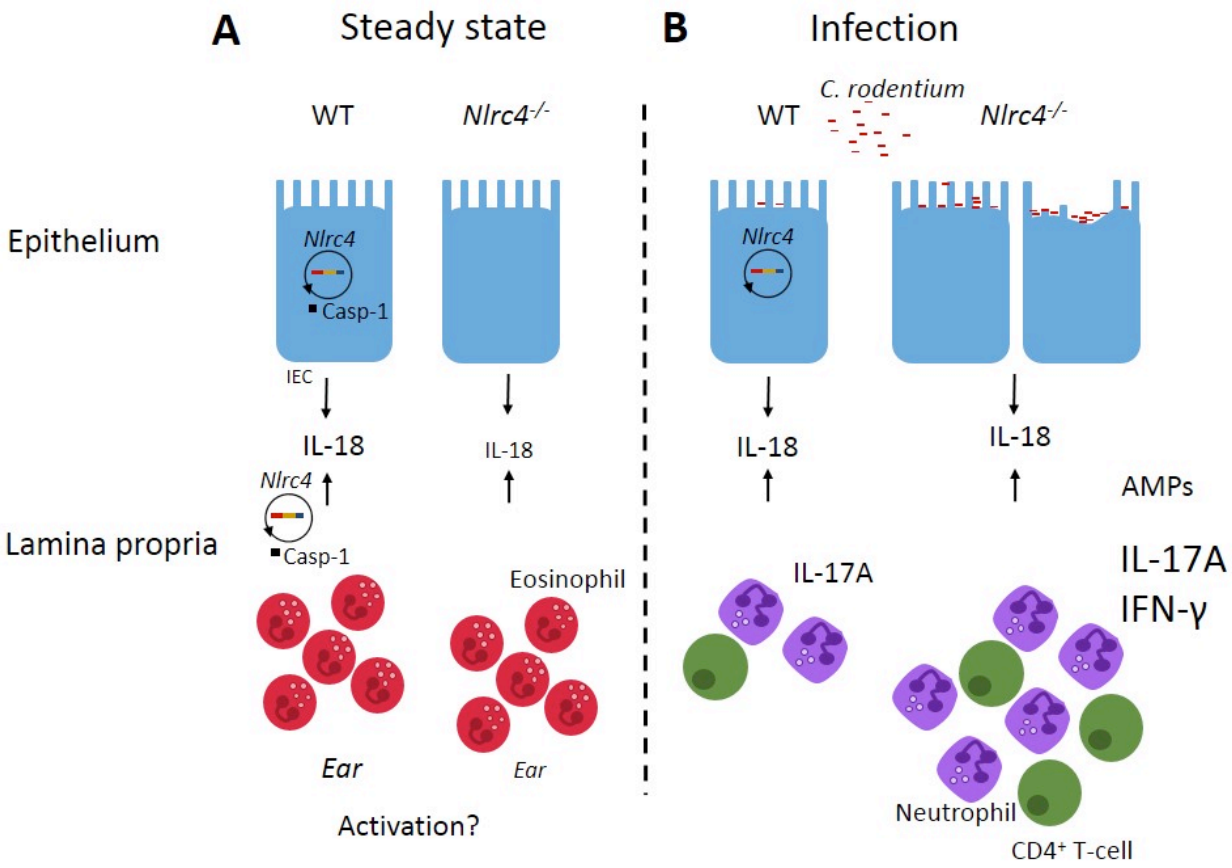


Figure 3.25 NLRC4 expression contributes to innate immunity in the large intestinal mucosa

(A) Steady state: NLRC4 contributes to basal immune activation in the mucosa. NLRC4 is expressed in both IEC and lamina propria leukocytes, but not in stromal cells. NLRC4 deficiency is linked with ablated caspase-1 activation and reduced production of IL-18. In addition, expression of several eosinophil associated Ear proteins are reduced in NLRC4 deficient mice, but eosinophil numbers in the lamina propria are equivalent to WT mice. This could suggest that NLRC4, directly or indirectly, affects activation status or functions in innate cells of the lamina propria. (B) Intestinal infection: NLRC4 expression in non-hematopoietic cells limits bacterial colonisation and subsequent immune activation and pathogenesis. NLRC4 deficiency is associated with increased bacterial colonisation and more potent innate and adaptive immune responses. Expression levels of AMPs are highly elevated, increased numbers of neutrophils are recruited to the tissue and IL-18 production is induced to levels equivalent to those in WT mice. The exacerbated pathology correlates with increased recruitment of Th1 and Th17 cells, as well as increased production of IFN- γ and IL-17A in the tissue.

Chapter 4: Role of NLRC4 in chronic bacterially triggered intestinal inflammation

4.1 Introduction

Infection of WT mice with the intestinal bacterium *H. hepaticus* results in life-long colonisation of the gut mucosa, but is normally not associated with any apparent pathological changes in immunocompetent hosts.[261] However, infection results in the expansion of *H. hepaticus* specific effector $CD4^+$ T-cell populations and the development of antigen specific serum IgG responses.[259, 262] *H. hepaticus* also induces dominant immunoregulatory Treg cell responses that suppress immunopathological $CD4^+$ T-cell responses in an IL-10-dependent manner.[263] Thus, IL-10R blockade by administration of anti-IL-10R mAb overcomes Treg-mediated suppression and allows the expression of *H. hepaticus*-specific effector $CD4^+$ T-cell responses resulting in severe typhlocolitis.[259, 263] In addition, anti-IL-10R mAb might have more general suppressive effects, considering that IL-10R is widely expressed by hematopoietic cells.[325] The IBD-like pathology induced by *H. hepaticus* in this dysregulated state has previously been shown to depend on IL-23 and was associated with potent Th1 and Th17 responses.[259, 263]

H. hepaticus is dependent on functional flagella for successful *in vivo* infection.[326] In addition, $CD4^+$ T-cells specific for *H. hepaticus* flagellar hook protein, FlgE, were able to produce IFN-γ and elicit intestinal inflammation when transferred into *H. hepaticus* infected B6*Rag1*$^{-/-}$ mice.[327] Furthermore, detection of flagellin by NLRC4 has been shown to be dependent on conserved motifs[328] and flagellin from *H. hepaticus* could be

a possible agonist. However, direct activation of NLRC4 has only been described in the context of bacterial pathogens carrying T3SS or T4SS. *H. hepaticus* does not express these secretion systems, although it was known to harbour a pathogenicity island (PAI), containing T4SS gene homologs.[329] PAI are large genomic segments, encoding virulence factors, thought to have been acquired through lateral gene transfer from other organisms.[330] More recently this *H. hepaticus* PAI was shown to encode a bacterial type 6 secretion system (T6SS).[331] *H. hepaticus* strains with complete or partial deletion of the PAI induced less severe hepatitis in susceptible A/JCr mice.[329]

A/JCr mice, which are known to develop hepatic carcinomas during long-term *H. hepaticus* colonisation, are carriers of a defective Naip5 allele, resulting in the production of a protein with reduced function.[332, 333] The cytosolic NLR Naip5 had been reported to respond to a conserved region of flagellin and Naip5 expression was essential for NLRC4 inflammasome activation in macrophages infected with *Legionella pneumophila*.[328] Thus, the potential reduction of NLRC4 signalling in mice susceptible to *H. hepaticus* infection suggested that NLRC4 might be important for host defence.

The aim of our studies was to investigate if NLRC4 contributed to immune responses during chronic, bacterially triggered intestinal inflammation. We used a T-cell mediated and an innate immune mediated model of intestinal inflammation, both based on infection with *H. hepaticus*. The use of complimentary models would allow for the study of the impact of NLRC4 on the development of pathogenic T-cell responses as well as innate immune circuits. Whether *H. hepaticus* could activate NLRC4 directly, or if the stimuli could be derived from the commensal flora, were open questions.

4.2 Results

4.2.1 NLRC4 is dispensable for the development of *Helicobacter hepaticus*-induced T-cell dependent intestinal inflammation

PRR circuits have been implicated in *H. hepaticus*-induced IBD as hematopoietic expression of the TLR adaptor molecule MyD88 is required for pathogenesis.[265] In order to investigate a possible contribution of NLRC4 in this process, we employed the *H. hepaticus* driven T-cell dependent IBD model by subjecting WT and *Nlrc4*$^{-/-}$ mice to *H. hepaticus* (Hh) infection and concomitant treatment with IL-10 receptor blocking mAb (αIL-10R).[259] Control groups included mice that were either infected with *H. hepaticus* or treated with αIL-10R alone. After 4 weeks mice were sacrificed and pathological changes in the cecum and colon were evaluated. As previously reported, αIL-10R treatment alone did not induce pathology in WT animals (Fig.4.1A). Similar results were obtained for *Nlrc4*$^{-/-}$ mice, confirming that the commensal flora alone could not induce pathology (Fig.4.1A). As expected, WT or *Nlrc4*$^{-/-}$ mice infected with *H. hepaticus* alone developed negligible disease in the cecum or colon, excluding any requirement for NLRC4 in inducing *H. hepaticus* protective Treg cell responses (Fig.4.1A,B). In contrast, WT mice that were infected with *H. hepaticus* and treated with αIL-10R mAb (Hh+αIL-10R) developed severe typhlitis and colitis, characterized by crypt hyperplasia, goblet cell depletion, crypt abscesses, edema and marked leukocytic infiltration (Fig.4.1A,B). We observed similarly severe inflammatory responses in the cecum and colon of *Nlrc4*$^{-/-}$ mice following Hh+αIL-10R treatment, indicating that NLRC4 was dispensable for the development of intestinal inflammation in response to *H. hepaticus* in the absence of regulatory IL-10 (Fig.4.1A, B).

Figure 4.1

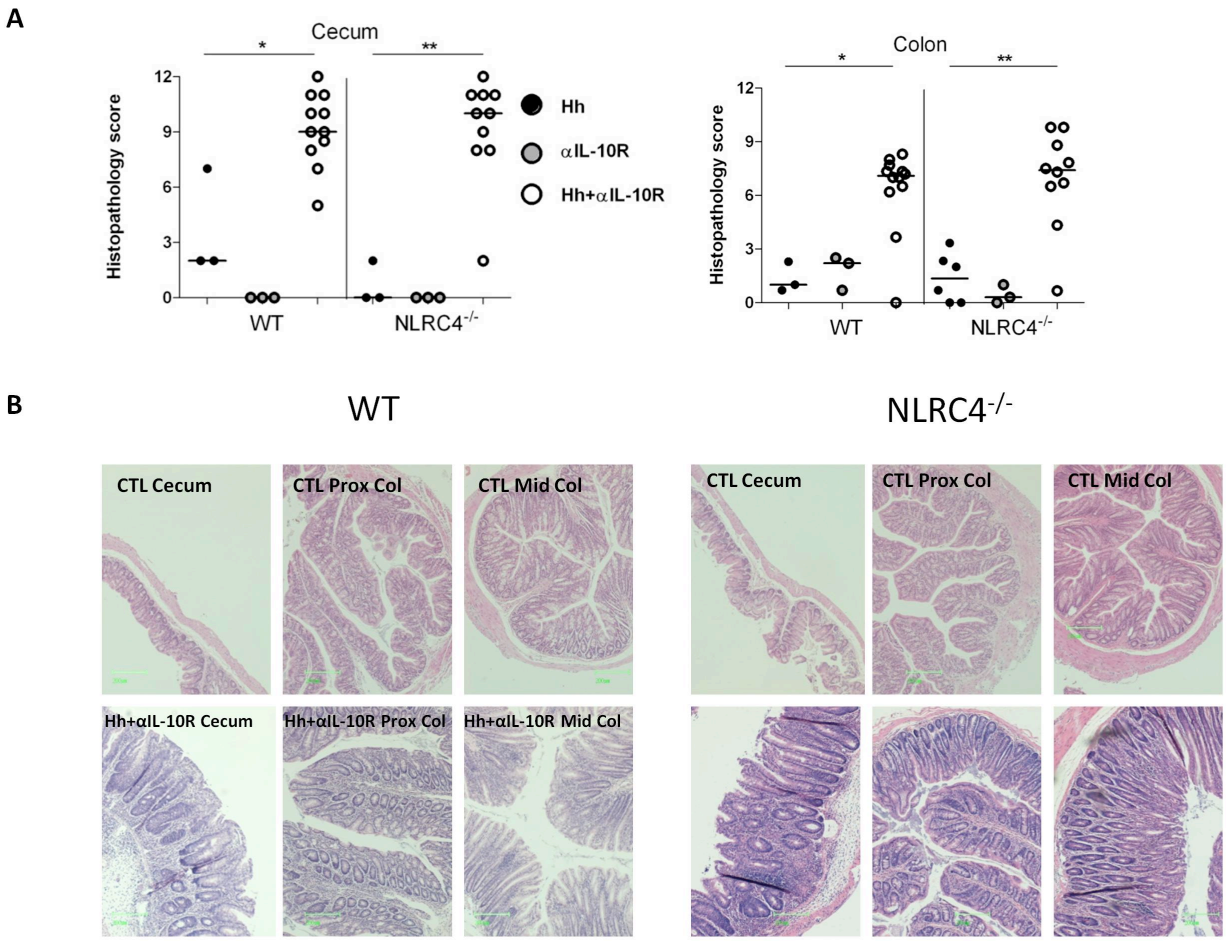


Figure 4.1 NLRC4 is dispensable for the development of *H. hepaticus* driven T-cell dependent intestinal inflammation.

WT and *Nlrc4*$^{-/-}$ mice were infected by oral gavage with approximately 10^8 CFU *H. hepaticus* and treated with 1 mg IL-10 receptor blocking antibody (Hh+αIL-10R) i.p. weekly for 4 wks. Controls included mice treated with αIL-10R alone (αIL-10R) or infected with *H. hepaticus* alone (Hh). (A) Intestinal pathology was evaluated in the cecum and colon. Each symbol represents an individual mouse and horizontal lines are group median values. Results are pooled from 2 independent experiments and the non-parametric Mann-Whitney test was used for statistical analysis, *P<0.05, **P<0.01. (B) Representative micrographs of cecum, proximal and mid colon. Magnification 5x. Control (CTL) sections are from animals that were untreated and uninfected.

4.2.2 NLRC4 is dispensable for the development of Th1 and Th17 responses in the intestine

H. hepaticus driven T-cell dependent IBD is characterized by the induction of Th1 and Th17 responses, and IFN-γ deficient animals developed reduced disease.[259] We isolated colonic LPL from Hh+αIL-10R treated WT or *Nlrc4*$^{-/-}$ mice, restimulated the cells with PMA and ionomycin and performed intracellular stains for IFN-γ and IL-17A. Consistent with the comparable levels of intestinal inflammation, quantification of cells recovered from LPL isolation showed equivalent total cell numbers in Hh+αIL-10R treated WT and *Nlrc4*$^{-/-}$ mice (Fig.4.2A). Furthermore, we found that Hh+αIL-10R treated WT and *Nlrc4*$^{-/-}$ mice had similar frequencies of Th1 and Th17 cells in colonic LPL (Fig.4.2B). In conjunction with intestinal inflammation, Hh+αIL-10R treatment induces systemic inflammation. We assessed spleen weights and spleen granulocyte numbers in Hh+αIL-10R treated mice and found that *Nlrc4*$^{-/-}$ mice developed systemic immune responses equivalent to WT mice (Fig.4.2C,D).

Figure 4.2

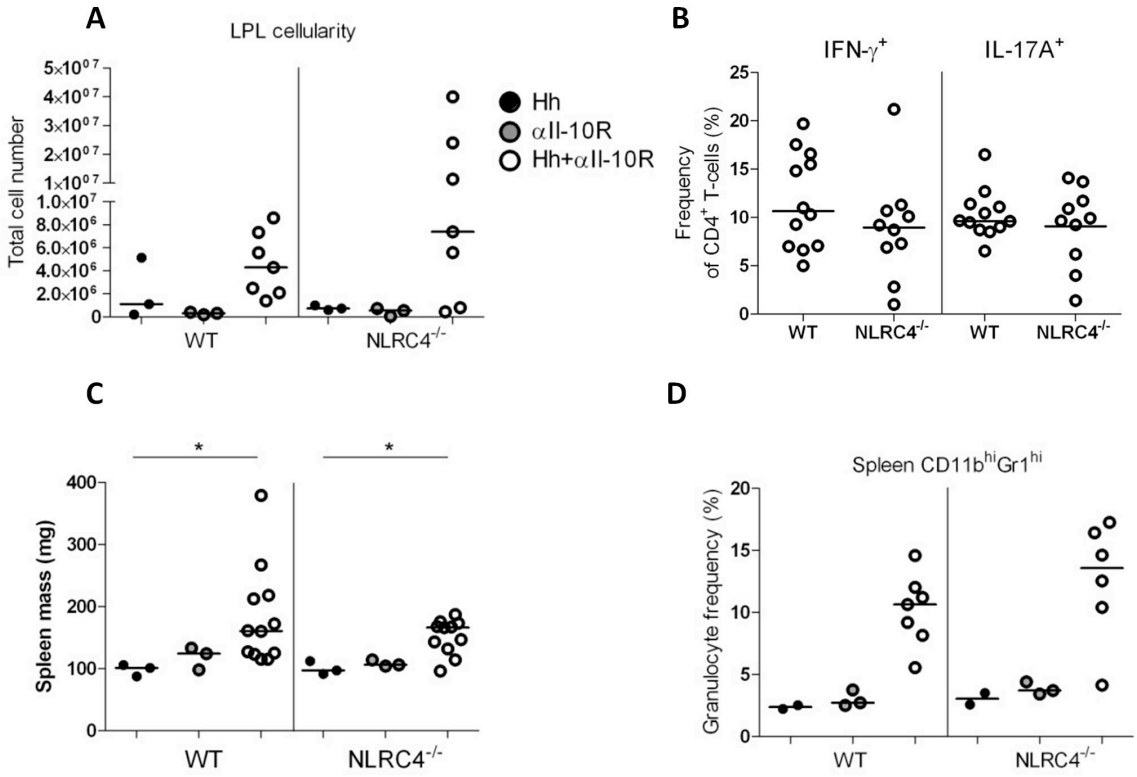


Figure 4.2 NLRC4 is dispensable for the development of *H. hepaticus*-driven pathogenic intestinal Th1 and Th17 responses.

WT and *Nlrc4*$^{-/-}$ mice were infected by oral gavage with approximately 10^8 CFU *H. hepaticus* and treated with 1 mg IL-10 receptor blocking antibody (Hh+αIL-10R) i.p. weekly for 4 wks. Controls included mice treated with αIL-10R alone (αIL-10R) or infected with *H. hepaticus* alone (Hh). LPL were isolated from the colon, restimulated with PMA (0.1µg/ml), ionomycin (1µg/ml) and Brefeldin A (10µg/ml) for 3h. Cell were stained for surface markers CD4 and TCRβ. Intracellular staining for IL-17A and IFN-γ was performed. (A) Total LPL cellularity. (B) Frequencies of IFN-γ^+ and IL-17^+ $CD4^+$ LPL (C) Spleen mass. (D) Spleen granulocyte frequencies. Each symbol represents an individual mouse and horizontal bars indicate group median values. (A) and (D) Data are representative of 1 experiment, n= 7 for Hh+αIL-10R, n=3 for Hh and αIL-10R respectively. For (B) and (C) data are pooled from 2 independent experiments, n=10-12 per group. Statistical analysis was performed using the non-parametric Mann-Whitney test, *P<0.05.

4.2.3 NLRC4 limits *H. hepaticus* colonisation during T-cell dependent intestinal inflammation

H. hepaticus has been shown to penetrate deep into the intestinal crypts in the large intestine.[260] A well-established system of quantifying *H. hepaticus* colonisation is by the isolation of DNA from cecal contents and subsequent qPCR.[285] We measured *H. hepaticus* colonisation levels in cecal contents of mice that had been infected and treated (Hh+ αIL-10R) for four weeks. Interestingly, we found that inflamed *Nlrc4*$^{-/-}$ mice (Hh+ αIL-10R) harboured significantly higher loads of *H. hepaticus* in the cecal contents compared with their WT counterparts (Fig.4.3). Although there was a similar trend in mice that were infected with *H. hepaticus* (Hh) alone, the small sample size of these groups precluded any firm conclusions (Fig.4.3). The higher *H. hepaticus*, colonisation levels found in the Hh+ αIL-10R treated *Nlrc4*$^{-/-}$ mice, and our findings that NLRC4 limited acute colonisation by *C. rodentium*, led us to hypothesise that NLRC4 might play a role in the initial stages of *H. hepaticus* infection. We therefore decided to investigate the responses in *Nlrc4*$^{-/-}$ mice during the onset of *H. hepaticus* driven T-cell dependent typhlocolitis.

Figure 4.3

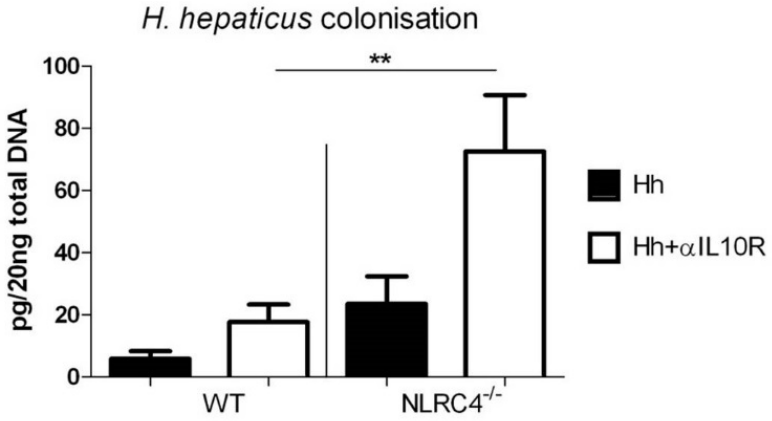


Figure 4.3 NLRC4 limits *H. hepaticus* colonisation during T-cell dependent intestinal inflammation.

WT and *Nlrc4*$^{-/-}$ mice were infected by oral gavage with approximately 10^8 CFU *H. hepaticus* and treated with 1mg IL-10 receptor blocking antibody (Hh+αIL-10R) i.p. weekly for 4 wks. Controls were infected with *H. hepaticus* alone (Hh). Mice were sacrificed after 4 wks, cecal contents were collected, DNA extracted and *H. hepaticus* colonisation levels assayed by qPCR. Data represent mean *H. hepaticus* DNA levels ±SEM pooled from 2 independent experiments; Hh, n=2 per group; Hh+αIL-10R, n=10-11 per group. The non-parametric Mann-Whitney statistical test was used, **P<0.01.

4.2.4 NLRC4 expression during the onset of *H. hepaticus* driven T-cell dependent colitis is dispensable for the development of intestinal inflammation

To study the onset of the disease at an earlier stage, WT and *Nlrc4*$^{-/-}$ mice were infected and treated (Hh+αIL-10R) for 2 weeks, with sacrifice on day 14 p.i. Although typhlitis was more variable in WT mice at this early time point, the majority had developed pathological changes in the cecal tissue (Fig.4.4A). Similarly, colon pathology in WT mice was also slightly reduced at 2wks p.i., with a median score of approximately 4 (Fig.4.4B), compared with a median score of around 7 at 4 wks p.i. (Fig.4.1B). We found that after 2 wks of Hh+αIL-10R treatment *Nlrc4*$^{-/-}$ mice had developed comparable typhlitis to WT mice (Fig.4.4A) and although they exhibited a trend towards increased colitis scores (Fig.4.4B), the difference was not statistically significant, suggesting that NLRC4 does not play a major role in regulating the onset of *H. hepaticus*-induced T cell-dependent IBD colitis (Fig.4.4A,B). Further supporting this conclusion was the finding that intestinal Th1 and Th17 responses were equivalent in both genotypes after 2 wks of Hh+αIL-10R treatment (Fig.4.4C). Conversely, the total accumulation of leukocytes in the colonic LP of *Nlrc4*$^{-/-}$ mice was significantly increased compared with WT mice after 2 wks of Hh+αIL-10R treatment, suggesting that enhanced immune activation was occurring (Fig.4.4D). We investigated this further by assessing the recruitment of innate leukocytes.

Figure 4.4

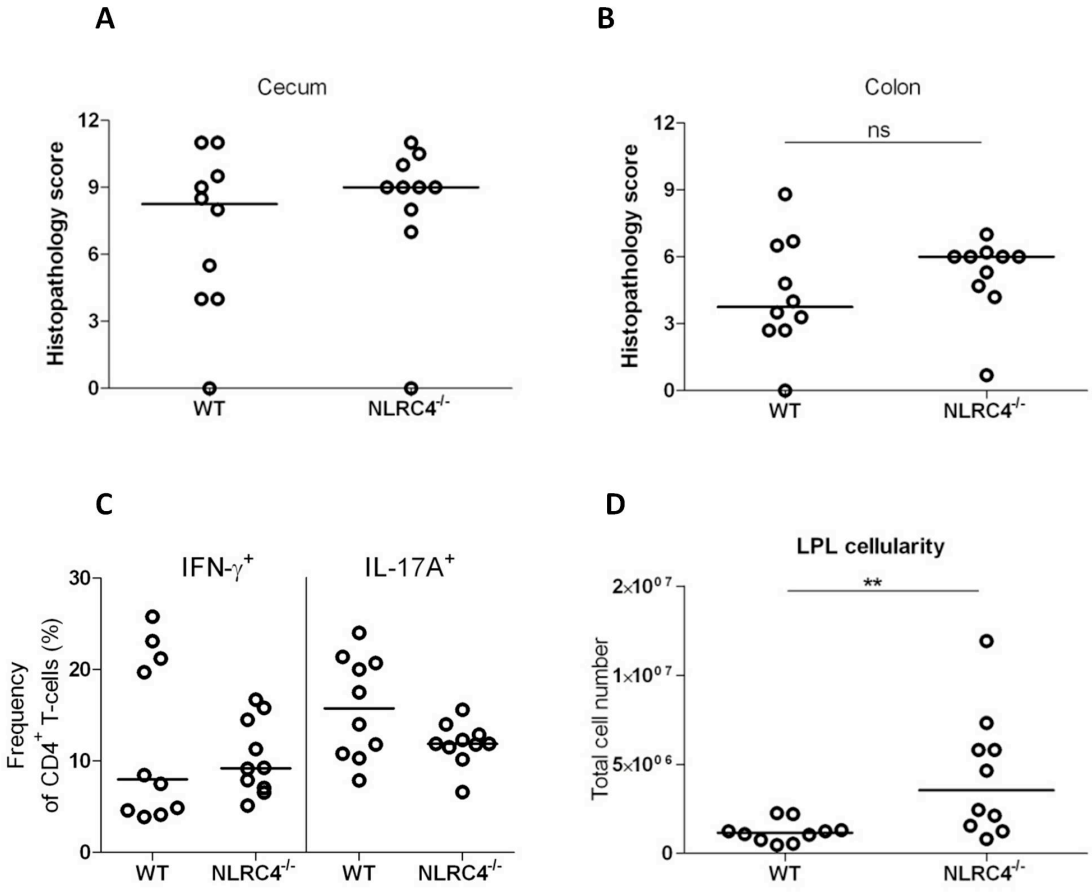


Figure 4.4 NLRC4 does not regulate the onset of *H. hepaticus* driven T-cell dependent intestinal inflammation.

WT and *Nlrc4*$^{-/-}$ mice were infected by oral gavage with approximately 10^8 CFU *H. hepaticus* and treated with 1 mg IL-10 receptor blocking antibody (Hh+αIL-10R) i.p. weekly for 2 wks. (A) Histopathology scores for cecum. (B) Histopathology scores for colon. (C) Frequencies of Th1 and Th17 CD4$^+$ T cells in colon LPL. (D) Total colon LPL cell numbers. Each symbol represents an individual mouse, horizontal bars represent group median values and data were pooled from 2 independent experiments (n=10 per group). The non-parametric Mann-Whitney statistical test was used for analysis, **P<0.01.

4.2.5 NLRC4 restrains systemic and local granulocyte accumulation during the onset of *H. hepaticus* mediated T-cell dependent colitis

To examine whether NLRC4 regulated the accumulation of innate leukocytes in the inflamed intestine during *H. hepaticus*-induced T cell-mediated IBD, we assessed the proportion of $CD11b^{hi}Ly6G^{+}$ granulocytes in colon LPL isolated from WT and *Nlrc4*$^{-/-}$ mice after 2 weeks of Hh+αIL-10R treatment. We found that granulocytes were barely detectable among LPL isolated from uninfected mice (Control) or mice infected with *H. hepaticus* alone (Hh) (Fig.4.5A). However, after 2 weeks of Hh+αIL-10R treatment, WT mice exhibited significant granulocyte recruitment to the colon LP, (Fig.4.5A). Furthermore, Hh+αIL-10R treated *Nlrc4*$^{-/-}$ animals had significantly increased granulocyte frequencies in the colon LP compared with WT animals (Fig.4.5A). In addition, at this early 2wk time point, Hh+αIL-10R treated *Nlrc4*$^{-/-}$ mice had significantly increased splenomegaly and spleen granulocyte numbers (Fig.4.5C) in comparison with their WT counterparts (Fig.4.5B,C). Finally, when we assessed *H. hepaticus* colonisation levels after 2 weeks of Hh+αIL-10R treatment, we found a strong trend towards increased bacterial burdens in *Nlrc4*$^{-/-}$ mice (Fig.4.5D). These results suggest that although NLRC4 might mediate protective effects by affecting *H. hepaticus* colonisation levels and restraining granulocyte accumulation at the early stages of infection, this is of minor impact for the overall induction and maintenance of chronic $CD4^{+}$ T-cell dependent intestinal inflammation.

Figure 4.5

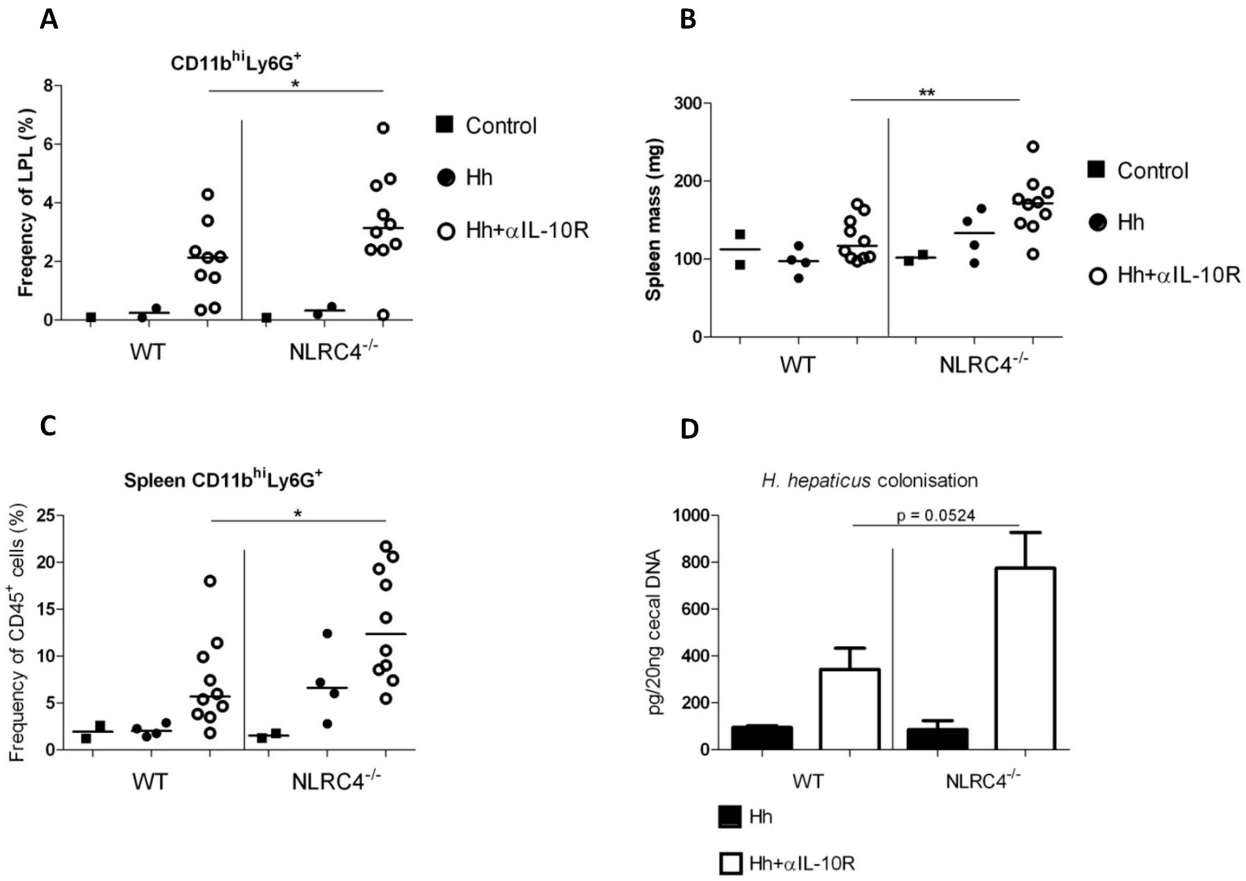


Figure 4.5 NLRC4 restrains granulocyte recruitment during the onset of *H. hepaticus* driven T-cell dependent colitis.

WT and *Nlrc4*$^{-/-}$ mice were infected by oral gavage with approximately 10^8 *H. hepaticus* and treated with 1 mg IL-10 receptor blocking antibody (Hh+αIL-10R) i.p. weekly for 2 wks. Controls included uninfected (Control; n=2 per genotype, pooled for 1 sample) and mice infected with *H. hepaticus* alone (Hh; n=4 per genotype, pooled for 2 samples). (A) Frequencies of CD11b^{hi}Ly6G$^+$ granulocytes in colon LPL. (B) Spleen weights. (C) Frequencies of CD11b^{hi}Ly6G$^+$ granulocytes in spleen. (D) *H. hepaticus* cecal DNA levels ±SEM. Each symbol represents an individual mouse, horizontal bars represent group median values and data were pooled from 2 independent experiments (Hh+αIL-10R, n=10 per group; Hh, n=4 per group). Statistical significance was assessed using the non-parametric Mann-Whitney test, *P<0.05, **P<0.01.

4.2.6 NLRC4 expression does not affect long-term *H. hepaticus* colonisation

In parallel with the characterisation of NLRC4 in *H. hepaticus* triggered T-cell dependent IBD, we performed long-term *H. hepaticus* infection experiments in order to assess whether NLRC4 influenced persistent colonisation and host responses. Thus, WT and *Nlrc4*$^{-/-}$ mice were infected with *H. hepaticus* for 10 or 20 weeks. We found that WT and *Nlrc4*$^{-/-}$ mice harboured equivalent amounts of *H. hepaticus* in the cecum after both 10 and 20 weeks of infection (Fig.4.6A). We measured endpoint secretory IgA (sIgA) levels in small intestinal lavage fluid and found that WT and *Nlrc4*$^{-/-}$ mice mounted similar responses after 10 weeks of infection (Fig.4.6B). After 20 weeks of infection *Nlrc4*$^{-/-}$ mice showed a trend towards increased *H. hepaticus*-specific sIgA responses, although this did not reach statistical significance (Fig.4.6C). We also measured the development of *H. hepaticus*-specific serum IgG responses by sampling the same cohorts of mice after 0, 4, 6 and 10 weeks of infection. We found that WT and *Nlrc4*$^{-/-}$ animals developed equivalent IgG responses over this period (Fig.4.6D). However, when we measured *H. hepaticus* specific serum IgG levels after 20 weeks of infection, *Nlrc4*$^{-/-}$ mice had significantly increased levels compared with WT mice (Fig.4.6E). However, neither WT nor *Nlrc4*$^{-/-}$ mice developed any overt pathology in the large intestine after 20 weeks of *H. hepaticus* infection alone (data not shown).

Figure 4.6

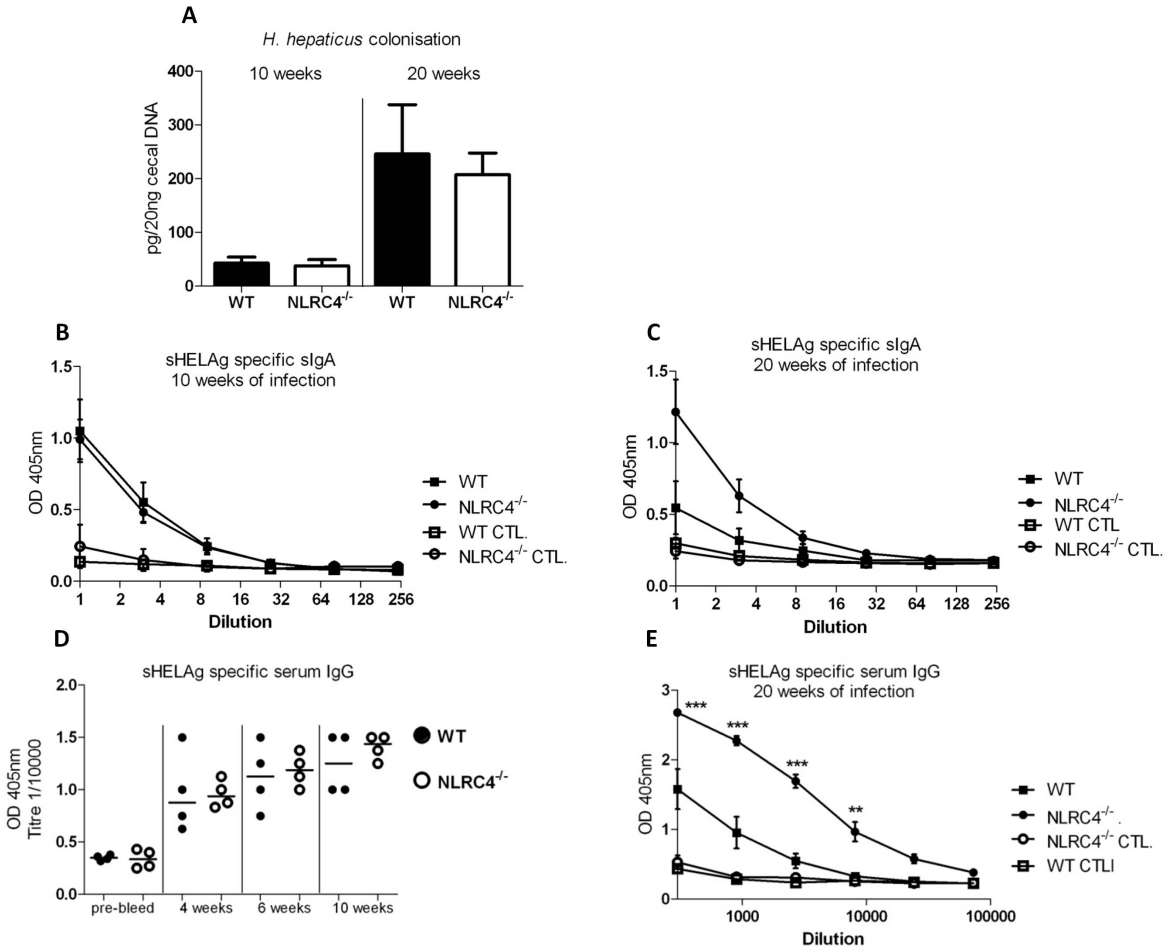


Figure 4.6 NLRC4 deficiency does not affect long-term *H. hepaticus* colonisation. WT and *Nlrc4*$^{-/-}$ mice were infected by oral gavage with approximately 10^8 CFU *H. hepaticus* and sacrificed after 10 weeks or 20 weeks. (A) *H. hepaticus* cecal DNA levels ±SEM at 10 or 20 weeks. (B) *H. hepaticus*-specific intestinal IgA levels ±SEM after 10 weeks of infection. (C) *H. hepaticus*-specific intestinal IgA levels ±SEM after 20 weeks of infection. (D) Systemic *H. hepaticus*-specific IgG responses in serum were monitored over 10 weeks of infection (E) Endpoint *H. hepaticus*-specific serum IgG ±SEM after 20 weeks of infection. Data are from independent experiments for 10 weeks (n=4 per genotype infected, n=3 per genotype uninfected) and 20 weeks (n=5 per genotype infected, n=2 per genotype uninfected). Statistical analysis was performed using two-way ANOVA, **P<0.01, ***P<0.001.

4.2.7 NLRC4 is dispensable for the development of *H. hepaticus* triggered T-cell independent intestinal inflammation

H. hepaticus has well described pathogenic properties in immunodeficient mice. Infection of 129SvEv*Rag2*$^{-/-}$ (*Rag2*$^{-/-}$) mice with *H. hepaticus* results in severe typhlocolitis and drives colon cancer development.[267, 269, 270, 334] To assess whether NLRC4 influenced innate immune typhlocolitis, we backcrossed B6*Nlrc4*$^{-/-}$ mice onto the 129*Rag2*$^{-/-}$ background (*Nlrc4*$^{-/-}$*Rag2*$^{-/-}$), using microsatellite markers to accelerate the process.[282] *Rag2*$^{-/-}$ mice and *Nlrc4*$^{-/-}$*Rag2*$^{-/-}$mice were infected with *H. hepaticus* for 12 weeks and intestinal pathology was assessed. As previously reported, *Rag2*$^{-/-}$ mice developed severe typhlocolitis after infection, characterised by marked epithelial hyperplasia, edema, goblet cell depletion and dense leukocytic infiltration (Fig.4.7A,B,C). We found that *Nlrc4*$^{-/-}$*Rag2*$^{-/-}$animals did not display any baseline abnormalities in the intestine and that they exhibited equivalent severe typhlocolitis to *Rag2*$^{-/-}$ mice following infection with *H. hepaticus* (Fig.4.7A,B,C).

Figure 4.7

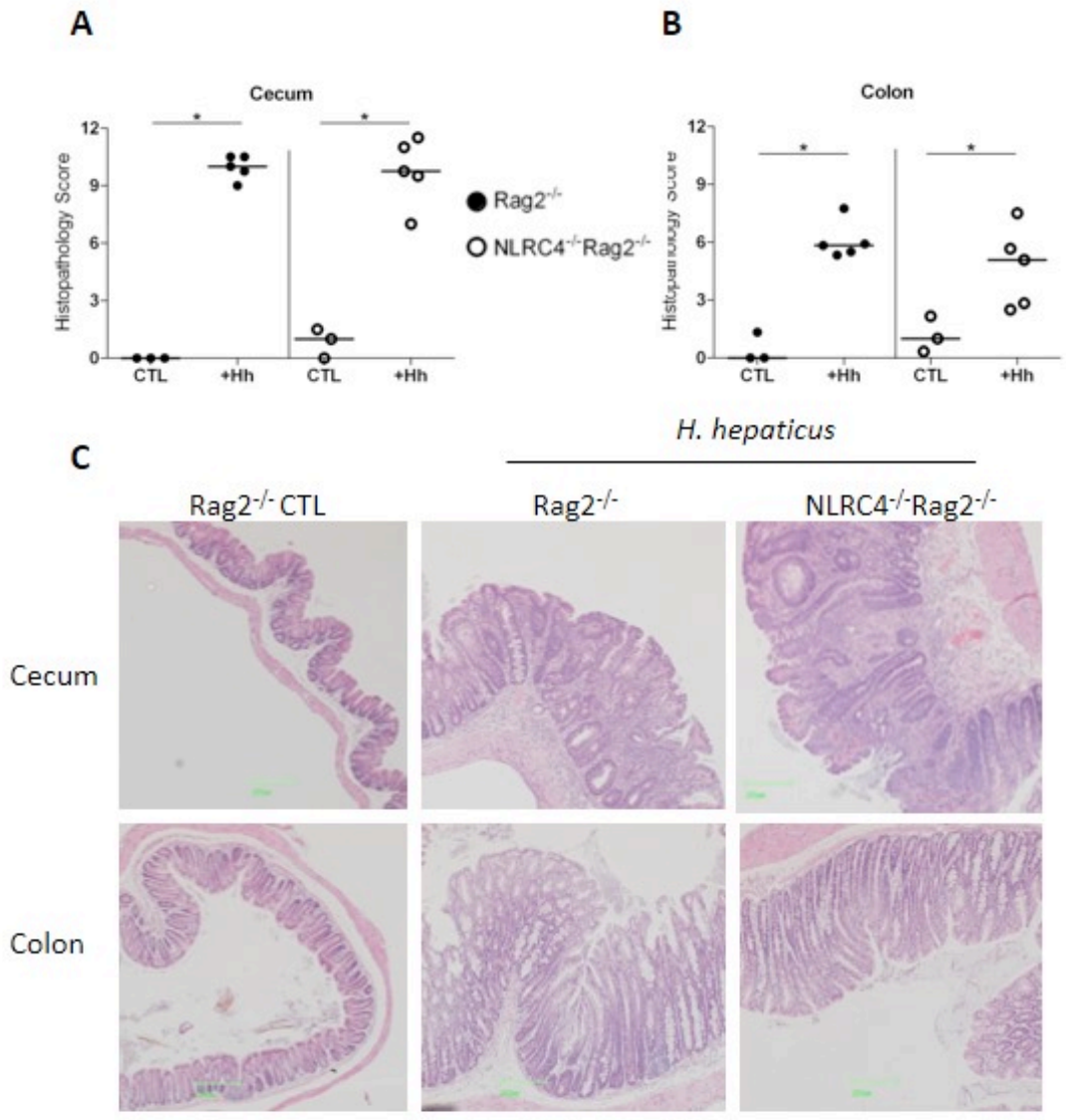


Figure 4.7 NLRC4 is dispensable for *H. hepaticus*-induced T-cell independent intestinal inflammation.

Rag2$^{-/-}$ *and Nlrc4*$^{-/-}$*Rag2*$^{-/-}$ animals were infected by oral gavage with approximately 10^8 CFU *H. hepaticus* and sacrificed after 12 weeks. (A) Histopathology scores for cecum. (B) Histopathology scores for colon. (C) Representative histology of cecum and distal colon. Control (*Rag2*$^{-/-}$ CTL) sections are from uninfected *Rag2*$^{-/-}$ mice. Data are from 1 experiment; each symbol represents an individual mouse and horizontal bars are group median values (n=5 per group). The non-parametric Mann-Whitney test was used for statistical analysis, *P<0.05.

4.2.8 NLRC4 is dispensable for systemic immune responses during *H. hepaticus* -induced T-cell independent intestinal inflammation

Innate intestinal inflammation driven by *H. hepaticus* also leads to systemic immune responses and granulocyte numbers in the spleen increase dramatically during infection.[267] Similar to what was observed in *Rag2*$^{-/-}$ mice, *Nlrc4*$^{-/-}$*Rag2*$^{-/-}$ mice developed marked splenomegaly and granulocyte frequencies in the spleen tripled following infection with *H. hepaticus* (Fig.4.8A,B). Granulocyte recruitment to the colonic LP is a feature of this IBD model and we found that *H. hepaticus*-infected *Nlrc4*$^{-/-}$*Rag2*$^{-/-}$mice and their NLRC4 sufficient *Rag2*$^{-/-}$ counterparts exhibited comparable recruitment of CD11b^{hi}Ly6G^{+} cells to the inflamed colon (Fig.4.8C). Lastly, *H. hepaticus* colonisation levels in cecal content were measured by qPCR and although there was a trend of reduced colonisation levels in *Nlrc4*$^{-/-}$*Rag2*$^{-/-}$mice compared with *Rag2*$^{-/-}$ mice, the difference was not statistically significant (Fig.4.8D), indicating that NLRC4 was redundant in *H. hepaticus*-induced innate inflammation.

Figure 4.8

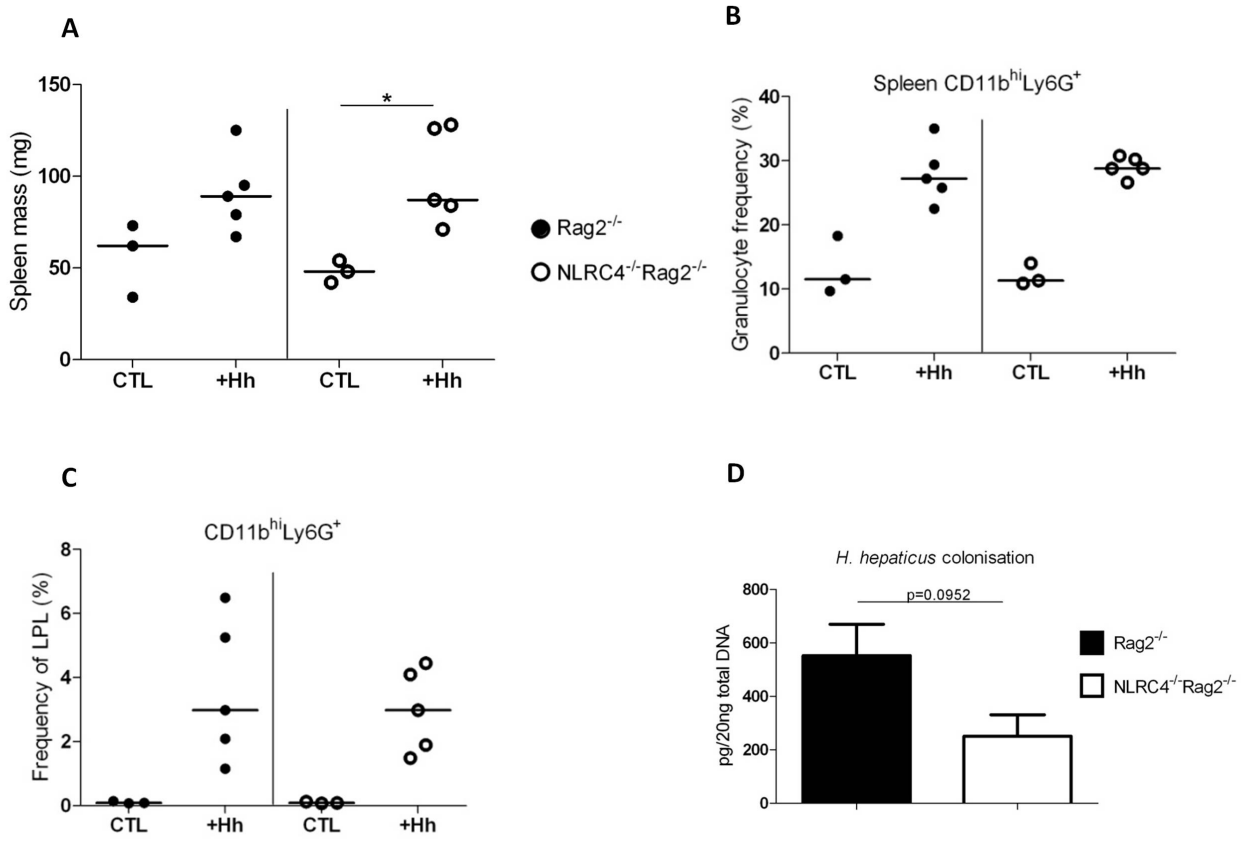


Figure 4.8 NLRC4 is dispensable for local and systemic granulocyte recruitment during *H. hepaticus*-triggered T-cell independent intestinal inflammation.

Rag2$^{-/-}$ and *Nlrc4*$^{-/-}$Rag2$^{-/-}$ animals were infected by oral gavage with approximately 10^8 *H. hepaticus* and sacrificed after 12 weeks. (A) Spleen weights. (B) Frequencies of CD11b^{hi}Ly6G^{+} granulocytes in spleen. (C) Frequencies of CD11b^{hi}Ly6G^{+} granulocytes in colon LPL. (D) *H. hepaticus* cecal DNA levels mean ±SEM. These data are from 1 experiment; each symbol represents an individual mouse and horizontal lines are group median values (n=3 per group control; n=5 per group *H. hepaticus*-infected). The non-parametric Mann-Whitney test was used for statistical analysis. *P<0.05.

4.2.9 NLRC4 does not regulate to the onset of *H. hepaticus*-induced T-cell independent intestinal inflammation

Immune cell recruitment to systemic and local sites is prominent during the initial stages of *H. hepaticus* infection in *Rag2*$^{-/-}$ animals.[269] To investigate a possible role for NLRC4 during the onset of *H. hepaticus*-triggered T-cell independent typhlocolitis, *Rag2*$^{-/-}$ and *Nlrc4*$^{-/-}$*Rag2*$^{-/-}$mice were infected with *H. hepaticus* and sacrificed at 3 weeks p.i. Assessment of cecal inflammation revealed comparable severe typhlitis in both *Rag2*$^{-/-}$ and *Nlrc4*$^{-/-}$*Rag2*$^{-/-}$animals at 3 weeks p.i. (Fig.4.9A). Similarly, although *Rag2*$^{-/-}$ mice exhibited slightly more variable colitis compared with *Nlrc4*$^{-/-}$*Rag2*$^{-/-}$mice, the overall colonic pathology was equivalent at 3 weeks p.i. (Fig.4.9A). Further characterisation of immune cell recruitment revealed that granulocyte accumulation in the colon LP was similar in *Rag2*$^{-/-}$ and *Nlrc4*$^{-/-}$*Rag2*$^{-/-}$mice at 3 weeks p.i. (Fig.4.9B), as were systemic immune responses, as evidenced by spleen weights (Fig.4.9C). Finally, quantification of *H. hepaticus* burdens in cecal contents showed that NLRC4 expression did not affect the initial stages of *H. hepaticus* colonisation in the intestine (Fig.4.9D). Our results indicated that NLRC4 did not contribute to innate immune signalling and pathogenesis in the initial stages of *H. hepaticus* innate colitis.

Figure 4.9

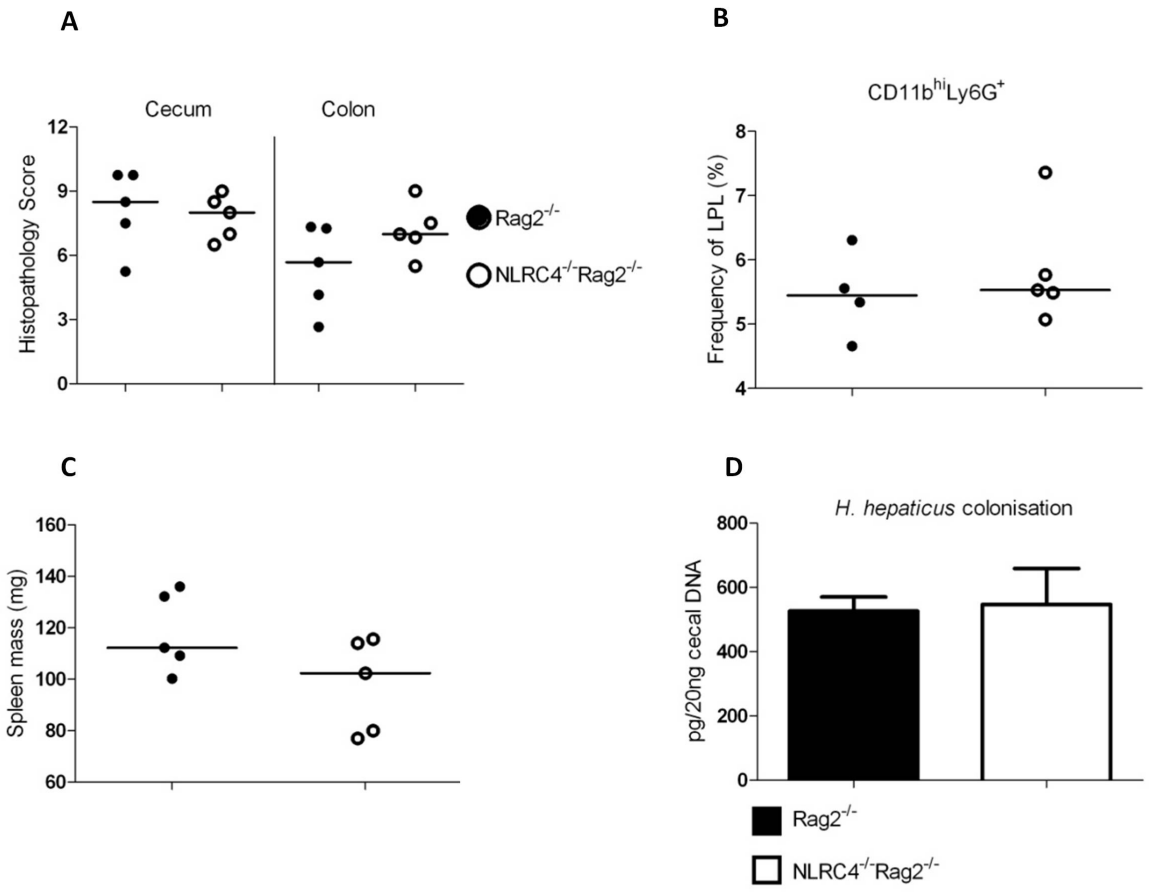


Figure 4.9 NLRC4 is dispensable during the development of chronic, T-cell independent intestinal inflammation.

Rag2$^{-/-}$ and *Nlrc4*$^{-/-}$*Rag2*$^{-/-}$ mice were infected by oral gavage with approximately 10^8 *H. hepaticus* and sacrificed after 3 weeks. (A) Histopathology scores for cecum and colon. (B) Frequencies of CD11b^{hi}Ly6G^{+} granulocytes in colon LPL. (C) Spleen weights. These data are from 1 experiment; each symbol represents an individual mouse and horizontal lines are group median values (n=5 per group).

4.3 Discussion

We had previously discovered that *Nlrc4*$^{-/-}$ mice displayed reduced levels of IL-18 and caspase-1 activation at steady state in the intestine. The NLRC4 inflammasome could thus be involved in both steady-state sensing of the commensal microflora and potentially in direct sensing of *H. hepaticus*. We could determine that NLRC4 was dispensable for the onset and maintenance of chronic, T-cell dependent colitis induced by *H. hepaticus*. However, we did detect elevated *H. hepaticus* colonisation levels and increased granulocyte recruitment in inflamed *Nlrc4*$^{-/-}$ animals, but these changes were not related to altered disease. To gain knowledge of the function of the inflammasome during chronic infection with extracellular bacteria, other *Helicobacter* species could provide insight. *Helicobacter felis* is a gastric *Helicobacter* species that induces gastritis in B6 WT mice.[335] It is used as a murine model of *Helicobacter pylori* driven gastritis, but similarly to *H. hepaticus*, the bacterium does not express the complete set of pathogenicity factors, such as a Type IV secretion system, which is present in *H. pylori*.[336, 337] Infection of Caspase-1$^{-/-}$, IL-1R$^{-/-}$ and IL-18$^{-/-}$ mice with *H. felis* revealed different roles of the inflammasome components. During 3 month infection, *Caspase-1*$^{-/-}$ and *IL-18*$^{-/-}$ mice developed exacerbated pathology and harboured lower bacterial burdens compared with WT mice, suggesting increased immune responses.[335] In contrast *IL-1r*$^{-/-}$ mice did not develop pathology and displayed elevated *H. felis* colonisation levels in the gastric mucosa.[335] The pathogenic properties of IL-1 cytokines during *H. felis* infection are in line with our findings in *H. hepaticus* mediated innate and T-cell dependent inflammation, in which blockade of IL-1β ameliorated colitis.[200, 338] Similarly to *H. felis* infection, it is possible that reduced inflammasome activation during *H. hepaticus* infection could have different effects depending on if the response is dominated by IL-18 or IL-1β. It is possible that the loss of epithelial NLRC4, and

possibly IL-18, could result in defective epithelial handling of *H. hepaticus* and subsequent increased immune activation. However, in contrast to global IL-18 deficiency described in the *H. felis* model of inflammation,[335] other inflammasomes and immune mechanisms could complement the response in *Nlrc4*$^{-/-}$ mice and prevent exacerbated pathology. *Nlrc4*$^{-/-}$ mice also developed increased *H. hepaticus* specific serum IgG reponses during long-term *H. hepaticus* infection in a non-inflamed setting. Although these latter data are based on a single experiment and would need to be confirmed, they could indicate heightened systemic immune activation in *Nlrc4*$^{-/-}$ mice. The quantification of inflammasome derived cytokines and caspase-1 activation, as well as the use of *Caspase-1*$^{-/-}$ mice, would assist in elucidating the role of inflammasome activation in response to *H. hepaticus* in a T-cell replete setting.

Although we have shown previously that IL-1β, and indirectly inflammasome activation, was pathogenic during *H. hepaticus* induced innate colitis,[200] we could conclude that NLRC4 was dispensable in this system. NLRC4 dependent IL-1β production has previously been shown to mediate protection in microbial infections of mucosal sites, such as infection of the lung with the invasive pathogen *Klebsiella pneumoniae*.[306] In this murine model of inflammation NLRC4 and IL-1β were associated with the development of inflammation, but were also essential for survival. Hematopoietic expression of NLRC4 resulted in increased granulocyte accumulation during *K. pneumoniae* infection, as did administration of recombinant IL-1β.[306] In contrast to our previous results in the *C. rodentium* model of acute inflammation, which suggested that IEC expression of NLRC4 conferred protective effects during infection with an extracellular pathogen, hematopoietic expression of inflammasomes might be more important for host defence during *H. hepaticus* driven disease. Intestinal macrophages are known to produce IL-1β and *H. hepaticus* mediated innate colitis

contains a strong element of hematopoietic cell accumulation and activation.[192, 200, 251] Furthermore, the severe pathology observed in *Nlrc4*$^{-/-}$ mice during *C. rodentium* infection was partially abrogated in mice of *Rag1*$^{-/-}$ background. Similarly, it is plausible that during innate, chronic inflammation mediated by extracellular bacteria, other pathways than NLRC4 inflammasome activation dominate the responses.

To further investigate potential protective or pathogenic effects of NLRC4 sensing of the commensal flora and resulting pathogenic T-cell responses, the T-cell transfer model of colitis[250] could be employed, using *Nlrc4*$^{-/-}$*Rag1*$^{-/-}$ recipient mice. Deletion of IL-18 in mainly epithelial cells, by the use of intrarectal administration of adenovirus carrying an IL-18 antisense construct, was reported to significantly reduce established T-cell transfer colitis.[339] The reduced pathology was associated with abrogated local production of IFN-γ.[339] Since pathogenesis in the T-cell transfer model of colitis is dependent on IFN-γ [253] and IL-18 potentiates Th1 responses,[79] epithelial NLRC4 expression and IL-18 production could promote pathogenesis.

Another important question is the contribution of innate signalling to the development of colitis associated cancer. *H. hepaticus* infection of 129SvEv*Rag2*$^{-/-}$ mice and treatment with the carcinogen AOM resulted in the development of colorectal-carcinoma.[270] Epithelial deletion of NLRC4 was shown to mediate increased susceptibility to colon cancer induced by repeated cycles of DSS and AOM injections, although this finding was contradicted by another study.[296, 297] NLRC4 was suggested to affect epithelial cell death and turnover, although the quantification of cell death was unclear and no mechanism was proposed.[340] Nevertheless, infection and treatment of *Nlrc4*$^{-/-}$*Rag2*$^{-/-}$ mice with *H. hepaticus* and AOM would elucidate potential effects of NLRC4 in preventing dysplasia, independent of effects on inflammation. Further

characterisation of NLRC4 in carcinogenesis would illuminate a potential role in intestinal homeostasis, beyond pathogen detection.

Chapter 5

Role of Toll-like receptor 5 in chronic intestinal inflammation

5.1 Introduction

Toll-like receptor 5 (TLR5) recognizes bacterial flagellin.[123] However, only monomeric flagellin is a ligand for TLR5, since the motifs recognized are buried within the polymeric helix of flagellin present in bacterial flagella.[341] Flagellin has previously been shown to be an immunodominant antigen in IBD and experimental colitis[127] and flagellin from commensal bacteria targeted by adaptive immune responses were found to exhibit sequences predicting intact TLR5 binding sites.[342]

In the intestine, TLR5 expression has been reported for epithelial cells,[343, 344] endothelial cells[345], submucosal myofibroblasts[29] and dendritic cells[279]. Expression was also described in sorted Treg from mouse and human.[346, 347] However, additional studies have suggested much more limited distribution and that expression is limited to defined sections in the large intestine [344, 348]and to specific DC subsets in the small intestine .[279] TLR5 has been suggested to be exclusively expressed on the basolateral side of the intestinal epithelium.[349] This compartmentalization would allow for the detection of flagellated, translocated bacteria but would exclude the luminal bacteria, thus distinguishing between pathogens and commensals.[349] However, this expression pattern was determined using polarized epithelial cell lines. Immunohistochemical analysis of murine, small intestinal tissue revealed TLR5 expression in the upper parts of the villi and in the apical side of the enterocytes. *Ex vivo* stimulation of gut tissue supported functional apical TLR5 signalling.[343] Furthermore, imaging of human colon tissue showed both apical and basolateral expression of TLR5 *in vivo*.[350] TLR5

expression and stimulation have been associated with protective effects during gastrointestinal bacterial infections.[131, 351, 352] Furthermore, TLR5 has also been shown to be protective during DSS colitis, in which the damaged epithelium is exposed to gut luminal antigens and bacteria.[275] In addition, prophylactic systemic administration of flagellin mediated survival from lethal irradiation in a TLR5-dependent fashion.[130] The mechanisms behind these cytoprotective effects are poorly understood, but injection with flagellin has been shown to reduce epithelial apoptosis *in vivo*. [129, 351] In the hematopoietic system, TLR5 activation in myeloid cells has been linked to IL-12[353] and IL-23 production, and subsequent tissue-protective and antimicrobial responses.[354] Furthermore, flagellin has been shown to promote the suppressive function of regulatory T-cells *in vitro*[346] and the class-switching of flagellin-specific B-cell cells into IgA producing cells in the MLN *in vivo*.[355]

Previous studies from our laboratory revealed that hematopoietic expression of MyD88 was necessary for chronic intestinal inflammation driven by *Helicobacter hepaticus,* whereas MyD88 signalling in non-hematopoietic cells was essential for survival of immune-deficient mice under SPF conditions.[265] Thus, TLR signalling in distinct cellular compartments can have either deleterious or protective effects in the intestine.

In addition, studies have indicated that TLR5 deficient mice harbour specific intestinal flora promoting pathology.[356, 357] In the light of these findings we chose to study the role of TLR5 signalling in well characterized models of intestinal inflammation. We used the T-cell transfer model of colitis,[250] which is dependent on commensal microflora. In addition, two separate systems of chronic inflammation based on infection with a known bacterium, *Helicobacter hepaticus*, were employed.[259, 267]

5.2 Results

5.2.1 TLR5 deficiency results in accelerated and exacerbated T cell transfer colitis

In order to examine if detection of commensal flagellin by TLR5 was important for the development of pathogenic T-cell responses and intestinal inflammation, we used the T-cell transfer model of colitis.[250, 358] To this end, *Tlr5*$^{-/-}$ mice were crossed to B-and T-cell deficient *Rag1*$^{-/-}$ mice to generate *Tlr5*$^{-/-}$*Rag1*$^{-/-}$ mice. Cohorts of control *Rag1*$^{-/-}$ and *Tlr5*$^{-/-}$*Rag1*$^{-/-}$ recipients were injected with 4x10^5 WT naïve CD4$^+$CD25$^-$CD45RB^{high} T-cells and the mice were weighed weekly and assessed for clinical signs of colitis. Although severe disease in this model typically occurs after 6-8wk, we observed that as early as 4 wk post-transfer *Tlr5*$^{-/-}$*Rag1*$^{-/-}$ recipients had significantly lower body weights compared to *Rag1*$^{-/-}$ recipients (Fig.5.1) Due to the onset of wasting disease in *Tlr5*$^{-/-}$ *Rag1*$^{-/-}$ mice, the experiment was ended at 4wk post-transfer and intestinal pathology assessed. We found that although the majority of *Rag1*$^{-/-}$ recipients exhibited only mild-to-moderate intestinal inflammation at this time point, *Tlr5*$^{-/-}$*Rag1*$^{-/-}$ recipients had developed significantly exacerbated pathology throughout the colon (Fig.5.2A,B). Severe disease was characterized by epithelial hyperplasia, cellular infiltration and tissue damage, such as crypt abscesses (Fig.5.2C).

Figure 5.1

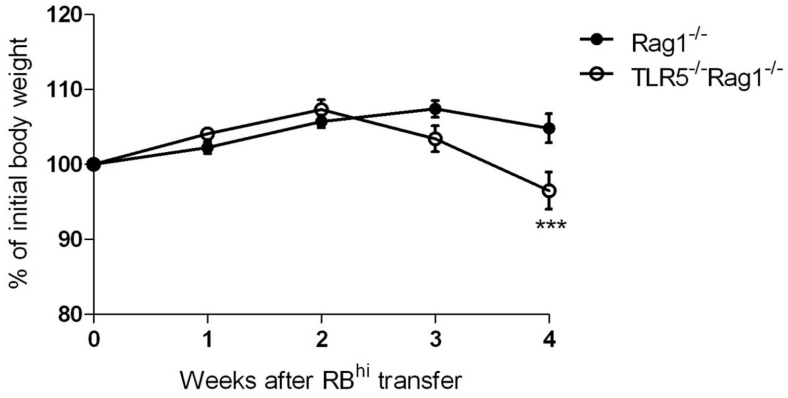


Figure 5.1 *Tlr5$^{-/-}$Rag1$^{-/-}$* mice develop accelerated wasting disease during T-cell transfer IBD

Rag1$^{-/-}$ and *Tlr5$^{-/-}$Rag1$^{-/-}$* mice were injected i.p. with 4x10^5 naïve CD4$^+$CD25$^-$CD45RB^{high} T-cells. Mice were sacrificed approximately 4 weeks post-transfer. Weight curves are shown as percentages of initial weight ± SEM and data were pooled from 3 independent experiments (n=22-23 per group). 2-way ANOVA was used for statistical analysis. ***P<0.001.

Figure 5.2

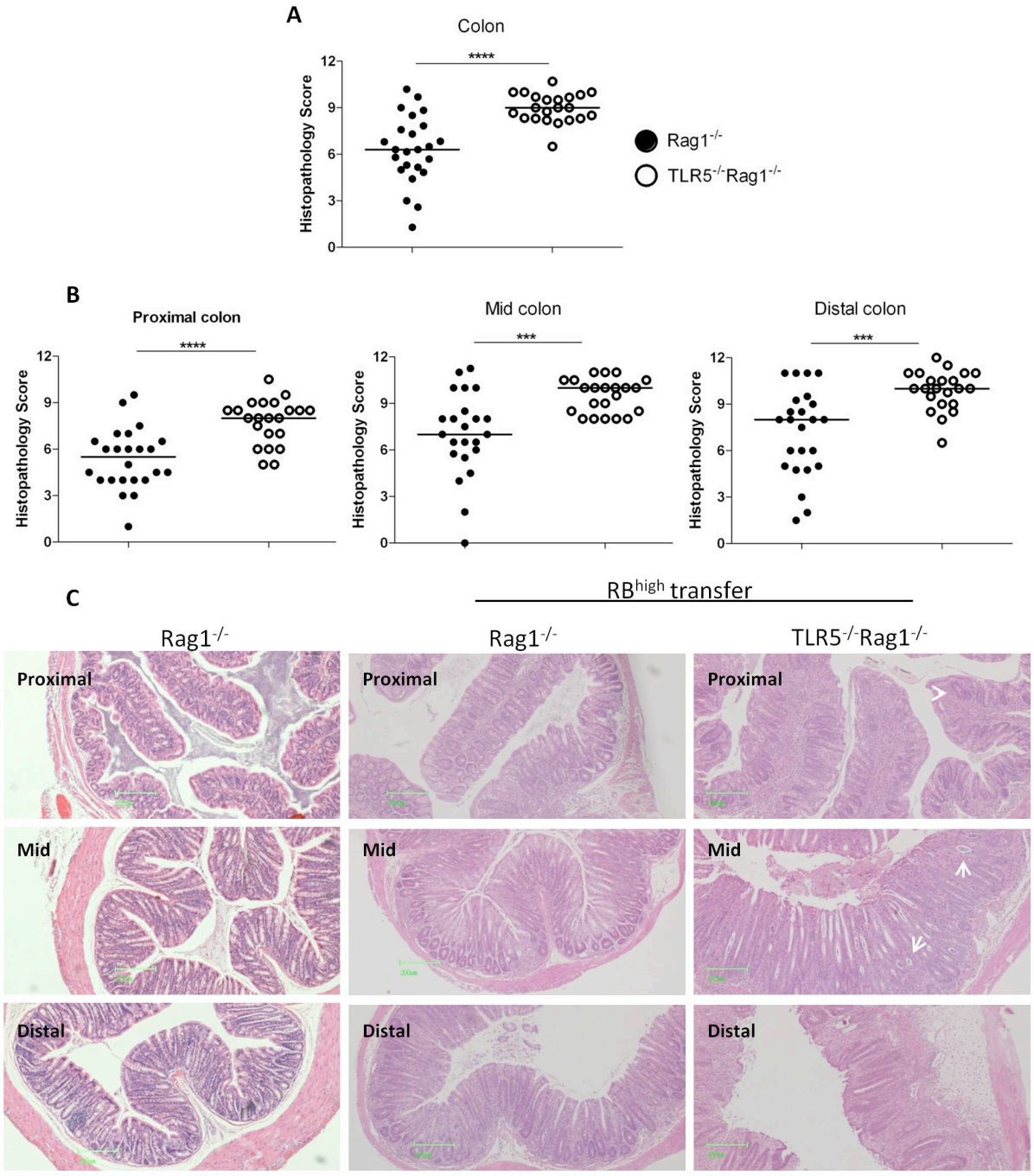


Figure 5.2 *Tlr5*$^{-/-}$*Rag1*$^{-/-}$ mice exhibit exacerbated pathology during T-cell transfer IBD*Rag1*$^{-/-}$ and *Tlr5*$^{-/-}$*Rag1*$^{-/-}$ mice were injected with 4x10^5 naïve CD4$^+$CD25$^-$CD45RB^{high} T-cells. Mice were sacrificed approximately 4 weeks post-transfer and intestinal pathology was evaluated. (A) Colon pathology scores. Mean colitis scores were calculated from proximal, mid and distal colon pathology scores from each animal. (B) Individual histopathology scores for colon regions. (C) Representative micrographs of colon. White arrows indicate crypt abscesses and white arrowhead denotes cellular infiltration. Green bars are equivalent to 200µm. Each symbol represents an individual mouse and horizontal bars are group median values. Data were pooled from 3 independent experiments (n=22-23 per group). The non-parametric Mann-Whitney test was used for statistical analysis, ***P<0.001, ****P<0.0001.

5.2.2 Exacerbated pathology in *Tlr5*$^{-/-}$*Rag1*$^{-/-}$ mice is not associated with increased Th1 or Th17 responses

Disease severity in T-cell mediated colitis is linked with the development of pathogenic Th1 responses and blocking of IFN-γ or the use of IFN-γ deficient naïve CD4^{+}T-cells attenuates colitis.[253, 259] To assess CD4^{+}T cell differentiation, colonic LPLs were isolated at sacrifice and stained intracellularly for IFN-γ and IL-17A. Surprisingly, *Tlr5*$^{-/-}$*Rag1*$^{-/-}$ mice had significantly reduced Th1 frequencies in the colon compared with *Rag1*$^{-/-}$ recipients (Fig.5.3A). Furthermore, only a small population of Th17 cells was detected among LPL in either genotype and the minor population of IL-17A^{+}IFN-γ^{+} cells was also significantly reduced in the *Tlr5*$^{-/-}$*Rag1*$^{-/-}$ mice (Fig.5.3B,C). Considering the increased inflammatory state in *Tlr5*$^{-/-}$*Rag1*$^{-/-}$ mice compared with *Rag1*$^{-/-}$ mice, we also assessed the total CD4^{+}T-cell recruitment to the colon LP. We observed a slight, but significant increase in CD4^{+} T-cell accumulation and total LPL cell numbers in *Tlr5*$^{-/-}$*Rag1*$^{-/-}$ mice (Fig.5.4A,B). Finally, we cultured colon explants and measured IFN-γ and IL-17A in the culture supernatants. We found comparable levels of IFN-γ and IL-17A in colon explants from *Tlr5*$^{-/-}$*Rag1*$^{-/-}$ recipients and *Rag1*$^{-/-}$ recipients (Fig.5.4C,D). Taken together, these results suggest that the severe pathology observed in TLR5 deficient animals could not be explained by increased effector CD4^{+} T cell responses in the colon.

Figure 5.3

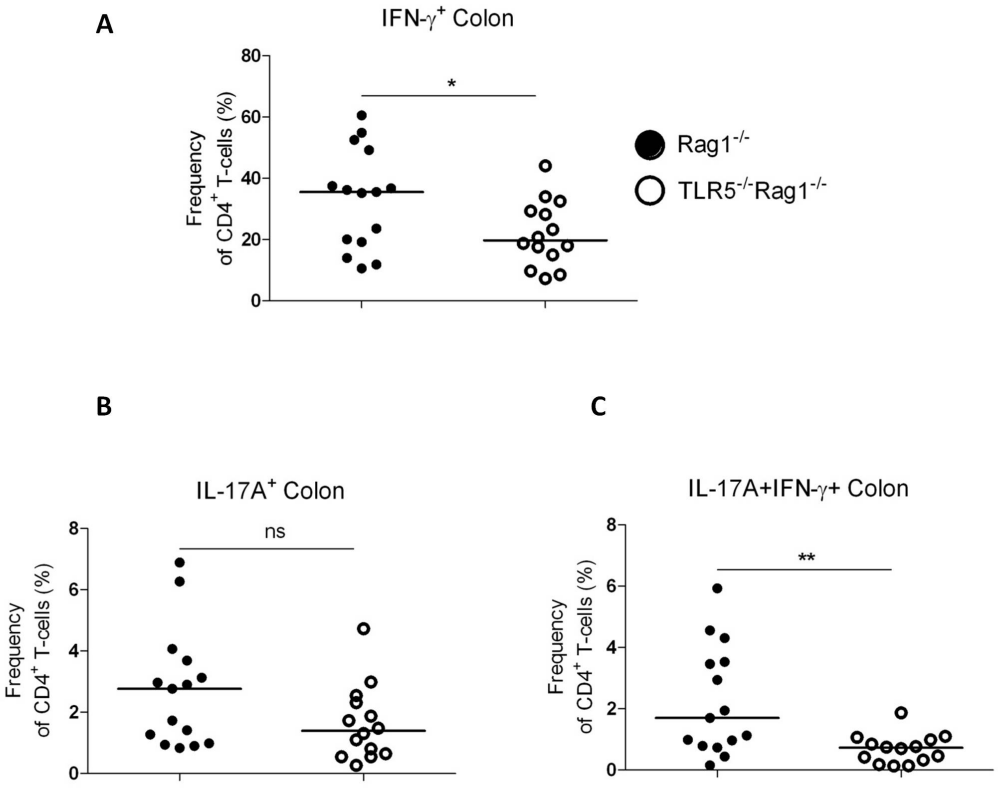


Figure 5.3 *Tlr5*$^{-/-}$*Rag1*$^{-/-}$ mice exhibit reduced frequencies of effector CD4$^+$ T-cells in the colon during T cell transfer IBD

Rag1$^{-/-}$ and *Tlr5*$^{-/-}$*Rag1*$^{-/-}$ mice were injected i.p. with 4x10^5 naïve CD4$^+$CD25$^-$CD45RB^{high} T-cells. Mice were sacrificed 4 weeks post-transfer and leukocytes from the colon lamina propria were isolated. Cells were restimulated with PMA (0.1μg/ml), ionomycin (1μg/ml) and Brefeldin A (10μg/ml) for 3h. LPL were surfaced stained for CD4 and TCRβ and stained intracellularly for IFN-γ and IL-17A. (A) Frequencies of IFN-γ$^+$ CD4$^+$ T-cells in colonic LPL (B) Frequencies of IL-17A$^+$ CD4$^+$ T-cells in colonic LPL (C) Frequencies of IL-17A$^+$IFN-γ$^+$ CD4$^+$ T-cells in colonic LPL. Each symbol represents and individual mouse and horizontal bars are group median values. Data were pooled from 2 independent experiments (n=14-15 per group) and the non-parametric Mann-Whitney was used for statistical analysis. *P<0.05, **P<0.01.

Figure 5.4

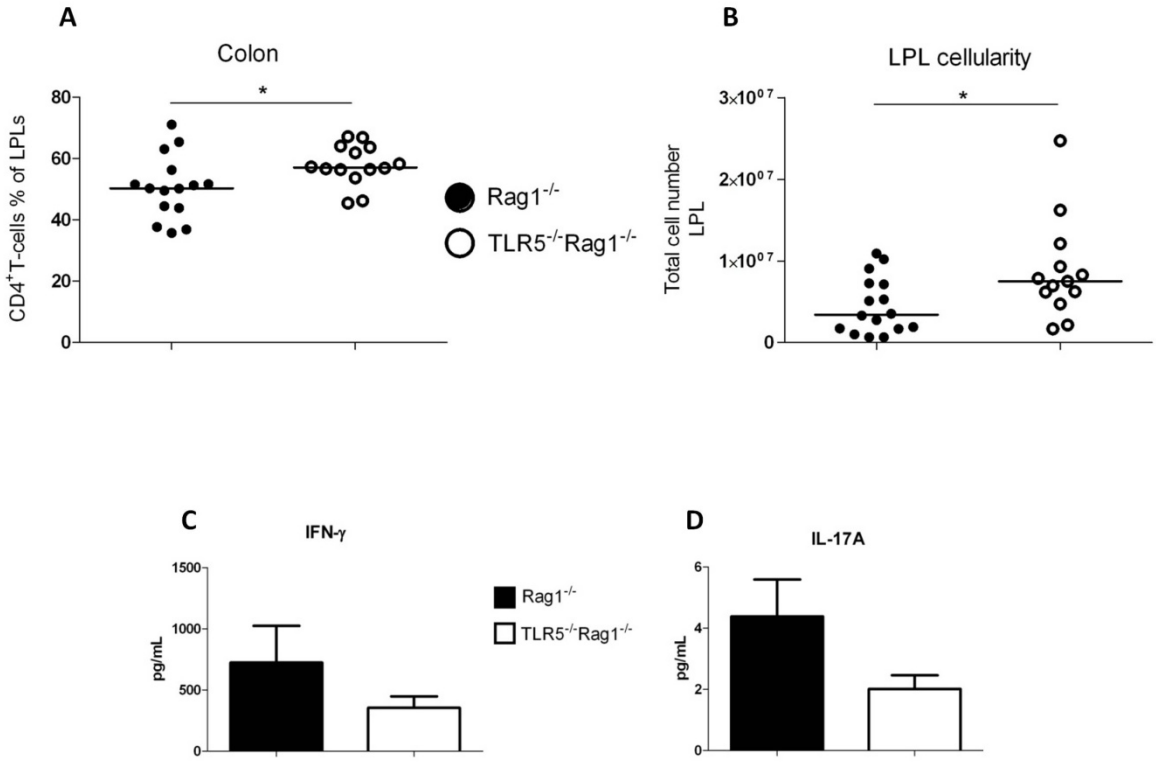


Figure 5.4 *Tlr5*$^{-/-}$*Rag1*$^{-/-}$ mice display increased tissue CD4^{+} T-cell accumulation during T-cell transfer colitis

Rag1$^{-/-}$ and *Tlr5*$^{-/-}$*Rag1*$^{-/-}$ mice were injected i.p. with 4x10^{5} naïve CD4^{+}CD25^{-}CD45RB^{high} T-cells and sacrificed 4 weeks later. (A) Frequencies of CD4^{+}TCRβ^{+} in colon LPL (B) Total cell numbers of LPL. Each symbol represents an individual mouse and horizontal bars are group median values. (C and D) Sections of mid colon were cultured overnight and levels of IFN-and IL-17-A in the culture supernatant assayed by bead based flow cytometry. Levels were normalised to tissue weight. Bar graphs represent mean values ±SEM. Data were pooled from 2 independent experiments (n=14-15 per group) and the non-parametric Mann-Whitney was used for statistical analysis. *P<0.05.

5.2.3 Exacerbated pathology in *Tlr5*$^{-/-}$*Rag1*$^{-/-}$ mice is not associated with increased local pro-inflammatory responses

T-cell transfer colitis is associated with the presence of neutrophils in the inflamed tissue[255] and TLR5 deficiency has previously been associated with increased neutrophil influx during infection with *Salmonella typhimurium*.[352] In order to gauge neutrophil accumulation in the colonic mucosa, LPL were stained for granulocyte markers CD11b and Gr1. We found that 4wks after naïve T cell transfer, *Tlr5*$^{-/-}$*Rag1*$^{-/-}$ recipients and *Rag1*$^{-/-}$ recipients harboured equivalent Cd11b^{hi}Gr1^{hi} frequencies in the gut tissue, although spleen neutrophil frequencies were significantly increased in *Tlr5*$^{-/-}$*Rag1*$^{-/-}$ mice (Fig.5.5A,B).

IL-23 is a key driving cytokine for intestinal inflammation during T-cell transfer colitis. [251] However, colonic levels of IL-23 mRNA were significantly reduced in *Tlr5*$^{-/-}$*Rag1*$^{-/-}$ recipients compared with *Rag1*$^{-/-}$ recipients during inflammation (Fig.5.6A). In addition, local tissue production of IL-22, which is strongly induced by IL-23, was similar in *Tlr5*$^{-/-}$*Rag1*$^{-/-}$ and *Rag1*$^{-/-}$ recipients, as were expression levels of the IL-22 associated AMPs, RegIIIγ and RegIIIβ (Fig.5.6.C). Furthermore, assessment of additional pro-inflammatory cytokines that have been associated with chronic intestinal inflammation revealed that they were either significantly reduced in *Tlr5*$^{-/-}$*Rag1*$^{-/-}$ recipients compared with *Rag1*$^{-/-}$ recipients (IL-12, Fig.5.6B), or were secreted at equivalent levels in both recipient genotypes (IL-6 and TNF-α, Fig.5.6 D). In conclusion, despite displaying exacerbated disease, *Tlr5*$^{-/-}$*Rag1*$^{-/-}$ mice did not exhibit increased Th1 responses or produce elevated levels of cytokines classically associated with T-cell transfer colitis. This suggests that other cell populations and pro-inflammatory cytokines could be involved or that regulatory mechanisms are reduced.

Figure 5.5

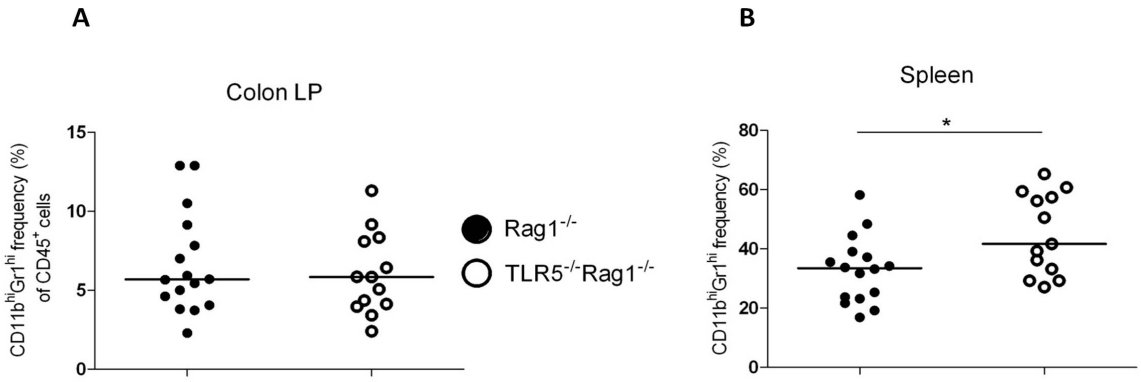


Figure 5.5 *Tlr5*$^{-/-}$*Rag1*$^{-/-}$ mice display increased splenic granulocyte accumulation during T-cell transfer colitis

4x10^5 naïve CD4$^+$CD25$^-$CD45RB^{high} T-cells were injected i.p. into *Rag1*$^{-/-}$ and *Tlr5*$^{-/-}$*Rag1*$^{-/-}$ mice and the mice were sacrificed 4wks later. (A) Accumulation of CD11b^{hi}Gr1^{hi} cells in colon LP. (B) Spleen granulocyte frequencies. Each symbol represents an individual mouse and horizontal bars are group median values. Data were pooled from 2 independent experiments (n=14-15 per group) and the non-parametric Mann-Whitney was used for statistical analysis, *P<0.05.

Figure 5.6

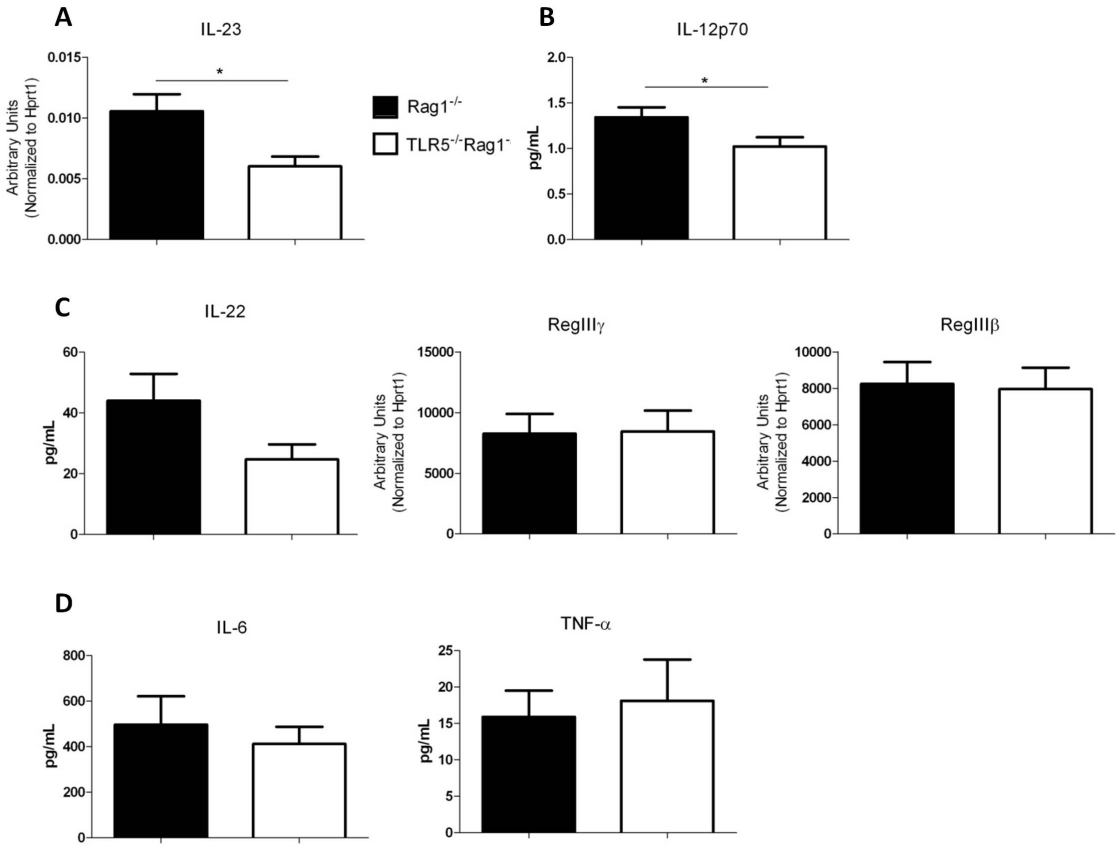


Figure 5.6 Expression of pro-inflammatory cytokines in *Tlr5*$^{-/-}$*Rag1*$^{-/-}$ and *Rag1*$^{-/-}$ recipients during T-cell transfer colitis

4x10^5 naïve CD4$^+$CD25$^-$CD45RB^{high} T-cells were injected i.p. into *Rag1*$^{-/-}$ and *Tlr5*$^{-/-}$*Rag1*$^{-/-}$ mice and the mice were sacrificed 4wks later. (A) IL-23 mRNA expression was evaluated in colon tissue by q-PCR. Values were normalized to Hprt. (B) Mid colon explants were cultured overnight and cytokine IL-12p70 measured in culture supernatant by a bead based assay and flow cytometry. (C). Production of IL-22 was assessed in colon explant culture supernatant, and mRNA expression of RegIIIγ and RegIIIβ in colon tissue were assayed by q-PCR (D). Explant culture supernatant levels of IL-6 and TNF-α were measured by bead based flow cytometry. Levels were normalised to tissue weight. Bar graphs represent mean values ±SEM. Data are pooled from 2 independent experiments and are displayed with mean ± SEM (n=14-15 per group). The non-parametric Mann-Whitney test was used to determine statistical significance, *P<0.05.

5.2.4 TLR5 deficiency in both non-hematopoietic and hematopoietic cells contributes to systemic disease

In order to elucidate the respective contributions of TLR5 signals in distinct cellular compartments to the exacerbated T-cell mediated colitis, bone-marrow (BM) chimeras were prepared, in which lethally-irradiated recipients were reconstituted with BM cells. Four groups were generated: Mice selectively deficient in TLR5 in the hematopoietic compartment (*Tlr5*$^{-/-}$*Rag1*$^{-/-}$ BM → *Rag1*$^{-/-}$); mice selectively deficient in TLR5 in the non-hematopoietic compartment (*Rag1*$^{-/-}$ BM → *Tlr5*$^{-/-}$*Rag1*$^{-/-}$); controls lacking TLR5 in both compartments (*Tlr5*$^{-/-}$*Rag1*$^{-/-}$ BM → *Tlr5*$^{-/-}$*Rag1*$^{-/-}$); and controls sufficient for TLR5 in both compartments (*Rag1*$^{-/-}$ → *Rag1*$^{-/-}$). BM chimeras were co-housed and left to reconstitute for 12 weeks, and were then injected with $4x10^5$ naïve WT $CD4^+$ T-cells to induce T cell transfer colitis. This experiment was performed twice, and although the course of disease varied between the two experiments, pooling of the data showed that mice deficient in TLR5 in both compartments (*Tlr5*$^{-/-}$*Rag1*$^{-/-}$ → *Tlr5*$^{-/-}$*Rag1*$^{-/-}$) developed significantly increased weight loss compared with the TLR5 sufficient chimeras (*Rag1*$^{-/-}$ → *Rag1*$^{-/-}$) at 3-4 weeks after transfer (Fig.5.7). In contrast, selective TLR5 deficiency in either the hematopoietic (*Tlr5*$^{-/-}$*Rag1*$^{-/-}$ → *Rag1*$^{-/-}$) or the non-hematopoietic (*Rag1*$^{-/-}$ → *Tlr5*$^{-/-}$*Rag1*$^{-/-}$) compartment did not result in increased systemic disease (Fig. 5.7), revealing that wasting disease is mediated by the loss of TLR5 signalling in both hematopoietic cells and radioresistant cells.

Figure 5.7

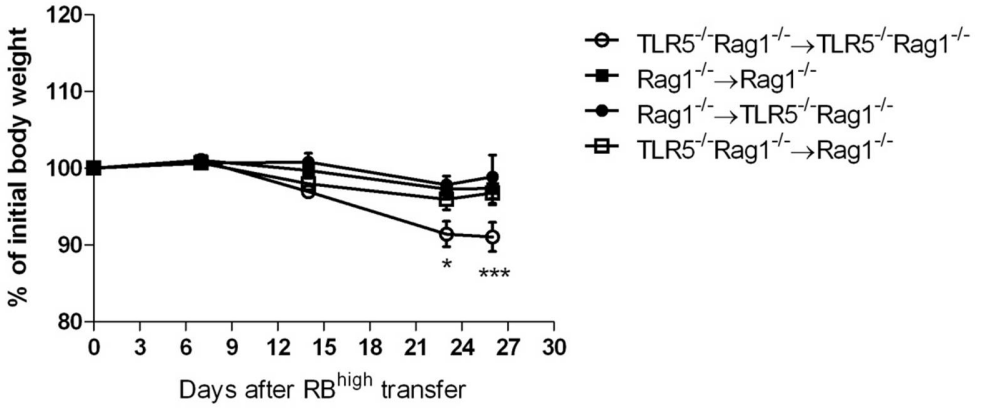


Figure 5.7 TLR5 signals in hematopoietic and non-hematopoietic cells protect from severe wasting disease during T-cell transfer colitis
Rag1$^{-/-}$ and *Tlr5*$^{-/-}$*Rag1*$^{-/-}$ were lethally irradiated and reconstituted with by i.p. injection of $10x10^6$ *Rag1*$^{-/-}$ or *Tlr5*$^{-/-}$*Rag1*$^{-/-}$ bone marrow (BM) cells. 12 wks later BM chimeric mice were injected i.p. with $4x10^5$ naïve $CD4^+CD25^-CD45RB^{high}$ T-cells (A) Weight curves representing pooled data from 2 independent experiments (n=11-13/group) are shown as percentages of the original weights with mean values ± SEM. Two-way ANOVA was used for statistical analysis. *P<0.05, ***P<0.001.

5.2.5 TLR5 signalling in hematopoietic cells protects from severe intestinal inflammation

Assessment of intestinal inflammation revealed that complete TLR5 deficient BM chimeras (*Tlr5*$^{-/-}$*Rag1*$^{-/-}$ → *Tlr5*$^{-/-}$*Rag1*$^{-/-}$) developed significantly exacerbated intestinal inflammation compared with the TLR5 sufficient (*Rag1*$^{-/-}$ → *Rag1*$^{-/-}$) control BM chimeras (Fig.5.8A,C). Evaluation of proximal, mid and distal colon regions separately, demonstrated that BM chimeras with complete TLR5 deficiency (*Tlr5*$^{-/-}$*Rag1*$^{-/-}$ → *Tlr5*$^{-/-}$ *Rag1*$^{-/-}$) exhibited increased pathology along the entire length of the colon (Fig.5.8B). In contrast, although BM chimeric mice that did not express TLR5 in the hematopoietic cells (*Tlr5*$^{-/-}$*Rag1*$^{-/-}$ → *Rag1*$^{-/-}$) also displayed significantly more severe colitis than TLR5 sufficient control chimeras (*Rag1*$^{-/-}$ → *Rag1*$^{-/-}$) (Fig.5.8A,C), they developed significantly more severe disease only in the proximal colon (Fig.5.8B,C). Conversely while BM chimeric mice that were selectively deficient in TLR5 in the non-hematopoietic compartment (*Rag1*$^{-/-}$ → *Tlr5*$^{-/-}$*Rag1*$^{-/-}$) did not have significantly elevated mean colitis scores (Fig.5.8A), they displayed significantly exacerbated intestinal inflammation in the distal colon (Fig.5.8B,C). In conclusion, these experiments showed that TLR5 deletion in both hematopoietic and non-hematopoietic cells contributed to increased disease severity in different parts of the large intestine. They also suggest that TLR5 signalling in hematopoietic cells plays a dominant role in protecting from severe T cell transfer colitis. Overall, BM chimeric mice developed less severe pathology 4 weeks post-RBhi transfer compared with conventional *Rag1*$^{-/-}$ and *Tlr5*$^{-/-}$*Rag1*$^{-/-}$ mice. Had the experiment been terminated when BM chimeric mice had suffered weight loss equivalent to non-irradiated *Tlr5*$^{-/-}$*Rag1*$^{-/-}$ mice, it is likely that *Rag1*$^{-/-}$ and *Tlr5*$^{-/-}$*Rag1*$^{-/-}$ mice would have displayed a similar degree of intestinal inflammation.

Figure 5.8

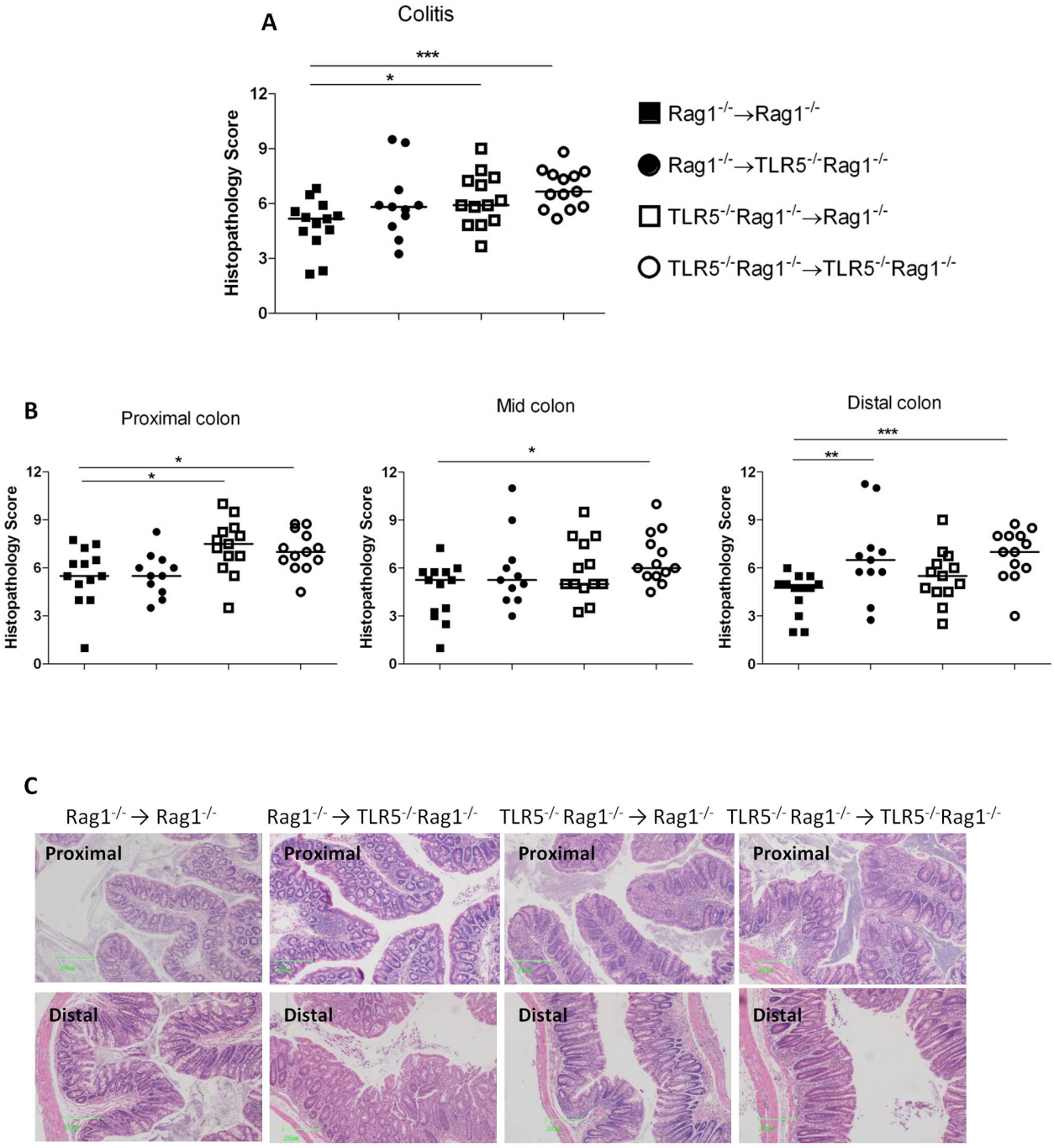


Figure 5.8 TLR5 signals in hematopoietic cells protect from severe T-cell transfer colitis*Rag1*$^{-/-}$ and *Tlr5*$^{-/-}$*Rag1*$^{-/-}$ were lethally irradiated and reconstituted with by i.p. injection of 10x10^6 *Rag1*$^{-/-}$ or *Tlr5*$^{-/-}$*Rag1*$^{-/-}$ bone marrow (BM) cells. 12 wks later BM chimeric mice were injected i.p. with 4x10^5 naïve CD4$^+$CD25$^-$CD45RB^{high} T-cells. Approximately 4 weeks after T-cell transfer mice were sacrificed and intestinal pathology assessed. (A) Mean colon pathology scores. (B) Pathology scores of the individual sections of the colon. (C) Representative micrographs of colon tissue. Each symbol represents an individual mouse and horizontal bars are group median values. Data are pooled from 2 independent experiments (n=11-15/group). The Mann-Whitney test was used for statistical analysis, *P<0.05, **P<0.01, ***P<0.001.

5.2.6 TLR5 is dispensable for T-cell independent innate intestinal inflammation

In order to investigate whether exacerbated colitis in TLR5 deficient animals was $CD4^+$ T-cell dependent, we employed a T-cell independent model of intestinal inflammation that is triggered by infection of 129SvEv*Rag2*$^{-/-}$ (*Rag2*$^{-/-}$) mice with the enteric bacterium *Helicobacter hepaticus*.[267] Our colony of C57BL/6 *Tlr5*$^{-/-}$ mice was backcrossed onto a 129SvEv*Rag2*$^{-/-}$ (*Rag2*$^{-/-}$) background and then co-housed *Rag2*$^{-/-}$ and *Tlr5*$^{-/-}$*Rag2*$^{-/-}$ mice were infected with *H. hepaticus*. At 8 wks post-infection pathology was assessed in the large intestine, revealing that *Rag2*$^{-/-}$ and *Tlr5*$^{-/-}$*Rag2*$^{-/-}$ mice had developed comparable severe typhlitis (Fig.5.9A) and moderate colitis (Fig.5.9B). In addition, *Tlr5*$^{-/-}$*Rag2*$^{-/-}$ mice did not display any spontaneous intestinal inflammation, excluding major effects of TLR5 in the steady state.

H. hepaticus infection of 129SvEv*Rag2*$^{-/-}$ also results in systemic immune activation.[267] We observed that, following *H. hepaticus* infection, *Rag2*$^{-/-}$ and *Tlr5*$^{-/-}$*Rag2*$^{-/-}$ mice exhibited similar splenomegaly and splenic granulocyte accumulation, implying that TLR5 deficiency in the absence of $CD4^+$T-cells did not affect systemic innate immune activation (Fig.5.10A,B). *H. hepaticus* driven innate intestinal inflammation is characterized by leukocyte infiltration of the tissue, including a small population of neutrophils.[269] Granulocyte specific staining of colonic LPL isolated from *H. hepaticus*-infected mice, revealed similar total LPL numbers and comparable neutrophil recruitment in *Tlr5*$^{-/-}$*Rag2*$^{-/-}$mice and *Rag2*$^{-/-}$ mice (Fig.5.10C,D). Finally, *H. hepaticus* colonisation levels were equivalent in *Tlr5*$^{-/-}$*Rag2*$^{-/-}$and *Rag2*$^{-/-}$ mice (Fig.5.11).

Recent work in our group revealed that *H. hepaticus* induced disease at the initial stage of infection appears to be of a different, more acute state. [269] Therefore, assessment of disease in *Tlr5*$^{-/-}$*Rag2*$^{-/-}$ and *Rag2*$^{-/-}$ mice was also performed after 3 wks of *H. hepaticus* infection. However, even at this early stage of infection, we could again determine that *Tlr5*$^{-/-}$*Rag2*$^{-/-}$ and *Rag2*$^{-/-}$ mice developed comparable severe cecal inflammation and moderate colitis (Fig.5.12A,B), as well as similar splenomegaly (Fig.5.12C).

Taken together, these data indicated that TLR5 was dispensable for pathogenesis and did not regulate disease severity in *H. hepaticus*-triggered innate immune IBD.

Figure 5.9

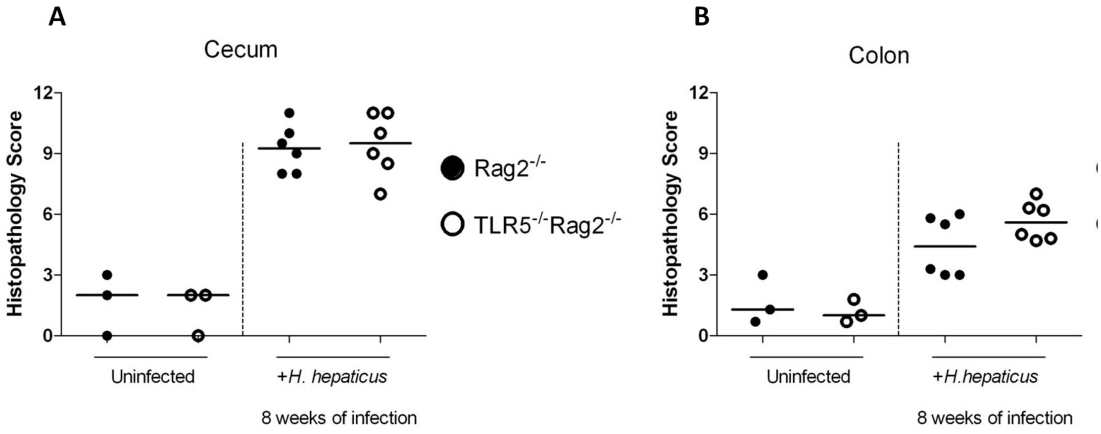


Figure 5.9 TLR5 is dispensable for *H. hepaticus* driven innate intestinal inflammation

Rag2$^{-/-}$ and *Tlr5*$^{-/-}$*Rag2*$^{-/-}$ mice were infected with approximately 10^8 CFU *H. hepaticus* p.o. and sacrificed after 8 wks of infection. (A) Intestinal pathology in cecum (B) Colon pathology scores. Uninfected animals were included as controls. Each symbol represents an individual mouse and horizontal bars are group median values. Data are from 1 experiment, (n=3-6 per group).

Figure 5.10

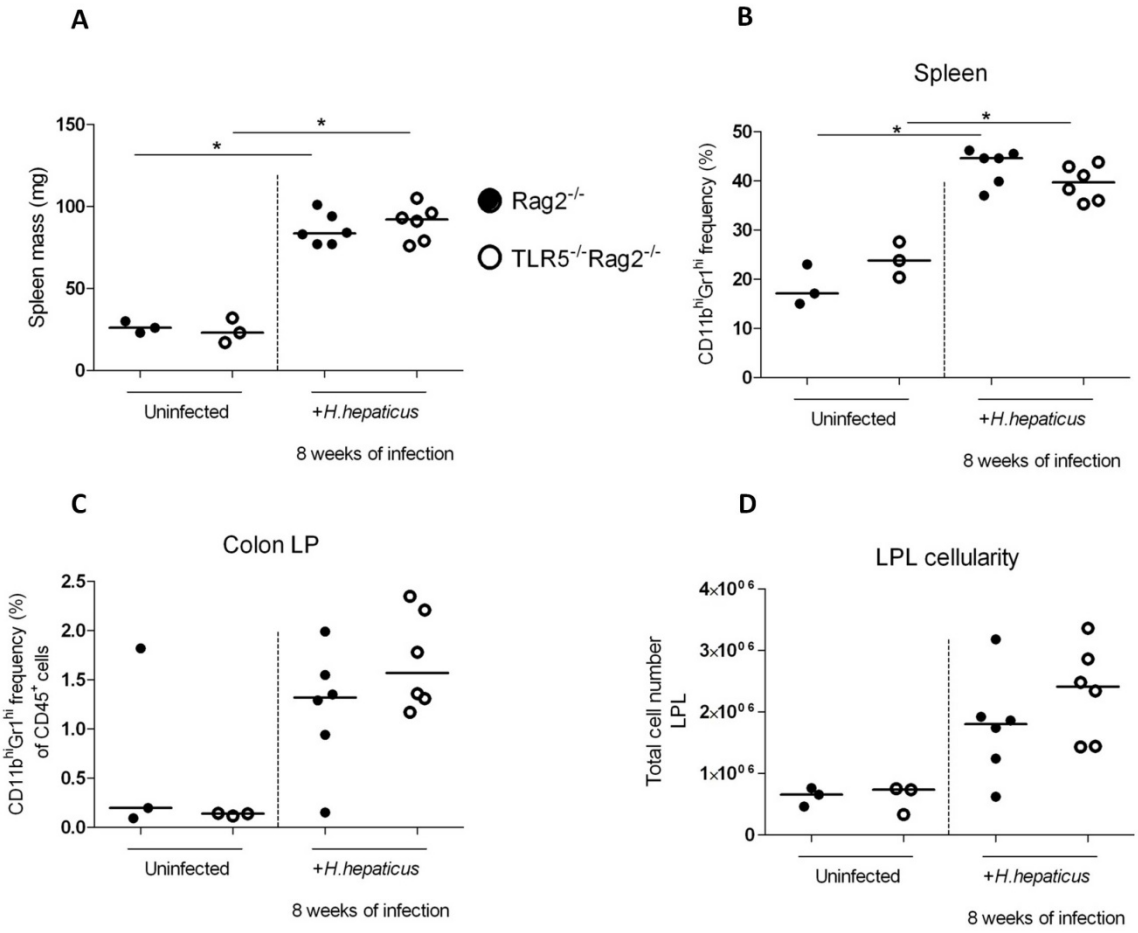


Figure 5.10 *Rag2*$^{-/-}$ and *Tlr5*$^{-/-}$*Rag2*$^{-/-}$ mice develop equivalent systemic and local inflammation during chronic *H. hepaticus*-induced innate IBD

Rag2$^{-/-}$ and *Tlr5*$^{-/-}$*Rag2*$^{-/-}$ mice were infected with approximately 10^8 CFU *H. hepaticus* p.o. and sacrificed after 8 wks of infection. (A) Systemic immune activation was assessed as spleen weights. (B) Accumulation of CD11b^{hi}Gr1^{hi}granulocytes in spleen. (C) Local granulocyte recruitment to the colon LP (D) Total cell numbers recovered from the colon LP. Each symbol represents an individual mouse and horizontal bars are group median values. Data shown are from 1 experiment (n=3-6 per group) and the Mann-Whitney test was used for statistical analysis. *P<0.05.

Figure 5.11

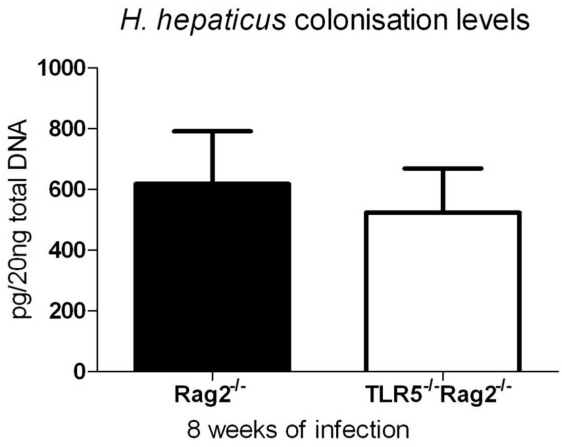


Figure 5.11 *H. hepaticus* colonisation levels are equivalent in *Rag2*$^{-/-}$ and *Tlr5*$^{-/-}$ *Rag2*$^{-/-}$ mice

Rag2$^{-/-}$ and *Tlr5*$^{-/-}$*Rag2*$^{-/-}$ mice were infected with approximately 10^8 CFU *H. hepaticus* p.o. and sacrificed after 8 wks of infection. DNA was extracted from cecal luminal contents and *H. hepaticus* colonisation levels were determined by qPCR. Bar graphs are displayed as mean values ± SEM.

Results are from 1 experiment (n=6 per group).

Figure 5.12

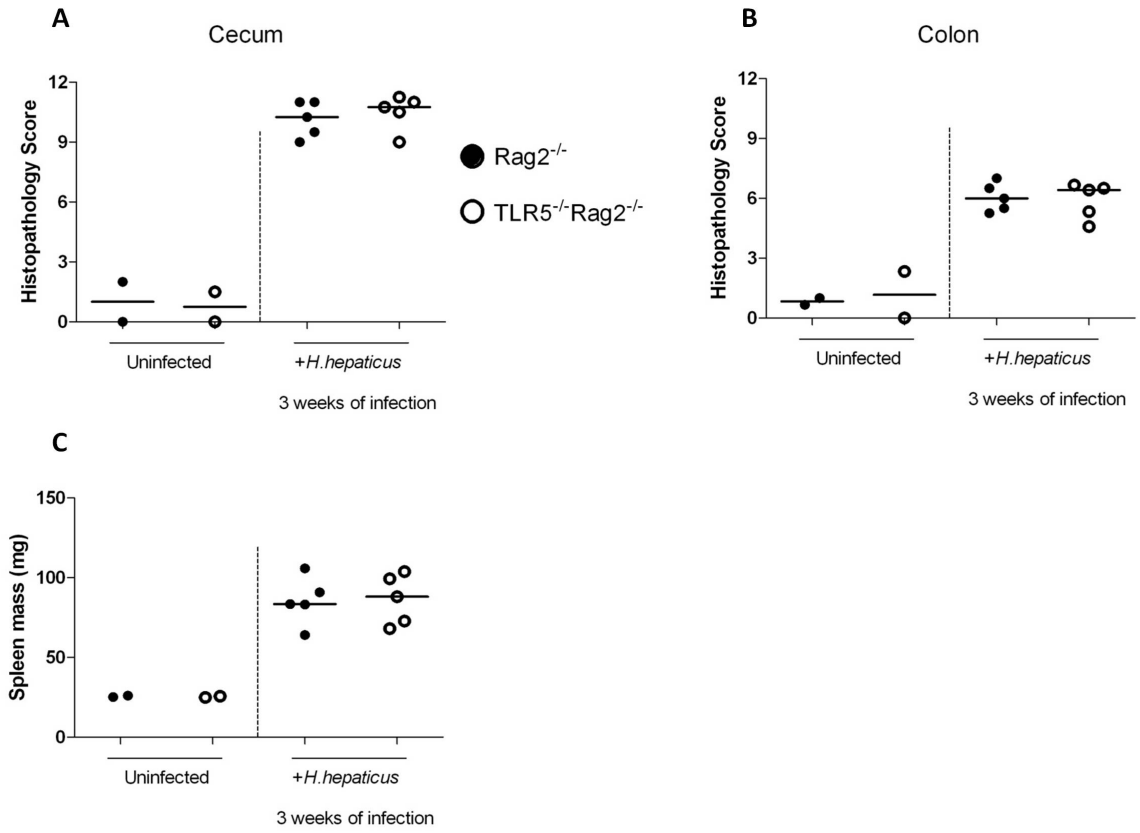


Figure 5.12 TLR5 is dispensable during the onset of *H. hepaticus*-triggered innate intestinal inflammation

Rag2$^{-/-}$ and *Tlr5*$^{-/-}$*Rag2*$^{-/-}$ mice were infected with approximately 10^8 CFU *H. hepaticus* p.o. and sacrificed after 3 wks of infection. (A) Pathology scores for cecum. (B) Colon pathology scores. (C) Splenomegaly. Each symbol represents an individual mouse and horizontal bars are group median values. Results are from 1 experiment (n=5 per group).

5.2.7 TLR5 deficiency results in accelerated and exacerbated *Helicobacter hepaticus* triggered T-cell dependent intestinal inflammation

Concurrent infection with the enteric bacterium *H. hepaticus* and systemic administration of antagonistic IL-10 receptor antibody (αIL-10R) induces severe intestinal inflammation in immunocompetent mice.[259] When maintained in our strict SPF animal facility, our *Tlr5*$^{-/-}$ mice did not exhibit any signs of spontaneous intestinal or systemic inflammation. Thus, C57BL/6 WT (WT) or *Tlr5*$^{-/-}$ mice were infected with *H. hepaticus* and injected with αIL-10R at the time of infection and again at day 7 post-infection (Hh+αIL-10R). On day 14 post-infection mice were sacrificed and intestinal inflammation was assessed. As expected, WT mice developed moderate typhlitis and mild colitis following Hh+αIL-10R treatment (Fig.5.13A,B,C). However, we found that *Tlr5*$^{-/-}$ mice exhibited significantly increased typhlitis and colitis compared with WT mice after Hh+αIL-10R treatment (Fig.5.13A,B,C). In addition, *Tlr5*$^{-/-}$ mice displayed a trend of increased splenomegaly after Hh+αIL-10R treatment, although this was not statistically significant (Fig.5.13D). Furthermore, local accumulation of neutrophils to the colon LP was similar in WT (WT) or *Tlr5*$^{-/-}$ mice after Hh+αIL-10R treatment (Fig.5.13E), suggesting that excessive granulocyte recruitment did not contribute to exacerbated disease.

Figure 5.13

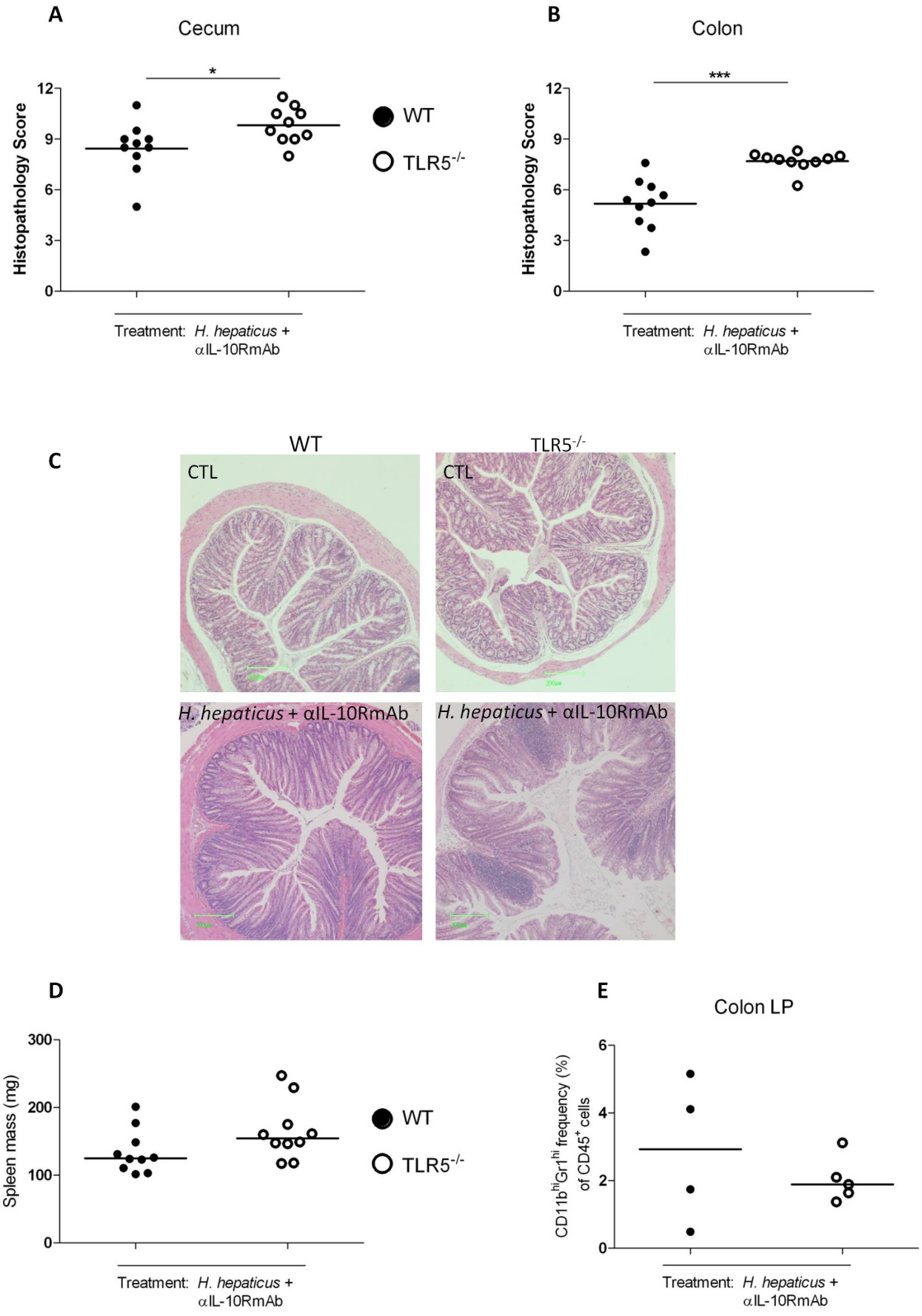

A
Cecum
*
Histopathology Score
12
9
6
3
0
WT
TLR5-/-
Treatment: H. hepaticus + αIL-10RmAb
B
Colon
***
Histopathology Score
12
9
6
3
0
Treatment: H. hepaticus + αIL-10RmAb
C
WT
TLR5-/-
CTL
CTL
H. hepaticus + αIL-10RmAb
H. hepaticus + αIL-10RmAb
D
Spleen mass (mg)
300
200
100
0
WT
TLR5-/-
Treatment: H. hepaticus + αIL-10RmAb
E
Colon LP
CD11bhiGr1hi frequency (%) of CD45+ cells
6
4
2
0
Treatment: H. hepaticus + αIL-10RmAb

Figure 5.13 TLR5 deficiency results in exacerbated bacterially triggered T-cell dependent intestinal inflammation

WT and *Tlr5*$^{-/-}$ mice were infected with approximately 10^8 CFU *H. hepaticus* p.o. and treated with weekly injections of αIL-10RmAb (1mg i.p.). At day 14 post-infection mice were sacrificed. (A) Intestinal pathology in cecum. (B) Colitis scores. (C) Representative micrographs of colon. Horizontal bars are equivalent to 200μm. (D) Spleen weights. (E) Local accumulation of granulocytes in colon LP. Results from 2 independent experiments were pooled for (A), (B) and (D) (n=10 per group). Data in (E) are from a single experiment (n=4-5 per group). Each symbol represents an individual mouse and horizontal bars are group median values. The Mann-Whitney test was used for determining statistical significance. *P<0.05, ***P<0.001.

5.2.8 TLR5 deficiency is not associated with increased Th1 or Th17 responses during *Helicobacter hepaticus* triggered T-cell dependent intestinal inflammation

H. hepaticus induced inflammation in lymphocyte replete animals is characterized by the induction of antigen specific Th1 and Th17 cells.[259] Evaluation of effector $CD4^+$ T-cell responses in the colonic LP on day 14 after Hh+αIL-10R treatment revealed that WT mice mounted potent Th17 responses while Th1 frequencies were low (Fig.5.14A,B,E). In comparison, Hh+αIL-10R treated *Tlr5*$^{-/-}$ mice had significantly reduced frequencies of Th17 cells and comparably low frequencies of IFN-γ producers as WT mice (Fig.5.14A,B,E). In addition, $CD4^+$ T-cell accumulation in the colon and total cell numbers recovered from the lamina propria were similar in WT and *Tlr5*$^{-/-}$ mice, (Fig. 5.14C,D). However, colon mRNA expression levels of IL-17A and IFN-γ in Hh+αIL-10R treated *Tlr5*$^{-/-}$ mice showed a trend of being increased compared with WT mice, although this was not statistically significant (Fig.5.14F). Finally, assessment of *H. hepaticus* colonisation levels suggested that bacterial levels were lower in the more severely inflamed *Tlr5*$^{-/-}$ mice, however there was considerable variation between the mice and this difference was not significant (Fig.5.15). However, although TLR5 deficient mice did not exhibit increased Th1 or Th17 responses, this does not exclude increased production of these cytokines by other cell populations. An increased number of samples and additional measurements, such as cytokine production by tissue explants, are needed to determine the levels of IFN-γ and IL-17A in the colon.

Figure 5.14

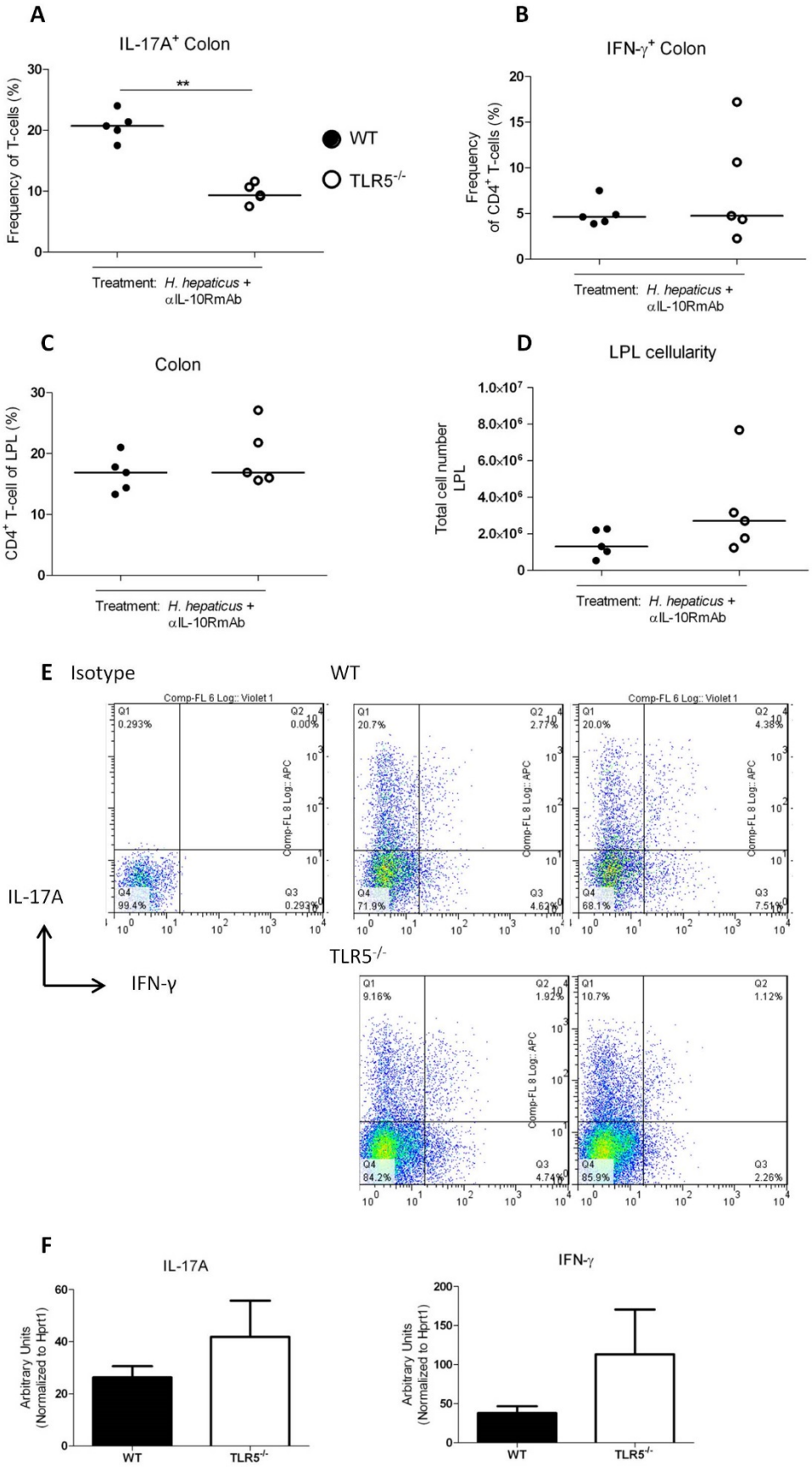

A
IL-17A+ Colon
Frequency of T-cells (%)
**
WT
TLR5-/-
Treatment: H. hepaticus + αIL-10RmAb
B
IFN-γ+ Colon
Frequency of CD4+ T-cells (%)
Treatment: H. hepaticus + αIL-10RmAb
C
Colon
CD4+ T-cell of LPL (%)
Treatment: H. hepaticus + αIL-10RmAb
D
LPL cellularity
Total cell number LPL
Treatment: H. hepaticus + αIL-10RmAb
E
Isotype
WT
TLR5-/-
IL-17A
IFN-γ
Comp-FL 6 Log:: Violet 1
Comp-FL 8 Log:: APC
Q1 0.293%
Q2 0.00%
Q4 99.4%
Q3 0.293%
Q1 20.7%
Q2 2.77%
Q4 71.9%
Q3 4.62%
Q1 20.0%
Q2 4.38%
Q4 68.1%
Q3 7.51%
Q1 9.16%
Q2 1.92%
Q4 84.2%
Q3 4.74%
Q1 10.7%
Q2 1.12%
Q4 85.9%
Q3 2.26%
F
IL-17A
IFN-γ
Arbitrary Units (Normalized to Hprt1)
WT
TLR5-/-

Figure 5.14 *Tlr5*$^{-/-}$ mice do not develop increased Th1 or Th17 responses during bacterially triggered T-cell dependent intestinal inflammation

WT and *Tlr5*$^{-/-}$ mice were infected with approximately 10^8 CFU *H. hepaticus* p.o. and treated with weekly injections of αIL-10RmAb (1mg i.p.). At day 14 post-infection mice were sacrificed, colonic lamina propria leukocytes (LPL) were isolated and restimulated with PMA (0.1μg/ml), ionomycin (1μg/ml) and Brefeldin A (10μg/ml) for 3h. LPL were surfaced stained for CD4 and TCRβ and i.c. stained for cytokines (A) Frequencies of IL-17A$^+$ CD4$^+$ T-cells in colon LP. (B) Frequencies of IFN-γ$^+$ CD4$^+$ T-cells in colon LP. (C) Total CD4$^+$ T-cell frequencies in colon LP. (D) Total LPL cell numbers. (E) Representative i.c. cytokine FACS stains, gated on CD4$^+$ colonic LP cells. (F) IL-17A and IFN-γ mRNA expression was determined in colon tissue by q-PCR and expressed relative to Hprt. Each symbol represents an individual mouse and horizontal bars are group median values. Bar graphs show mean ± SEM. Data displayed are from 1 experiment (n=5 per group). The non-parametric Mann-Whitney test was used for statistical analysis. **P<0.01.

Figure 5.15

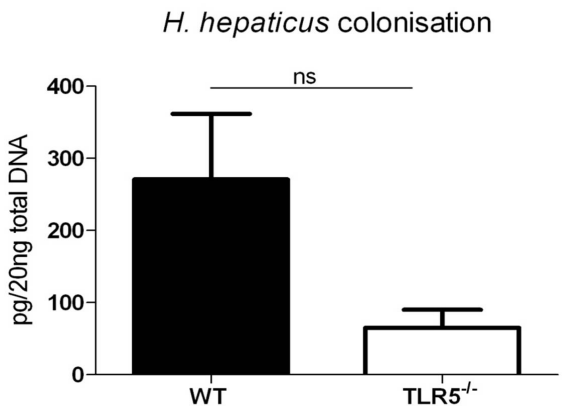


Figure 5.15 *H. hepaticus* levels during bacterially triggered T-cell dependent chronic colitis in WT and *Tlr5*$^{-/-}$ mice.
WT and *Tlr5*$^{-/-}$ mice were infected with approximately 10^8 CFU *H. hepaticus* p.o. and treated with weekly injections of αIL-10RmAb (1mg i.p.). At day 14 post-infection and treatment mice were sacrificed. *H. hepaticus* colonisation levels were determined by qPCR analysis of total DNA in luminal cecal content. Bar graphs show mean ± SEM. Results are pooled from 2 independent experiments (n=10 per group).

5.3 Discussion

We found that deletion of TLR5 in *Rag1*$^{-/-}$ recipient animals resulted in increased systemic and local pathology following transfer of naïve CD4^{+} T-cells. T-cell transfer colitis exhibits pathology traits of both UC and CD. Similarly to UC the pathology mainly develops in the colon and appears continuous. Features in common with CD include transmural disease and a Th1 signature.[1, 253, 255] Although the presence of Th1 cells and production of IFN-γ are correlated with the development of both weight loss and intestinal inflammation in this model,[94, 252] increased pathology in *Tlr5*$^{-/-}$*Rag1*$^{-/-}$ did not correspond with increased Th1 responses. We observed significantly reduced Th1 frequencies in *Tlr5*$^{-/-}$*Rag1*$^{-/-}$ mice and although total CD4^{+}T-cell numbers were slightly increased, tissue production of IFN-γ was not elevated. It is possible that effector T-cell recruitment and differentiation could be accelerated in *Tlr5*$^{-/-}$*Rag1*$^{-/-}$ mice and that these animals were exposed to Th1 cytokines for a longer period of time than *Rag1*$^{-/-}$ animals. However, the fact that the less inflamed *Rag1*$^{-/-}$ mice produced similar amounts of IFN-γ argued against a cumulative effect. An effect of increased systemic IFN-γ production cannot be excluded, but the severe local inflammation displayed by *Tlr5*$^{-/-}$*Rag1*$^{-/-}$ animals appeared to be uncoupled from excessive intestinal Th1 responses.

Previous studies in our laboratory showed that the development of T-cell transfer colitis was dependent on IL-23 production in recipient *Rag1*$^{-/-}$ mice and on IL-23 receptor expression by transferred naive CD4^{+} T-cells.[94, 252] Analysis of IL-23 mRNA levels in colon tissue after T cell transfer revealed reduced expression in *Tlr5*$^{-/-}$*Rag1*$^{-/-}$ mice relative to *Rag1*$^{-/-}$ recipients. However, in order to determine whether TLR5 deficient animals exhibited reduced induction or diminished steady state production of IL-23, baseline expression levels in *Tlr5*$^{-/-}$*Rag1*$^{-/-}$ and *Rag1*$^{-/-}$ mice would need to be assessed.

Small intestinal lamina propria DCs were reported to produce IL-23 in a TLR5 dependent fashion in response to systemic administration of flagellin.[354] In turn, intestinal IL-23 induced IL-22 production by ILCs and subsequent expression of the AMP RegIIIγ, which conferred protective effects during pathogenic infection.[131, 354] IL-23 and IL-22 were induced within 2 hours of flagellin injection, suggesting that sub-epithelial DC rapidly respond to a breach of barrier.[354] Although IL-22 is induced during T-cell transfer colitis,[359] we did not find any significant differences in IL-22 production and induction of downstream effectors, such as RegIIIγ, in *Tlr5*$^{-/-}$*Rag1*$^{-/-}$ recipients of naive CD4^{+} T cells, compared with *Rag1*$^{-/-}$ recipients. Hypothetically, a general defect in IL-22 and AMPs could lead to increased barrier permeability and microbial translocation at steady state that could enhance priming and activation of naïve T-cells. A comparison between *Rag1*$^{-/-}$ and *Tlr5*$^{-/-}$*Rag1*$^{-/-}$ mice for steady state barrier function and IL-22 production would further elucidate possible homeostatic functions dependent on TLR5.

TLR5 expression has been reported to be confined mainly to the cecum and proximal colon,[344, 360] with expression in both mononuclear cells of the lamina propria and in IECs.[360] In addition, TLR5 expression was reported to be reduced during acute intestinal inflammation, induced by DSS.[344] To characterise the effects of TLR5 signalling in distinct cellular compartments during colitis, we generated *Rag1*$^{-/-}$ BM chimeras selectively lacking TLR5 in either the haematopoietic or stromal compartments. The T-cell transfer experiments using BM chimera indicated that the absence of TLR5 expression in IEC or stroma resulted in increased pathology in the distal colon. However, the distal colon harbours a high antigenic load and conventional *Rag1*$^{-/-}$ mice displayed marked variability in disease at this site. Evaluation of TLR5 expression by mRNA or immunohistochemistry in inflamed and non-inflamed *Rag1*$^{-/-}$

mice in the different regions of the colon would be needed in order to validate the expression levels of epithelial TLR5 at this site.

Studies using the BM chimeric mice further revealed that the absence of TLR5 expression in host hematopoietic cells mediated increased mean pathology, as well as exacerbated pathology in the proximal colon. One study reported that small intestinal TLR5 expression was confined to lamina propria $CD11c^+$ cells, while expression in IECs and lymphocytes was negligible.[279] Although the use of different cell surface markers and gating strategies renders comparisons across studies difficult, TLR5 expressing DCs in the small intestinal LP were shown to promote intestinal IgA production[353] to accumulate in the MLN[355] and to produce IL-23[354] following administration of flagellin.[354] TLR5 expression among distinct hematopoietic cell populations in the colonic mucosa has not been described and whether IL-23 production by colonic DC can occur in a TLR5 dependent manner remains to be determined. During T-cell transfer colitis, IL-23mRNA expression was highly increased in $CD11b^+$ and $CD11c^+$ cells isolated from the colonic lamina propria, suggesting that these cells could be a major source of IL-23 in the inflamed colon.[361]

Another possible explanation for the exacerbated T cell transfer colitis in *Tlr5*$^{-/-}$*Rag1*$^{-/-}$ mice could be impairments of regulatory circuits. Indeed, even in the absence of host IL-23, naïve $CD4^+$ T-cells mediated colitis in *Rag*$^{-/-}$ recipients when regulatory cytokines IL-10 or TGF-β were neutralised.[252] There is some limited development of $FoxP3^+$ Tregs from the adoptively transferred naive $CD4^+$ T cells.[252] Attempts were made to assess regulatory T-cell development in the colonic lamina propria by isolating LPL and performing ic stain for FoxP3. However, no clear induction of $FoxP3^+$ cells could be discerned. An alternative way of determining regulation would be to measure IL-10 production in tissue explant cultures or from isolated LPL, or to use naïve $CD4^+$

T-cells from IL-10-GFP reporter mice, which co-express IL-10 and GFP.[280] In contrast to a potential regulatory effect of myeloid cells, transfer of naïve T-cells into an IL-10 deficient host was reported to result in wasting disease and pathology of the same kinetics and severity as in an IL-10 sufficient recipient, suggesting that host-derived IL-10 was dispensable for disease development. [362] This observation suggests that host myeloid cell production of IL-10, and possible defects in this axis in *Tlr5*$^{-/-}$*Rag1*$^{-/-}$ mice, would likely only have a minor impact on T cell-mediated colitis. However, lamina propria DC expressing TLR5, isolated from the small intestine, expressed retinaldehyde dehydrogenase which is needed for synthesis of retinoic acid (RA).[353] RA production by these cells induced Th17 cells *in vitro*[353]. However, RA is also associated with Treg induction,[363] arguing for a dual role of these TLR5 expressing myeloid cells.

Consistent with a regulatory role for TLR5 in limiting T cell-mediated colitis, we found that lymphocyte replete *Tlr5*$^{-/-}$ mice developed exacerbated T-cell dependent typhlocolitis when infected with *H. hepaticus* and concomitantly treated with α-IL-10R mAb. Again, it was difficult to see any clear exacerbation of well-described pathogenetic effector mechanisms in this model, with similar frequencies of Th1 cells and neutrophils present in the intestine in WT and *Tlr5*$^{-/-}$ mice. Although the frequencies of Th17 cells were reduced in *Tlr5*$^{-/-}$ mice relative to WT mice after Hh+ α-IL-10R treatment, comparative analyses of IL-17A and IFN-γ mRNA levels showed a trend towards increased expression in the colon of *Tlr5*$^{-/-}$ mice. In addition to effector CD4^{+} T cells, these cytokines can be produced by various innate leukocytes in the intestine, most notably by NK cells and ILCs.[58] Indeed ILC-derived IL-17A and IFN-γ mRNA has been shown to contribute to innate intestinal inflammation triggered by *H. hepaticus*,[63] although, as discussed below, we did not see exacerbated disease in this model in the absence of TLR5. Thus, further studies are required in order to identify the

non-T cell sources of inflammatory cytokines in colitic *Tlr5*$^{-/-}$ mice and their contribution to disease.

In contrast to our findings of increased susceptibility of *Rag1*$^{-/-}$*Tlr5*$^{-/-}$ mice in the T-cell transfer model of colitis, a recent study reported that transfer of sorted splenic CD4^{+}FOXP3^{-} T-cells into *Tlr5*$^{-/-}$*Tcrβ*$^{-/-}$ mice or *Tlr5*$^{+/+}$*Tcrβ*$^{-/-}$ mice resulted in reduced wasting disease in *Tlr5*$^{-/-}$*Tcrβ*$^{-/-}$ mice, but similar intestinal inflammation in both genitypes.[347] Possible explanations for the discrepancies between these results and our findings could be the different sorting protocols employed, as not only naïve CD4^{+} T-cells were transferred to recipient animals in this study, and that the recipients were of a different genotype.

We found that TLR5 expression was dispensable for the development of *H. hepaticus* innate, intestinal inflammation. Previous studies had shown that MyD88 signalling in myeloid cells was required for pathogenesis in this model and that TLR2 signaling was redundant.[265, 287] In the case of direct detection of *H. hepaticus* by TLR5, it is known that enteric ε-proteobacteria, which include the *Helicobacter* and *Campylobacter* genera, have developed altered forms of flagellin which have little or no TLR5 activating effect.[266] Since the structures involved in TLR5 binding are essential for motility, these bacteria have evolved flagellin with compensatory amino acid changes and remain motile.[266] Recently, TLR11, which is expressed in mice but not humans, was reported to detect bacterial flagellin.[119] Interestingly, small intestinal LP-DCs expressed both TLR5 and TLR11 and the two sensors could form heterodimers.[119] However, TLR11 expression in colonic DCs has not been described and it is unclear whether *Helicobacter* flagellin would be a putative ligand.

TLR5 deficient mice have previously been reported to harbour distinct microbial flora that could affect metabolic status and alter basal inflammatory gene expression.[356, 357] 25% of *Tlr5*$^{-/-}$ mice from a specific colony exhibited severe intestinal inflammation, characterized by shortening of the colon, neutrophil recruitment to the mucosa, increased levels of adherent bacteria in the gut tissue and systemic translocation of bacteria to the spleen and liver.[357] Further studies showed that standardisation of the microflora by embryonic rederivation abrogated spontaneous colitis, but that *Tlr5*$^{-/-}$ mice developed metabolic syndrome.[356] Despite the rederivation this effect was dependent on gut microbiota and could be transferred to germ-free WT mice.[356] These findings have been challenged and TLR5 deficient animals from a different colony did not display either spontaneous colitis or metabolic syndrome.[364] Furthermore, different TLR deficient animals were confirmed to harbour distinct flora, but the composition was maternally derived and not a result of altered TLR signalling. [365] However, as a consequence of these studies intestinal microflora needs to be considered. Experiments using the *H. hepaticus* αIL-10R model of colitis exclusively included male animals and the different genotypes were not co-housed at any point. Measures to equalise intestinal flora would need to be undertaken in order to determine whether TLR5 deficiency directly results in exacerbated pathology during *H. hepaticus* driven T-cell mediated intestinal inflammation. Studies showed that non-colitic *Tlr5*$^{-/-}$ mice[356] developed intestinal inflammation following treatment with αIL-10R antibody.[366] The disease was driven by IL-1R signalling and assessment of IL-1 levels in our experimental setting should be performed.

In contrast to the *H. hepaticus* +αIL-10R experiments, *Rag1*$^{-/-}$ and *Tlr5*$^{-/-}$*Rag1*$^{-/-}$ mice were either kept separately, co-housed during or co-housed before and during the T-cell transfer experiment. The different settings all resulted in the same TLR5 phenotype.

BM chimeric mice were co-housed extensively during reconstitution and RB^{high} transfer. The TLR5 deficient mice remained susceptible, arguing against a role of colitogenic flora in this model. Since IL-23 is protective during acute bacterially triggered intestinal inflammation,[244] an alternative explanation could be that TLR5 deficient animals display baseline or initial innate immune deficiencies, which at an early, more acute, stage of chronic inflammation contributes to exacerbated pathology. Further analysis of TLR5 expression in mucosal tissue and intestinal cell populations, as well as steady state characteristics of TLR5 deficient animals, are needed to elucidate the protective and pathogenic effects of TLR5 in the intestine.

Chapter 6 Effects of the *Helicobacter hepaticus* Type 6 secretion system in infection and inflammation

6.1 Introduction

Helicobacter hepaticus is a gram-negative, enteric bacterium that is present in many mouse colonies around the world. [367] It is unknown how *H. hepaticus* persists in close proximity of epithelial cells in the intestinal crypts without triggering adaptive immune responses that could result in eradication, but the regulatory cytokine IL-10 has been shown to be imperative for suppressing inflammatory cues.[262, 263] Relatively few colonisation or pathogenicity factors have been identified for *H. hepaticus*. Motility is essential for colonisation, and various flagellar mutants were attenuated during *in vivo* infection.[326] The urease enzyme, which catalyses the conversion of urea into ammonia and carbon dioxide, is a colonisation factor of gastric *Helicobacter* species[368, 369]. Recent studies in our laboratory showed that deletion of the *H. hepaticus* urease *ureA* gene resulted in delayed colonisation and reduced pathology in both innate and adaptive models of colitis.[370] Furthermore, cytolethal distending toxin (CDT), a protein with cytotoxic properties *in vitro*, was shown to contribute to colonisation, pathology and long-term persistence of *H. hepaticus*.[291, 371-373]

Recently, *H. hepaticus* was shown to express a functional type 6 secretion system (T6SS).[331]Bacterial T6SS are considered to be present in up to 25% of all sequenced bacterial genomes and appear to be a property of the proteobacteria.[374] The precise structure of the system has not been determined, but it has been suggested to be similar to a bacteriophage like needle complex.[375] Activation is seemingly dependent on cell-cell contact. TTS6 systems consist of a genomic island of approximately 15-20 conserved genes, although individual genes of the system can be found in other parts of

the genome. *IcmF* is a transmembrane protein present in all T6SS described so far. Valine-glycine-repeat proteins (VgrG) and hemolysin coregulated protein (Hcp) are hallmark substrates and structural proteins of the T6SS. The detection of Hcp protein in culture medium indicates the presence of an active T6SS.[376-380] So far relatively few effector proteins have been identified, but *Vibrio cholera* has been reported to express a VgrG protein with actin cross-linking enzymatic activity. [381] T6SS have been implicated in a wide array of functions, including inter-bacterial competition and the killing of eukaryotic predators.[382-384] In the case of enteric bacteria, studies using different species of the *Salmonella* genus have mainly concluded that the T6SS confers fitness and contributes to colonisation, persistence and intracellular replication. *Salmonella* T6SS deletion mutants displayed attenuated phenotypes during *in vivo* infection.[385-388]

Sequencing analyses of different *H. hepaticus* isolates identified a pathogenicity island, termed HHGI1, in some strains.[389] Deletion of the *H. hepaticus* genomic island HHGI1 resulted in attenuated development of liver disease and intestinal inflammation in susceptible hosts.[329, 390] *In silico* analysis revealed that HHGI1 likely encoded for T6SS factors and VgrG, Hcp and IcmF proteins were subsequently identified.[331] The *H. hepaticus* T6SS has been described to promote anti-inflammatory, symbiotic effects in a model of intestinal inflammation based on adoptive transfer of naïve T-cells.[331] Infection of *Rag1*$^{-/-}$ mice with an *IcmF* deletion mutant following adoptive transfer of naïve CD4^{+} T-cells resulted in increased colonisation levels and elevated expression of pro-inflammatory cytokines in colon tissue. Furthermore, MLN lymphocytes from infected animals displayed increased ability to produce IL-17A during *in vitro* stimulation with PMA and ionomycin or α-CD3 and α-CD28.[331] However, despite claiming that the *IcmF* mutant induced increased inflammatory responses, no

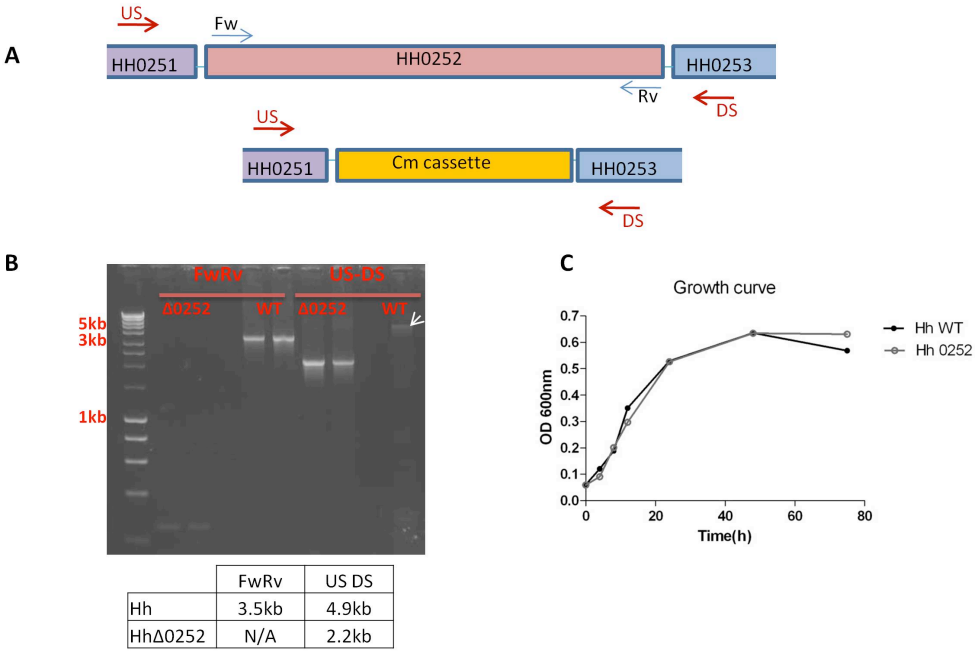
significant differences in intestinal pathology *in vivo* were reported. In order to evaluate the role of the *H. hepaticus* T6SS in the regulation of chronic innate and adaptive intestinal pathology, we generated a *H. hepaticus IcmF* deletion mutant and assessed the course of infection in both pathogenic and non-pathogenic settings.

6.2 Results

6.2.1 Generation of a *H. hepaticus IcmF* deletion mutant

In order to investigate the impact of T6SS in *H. hepaticus* pathogenicity, an *IcmF* deletion mutant (HhΔ0252) was generated. Gene HH0252 was replaced with a chloramphenicol (Cm) resistance cassette via homologous recombination (Fig.6.1A).[291] PCR and sequencing confirmed that gene HH0252 was deleted in HhΔ0252 and that insertion of the Cm-cassette resulted in a smaller product when primers binding to flanking regions (US,DS) were used for PCR amplification (Fig.6.1A,B). The deletion mutant appeared fully motile when observed under the microscope and did not display altered growth characteristics compared with the parental WT *H. hepaticus* strain (Hh WT) *in vitro* (Fig.6.1C).

Figure 6.1



	FwRv	US DS
Hh	3.5kb	4.9kb
HhΔ0252	N/A	2.2kb

Figure 6.1 Generation of a *H. hepaticus IcmF* deletion mutant

(A) Schematic representation of HhΔ0252 deletion mutant where the *H. hepaticus IcmF* gene, HH0252, was replaced with a chloramphenicol (Cm) resistance cassette. (B) The deletion of HH0252 (Δ0252) was confirmed by PCR for an intragenic sequence (Fw-Rv) and for sequences flanking the deleted area (US-DS). The white arrow indicates a PCR product of approximately 5kb. (C) Growth curves for WT *H. hepaticus* (Hh WT) and the IcmF deletion mutant (HhΔ0252) were generated. Cultures were grown in TSB supplemented with TVP. Data are from 1 experiment.

6.2.2 Intestinal inflammation is delayed during infection with a *H. hepaticus* T6SS deletion mutant

To examine the role of the T6SS in the regulation of innate immune pathology, cohorts of 129SvEv*Rag2*$^{-/-}$(*Rag2*$^{-/-}$) mice were infected with 10^8 CFU Hh WT or HhΔ0252 and were sacrificed after 2, 4, 8 or 12 weeks of infection. Intestinal pathology was evaluated in the cecum and the colon. As expected, *Rag2*$^{-/-}$ mice infected with Hh WT developed cecal inflammation, with moderate typhlitis observed as early as 2wks p.i. and severe pathology present in all mice by 8 weeks p.i. (Fig.6.2A,C). Colitis scores in *Rag2*$^{-/-}$ mice infected with Hh WT were more variable, with mild colitis at 2wks and 4wks p.i., but severe colitis present after 12 wks of colonisation (Fig.6.2B). In contrast, *Rag2*$^{-/-}$ mice infected with HhΔ0252 exhibited significantly reduced typhlitis at 2 and 4 wks p.i. (Fig.6.2A,C). Similarly, infection of *Rag2*$^{-/-}$ mice with HhΔ0252 resulted in significantly lower colitis scores at 2 and 4 wks p.i. (Fig.6.2 B). However, after 8-12 wks of colonisation, comparably severe inflammatory pathology was observed in the cecum and colon of *Rag2*$^{-/-}$ mice infected with Hh WT or with HhΔ0252 (Fig.6.2A,B), indicating that long-term pathogenicity of HhΔ0252 was not altered.

Figure 6.2

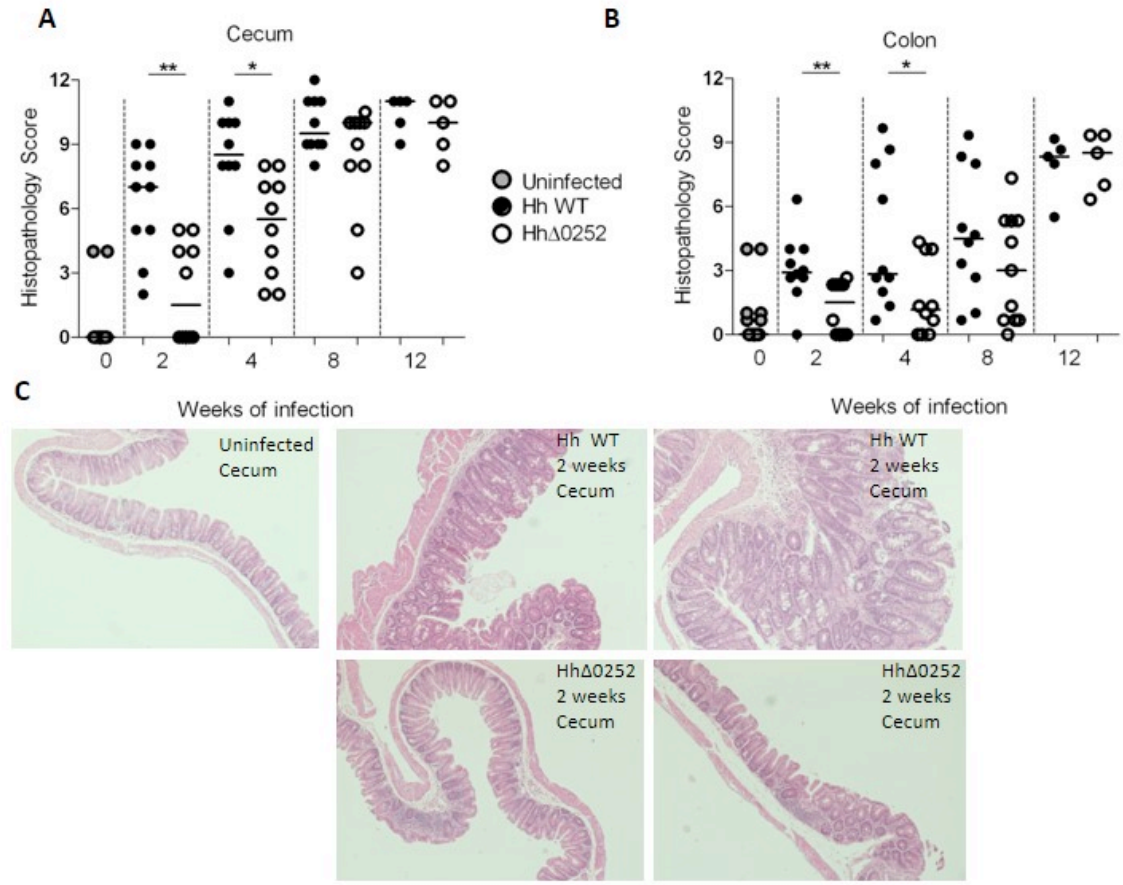


Figure 6.2 Delayed development of typhlocolitis during infection with a *H. hepaticus* T6SS deletion mutant

129SvEv*Rag2*$^{-/-}$mice were infected by oral gavage with approximately 10^8 CFU Hh WT or HhΔ0252 and sacrificed after 2, 4, 8 or 12 weeks of infection. (A) Typhlitis scores (B) Colitis scores. (C) Representative micrographs of cecum after 0 or 2 weeks of infection. Data were pooled from 2 independent experiments for the 2 week, 4 week and 8 week time points, n=10 per group. Data for the 12 week time point are from 1 experiment, n=5 per group. Uninfected controls n=13. Horizontal bars are median values and the non-parametric Mann-Whitney test was used for statistical analysis, *P<0.05, **P<0.01.

6.2.3 Local and systemic immune responses are delayed during infection with a *H. hepaticus*T6SS deletion mutant

Concurrent with the onset of intestinal pathology, *Rag2*$^{-/-}$ mice infected with Hh WT displayed significant neutrophil accumulation in the colon LP after 2 wks of infection, whereas no significant neutrophil recruitment was found in the colon LP in *Rag2*$^{-/-}$ mice infected with HhΔ0252 at this early time point (Fig.6.3A). However, by 8 weeks p.i. neutrophil recruitment to the colonic tissue in *Rag2*$^{-/-}$ mice infected with HhΔ0252 was comparable to that found in *Rag2*$^{-/-}$ mice infected with Hh WT (Fig.6.3A). Quantification of total cell numbers recovered from the colon LP confirmed the significantly reduced early leukocyte accumulation in *Rag2*$^{-/-}$ mice inoculated with HhΔ0252 compared to those infected with Hh WT (Fig. 6.3B). Assessment of splenomegaly revealed that *Rag2*$^{-/-}$ mice infected with Hh WT developed significant splenomegaly as early as 2 wks p.i., which rapidly increased during the course of infection (Fig.6.3C). In contrast, *Rag2*$^{-/-}$ mice infected with HhΔ0252 displayed unaltered spleen weights at 2 wks p.i. and splenomegaly was still significantly lower in *Rag2*$^{-/-}$ mice infected with HhΔ0252 compared with Hh WT at 4 and 8 wks p.i. (Fig.6.3C). However, after 12 weeks of colonisation spleen weights reached equivalent levels in *Rag2*$^{-/-}$ mice infected with Hh WT or HhΔ0252 (Fig.6.3C), indicating that long-term systemic immune responses to HhΔ0252 compared with Hh WT were equivalent.

Figure 6.3

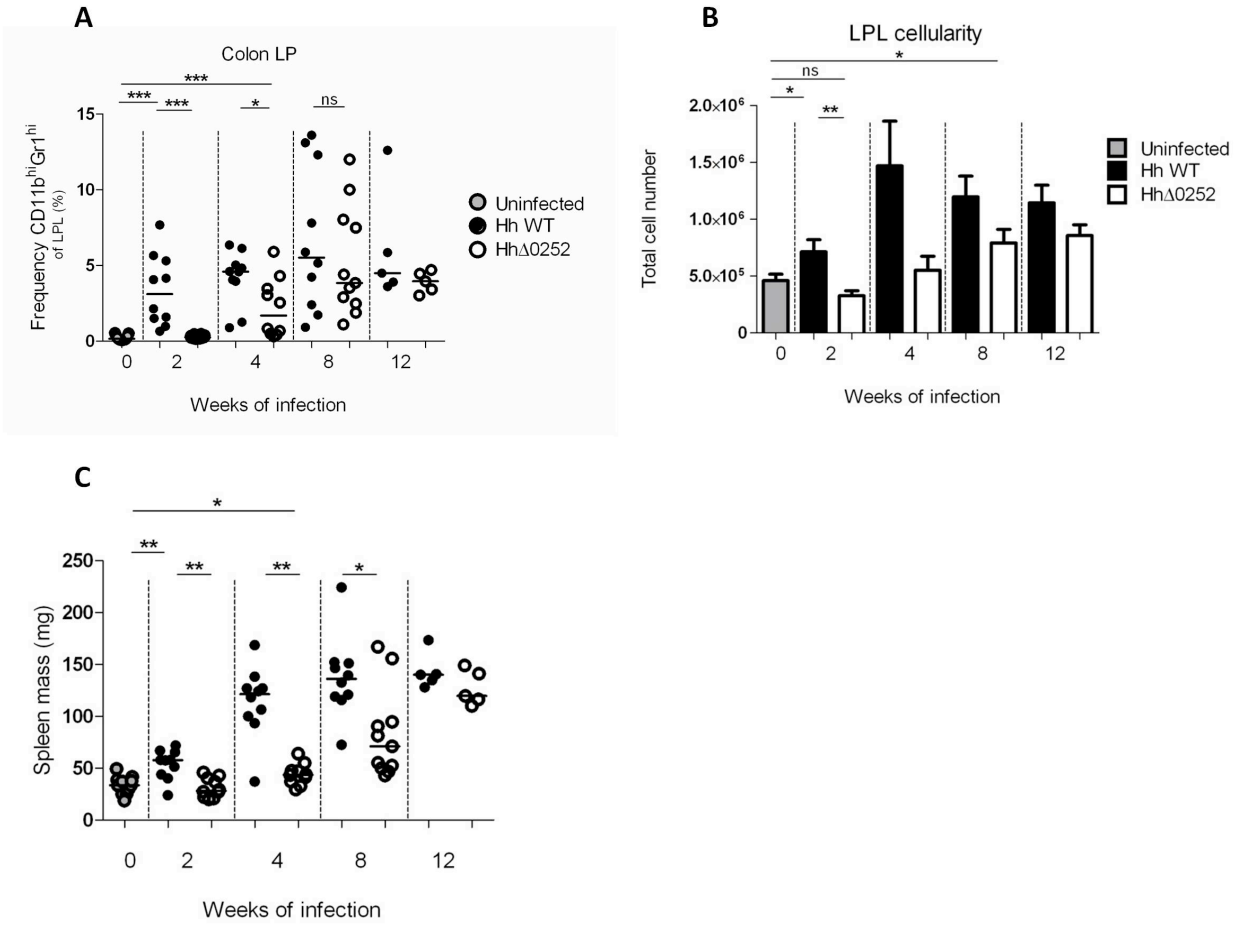


Figure 6.3 Local and systemic immune responses are delayed during infection with a *H. hepaticus*T6SS deletion mutant

129SvEv*Rag2*$^{-/-}$mice were infected by oral gavage with approximately 10^8 CFU Hh WT or HhΔ0252 and sacrificed after 2, 4, 8 or 12 weeks of infection. (A) Lamina propria leukocytes were isolated from colonic tissue and granulocyte ($CD11b^{hi}Gr1^{hi}$) accumulation was assessed. (B) Total cell numbers recovered from colon LP were quantified. (C) Spleen weights. Data were pooled from 2 independent experiments for the 2 week, 4 week and 8 week time point (n=10/group). For the 12 week time point, data were from 1 experiment, n=5 per group. Uninfected controls n=13. Horizontal bars indicate median values. Bar graphs are shown with mean ± SEM. The non-parametric Mann-Whitney test was used for statistical analysis. *P<0.05, **P<0.01, ***P<0.001

6.2.4 The *H. hepaticus* T6SS deletion mutant exhibits a colonisation defect

Assessment of *H. hepaticus* colonisation of the intestinal tract of *Rag2*$^{-/-}$ mice was performed by *H. hepaticus* specific qPCR of total DNA extracted from cecal luminal content.[285] Consistent with the reduced local and systemic immune responses, colonisation levels in *Rag2*$^{-/-}$ mice infected with HhΔ0252 were significantly reduced compared with *Rag2*$^{-/-}$ mice infected with Hh WT at 2 wks p.i. (Fig.6.A). However, at subsequent time points, *H. hepaticus* colonisation levels were comparable in *Rag2*$^{-/-}$ mice infected with HhΔ0252 or Hh WT (Fig.6.A). To investigate levels of tissue-associated *H. hepaticus*, DNA from whole cecal tissue was isolated and *H. hepaticus* specific qPCR carried out. Although levels of *H. hepaticus* were generally lower in tissue samples compared with cecal luminal contents, *Rag2*$^{-/-}$ mice infected with HhΔ0252 harboured significantly less *H. hepaticus* in the tissue compared to those infected with Hh WT at 2 wks p.i. (Fig.6.4B). However, by 12 wks p.i. tissue-associated levels of HhΔ0252 were equivalent to levels of Hh WT in infected *Rag2*$^{-/-}$ mice (Fig.6.4B), indicating that the *H. hepaticus* T6SS modulated initial, but not long-term, colonisation.

Figure 6.4

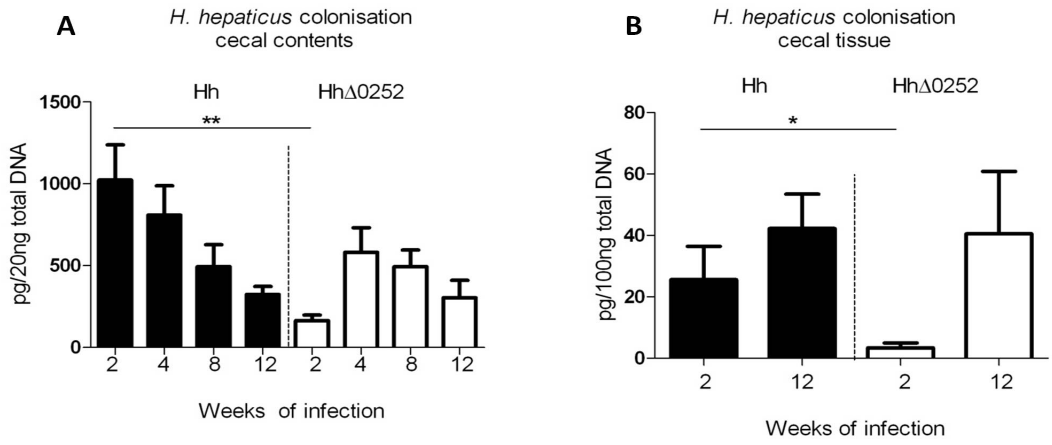


Figure 6.4 The *H. hepaticus* T6SS deletion mutant exhibits a colonisation defect
129SvEv*Rag2*$^{-/-}$mice were infected by oral gavage with approximately 10^8 CFU Hh WT or HhΔ0252 and sacrificed after 2, 4, 8 or 12 weeks of infection. (A) *H. hepaticus* colonisation levels. Total DNA was extracted from cecal contents and levels of *H. hepaticus* was determined by qPCR. (B) *H. hepaticus* levels in cecal tissue. Cecal tissue was snap-frozen at necropsy, total DNA was isolated and *H. hepaticus* colonisation levels were determined by qPCR. In (A) data were pooled from 2 independent experiments for the 2 week, 4 week and 8 week time point (n=10/group). For the 12 week time point, data were from 1 experiment, n=5 per group. In (B) data represent 1 experiment, n=5 per group. Bar graphs are shown with mean ± SEM. The non-parametric Mann-Whitney test was used for statistical analysis. *P<0.05, **P<0.01.

6.2.5 Impaired IL-10$^+$ Foxp3$^+$ Treg cell induction during infection with a *H. hepaticus* T6SS deletion mutant

Infection of WT mice with *H. hepaticus* results in the induction of IL-10 production by CD25$^+$CD45RB^{low}CD4$^+$ and CD25$^-$CD45RB^{low}CD4$^+$T-cells.[263] The CD25$^+$RB^{low}CD4$^+$ population has been identified to contain the regulatory T-cells.[264] Blocking the IL-10 receptor concurrent with *H. hepaticus* infection or exposing mice deficient in IL-10 to *H. hepaticus*, culminates in severe intestinal inflammation.[259, 262] The *H. hepaticus* T6SS was suggested to mediate immunosuppressive effects.[331] In order to track development of IL-10 induction in Treg during *H. hepaticus* infection, FOXP3-IL-10 reporter mice were used.[280, 281] Mice homozygous for both GFP-linked IL-10 and FOXP3 linked to a human CD2_CD52 fusion protein (hCD2) were crossed with mice homozygous for FOXP3-hCD2. In the resulting offspring, cells expressing mRNA for IL-10 could be tracked through GFP expression and cells expressing Foxp3 could be distinguished by coexpression of surface human CD2_CD52 fusion protein. IL-10 expressing Treg could thus be distinguished by flow cytometry. The FOXP3-IL-10 reporter mice were inoculated with Hh WT or HhΔ0252 and were sacrificed after 14 days of infection. No mice displayed any overt intestinal inflammation, in line with functional IL-10 production. Leukocytes were isolated from cecal and colonic tissue and intestinal CD4$^+$ T cells were analysed by flow cytometry. In uninfected mice, IL-10 expressing Foxp3$^+$ Treg constituted approximately 30% of the total Foxp3$^+$ Treg population in the cecum and colon (Fig.6.5A,B). We found that mice infected with Hh WT exhibited significantly increased frequencies of IL-10$^+$ Foxp3$^+$ Treg in both cecum and colon compared with uninfected mice (Fig. Fig.6.5A,B). In mice infected with HhΔ0252 the frequencies of IL-10$^+$ Foxp3$^+$ Treg were similar in the cecum but were significantly reduced in the colon compared to those found in mice infected with Hh

WT (Fig.6.5A,B). Assessment of *H. hepaticus* colonisation levels in cecal contents revealed that although levels of HhΔ0252 were not significantly reduced, colonisation levels with the mutant were very low in some individual mice (Fig.6.5C), corresponding to similarly low frequencies of IL-10 expressing Treg (Fig.6.5D). Thus, the low colonisation levels of HhΔ0252 in a proportion of animals suggested that although HhΔ0252 might induce less IL-10 expression, this could be an effect of delayed colonisation.

Figure 6.5

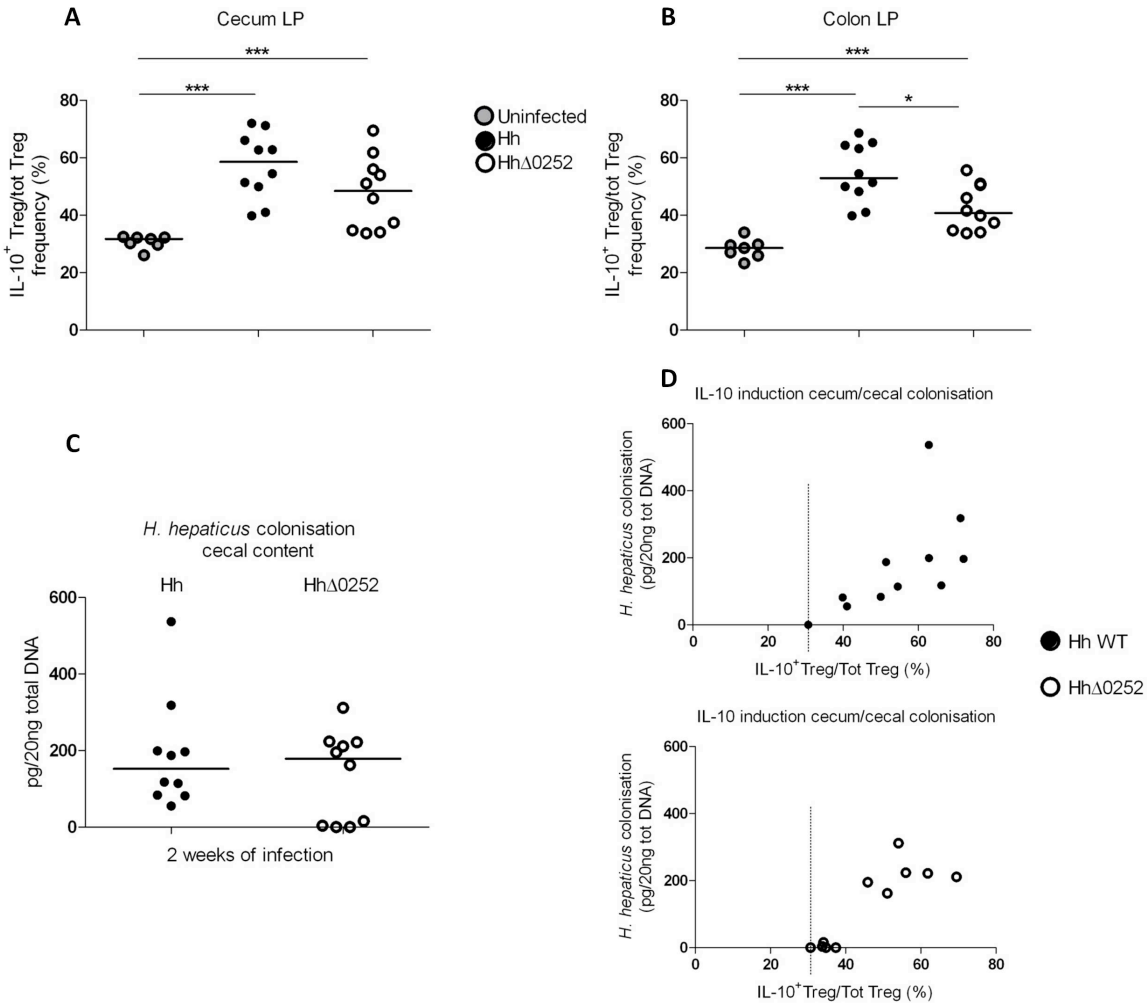


Figure 6.5 Induction of IL-10 expressing regulatory T-cells is impaired during infection with a *H. hepaticus* T6SS deletion mutant

FOXP3-IL-10 reporter mice were infected by oral gavage with approximately 10^8 CFU Hh WT or HhΔ0252 and sacrificed after 14 days of infection. (A) Frequencies of IL-10 expressing Treg among total Treg in cecal lamina propria. (B) Frequencies of IL-10 expressing Treg among total Treg in colonic lamina propria. (C) *H. hepaticus* colonisation levels. Total DNA was isolated from cecal contents at necropsy and *H. hepaticus* speficic qPCR was performed. (D) Correlation between cecal colonisation levels and frequencies of IL-10 expressing Treg among total Treg in cecum lamina propria. Data were pooled from 2 independent experiments (n=10/group infected, n=7 uninfected). Horizontal bars indicate group median values. In (D) vertical dotted lines indicate cut off value for uninfected animals. Bar graphs are shown with mean ± SEM. The non-parametric Mann-Whitney test was used for statistical analysis. *P<0.05, ***P<0.001.

6.3 Discussion

Our findings indicate that infection with a *Helicobacter hepaticus IcmF* deletion mutant resulted in delayed disease development in a model of *H. hepaticus* induced innate intestinal inflammation. The reduced pathology at early stage infection was correlated with reduced initial colonisation, suggesting that the *H. hepaticus* T6SS contributed to the establishment of a niche in the host. A previous study using various *H. hepaticus* T6SS mutants revealed that although T6SS genes were expressed during *in vitro* culture, only Hcp could be detected after long term infection *in vivo*.[391] T6SS components Hcp and Vgrg1 were detected in culture supernatant of WT *H. hepaticus*, but only detected in bacterial lysates of *IcmF* mutant *H. hepaticus*.[391] The *IcmF* deletion mutant was therefore considered a functional T6SS mutant.[391]

A previous report revealed increased colonisation of a *H. hepaticus IcmF* mutant in colonic and cecal tissue of mono colonised lymphocyte replete, WT mice after 2-13 weeks of infection.[331] Colonisation levels were assessed both by qPCR for *H. hepaticus* DNA levels and by culture of tissue homogenates for CFU enumeration.[331] Furthermore, conventional SPF mice were shown to harbour increased intracellular levels of the *IcmF* mutant in colonic epithelial cells, as shown by *ex vivo* culturing of IEC isolates, and the increased invasion of epithelial cells could be replicated *in vitro* by the use of an epithelial cell line.[331] This would suggest that the *H. hepaticus* T6SS limited invasive properties. *H. hepaticus* has not previously been described as an intracellular bacterium and the immunohistochemistry images from the *in vivo* infection of the aforementioned study did not support increased invasion of IEC.[331] We assessed *H. hepaticus* colonisation levels in cecal tissue of *Rag2*$^{-/-}$mice infected with Hh WT or HhΔ0252 for 2 weeks and 12 weeks by qPCR of DNA levels. We could not detect an increase in tissue resident bacteria in mice infected with HhΔ0252 compared with Hh

WT. On the contrary, levels of tissue-associated HhΔ0252 were significantly lower after 2 weeks of infection compared with Hh WT, supporting a colonisation defect. Different technical approaches could explain the discrepancies between our results and the published study. Colonisation of germ free mice is difficult to compare with SPF mice. Regarding invasion of IEC, the culturing of *H. hepaticus* from *in vivo* samples requires more than week long incubation and the discerning of distinct *H. hepaticus* colonies is challenging due to motility of the bacteria. In order to draw final conclusions regarding the impact of the T6SS on *H. hepaticus* invasiveness, we would need to assess colonisation levels in isolated IEC using our settings.

A second study reported reduced pathogenic properties of T6SS mutant *H. hepaticus*.[391] B6*Rag2*$^{-/-}$ mice were inoculated with *H. hepaticus* one week prior to adoptive transfer of naïve CD4^{+} T-cells. Infection with an *IcmF* deletion mutant resulted in similar colonisation levels, as assessed by CFU enumeration of total tissue homogenates, and pathogenicity as WT *H. hepaticus*.[391] Infection with a *VgrG1* deletion mutant however resulted in increased colonisation levels and abrogated disease.[391] Due to technical differences, the two opposing studies are difficult to compare. In the study that reported immunosuppressive effects and increased pathogenicity of the *H. hepaticus* T6SS, mice that had already been injected with naïve CD4^{+} T-cells were infected.[331] In the second study, which reported reduced pathology, mice were already infected at the time of adoptive transfer.[391] Thus, *H. hepaticus* colonisation did not occur in comparable mucosal environments. The *H. hepaticus* T6SS could potentially mediate different effects when colonising uninflamed or inflamed tissue.

Our studies have shown that an *H. hepaticus* T6SS deletion mutant exhibited delayed colonisation and reduced intestinal inflammation in a model of chronic typhlocolitis. However, the T6SS mutant bacteria overcame this initial defect and by 12 weeks of

infection local and systemic responses, as well as luminal and tissue-associated colonisation levels, were equivalent in mice infected with WT or *H. hepaticus* T6SS mutant. In order to extract possible immunomodulatory effects of the *H. hepaticus* T6SS from a general colonisation defect, factors or induced effects need to be identified *in vitro* and subsequently modulated *in vivo*. Overall, our data suggest that the *H. hepaticus* T6SS confers advantageous properties during initial infection and could be viewed as an early colonisation factor.

Chapter 7 General discussion

7.1 Innate sensing of flagellin contributes to tissue protection in the intestine

Flagellin is a highly immunogenic bacterial protein that is recognised by at least two different PRRs; the cytosolic NLRC4 and the transmembrane TLR5. The two flagellin PRRs differ considerably. The NLRC4 inflammasome recognises bacterial components other than flagellin and represents a potent mechanism for the generation of pro-inflammatory effects, including cell death. TLR5 modulates DC function and promotes epithelial protection. The aim of this thesis was to investigate the impact of innate immune responses to flagellin on the development of intestinal inflammation.

By using different models of experimental intestinal inflammation and mice deficient in either NLRC4 or TLR5, various properties of these PRRs have been studied. The results clearly show that NLRC4 and TLR5 mediate protective effects in acute and chronic intestinal inflammation. During the development of these projects, it became apparent that NLRC4 most likely did not only detect flagellin in our models of inflammation but also components of the bacterial T3SS.[176-178] We hypothesised that the *C. rodentium* T3SS was detected by NLRC4 but that commensal flagellin could provide the activating signal at steady state. The NLRC4 inflammasome was therefore viewed as a collective unit for the sensing of flagellin and the T3SS.

The results presented in this thesis can be aligned with several emerging perspectives of PRR activation and function. These include; the functional consequences of cell-specific expression of different PRRs; the effects of PRR activation on epithelial cell turn-over; the absence of redundancy in PRR regulation of intestinal homeostasis; and microbial modulatory effects on PRR function.

7.2 Inflammasomes and the intestinal epithelium

Inflammasomes have traditionally been observed and studied in *in vitro* systems using bone-marrow derived macrophages (BMDMs). BMDMs provide a high-throughput system, allow the study of the impact of single genes and serve as relevant, although not identical, representatives of the intestinal macrophage. However, growing evidence suggests that inflammasome activation in other cell types contributes to intestinal homeostasis and provide protection during conditions of infection and damage.[392]

Little is known about inflammasome activation in the intestinal epithelium. Colonic epithelial cells produce IL-18 during intestinal inflammation and express mRNA for caspase-1, ASC, NLRP6 and NLRC4.[157, 296, 392] NLRP1, but not NLRP3, is expressed in human IECs.[393] Our experiments suggest that the NLRC4 inflammasome is active during steady state in the colon and that the NLRC4 inflammasome exerts limiting effects on pathogen colonisation of the intestinal epithelium very early during infection. The protective effects of NLRC4 during *C. rodentium* infection could be a combination of baseline activation and induced responses. The outcome could be modulated by the classical inflammasome derived cytokines and/or by pyroptosis, but could also be the result of the production of unknown antimicrobial factors (Fig. 7.1).

In order to fully study classical inflammasome activation in IEC in terms of IL-18, IL-1β and pyroptosis, a more reproducible *in vitro* or *ex vivo* system would need to be employed. Isolated primary IECs are challenging to culture *in vitro* and *C. rodentium* does not adhere to the majority of available intestinal epithelial cell lines (personal communication Professor Gad Frankel, Imperial College, London). An alternative approach to exploring interactions between *C. rodentium* and primary IEC, would be to establish organoid cultures.[318] Organoids originate from isolated intestinal stem cells

that have been cultured in a matrix containing a cocktail of growth factors. The protocol results in aggregates resembling intestinal crypts, composed of IECs.[318] The cultures could be generated from mice of specific genotypes in order to study different components of the inflammasome. Organoids are organised as hollow structures and the resulting cavity is equivalent to the intestinal lumen.[318] In order to infect organoids with bacteria or to treat the cells from the luminal side, a procedure of microinjection would have to be developed. Another approach would be to refine the organoid cultures and attempt to co-culture monolayers of organoids and stromal cells. IEC and stromal co-cultures would also resemble the actual architecture of the intestinal mucosa, provide the IEC with stromal derived cues[26] and afford a possibility to introduce immune cells to the cultures.

Epithelial NLRP3 and IL-18 mediate protective effects in the DSS model of intestinal inflammation.[157] The protective effects of recombinant IL-18 administration on DSS colitis are manifested as reduced weight loss and ameliorated pathology.[157, 214] However, the actual mechanisms of IL-18 mediated protection is less characterised. The IL-18R complex is expressed in a variety of different cells, including macrophages, neutrophils and endothelial cells, and is inducible in naïve $CD4^+$ T-cells.[394] One possibility is that IL-18 exerts its effect indirectly by potentiating the activity of IL-22, a cytokine that has been shown to promote IEC proliferation during inflammatory conditions.[270] IL-18 also mediated reduced expression of the soluble IL-22 receptor, IL-22 binding protein, by DCs, which potentially could increase the stimulatory capacity of IL-22.[395] In a model of intestinal inflammation and carcinogenesis based on AOM and DSS administration, mice deficient in IL-22 binding protein exhibited increased tumour numbers, in line with excessive IL-22 driven responses.[395] During the course of intestinal infection with *C. rodentium*, early stage inflammasome activation and IL-18

release in the epithelium could enhance IL-22 directed repair via IL-18 mediated downregulation of IL-22 binding protein. This in turn could prevent excessive immune activation and damage.

Pyroptosis is a lytic type of cell death that is associated with inflammasome activation.[145] The intestinal epithelium is constantly replaced and IECs are shed through a process called anoikis. Studies showed that cell-cell adherence was reduced before anoikis. Shedding resulted in gaps, which were found to be impermeable to aqueous dyes that were used in experimental settings.[396] Before shedding, surrounding cells extended processes beneath and around the cell destined to be lost, resulting in an actin and myosin dependent contraction.[397] Cells that were expelled from the monolayer were positive for cleaved caspase-3, confirming that apoptosis had occurred.[398] Pyroptosis does not result in caspase-3 processing.[399] Considering that cell shedding is a highly co-ordinated process between neighbouring cells, it is unclear how pyroptosis would fit in this system. Pyroptosis could be a mechanism of limiting pathogen colonisation by shedding single, infected cells, or by exporting factors through the formed pores into the lumen. The use of organoid cultures and *in vitro* infection could shed light on this rapid process.

Although mice deficient in IL-18R develop increased pathology in response to *C. rodentium* infection, the disease is less severe compared with inflammasome deficient animals (Personal communication, George Song-Zhao). Our experiments do not reveal increased release of IL-1β during infection, indicating that the mucosal production of IL-18 and IL-1β alone does not replicate the absence if inflammasome activation. In order to identify potentially novel inflammasome dependent factors in IECs, one approach would be to undertake a screening. A microarray analysis of isolated IEC could be performed. Alternatively, since the isolation process of IECs could alter gene

expression, an analysis of the proteome could be preferable. A standard procedure of mass spectrometry analysis of cell lines is the use of metabolic labelling, such as stable isotype labelling in cell culture (SILAC)[400] Since *C. rodentium* does not adhere to epithelial cell lines, organoid cultures could be an alternative *in vitro* system. The use of organoid cultures would not allow normalisation of cell numbers and techniques other than SILAC would need to be used. One possibility would be chemical labelling by dimethylation of peptides.[400, 401] Organoid cultures of different conditions could be grown and fractionated in parallel, and labelled as peptides. Samples would then be pooled and analysed by mass spectrometry.

Finally, tissue specific deletion of NLRs using the well characterised Cre/lox system would provide formal evidence of the importance and function of epithelial inflammasome activation. The Cre recombinase is of prokaryotic origin and once expressed, it recognises loxP sites and catalyses reciprocal recombination between these sites. As a result any gene flanked by two loxP sites will be excised.[402] To generate tissue specific deletion, Cre recombinase expression can be coupled to tissue specific promoters, such as the regulatory region of the villin gene that is selectively expressed in epithelial cells.[403] The Cre recombinase can also be coupled to an inducible element such as the human estrogen receptor. Adminstration of tamoxifen will result in ligand binding of the estrogen receptor and Cre recombinase activation.[403] This system would allow insight into the timeline of epithelial inflammasome expression and provide further understanding of this process *in vivo*. Whether the mechanisms of inflammasome activation and effector pathways that have derived from studies with myeloid cells are conserved in IECs is a key question that remains to be answered.

Figure 7.1

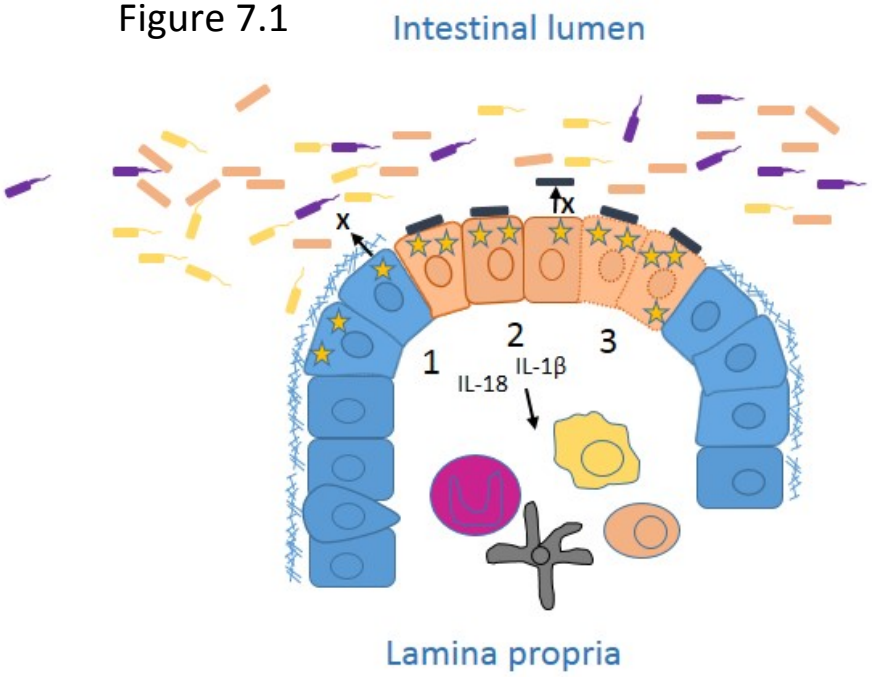


Figure 7.1 Epithelial inflammasomes contribute to tissue protection at steady state and during infection

Inflammasomes (stars) are active in IECs at steady state and during infection with an extracellular enteric pathogen. Inflammasome activation in IEC could contribute to several processes: (1) Contribution to tissue maintenance at steady state via IL-18 and potentially the generation of antimicrobial factors (X). (2) Production of active IL-1β and IL-18 during infection, with effects on immune cell recruitment and activity. (3) Triggering of pyroptosis and subsequent shedding during infection.

7.3 Inflammasomes and cell death

Caspases are cysteine proteases necessary for cell death. Mice and humans express 10 and 11 distinct caspases, respectively, divided into initiator caspases, which include caspases -1, -2, -4, -5, -8, -9, -10, -11 and -12, and effector caspases, which include caspase -3, -6, -7 and -14.[404] Initiator caspases associate with adaptor molecules through homotypic interactions and form a number of caspase activating complexes, namely the apoptosome, the death inducing signaling complex, the inflammasome and the caspase-2 activating PIDDosome complex.[404] Effector caspases induce apoptosis following activation.[404] The inflammasome associated caspases are caspase-1, -11 and -12 in mice, and caspase- 1, -4 and -5 in humans.[404, 405] Caspase-8 is traditionally activated via an external signal, typically the ligation of cell surface receptors with Fas ligand or TNF-α, which results in the formation of the death inducing complex and subsequent activation of effector caspases.[405] However, a recent report revealed that caspase-8 also could process IL-1β in response to binding of Fas ligand, independently of caspase-1 and caspase-11.[406] Other studies have revealed that caspase-8 interacts with the AIM2 and NLRP3 inflammasomes[407] and that, following ubiquitination, NLRC4 also interacts with caspase-8.[408] In the context of AIM2 and NLRP3 activating stimuli, caspase-8 activation mediated apoptosis, which was dependent on ASC and occurred in parallel with classical caspase-1 mediated pyroptosis.[407] Caspase-8 and ASC co-localised in specks following inflammasome stimuli and interacted via pyrin domains and IL-1β was processed, but not into the active species. A lower dose of the stimuli promoted caspase-8 and caspase-3 mediated apoptosis, while higher levels of stimuli favoured caspase-1 dependent pyroptosis.[407] In addition to caspase-1 proteolysis, caspase-8 activation is emerging as an alternative inflammasome-associated apoptotic pathway.

The majority of the aforementioned data were derived from BMDMs. The implications for the intestinal epithelium could be different, since IECs rapidly proceed through differentiation and apoptosis. Complete deletion of caspase-8 is embryonically lethal,[409] but mice with IEC-specific caspase-8 deficiency developed severe spontaneous intestinal inflammation in the distal ileum that was associated with reduced numbers of goblet cells and Paneth cells.[410] In the absence of caspase-8 mediated apoptosis in IECs a different type of cell death, termed necroptosis, dominated. Necroptosis could be induced by TNF-α and was mediated by the Rip3 kinase.[410, 411] Necroptotic cells were TUNEL positive, displayed vacuole formation and mitochondrial swelling but did not exhibit typical apoptotic characteristics such as membrane blebbing and were negative for caspase-3.[410] Interestingly, increased paneth cell depletion and necroptotic features constitute shared histological findings with Crohn's disease patients.[410]

In the context of *C. rodentium* infection of IECs, it is possible that low level, tonic stimulation by the commensal microflora could activate caspase-8 and trigger apoptosis. During infection with *C. rodentium*, increased inflammasome activation would induce caspase-1 mediated pyroptosis, which would attract leukocytes and possibly provide a mechanism of rapid shedding. In the absence of functional inflammasomes and subsequent apoptosis and pyroptosis, deleterious necroptosis could be promoted, resulting in increased damage.

7.4 Inflammasomes and NLR redundancy

Inflammasomes are formed in response to cytosolic presence of specific ligands. The NLRP3, NLRP6, NLRP12 and the NLRC4 inflammasomes all mediate protection in response to intestinal damage induced by DSS and little redundancy appears to exist.[157, 159, 160, 165, 166, 190] However, an *in vivo* infection study suggested that redundancy existed between NLRC4 and NLRP3 in protection to *Salmonella typhimurium*, perhaps to combat active immune evasion by bacteria.[143] In the case of *C. rodentium* infection, *Nlrp3*$^{-/-}$ mice displayed similar characteristics to *Nlrc4*$^{-/-}$ mice (Personal communication George Song-Zhao), further indicating that NLR redundancy is the exception rather than the rule. A possible explanation could be restricted expression of NLRs, both in cell types and over time. For example, NLRP3 is induced by NF-κB signalling while ASC and NLRP6 are constitutively expressed in the intestine.[156, 392, 412] NLRP12 is predominantly expressed in hematopoietic cells while NLRP6 expression mainly is epithelial.[166, 392] Thus, defects in individual components of diverse inflammasomes would result in the same end condition of exacerbated intestinal inflammation in response to DSS challenge. In addition, accumulating evidence suggests that the inflammasome NLRs are not only involved in caspase-1 mediated cytokine processing, but also in apoptosis, inhibition of NF-κB activation and embryonic development.[413] The lack of redundancy of inflammasomes in the intestine suggests that individual NLRs might contribute to cellular mechanisms that are essential in situations of stress and damage, such as protective immunity and appropriate cell death pathways.

7.5 Inflammasomes and immune evasion

The inflammasome provides an efficient effector mechanism for eradicating pathogens. For example, *Listeria monocytogenes* that were mutated to constitutively express flagellin were swiftly eliminated via the NLRC4 inflammasome.[303] Thus, pathogens may have evolved strategies to limit or avoid inflammasome activation. For instance, once in an intracellular location, *Salmonella typhimurium* evades the NLRC4 inflammasome by repressing flagellin production and expressing a T3SS that does not activate the inflammasome.[178] Furthermore, direct repression of the inflammasome by pathogens has also been reported. Thus, B-cells infected with *S. typhimurium* do not undergo cell death and therefore might serve as reservoirs for the bacterium.[414] Although B-cells express comparatively low levels of NLRC4, *S. typhimurium* was reported to induce down-regulation of NLRC4 and thereby reduce production of IL-1β.[414] This inhibitory effect was dependent on the T3SS of the SPI1 system.[187] Other bacterial virulence factors delivered through a T3SS have recently been shown to inhibit caspase-8 mediated apoptotic signalling, which, as described above, has been linked to inflammasome activation. The EPEC T3SS associated factor NleB1 could bind to components of the caspase-8 death inducing complex and inhibit Fas ligand or TNF-α mediated signalling.[415] Thus, when mice were infected with *Citrobacter rodentium*, few IECs were positive for processed caspase-8. However when *nleB* mutant *C. rodentium* were used for infection, caspase-8 activation was evident in IECs and cells positive for activation had been shed intro the lumen.[415] In addition colonisation was markedly increased in mice deficient in Fas ligand signalling, confirming that bacterial interference with apoptosis is a strategy employed to avoid elimination.[415]

Caspase-1 is also a target for bacterial inhibition. *Yersinia pestis* expresses the protein YopM which is translocated into the cytosol via a T3SS and was reported to bind caspase-1.[416]This blocked inflammasome formation and promoted bacterial survival. YopM exhibited a protein sequence with similarities to a caspase-1 substrate, YVAD, which can bind both active caspase-1 and the zymogen pro-caspase-1.[416] However, in other instances, triggering of the inflammasome and subsequent pyroptosis could be beneficial for bacterial dissemination. *Shigella flexneri* expresses IpaB which could associate with caspase-1 and induce macrophage death.[417] In conclusion, the inflammasome is a target for microbial effectors from several pathogens. Bacterial strategies range from highly elaborate evasion mechanisms to detection by multiple inflammasomes. It is plausible that the most beneficial strategy varies with site of invasion, cell type and stage of infection.

7.6 Endogenous flagellin and the intestinal immune system

Research into innate immune sensing of flagellin by TLR5 has generated an image of surprising complexity, with reports of spontaneous intestinal inflammation and the development of metabolic syndrome in *Tlr5*$^{-/-}$ mice.[356, 357] These findings have been disputed and the incidence of colitis in the affected colony was attenuated after rederivation.[356, 364] The research group reporting a spontaneous inflammatory phenotype of *Tlr5*$^{-/-}$ animals mice also showed that pathogenicity was dependent on IL-1R signalling.[366] Furthermore, TLR5 mediated the production of secretory IL-1R antagonist in the colon in response to challenge with systemic flagellin.[418] The implications of increased ligation of the IL-1R could be several, for example affecting cellular migration. A study of Influenza A viral infection of the lung, showed that IL-1β promoted CCR7 expression and migration of DCs to lymph nodes and efficient priming of CD8^{+} T-cells.[419] In the case of chronic intestinal inflammation, our own studies have

revealed that the absence of IL-1R signalling in $CD4^+$ T-cells reduced the rate of pathogenesis in the T-cell transfer model of colitis. In addition, blocking IL-1β reduced the recruitment and activation of innate inflammatory cells.[200] We did detect elevated cell numbers in the colon LP of inflamed *Tlr5*$^{-/-}$ and *Tlr5*$^{-/-}$ *Rag1*$^{-/-}$ mice, although cytokines normally associated with pathology were not increased. Furthermore, IL-1R signalling promoted survival of $CD4^+$ T-cells *in vitro*, under conditions of TCR stimulation.[200] It remains to be determined if single PRRs could affect the overall balance of available IL-1β in mucosal tissues and subsequent cell recruitment and survival. Considering the wide expression and pleiotropic effects of IL-1 cytokines, this remains a valid target for future investigation.

7.7 Concluding remarks

The mucosal immune system is a complex network of hardwired innate immune mechanisms and pliable adaptive responses. The interplay between the intestinal microflora and innate PRRs provides cues for distinct immune pathways. Bacterial flagellin is a highly immunogenic protein present in the intestinal lumen, but the role of innate sensing of flagellin in the development of intestinal inflammation was not clear. Our studies revealed that cell type specific expression of flagellin sensors could have a determining effect on subsequent immune activation and development of pathology. Surprisingly little redundancy appears to exist, confirming that PRR circuits are integral for protection during situations of intestinal infection and invasion. The relative contribution of PRRs to breakdown of tolerance and the development of IBD could be viewed not only as a module of innate immunity, but also as disrupted responses in individual cell types.

References

1. Bouma G, Strober W. The immunological and genetic basis of inflammatory bowel disease. *Nat Rev Immunol* 2003; **3**(7)**:** 521-533.

2. Magalhaes JG, Tattoli I, Girardin SE. The intestinal epithelial barrier: how to distinguish between the microbial flora and pathogens. *Seminars in immunology* 2007; **19**(2)**:** 106-115.

3. Schonhoff SE, Giel-Moloney M, Leiter AB. Minireview: Development and differentiation of gut endocrine cells. *Endocrinology* 2004; **145**(6)**:** 2639-2644.

4. Brandl K, Plitas G, Schnabl B, DeMatteo RP, Pamer EG. MyD88-mediated signals induce the bactericidal lectin RegIII gamma and protect mice against intestinal Listeria monocytogenes infection. *J Exp Med* 2007; **204**(8)**:** 1891-1900.

5. Clevers HC, Bevins CL. Paneth cells: maestros of the small intestinal crypts. *Annual review of physiology* 2013; **75:** 289-311.

6. Muniz LR, Knosp C, Yeretssian G. Intestinal antimicrobial peptides during homeostasis, infection, and disease. *Front Immunol* 2012; **3:** 310.

7. Vaishnava S, Behrendt CL, Ismail AS, Eckmann L, Hooper LV. Paneth cells directly sense gut commensals and maintain homeostasis at the intestinal host-microbial interface. *Proc Natl Acad Sci U S A* 2008; **105**(52)**:** 20858-20863.

8. Johansson ME, Phillipson M, Petersson J, Velcich A, Holm L, Hansson GC. The inner of the two Muc2 mucin-dependent mucus layers in colon is devoid of bacteria. *Proc Natl Acad Sci U S A* 2008; **105**(39)**:** 15064-15069.

9. Linden SK, Sutton P, Karlsson NG, Korolik V, McGuckin MA. Mucins in the mucosal barrier to infection. *Mucosal Immunol* 2008; **1**(3)**:** 183-197.

10. Sonnenburg JL, Angenent LT, Gordon JI. Getting a grip on things: how do communities of bacterial symbionts become established in our intestine? *Nat Immunol* 2004; **5**(6)**:** 569-573.

11. Heazlewood CK, Cook MC, Eri R, Price GR, Tauro SB, Taupin D *et al.* Aberrant mucin assembly in mice causes endoplasmic reticulum stress and spontaneous inflammation resembling ulcerative colitis. *PLoS medicine* 2008; **5**(3)**:** e54.

12. Frey A, Giannasca KT, Weltzin R, Giannasca PJ, Reggio H, Lencer WI *et al.* Role of the glycocalyx in regulating access of microparticles to apical plasma membranes of intestinal epithelial cells: implications for microbial attachment and oral vaccine targeting. *J Exp Med* 1996; **184**(3)**:** 1045-1059.

13. Mabbott NA, Donaldson DS, Ohno H, Williams IR, Mahajan A. Microfold (M) cells: important immunosurveillance posts in the intestinal epithelium. *Mucosal Immunol* 2013; **6**(4)**:** 666-677.

14. Miller H, Zhang J, Kuolee R, Patel GB, Chen W. Intestinal M cells: the fallible sentinels? *World J Gastroenterol* 2007; **13**(10)**:** 1477-1486.

15. van der Flier LG, Clevers H. Stem cells, self-renewal, and differentiation in the intestinal epithelium. *Annual review of physiology* 2009; **71:** 241-260.

16. Fukata M, Arditi M. The role of pattern recognition receptors in intestinal inflammation. *Mucosal Immunol* 2013; **6**(3)**:** 451-463.

17. Marques R, Boneca IG. Expression and functional importance of innate immune receptors by intestinal epithelial cells. *Cellular and molecular life sciences : CMLS* 2011; **68**(22)**:** 3661-3673.

18. He B, Xu W, Santini PA, Polydorides AD, Chiu A, Estrella J *et al.* Intestinal bacteria trigger T cell-independent immunoglobulin A(2) class switching by inducing epithelial-cell secretion of the cytokine APRIL. *Immunity* 2007; **26**(6)**:** 812-826.

19. Szabady RL, McCormick BA. Control of neutrophil inflammation at mucosal surfaces by secreted epithelial products. *Front Immunol* 2013; **4:** 220.

20. Mostov KE. Transepithelial transport of immunoglobulins. *Annual review of immunology* 1994; **12:** 63-84.

21. Hecht G, Pothoulakis C, LaMont JT, Madara JL. Clostridium difficile toxin A perturbs cytoskeletal structure and tight junction permeability of cultured human intestinal epithelial monolayers. *J Clin Invest* 1988; **82**(5)**:** 1516-1524.

22. Turner JR. Molecular basis of epithelial barrier regulation: from basic mechanisms to clinical application. *Am J Pathol* 2006; **169**(6)**:** 1901-1909.

23. Owens BM, Simmons A. Intestinal stromal cells in mucosal immunity and homeostasis. *Mucosal Immunol* 2013; **6**(2)**:** 224-234.

24. Pinchuk IV, Mifflin RC, Saada JI, Powell DW. Intestinal mesenchymal cells. *Current gastroenterology reports* 2010; **12**(5)**:** 310-318.

25. Powell DW, Pinchuk IV, Saada JI, Chen X, Mifflin RC. Mesenchymal cells of the intestinal lamina propria. *Annual review of physiology* 2011; **73:** 213-237.

26. Farin HF, Van Es JH, Clevers H. Redundant sources of Wnt regulate intestinal stem cells and promote formation of Paneth cells. *Gastroenterology* 2012; **143**(6)**:** 1518-1529 e1517.

27. Andoh A, Shioya M, Nishida A, Bamba S, Tsujikawa T, Kim-Mitsuyama S *et al.* Expression of IL-24, an activator of the JAK1/STAT3/SOCS3 cascade, is enhanced in inflammatory bowel disease. *J Immunol* 2009; **183**(1)**:** 687-695.

28. Kim YG, Kamada N, Shaw MH, Warner N, Chen GY, Franchi L *et al.* The Nod2 sensor promotes intestinal pathogen eradication via the chemokine CCL2-dependent recruitment of inflammatory monocytes. *Immunity* 2011; **34**(5)**:** 769-780.

29. Otte JM, Rosenberg IM, Podolsky DK. Intestinal myofibroblasts in innate immune responses of the intestine. *Gastroenterology* 2003; **124**(7)**:** 1866-1878.

30. Persson EK, Scott CL, Mowat AM, Agace WW. Dendritic cell subsets in the intestinal lamina propria: Ontogeny and function. *Eur J Immunol* 2013.

31. Rivollier A, He J, Kole A, Valatas V, Kelsall BL. Inflammation switches the differentiation program of Ly6Chi monocytes from antiinflammatory macrophages to inflammatory dendritic cells in the colon. *J Exp Med* 2012; **209**(1)**:** 139-155.

32. Mowat AM, Bain CC. Mucosal macrophages in intestinal homeostasis and inflammation. *Journal of innate immunity* 2011; **3**(6)**:** 550-564.

33. Cerovic V, Houston SA, Scott CL, Aumeunier A, Yrlid U, Mowat AM *et al.* Intestinal CD103(-) dendritic cells migrate in lymph and prime effector T cells. *Mucosal Immunol* 2013; **6**(1)**:** 104-113.

34. Farache J, Koren I, Milo I, Gurevich I, Kim KW, Zigmond E *et al.* Luminal bacteria recruit CD103+ dendritic cells into the intestinal epithelium to sample bacterial antigens for presentation. *Immunity* 2013; **38**(3)**:** 581-595.

35. Worbs T, Bode U, Yan S, Hoffmann MW, Hintzen G, Bernhardt G *et al.* Oral tolerance originates in the intestinal immune system and relies on antigen carriage by dendritic cells. *J Exp Med* 2006; **203**(3)**:** 519-527.

36. Iwata M, Hirakiyama A, Eshima Y, Kagechika H, Kato C, Song SY. Retinoic acid imprints gut-homing specificity on T cells. *Immunity* 2004; **21**(4)**:** 527-538.

37. Denning TL, Norris BA, Medina-Contreras O, Manicassamy S, Geem D, Madan R *et al.* Functional specializations of intestinal dendritic cell and macrophage subsets that control Th17 and regulatory T cell responses are dependent on the T cell/APC ratio, source of mouse strain, and regional localization. *J Immunol* 2011; **187**(2)**:** 733-747.

38. Persson EK, Uronen-Hansson H, Semmrich M, Rivollier A, Hagerbrand K, Marsal J *et al.* IRF4 transcription-factor-dependent CD103(+)CD11b(+) dendritic cells drive mucosal T helper 17 cell differentiation. *Immunity* 2013; **38**(5)**:** 958-969.

39. Fujimoto K, Karuppuchamy T, Takemura N, Shimohigoshi M, Machida T, Haseda Y *et al.* A new subset of CD103+CD8alpha+ dendritic cells in the small intestine expresses TLR3, TLR7, and TLR9 and induces Th1 response and CTL activity. *J Immunol* 2011; **186**(11)**:** 6287-6295.

40. Bain CC, Scott CL, Uronen-Hansson H, Gudjonsson S, Jansson O, Grip O *et al.* Resident and pro-inflammatory macrophages in the colon represent alternative context-dependent fates of the same Ly6Chi monocyte precursors. *Mucosal Immunol* 2013; **6**(3)**:** 498-510.

41. Schulz O, Jaensson E, Persson EK, Liu X, Worbs T, Agace WW *et al.* Intestinal CD103+, but not CX3CR1+, antigen sampling cells migrate in lymph and serve classical dendritic cell functions. *J Exp Med* 2009; **206**(13)**:** 3101-3114.

42. Hoshi N, Schenten D, Nish SA, Walther Z, Gagliani N, Flavell RA *et al.* MyD88 signalling in colonic mononuclear phagocytes drives colitis in IL-10-deficient mice. *Nature communications* 2012; **3:** 1120.

43. Carlens J, Wahl B, Ballmaier M, Bulfone-Paus S, Forster R, Pabst O. Common gamma-chain-dependent signals confer selective survival of eosinophils in the murine small intestine. *J Immunol* 2009; **183**(9)**:** 5600-5607.

44. Mowat AM. The curious case of the intestinal eosinophil. *Mucosal Immunology* 2010; **3**(5)**:** 420-421.

45. Svensson-Frej M. Immunobiology of intestinal eosinophils - a dogma in the changing? *Journal of innate immunity* 2011; **3**(6)**:** 565-576.

46. Zhang JQ, Biedermann B, Nitschke L, Crocker PR. The murine inhibitory receptor mSiglec-E is expressed broadly on cells of the innate immune system whereas mSiglec-F is restricted to eosinophils. *Eur J Immunol* 2004; **34**(4)**:** 1175-1184.

47. Mishra A, Hogan SP, Lee JJ, Foster PS, Rothenberg ME. Fundamental signals that regulate eosinophil homing to the gastrointestinal tract. *J Clin Invest* 1999; **103**(12)**:** 1719-1727.

48. Hogan SP, Rosenberg HF, Moqbel R, Phipps S, Foster PS, Lacy P *et al.* Eosinophils: biological properties and role in health and disease. *Clin Exp Allergy* 2008; **38**(5)**:** 709-750.

49. Bercovitz ZT, Sommers SC. Altered inflammatory reaction in nonspecific ulcerative colitis. *Archives of internal medicine* 1966; **117**(4)**:** 504-510.

50. Hogan SP, Waddell A, Fulkerson PC. Eosinophils in infection and intestinal immunity. *Current opinion in gastroenterology* 2013; **29**(1)**:** 7-14.

51. Ahrens R, Waddell A, Seidu L, Blanchard C, Carey R, Forbes E *et al.* Intestinal macrophage/epithelial cell-derived CCL11/eotaxin-1 mediates eosinophil recruitment and function in pediatric ulcerative colitis. *J Immunol* 2008; **181**(10)**:** 7390-7399.

52. Nagase H, Okugawa S, Ota Y, Yamaguchi M, Tomizawa H, Matsushima K *et al.* Expression and function of Toll-like receptors in eosinophils: activation by Toll-like receptor 7 ligand. *J Immunol* 2003; **171**(8)**:** 3977-3982.

53. Sabroe I, Jones EC, Usher LR, Whyte MK, Dower SK. Toll-like receptor (TLR)2 and TLR4 in human peripheral blood granulocytes: a critical role for monocytes in leukocyte lipopolysaccharide responses. *J Immunol* 2002; **168**(9)**:** 4701-4710.

54. Brinkmann V, Reichard U, Goosmann C, Fauler B, Uhlemann Y, Weiss DS *et al.* Neutrophil extracellular traps kill bacteria. *Science* 2004; **303**(5663)**:** 1532-1535.

55. Yousefi S, Gold JA, Andina N, Lee JJ, Kelly AM, Kozlowski E *et al.* Catapult-like release of mitochondrial DNA by eosinophils contributes to antibacterial defense. *Nat Med* 2008; **14**(9)**:** 949-953.

56. Linch SN, Kelly AM, Danielson ET, Pero R, Lee JJ, Gold JA. Mouse eosinophils possess potent antibacterial properties in vivo. *Infect Immun* 2009; **77**(11)**:** 4976-4982.

57. Lee JJ, Dimina D, Macias MP, Ochkur SI, McGarry MP, O'Neill KR *et al.* Defining a link with asthma in mice congenitally deficient in eosinophils. *Science* 2004; **305**(5691)**:** 1773-1776.

58. Spits H, Di Santo JP. The expanding family of innate lymphoid cells: regulators and effectors of immunity and tissue remodeling. *Nat Immunol* 2011; **12**(1)**:** 21-27.

59. Sonnenberg GF, Monticelli LA, Elloso MM, Fouser LA, Artis D. CD4(+) lymphoid tissue-inducer cells promote innate immunity in the gut. *Immunity* 2011; **34**(1)**:** 122-134.

60. Zheng Y, Valdez PA, Danilenko DM, Hu Y, Sa SM, Gong Q *et al.* Interleukin-22 mediates early host defense against attaching and effacing bacterial pathogens. *Nat Med* 2008; **14**(3)**:** 282-289.

61. Spits H, Cupedo T. Innate lymphoid cells: emerging insights in development, lineage relationships, and function. *Annual review of immunology* 2012; **30:** 647-675.

62. Sawa S, Lochner M, Satoh-Takayama N, Dulauroy S, Berard M, Kleinschek M *et al.* RORgammat+ innate lymphoid cells regulate intestinal homeostasis by integrating negative signals from the symbiotic microbiota. *Nat Immunol* 2011; **12**(4)**:** 320-326.

63. Buonocore S, Ahern PP, Uhlig HH, Ivanov, II, Littman DR, Maloy KJ *et al.* Innate lymphoid cells drive interleukin-23-dependent innate intestinal pathology. *Nature* 2010; **464**(7293)**:** 1371-1375.

64. Lochner M, Ohnmacht C, Presley L, Bruhns P, Si-Tahar M, Sawa S *et al.* Microbiota-induced tertiary lymphoid tissues aggravate inflammatory disease in the absence of RORgamma t and LTi cells. *J Exp Med* 2011; **208**(1)**:** 125-134.

65. Tsuji M, Suzuki K, Kitamura H, Maruya M, Kinoshita K, Ivanov, II *et al.* Requirement for lymphoid tissue-inducer cells in isolated follicle formation and T cell-independent immunoglobulin A generation in the gut. *Immunity* 2008; **29**(2)**:** 261-271.

66. Cheroutre H, Lambolez F, Mucida D. The light and dark sides of intestinal intraepithelial lymphocytes. *Nat Rev Immunol* 2011; **11**(7)**:** 445-456.

67. Umesaki Y, Setoyama H, Matsumoto S, Okada Y. Expansion of alpha beta T-cell receptor-bearing intestinal intraepithelial lymphocytes after microbial colonization in germ-free mice and its independence from thymus. *Immunology* 1993; **79**(1)**:** 32-37.

68. Jensen KD, Shin S, Chien YH. Cutting edge: Gammadelta intraepithelial lymphocytes of the small intestine are not biased toward thymic antigens. *J Immunol* 2009; **182**(12)**:** 7348-7351.

69. Schild H, Mavaddat N, Litzenberger C, Ehrich EW, Davis MM, Bluestone JA *et al.* The nature of major histocompatibility complex recognition by gamma delta T cells. *Cell* 1994; **76**(1)**:** 29-37.

70. Tanaka Y, Morita CT, Tanaka Y, Nieves E, Brenner MB, Bloom BR. Natural and synthetic non-peptide antigens recognized by human gamma delta T cells. *Nature* 1995; **375**(6527)**:** 155-158.

71. Dalton JE, Cruickshank SM, Egan CE, Mears R, Newton DJ, Andrew EM *et al.* Intraepithelial gammadelta+ lymphocytes maintain the integrity of intestinal epithelial tight junctions in response to infection. *Gastroenterology* 2006; **131**(3)**:** 818-829.

72. Roberts SJ, Smith AL, West AB, Wen L, Findly RC, Owen MJ *et al.* T-cell alpha beta + and gamma delta + deficient mice display abnormal but distinct phenotypes toward a natural, widespread infection of the intestinal epithelium. *Proc Natl Acad Sci U S A* 1996; **93**(21)**:** 11774-11779.

73. Chen Y, Chou K, Fuchs E, Havran WL, Boismenu R. Protection of the intestinal mucosa by intraepithelial gamma delta T cells. *Proc Natl Acad Sci U S A* 2002; **99**(22)**:** 14338-14343.

74. Komano H, Fujiura Y, Kawaguchi M, Matsumoto S, Hashimoto Y, Obana S *et al.* Homeostatic regulation of intestinal epithelia by intraepithelial gamma delta T cells. *Proc Natl Acad Sci U S A* 1995; **92**(13)**:** 6147-6151.

75. Basu R, Hatton RD, Weaver CT. The Th17 family: flexibility follows function. *Immunol Rev* 2013; **252**(1)**:** 89-103.

76. Zhu J, Yamane H, Paul WE. Differentiation of effector CD4 T cell populations (*). *Annual review of immunology* 2010; **28:** 445-489.

77. Mosmann TR, Cherwinski H, Bond MW, Giedlin MA, Coffman RL. Two types of murine helper T cell clone. I. Definition according to profiles of lymphokine activities and secreted proteins. *J Immunol* 1986; **136**(7)**:** 2348-2357.

78. Amsen D, Spilianakis CG, Flavell RA. How are T(H)1 and T(H)2 effector cells made? *Curr Opin Immunol* 2009; **21**(2)**:** 153-160.

79. Kohno K, Kataoka J, Ohtsuki T, Suemoto Y, Okamoto I, Usui M *et al.* IFN-gamma-inducing factor (IGIF) is a costimulatory factor on the activation of Th1 but not Th2 cells and exerts its effect independently of IL-12. *J Immunol* 1997; **158**(4)**:** 1541-1550.

80. Stout RD, Bottomly K. Antigen-specific activation of effector macrophages by IFN-gamma producing (TH1) T cell clones. Failure of IL-4-producing (TH2) T cell clones to activate effector function in macrophages. *J Immunol* 1989; **142**(3)**:** 760-765.

81. Berberich C, Ramirez-Pineda JR, Hambrecht C, Alber G, Skeiky YA, Moll H. Dendritic cell (DC)-based protection against an intracellular pathogen is dependent upon DC-derived IL-12 and can be induced by molecularly defined antigens. *J Immunol* 2003; **170**(6)**:** 3171-3179.

82. Snapper CM, Paul WE. Interferon-gamma and B cell stimulatory factor-1 reciprocally regulate Ig isotype production. *Science* 1987; **236**(4804)**:** 944-947.

83. Monteleone G, Biancone L, Marasco R, Morrone G, Marasco O, Luzza F *et al.* Interleukin 12 is expressed and actively released by Crohn's disease intestinal lamina propria mononuclear cells. *Gastroenterology* 1997; **112**(4)**:** 1169-1178.

84. Monteleone G, Trapasso F, Parrello T, Biancone L, Stella A, Iuliano R *et al.* Bioactive IL-18 expression is up-regulated in Crohn's disease. *J Immunol* 1999; **163**(1)**:** 143-147.

85. Harrington LE, Hatton RD, Mangan PR, Turner H, Murphy TL, Murphy KM *et al.* Interleukin 17-producing CD4+ effector T cells develop via a lineage distinct from the T helper type 1 and 2 lineages. *Nat Immunol* 2005; **6**(11)**:** 1123-1132.

86. Moseley TA, Haudenschild DR, Rose L, Reddi AH. Interleukin-17 family and IL-17 receptors. *Cytokine & growth factor reviews* 2003; **14**(2)**:** 155-174.

87. Ishigame H, Kakuta S, Nagai T, Kadoki M, Nambu A, Komiyama Y *et al.* Differential roles of interleukin-17A and -17F in host defense against mucoepithelial bacterial infection and allergic responses. *Immunity* 2009; **30**(1)**:** 108-119.

88. Yang XO, Chang SH, Park H, Nurieva R, Shah B, Acero L *et al.* Regulation of inflammatory responses by IL-17F. *J Exp Med* 2008; **205**(5)**:** 1063-1075.

89. Ivanov, II, Atarashi K, Manel N, Brodie EL, Shima T, Karaoz U *et al.* Induction of intestinal Th17 cells by segmented filamentous bacteria. *Cell* 2009; **139**(3)**:** 485-498.

90. Curtis MM, Way SS. Interleukin-17 in host defence against bacterial, mycobacterial and fungal pathogens. *Immunology* 2009; **126**(2)**:** 177-185.

91. Ghoreschi K, Laurence A, Yang XP, Tato CM, McGeachy MJ, Konkel JE *et al.* Generation of pathogenic T(H)17 cells in the absence of TGF-beta signalling. *Nature* 2010; **467**(7318)**:** 967-971.

92. Codarri L, Gyulveszi G, Tosevski V, Hesske L, Fontana A, Magnenat L *et al.* RORgammat drives production of the cytokine GM-CSF in helper T cells, which is essential for the effector phase of autoimmune neuroinflammation. *Nat Immunol* 2011; **12**(6)**:** 560-567.

93. Hirota K, Duarte JH, Veldhoen M, Hornsby E, Li Y, Cua DJ *et al.* Fate mapping of IL-17-producing T cells in inflammatory responses. *Nat Immunol* 2011; **12**(3)**:** 255-263.

94. Ahern PP, Schiering C, Buonocore S, McGeachy MJ, Cua DJ, Maloy KJ *et al.* Interleukin-23 drives intestinal inflammation through direct activity on T cells. *Immunity* 2010; **33**(2)**:** 279-288.

95. Morrison PJ, Bending D, Fouser LA, Wright JF, Stockinger B, Cooke A *et al.* Th17-cell plasticity in Helicobacter hepaticus-induced intestinal inflammation. *Mucosal Immunol* 2013.

96. Muranski P, Borman ZA, Kerkar SP, Klebanoff CA, Ji Y, Sanchez-Perez L *et al.* Th17 cells are long lived and retain a stem cell-like molecular signature. *Immunity* 2011; **35**(6)**:** 972-985.

97. Veldhoen M, Hirota K, Westendorf AM, Buer J, Dumoutier L, Renauld JC *et al.* The aryl hydrocarbon receptor links TH17-cell-mediated autoimmunity to environmental toxins. *Nature* 2008; **453**(7191)**:** 106-109.

98. Basu R, O'Quinn DB, Silberger DJ, Schoeb TR, Fouser L, Ouyang W *et al.* Th22 cells are an important source of IL-22 for host protection against enteropathogenic bacteria. *Immunity* 2012; **37**(6)**:** 1061-1075.

99. Schmechel S, Konrad A, Diegelmann J, Glas J, Wetzke M, Paschos E *et al.* Linking genetic susceptibility to Crohn's disease with Th17 cell function: IL-22 serum levels are increased in Crohn's disease and correlate with disease activity and IL23R genotype status. *Inflamm Bowel Dis* 2008; **14**(2)**:** 204-212.

100. Barnes MJ, Powrie F. Regulatory T cells reinforce intestinal homeostasis. *Immunity* 2009; **31**(3)**:** 401-411.

101. Chen W, Jin W, Hardegen N, Lei KJ, Li L, Marinos N *et al.* Conversion of peripheral CD4+CD25- naive T cells to CD4+CD25+ regulatory T cells by TGF-beta induction of transcription factor Foxp3. *J Exp Med* 2003; **198**(12)**:** 1875-1886.

102. Singh B, Read S, Asseman C, Malmstrom V, Mottet C, Stephens LA *et al.* Control of intestinal inflammation by regulatory T cells. *Immunol Rev* 2001; **182:** 190-200.

103. Atarashi K, Tanoue T, Shima T, Imaoka A, Kuwahara T, Momose Y *et al.* Induction of colonic regulatory T cells by indigenous Clostridium species. *Science* 2011; **331**(6015)**:** 337-341.

104. Moran CJ, Walters TD, Guo CH, Kugathasan S, Klein C, Turner D *et al.* IL-10R polymorphisms are associated with very-early-onset ulcerative colitis. *Inflamm Bowel Dis* 2013; **19**(1)**:** 115-123.

105. Wildin RS, Smyk-Pearson S, Filipovich AH. Clinical and molecular features of the immunodysregulation, polyendocrinopathy, enteropathy, X linked (IPEX) syndrome. *Journal of medical genetics* 2002; **39**(8)**:** 537-545.

106. Cong Y, Feng T, Fujihashi K, Schoeb TR, Elson CO. A dominant, coordinated T regulatory cell-IgA response to the intestinal microbiota. *Proc Natl Acad Sci U S A* 2009; **106**(46)**:** 19256-19261.

107. Rubtsov YP, Rasmussen JP, Chi EY, Fontenot J, Castelli L, Ye X *et al.* Regulatory T cell-derived interleukin-10 limits inflammation at environmental interfaces. *Immunity* 2008; **28**(4)**:** 546-558.

108. Macpherson AJ, Uhr T. Induction of protective IgA by intestinal dendritic cells carrying commensal bacteria. *Science* 2004; **303**(5664)**:** 1662-1665.

109. Zhou X, Bailey-Bucktrout SL, Jeker LT, Penaranda C, Martinez-Llordella M, Ashby M *et al.* Instability of the transcription factor Foxp3 leads to the generation of pathogenic memory T cells in vivo. *Nat Immunol* 2009; **10**(9)**:** 1000-1007.

110. Miyao T, Floess S, Setoguchi R, Luche H, Fehling HJ, Waldmann H *et al.* Plasticity of Foxp3(+) T cells reflects promiscuous Foxp3 expression in conventional T cells but not reprogramming of regulatory T cells. *Immunity* 2012; **36**(2)**:** 262-275.

111. Rubtsov YP, Niec RE, Josefowicz S, Li L, Darce J, Mathis D *et al.* Stability of the regulatory T cell lineage in vivo. *Science* 2010; **329**(5999)**:** 1667-1671.

112. Cannons JL, Lu KT, Schwartzberg PL. T follicular helper cell diversity and plasticity. *Trends in immunology* 2013; **34**(5)**:** 200-207.

113. Ma CS, Deenick EK, Batten M, Tangye SG. The origins, function, and regulation of T follicular helper cells. *J Exp Med* 2012; **209**(7)**:** 1241-1253.

114. Uematsu S, Fujimoto K. The innate immune system in the intestine. *Microbiology and immunology* 2010; **54**(11)**:** 645-657.

115. Zelenay S, Reis e Sousa C. Adaptive immunity after cell death. *Trends in immunology* 2013; **34**(7)**:** 329-335.

116. Kawai T, Akira S. The role of pattern-recognition receptors in innate immunity: update on Toll-like receptors. *Nat Immunol* 2010; **11**(5)**:** 373-384.

117. Koblansky AA, Jankovic D, Oh H, Hieny S, Sungnak W, Mathur R *et al.* Recognition of profilin by Toll-like receptor 12 is critical for host resistance to Toxoplasma gondii. *Immunity* 2013; **38**(1)**:** 119-130.

118. Oldenburg M, Kruger A, Ferstl R, Kaufmann A, Nees G, Sigmund A *et al.* TLR13 recognizes bacterial 23S rRNA devoid of erythromycin resistance-forming modification. *Science* 2012; **337**(6098)**:** 1111-1115.

119. Mathur R, Oh H, Zhang D, Park SG, Seo J, Koblansky A *et al.* A mouse model of Salmonella typhi infection. *Cell* 2012; **151**(3)**:** 590-602.

120. McGettrick AF, O'Neill LA. Localisation and trafficking of Toll-like receptors: an important mode of regulation. *Curr Opin Immunol* 2010; **22**(1)**:** 20-27.

121. Hornef MW, Normark BH, Vandewalle A, Normark S. Intracellular recognition of lipopolysaccharide by toll-like receptor 4 in intestinal epithelial cells. *J Exp Med* 2003; **198**(8)**:** 1225-1235.

122. Yoon SI, Kurnasov O, Natarajan V, Hong M, Gudkov AV, Osterman AL *et al.* Structural basis of TLR5-flagellin recognition and signaling. *Science* 2012; **335**(6070)**:** 859-864.

123. Hayashi F, Smith KD, Ozinsky A, Hawn TR, Yi EC, Goodlett DR *et al.* The innate immune response to bacterial flagellin is mediated by Toll-like receptor 5. *Nature* 2001; **410**(6832)**:** 1099-1103.

124. Letran SE, Lee SJ, Atif SM, Uematsu S, Akira S, McSorley SJ. TLR5 functions as an endocytic receptor to enhance flagellin-specific adaptive immunity. *Eur J Immunol* 2011; **41**(1)**:** 29-38.

125. Bates JT, Uematsu S, Akira S, Mizel SB. Direct stimulation of tlr5+/+ CD11c+ cells is necessary for the adjuvant activity of flagellin. *J Immunol* 2009; **182**(12)**:** 7539-7547.

126. Vicente-Suarez I, Brayer J, Villagra A, Cheng F, Sotomayor EM. TLR5 ligation by flagellin converts tolerogenic dendritic cells into activating antigen-presenting cells that preferentially induce T-helper 1 responses. *Immunology letters* 2009; **125**(2)**:** 114-118.

127. Lodes MJ, Cong Y, Elson CO, Mohamath R, Landers CJ, Targan SR *et al.* Bacterial flagellin is a dominant antigen in Crohn disease. *J Clin Invest* 2004; **113**(9)**:** 1296-1306.

128. Van Maele L, Carnoy C, Cayet D, Songhet P, Dumoutier L, Ferrero I *et al.* TLR5 signaling stimulates the innate production of IL-17 and IL-22 by CD3(neg)CD127+ immune cells in spleen and mucosa. *J Immunol* 2010; **185**(2)**:** 1177-1185.

129. Jones RM, Sloane VM, Wu H, Luo L, Kumar A, Kumar MV *et al.* Flagellin administration protects gut mucosal tissue from irradiation-induced apoptosis via MKP-7 activity. *Gut* 2011; **60**(5)**:** 648-657.

130. Vijay-Kumar M, Aitken JD, Sanders CJ, Frias A, Sloane VM, Xu J *et al.* Flagellin treatment protects against chemicals, bacteria, viruses, and radiation. *J Immunol* 2008; **180**(12)**:** 8280-8285.

131. Kinnebrew MA, Ubeda C, Zenewicz LA, Smith N, Flavell RA, Pamer EG. Bacterial flagellin stimulates Toll-like receptor 5-dependent defense against vancomycin-resistant Enterococcus infection. *J Infect Dis* 2010; **201**(4)**:** 534-543.

132. Davis BK, Wen H, Ting JP. The inflammasome NLRs in immunity, inflammation, and associated diseases. *Annual review of immunology* 2011; **29:** 707-735.

133. Schroder K, Tschopp J. The inflammasomes. *Cell* 2010; **140**(6)**:** 821-832.

134. Maekawa T, Kufer TA, Schulze-Lefert P. NLR functions in plant and animal immune systems: so far and yet so close. *Nat Immunol* 2011; **12**(9)**:** 817-826.

135. Kobayashi KS, van den Elsen PJ. NLRC5: a key regulator of MHC class I-dependent immune responses. *Nat Rev Immunol* 2012; **12**(12)**:** 813-820.

136. Chamaillard M, Hashimoto M, Horie Y, Masumoto J, Qiu S, Saab L *et al.* An essential role for NOD1 in host recognition of bacterial peptidoglycan containing diaminopimelic acid. *Nat Immunol* 2003; **4**(7)**:** 702-707.

137. Girardin SE, Boneca IG, Viala J, Chamaillard M, Labigne A, Thomas G *et al.* Nod2 is a general sensor of peptidoglycan through muramyl dipeptide (MDP) detection. *J Biol Chem* 2003; **278**(11)**:** 8869-8872.

138. Hugot JP, Chamaillard M, Zouali H, Lesage S, Cezard JP, Belaiche J *et al.* Association of NOD2 leucine-rich repeat variants with susceptibility to Crohn's disease. *Nature* 2001; **411**(6837)**:** 599-603.

139. Fritz T, Niederreiter L, Adolph T, Blumberg RS, Kaser A. Crohn's disease: NOD2, autophagy and ER stress converge. *Gut* 2011; **60**(11)**:** 1580-1588.

140. Watanabe T, Kitani A, Murray PJ, Strober W. NOD2 is a negative regulator of Toll-like receptor 2-mediated T helper type 1 responses. *Nat Immunol* 2004; **5**(8)**:** 800-808.

141. Martinon F, Burns K, Tschopp J. The inflammasome: a molecular platform triggering activation of inflammatory caspases and processing of proIL-beta. *Mol Cell* 2002; **10**(2)**:** 417-426.

142. Srinivasula SM, Poyet JL, Razmara M, Datta P, Zhang Z, Alnemri ES. The PYRIN-CARD protein ASC is an activating adaptor for caspase-1. *J Biol Chem* 2002; **277**(24)**:** 21119-21122.

143. Broz P, Newton K, Lamkanfi M, Mariathasan S, Dixit VM, Monack DM. Redundant roles for inflammasome receptors NLRP3 and NLRC4 in host defense against Salmonella. *J Exp Med* 2010; **207**(8)**:** 1745-1755.

144. Latz E, Xiao TS, Stutz A. Activation and regulation of the inflammasomes. *Nat Rev Immunol* 2013; **13**(6)**:** 397-411.

145. Miao EA, Rajan JV, Aderem A. Caspase-1-induced pyroptotic cell death. *Immunol Rev* 2011; **243**(1)**:** 206-214.

146. Vladimer GI, Marty-Roix R, Ghosh S, Weng D, Lien E. Inflammasomes and host defenses against bacterial infections. *Current opinion in microbiology* 2013; **16**(1)**:** 23-31.

147. Tschopp J, Martinon F, Burns K. NALPs: a novel protein family involved in inflammation. *Nature reviews Molecular cell biology* 2003; **4**(2)**:** 95-104.

148. Boyden ED, Dietrich WF. Nalp1b controls mouse macrophage susceptibility to anthrax lethal toxin. *Nat Genet* 2006; **38**(2)**:** 240-244.

149. Kovarova M, Hesker PR, Jania L, Nguyen M, Snouwaert JN, Xiang Z *et al.* NLRP1-dependent pyroptosis leads to acute lung injury and morbidity in mice. *J Immunol* 2012; **189**(4)**:** 2006-2016.

150. Masters SL, Gerlic M, Metcalf D, Preston S, Pellegrini M, O'Donnell JA *et al.* NLRP1 inflammasome activation induces pyroptosis of hematopoietic progenitor cells. *Immunity* 2012; **37**(6)**:** 1009-1023.

151. Franchi L, Kanneganti TD, Dubyak GR, Nunez G. Differential requirement of P2X7 receptor and intracellular K+ for caspase-1 activation induced by intracellular and extracellular bacteria. *J Biol Chem* 2007; **282**(26)**:** 18810-18818.

152. Mariathasan S, Weiss DS, Newton K, McBride J, O'Rourke K, Roose-Girma M *et al.* Cryopyrin activates the inflammasome in response to toxins and ATP. *Nature* 2006; **440**(7081)**:** 228-232.

153. Hornung V, Bauernfeind F, Halle A, Samstad EO, Kono H, Rock KL *et al.* Silica crystals and aluminum salts activate the NALP3 inflammasome through phagosomal destabilization. *Nat Immunol* 2008; **9**(8)**:** 847-856.

154. Zhou R, Yazdi AS, Menu P, Tschopp J. A role for mitochondria in NLRP3 inflammasome activation. *Nature* 2011; **469**(7329)**:** 221-225.

155. Shimada K, Crother TR, Karlin J, Dagvadorj J, Chiba N, Chen S *et al.* Oxidized mitochondrial DNA activates the NLRP3 inflammasome during apoptosis. *Immunity* 2012; **36**(3)**:** 401-414.

156. O'Connor W, Jr., Harton JA, Zhu X, Linhoff MW, Ting JP. Cutting edge: CIAS1/cryopyrin/PYPAF1/NALP3/CATERPILLER 1.1 is an inducible inflammatory mediator with NF-kappa B suppressive properties. *J Immunol* 2003; **171**(12)**:** 6329-6333.

157. Zaki MH, Boyd KL, Vogel P, Kastan MB, Lamkanfi M, Kanneganti TD. The NLRP3 inflammasome protects against loss of epithelial integrity and mortality during experimental colitis. *Immunity* 2010; **32**(3)**:** 379-391.

158. Liu Z, Zaki MH, Vogel P, Gurung P, Finlay BB, Deng W *et al.* Role of inflammasomes in host defense against Citrobacter rodentium infection. *J Biol Chem* 2012; **287**(20)**:** 16955-16964.

159. Chen GY, Liu M, Wang F, Bertin J, Nunez G. A functional role for Nlrp6 in intestinal inflammation and tumorigenesis. *J Immunol* 2011; **186**(12)**:** 7187-7194.

160. Normand S, Delanoye-Crespin A, Bressenot A, Huot L, Grandjean T, Peyrin-Biroulet L *et al.* Nod-like receptor pyrin domain-containing protein 6 (NLRP6) controls epithelial self-renewal and colorectal carcinogenesis upon injury. *Proc Natl Acad Sci U S A* 2011; **108**(23)**:** 9601-9606.

161. Wang L, Manji GA, Grenier JM, Al-Garawi A, Merriam S, Lora JM *et al.* PYPAF7, a novel PYRIN-containing Apaf1-like protein that regulates activation of NF-kappa B and caspase-1-dependent cytokine processing. *J Biol Chem* 2002; **277**(33)**:** 29874-29880.

162. Elinav E, Strowig T, Kau AL, Henao-Mejia J, Thaiss CA, Booth CJ *et al.* NLRP6 inflammasome regulates colonic microbial ecology and risk for colitis. *Cell* 2011; **145**(5)**:** 745-757.

163. Anand PK, Malireddi RK, Lukens JR, Vogel P, Bertin J, Lamkanfi M *et al.* NLRP6 negatively regulates innate immunity and host defence against bacterial pathogens. *Nature* 2012; **488**(7411)**:** 389-393.

164. Vladimer GI, Weng D, Paquette SW, Vanaja SK, Rathinam VA, Aune MH *et al.* The NLRP12 inflammasome recognizes Yersinia pestis. *Immunity* 2012; **37**(1)**:** 96-107.

165. Allen IC, Wilson JE, Schneider M, Lich JD, Roberts RA, Arthur JC *et al.* NLRP12 suppresses colon inflammation and tumorigenesis through the negative regulation of noncanonical NF-kappaB signaling. *Immunity* 2012; **36**(5)**:** 742-754.

166. Zaki MH, Vogel P, Malireddi RK, Body-Malapel M, Anand PK, Bertin J *et al.* The NOD-like receptor NLRP12 attenuates colon inflammation and tumorigenesis. *Cancer cell* 2011; **20**(5)**:** 649-660.

167. Fernandes-Alnemri T, Yu JW, Datta P, Wu J, Alnemri ES. AIM2 activates the inflammasome and cell death in response to cytoplasmic DNA. *Nature* 2009; **458**(7237)**:** 509-513.

168. DeYoung KL, Ray ME, Su YA, Anzick SL, Johnstone RW, Trapani JA *et al.* Cloning a novel member of the human interferon-inducible gene family associated with control of tumorigenicity in a model of human melanoma. *Oncogene* 1997; **15**(4)**:** 453-457.

169. Hornung V, Ablasser A, Charrel-Dennis M, Bauernfeind F, Horvath G, Caffrey DR *et al.* AIM2 recognizes cytosolic dsDNA and forms a caspase-1-activating inflammasome with ASC. *Nature* 2009; **458**(7237)**:** 514-518.

170. Roberts TL, Idris A, Dunn JA, Kelly GM, Burnton CM, Hodgson S *et al.* HIN-200 proteins regulate caspase activation in response to foreign cytoplasmic DNA. *Science* 2009; **323**(5917)**:** 1057-1060.

171. Fernandes-Alnemri T, Yu JW, Juliana C, Solorzano L, Kang S, Wu J *et al.* The AIM2 inflammasome is critical for innate immunity to Francisella tularensis. *Nat Immunol* 2010; **11**(5)**:** 385-393.

172. Rathinam VA, Jiang Z, Waggoner SN, Sharma S, Cole LE, Waggoner L *et al.* The AIM2 inflammasome is essential for host defense against cytosolic bacteria and DNA viruses. *Nat Immunol* 2010; **11**(5)**:** 395-402.

173. Hu Z, Yan C, Liu P, Huang Z, Ma R, Zhang C *et al.* Crystal structure of NLRC4 reveals its autoinhibition mechanism. *Science* 2013; **341**(6142)**:** 172-175.

174. Broz P, von Moltke J, Jones JW, Vance RE, Monack DM. Differential requirement for Caspase-1 autoproteolysis in pathogen-induced cell death and cytokine processing. *Cell Host Microbe* 2010; **8**(6)**:** 471-483.

175. Miao EA, Leaf IA, Treuting PM, Mao DP, Dors M, Sarkar A *et al.* Caspase-1-induced pyroptosis is an innate immune effector mechanism against intracellular bacteria. *Nat Immunol* 2010; **11**(12)**:** 1136-1142.

176. Franchi L, Amer A, Body-Malapel M, Kanneganti TD, Ozoren N, Jagirdar R *et al.* Cytosolic flagellin requires Ipaf for activation of caspase-1 and interleukin 1beta in salmonella-infected macrophages. *Nat Immunol* 2006; **7**(6)**:** 576-582.

177. Miao EA, Alpuche-Aranda CM, Dors M, Clark AE, Bader MW, Miller SI *et al.* Cytoplasmic flagellin activates caspase-1 and secretion of interleukin 1beta via Ipaf. *Nat Immunol* 2006; **7**(6)**:** 569-575.

178. Miao EA, Mao DP, Yudkovsky N, Bonneau R, Lorang CG, Warren SE *et al.* Innate immune detection of the type III secretion apparatus through the NLRC4 inflammasome. *Proc Natl Acad Sci U S A* 2010; **107**(7)**:** 3076-3080.

179. Kofoed EM, Vance RE. Innate immune recognition of bacterial ligands by NAIPs determines inflammasome specificity. *Nature* 2011; **477**(7366)**:** 592-595.

180. Zhao Y, Yang J, Shi J, Gong YN, Lu Q, Xu H *et al.* The NLRC4 inflammasome receptors for bacterial flagellin and type III secretion apparatus. *Nature* 2011; **477**(7366)**:** 596-600.

181. Kofoed EM, Vance RE. NAIPs: building an innate immune barrier against bacterial pathogens. NAIPs function as sensors that initiate innate immunity by detection of bacterial proteins in the host cell cytosol. *Bioessays* 2012; **34**(7)**:** 589-598.

182. Yang J, Zhao Y, Shi J, Shao F. Human NAIP and mouse NAIP1 recognize bacterial type III secretion needle protein for inflammasome activation. *Proc Natl Acad Sci U S A* 2013; **110**(35)**:** 14408-14413.

183. Qu Y, Misaghi S, Izrael-Tomasevic A, Newton K, Gilmour LL, Lamkanfi M *et al.* Phosphorylation of NLRC4 is critical for inflammasome activation. *Nature* 2012; **490**(7421)**:** 539-542.

184. Poyet JL, Srinivasula SM, Tnani M, Razmara M, Fernandes-Alnemri T, Alnemri ES. Identification of Ipaf, a human caspase-1-activating protein related to Apaf-1. *J Biol Chem* 2001; **276**(30)**:** 28309-28313.

185. Damiano JS, Stehlik C, Pio F, Godzik A, Reed JC. CLAN, a novel human CED-4-like gene. *Genomics* 2001; **75**(1-3)**:** 77-83.

186. Mariathasan S, Newton K, Monack DM, Vucic D, French DM, Lee WP *et al.* Differential activation of the inflammasome by caspase-1 adaptors ASC and Ipaf. *Nature* 2004; **430**(6996)**:** 213-218.

187. Miao EA, Rajan JV. Salmonella and Caspase-1: A complex Interplay of Detection and Evasion. *Front Microbiol* 2011; **2:** 85.

188. Suzuki T, Franchi L, Toma C, Ashida H, Ogawa M, Yoshikawa Y *et al.* Differential regulation of caspase-1 activation, pyroptosis, and autophagy via Ipaf and ASC in Shigella-infected macrophages. *PLoS Pathog* 2007; **3**(8)**:** e111.

189. Sutterwala FS, Mijares LA, Li L, Ogura Y, Kazmierczak BI, Flavell RA. Immune recognition of Pseudomonas aeruginosa mediated by the IPAF/NLRC4 inflammasome. *J Exp Med* 2007; **204**(13)**:** 3235-3245.

190. Carvalho FA, Nalbantoglu I, Aitken JD, Uchiyama R, Su Y, Doho GH *et al.* Cytosolic flagellin receptor NLRC4 protects mice against mucosal and systemic challenges. *Mucosal Immunol* 2012; **5**(3)**:** 288-298.

191. Griffin AJ, McSorley SJ. Development of protective immunity to Salmonella, a mucosal pathogen with a systemic agenda. *Mucosal Immunol* 2011; **4**(4)**:** 371-382.

192. Franchi L, Kamada N, Nakamura Y, Burberry A, Kuffa P, Suzuki S *et al.* NLRC4-driven production of IL-1beta discriminates between pathogenic and commensal bacteria and promotes host intestinal defense. *Nat Immunol* 2012; **13**(5)**:** 449-456.

193. Amer A, Franchi L, Kanneganti TD, Body-Malapel M, Ozoren N, Brady G *et al.* Regulation of Legionella phagosome maturation and infection through flagellin and host Ipaf. *J Biol Chem* 2006; **281**(46)**:** 35217-35223.

194. Akhter A, Gavrilin MA, Frantz L, Washington S, Ditty C, Limoli D *et al.* Caspase-7 activation by the Nlrc4/Ipaf inflammasome restricts Legionella pneumophila infection. *PLoS Pathog* 2009; **5**(4)**:** e1000361.

195. Allen IC, TeKippe EM, Woodford RM, Uronis JM, Holl EK, Rogers AB *et al.* The NLRP3 inflammasome functions as a negative regulator of tumorigenesis during colitis-associated cancer. *J Exp Med* 2010; **207**(5)**:** 1045-1056.

196. van de Veerdonk FL, Netea MG. New Insights in the Immunobiology of IL-1 Family Members. *Front Immunol* 2013; **4:** 167.

197. Dinarello CA. Immunological and inflammatory functions of the interleukin-1 family. *Annual review of immunology* 2009; **27:** 519-550.

198. Gross O, Yazdi AS, Thomas CJ, Masin M, Heinz LX, Guarda G *et al.* Inflammasome activators induce interleukin-1alpha secretion via distinct pathways with differential requirement for the protease function of caspase-1. *Immunity* 2012; **36**(3)**:** 388-400.

199. Shaw MH, Kamada N, Kim YG, Nunez G. Microbiota-induced IL-1beta, but not IL-6, is critical for the development of steady-state TH17 cells in the intestine. *J Exp Med* 2012; **209**(2)**:** 251-258.

200. Coccia M, Harrison OJ, Schiering C, Asquith MJ, Becher B, Powrie F *et al.* IL-1beta mediates chronic intestinal inflammation by promoting the accumulation of IL-17A secreting innate lymphoid cells and CD4(+) Th17 cells. *J Exp Med* 2012; **209**(9)**:** 1595-1609.

201. Hirsch E, Irikura VM, Paul SM, Hirsh D. Functions of interleukin 1 receptor antagonist in gene knockout and overproducing mice. *Proc Natl Acad Sci U S A* 1996; **93**(20)**:** 11008-11013.

202. Ludwiczek O, Vannier E, Borggraefe I, Kaser A, Siegmund B, Dinarello CA *et al.* Imbalance between interleukin-1 agonists and antagonists: relationship to severity of inflammatory bowel disease. *Clin Exp Immunol* 2004; **138**(2)**:** 323-329.

203. McAlindon ME, Hawkey CJ, Mahida YR. Expression of interleukin 1 beta and interleukin 1 beta converting enzyme by intestinal macrophages in health and inflammatory bowel disease. *Gut* 1998; **42**(2)**:** 214-219.

204. Arend WP, Palmer G, Gabay C. IL-1, IL-18, and IL-33 families of cytokines. *Immunol Rev* 2008; **223:** 20-38.

205. Novick D, Kim SH, Fantuzzi G, Reznikov LL, Dinarello CA, Rubinstein M. Interleukin-18 binding protein: a novel modulator of the Th1 cytokine response. *Immunity* 1999; **10**(1)**:** 127-136.

206. Paulukat J, Bosmann M, Nold M, Garkisch S, Kampfer H, Frank S *et al.* Expression and release of IL-18 binding protein in response to IFN-gamma. *J Immunol* 2001; **167**(12)**:** 7038-7043.

207. Kanai T, Watanabe M, Okazawa A, Sato T, Yamazaki M, Okamoto S *et al.* Macrophage-derived IL-18-mediated intestinal inflammation in the murine model of Crohn's disease. *Gastroenterology* 2001; **121**(4)**:** 875-888.

208. Siegmund B. Interleukin-18 in intestinal inflammation: friend and foe? *Immunity* 2010; **32**(3)**:** 300-302.

209. Pizarro TT, Michie MH, Bentz M, Woraratanadharm J, Smith MF, Jr., Foley E *et al.* IL-18, a novel immunoregulatory cytokine, is up-regulated in Crohn's disease: expression and localization in intestinal mucosal cells. *J Immunol* 1999; **162**(11)**:** 6829-6835.

210. Leach ST, Messina I, Lemberg DA, Novick D, Rubenstein M, Day AS. Local and systemic interleukin-18 and interleukin-18-binding protein in children with inflammatory bowel disease. *Inflamm Bowel Dis* 2008; **14**(1)**:** 68-74.

211. Fink SL, Cookson BT. Caspase-1-dependent pore formation during pyroptosis leads to osmotic lysis of infected host macrophages. *Cell Microbiol* 2006; **8**(11)**:** 1812-1825.

212. Chen S, Sun B. Negative regulation of NLRP3 inflammasome signaling. *Protein & cell* 2013; **4**(4)**:** 251-258.

213. Saleh M, Mathison JC, Wolinski MK, Bensinger SJ, Fitzgerald P, Droin N *et al.* Enhanced bacterial clearance and sepsis resistance in caspase-12-deficient mice. *Nature* 2006; **440**(7087)**:** 1064-1068.

214. Dupaul-Chicoine J, Yeretssian G, Doiron K, Bergstrom KS, McIntire CR, LeBlanc PM *et al.* Control of intestinal homeostasis, colitis, and colitis-associated colorectal cancer by the inflammatory caspases. *Immunity* 2010; **32**(3)**:** 367-378.

215. Guarda G, Dostert C, Staehli F, Cabalzar K, Castillo R, Tardivel A *et al.* T cells dampen innate immune responses through inhibition of NLRP1 and NLRP3 inflammasomes. *Nature* 2009; **460**(7252)**:** 269-273.

216. Shi CS, Shenderov K, Huang NN, Kabat J, Abu-Asab M, Fitzgerald KA *et al.* Activation of autophagy by inflammatory signals limits IL-1beta production by targeting ubiquitinated inflammasomes for destruction. *Nat Immunol* 2012; **13**(3)**:** 255-263.

217. Saitoh T, Fujita N, Jang MH, Uematsu S, Yang BG, Satoh T *et al.* Loss of the autophagy protein Atg16L1 enhances endotoxin-induced IL-1beta production. *Nature* 2008; **456**(7219)**:** 264-268.

218. Neurath MF. Animal models of inflammatory bowel diseases: illuminating the pathogenesis of colitis, ileitis and cancer. *Digestive diseases* 2012; **30 Suppl 1:** 91-94.

219. Khor B, Gardet A, Xavier RJ. Genetics and pathogenesis of inflammatory bowel disease. *Nature* 2011; **474**(7351)**:** 307-317.

220. Whitman WB, Coleman DC, Wiebe WJ. Prokaryotes: the unseen majority. *Proc Natl Acad Sci U S A* 1998; **95**(12)**:** 6578-6583.

221. Sellon RK, Tonkonogy S, Schultz M, Dieleman LA, Grenther W, Balish E *et al.* Resident enteric bacteria are necessary for development of spontaneous colitis and immune system activation in interleukin-10-deficient mice. *Infect Immun* 1998; **66**(11)**:** 5224-5231.

222. Darfeuille-Michaud A, Neut C, Barnich N, Lederman E, Di Martino P, Desreumaux P *et al.* Presence of adherent Escherichia coli strains in ileal mucosa of patients with Crohn's disease. *Gastroenterology* 1998; **115**(6)**:** 1405-1413.

223. Baumgart DC, Sandborn WJ. Inflammatory bowel disease: clinical aspects and established and evolving therapies. *Lancet* 2007; **369**(9573)**:** 1641-1657.

224. Geremia A, Biancheri P, Allan P, Corazza GR, Di Sabatino A. Innate and adaptive immunity in inflammatory bowel disease. *Autoimmunity reviews* 2013.

225. Fujino S, Andoh A, Bamba S, Ogawa A, Hata K, Araki Y *et al.* Increased expression of interleukin 17 in inflammatory bowel disease. *Gut* 2003; **52**(1)**:** 65-70.

226. Zhou L, Ivanov, II, Spolski R, Min R, Shenderov K, Egawa T *et al.* IL-6 programs T(H)-17 cell differentiation by promoting sequential engagement of the IL-21 and IL-23 pathways. *Nat Immunol* 2007; **8**(9)**:** 967-974.

227. Duerr RH, Taylor KD, Brant SR, Rioux JD, Silverberg MS, Daly MJ *et al.* A genome-wide association study identifies IL23R as an inflammatory bowel disease gene. *Science* 2006; **314**(5804)**:** 1461-1463.

228. Mundy R, MacDonald TT, Dougan G, Frankel G, Wiles S. Citrobacter rodentium of mice and man. *Cell Microbiol* 2005; **7**(12)**:** 1697-1706.

229. Luperchio SA, Schauer DB. Molecular pathogenesis of Citrobacter rodentium and transmissible murine colonic hyperplasia. *Microbes Infect* 2001; **3**(4)**:** 333-340.

230. Deng W, Puente JL, Gruenheid S, Li Y, Vallance BA, Vazquez A *et al.* Dissecting virulence: systematic and functional analyses of a pathogenicity island. *Proc Natl Acad Sci U S A* 2004; **101**(10)**:** 3597-3602.

231. Deng W, Vallance BA, Li Y, Puente JL, Finlay BB. Citrobacter rodentium translocated intimin receptor (Tir) is an essential virulence factor needed for actin condensation, intestinal colonization and colonic hyperplasia in mice. *Mol Microbiol* 2003; **48**(1)**:** 95-115.

232. Wiles S, Clare S, Harker J, Huett A, Young D, Dougan G *et al.* Organ specificity, colonization and clearance dynamics in vivo following oral challenges with the murine pathogen Citrobacter rodentium. *Cell Microbiol* 2004; **6**(10)**:** 963-972.

233. Owen RL, Piazza AJ, Ermak TH. Ultrastructural and cytoarchitectural features of lymphoreticular organs in the colon and rectum of adult BALB/c mice. *The American journal of anatomy* 1991; **190**(1)**:** 10-18.

234. Wiles S, Dougan G, Frankel G. Emergence of a 'hyperinfectious' bacterial state after passage of Citrobacter rodentium through the host gastrointestinal tract. *Cell Microbiol* 2005; **7**(8)**:** 1163-1172.

235. Bishop AL, Wiles S, Dougan G, Frankel G. Cell attachment properties and infectivity of host-adapted and environmentally adapted Citrobacter rodentium. *Microbes Infect* 2007; **9**(11)**:** 1316-1324.

236. Simmons CP, Clare S, Ghaem-Maghami M, Uren TK, Rankin J, Huett A *et al.* Central role for B lymphocytes and CD4+ T cells in immunity to infection by the attaching and effacing pathogen Citrobacter rodentium. *Infect Immun* 2003; **71**(9)**:** 5077-5086.

237. Shiomi H, Masuda A, Nishiumi S, Nishida M, Takagawa T, Shiomi Y *et al.* Gamma interferon produced by antigen-specific CD4+ T cells regulates the mucosal immune responses to Citrobacter rodentium infection. *Infect Immun* 2010; **78**(6)**:** 2653-2666.

238. Barthold SW, Coleman GL, Jacoby RO, Livestone EM, Jonas AM. Transmissible murine colonic hyperplasia. *Veterinary pathology* 1978; **15**(2)**:** 223-236.

239. Gibson DL, Ma C, Bergstrom KS, Huang JT, Man C, Vallance BA. MyD88 signalling plays a critical role in host defence by controlling pathogen burden and promoting epithelial cell homeostasis during Citrobacter rodentium-induced colitis. *Cell Microbiol* 2008; **10**(3)**:** 618-631.

240. Lebeis SL, Bommarius B, Parkos CA, Sherman MA, Kalman D. TLR signaling mediated by MyD88 is required for a protective innate immune response by neutrophils to Citrobacter rodentium. *J Immunol* 2007; **179**(1)**:** 566-577.

241. Lebeis SL, Powell KR, Merlin D, Sherman MA, Kalman D. Interleukin-1 receptor signaling protects mice from lethal intestinal damage caused by the attaching and effacing pathogen Citrobacter rodentium. *Infect Immun* 2009; **77**(2)**:** 604-614.

242. Gibson DL, Ma C, Rosenberger CM, Bergstrom KS, Valdez Y, Huang JT *et al.* Toll-like receptor 2 plays a critical role in maintaining mucosal integrity during Citrobacter rodentium-induced colitis. *Cell Microbiol* 2008; **10**(2)**:** 388-403.

243. Khan MA, Ma C, Knodler LA, Valdez Y, Rosenberger CM, Deng W *et al.* Toll-like receptor 4 contributes to colitis development but not to host defense during Citrobacter rodentium infection in mice. *Infect Immun* 2006; **74**(5)**:** 2522-2536.

244. Mangan PR, Harrington LE, O'Quinn DB, Helms WS, Bullard DC, Elson CO *et al.* Transforming growth factor-beta induces development of the T(H)17 lineage. *Nature* 2006; **441**(7090)**:** 231-234.

245. Rutz S, Eidenschenk C, Ouyang W. IL-22, not simply a Th17 cytokine. *Immunol Rev* 2013; **252**(1)**:** 116-132.

246. Bergstrom KS, Guttman JA, Rumi M, Ma C, Bouzari S, Khan MA *et al.* Modulation of intestinal goblet cell function during infection by an attaching and effacing bacterial pathogen. *Infect Immun* 2008; **76**(2)**:** 796-811.

247. Vallance BA, Deng W, Knodler LA, Finlay BB. Mice lacking T and B lymphocytes develop transient colitis and crypt hyperplasia yet suffer impaired bacterial clearance during Citrobacter rodentium infection. *Infect Immun* 2002; **70**(4)**:** 2070-2081.

248. Simmons CP, Goncalves NS, Ghaem-Maghami M, Bajaj-Elliott M, Clare S, Neves B *et al.* Impaired resistance and enhanced pathology during infection with a noninvasive, attaching-effacing enteric bacterial pathogen, Citrobacter rodentium, in mice lacking IL-12 or IFN-gamma. *J Immunol* 2002; **168**(4)**:** 1804-1812.

249. Higgins LM, Frankel G, Douce G, Dougan G, MacDonald TT. Citrobacter rodentium infection in mice elicits a mucosal Th1 cytokine response and lesions similar to those in murine inflammatory bowel disease. *Infect Immun* 1999; **67**(6)**:** 3031-3039.

250. Powrie F, Leach MW, Mauze S, Caddle LB, Coffman RL. Phenotypically distinct subsets of CD4+ T cells induce or protect from chronic intestinal inflammation in C. B-17 scid mice. *Int Immunol* 1993; **5**(11)**:** 1461-1471.

251. Hue S, Ahern P, Buonocore S, Kullberg MC, Cua DJ, McKenzie BS *et al.* Interleukin-23 drives innate and T cell-mediated intestinal inflammation. *J Exp Med* 2006; **203**(11)**:** 2473-2483.

252. Izcue A, Hue S, Buonocore S, Arancibia-Carcamo CV, Ahern PP, Iwakura Y *et al.* Interleukin-23 restrains regulatory T cell activity to drive T cell-dependent colitis. *Immunity* 2008; **28**(4)**:** 559-570.

253. Powrie F, Leach MW, Mauze S, Menon S, Caddle LB, Coffman RL. Inhibition of Th1 responses prevents inflammatory bowel disease in scid mice reconstituted with CD45RBhi CD4+ T cells. *Immunity* 1994; **1**(7)**:** 553-562.

254. Simpson SJ, Shah S, Comiskey M, de Jong YP, Wang B, Mizoguchi E *et al.* T cell-mediated pathology in two models of experimental colitis depends predominantly on the interleukin 12/Signal transducer and activator of transcription (Stat)-4 pathway, but is not conditional on interferon gamma expression by T cells. *J Exp Med* 1998; **187**(8)**:** 1225-1234.

255. Leach MW, Bean AG, Mauze S, Coffman RL, Powrie F. Inflammatory bowel disease in C.B-17 scid mice reconstituted with the CD45RBhigh subset of CD4+ T cells. *Am J Pathol* 1996; **148**(5)**:** 1503-1515.

256. Annunziato F, Cosmi L, Santarlasci V, Maggi L, Liotta F, Mazzinghi B *et al.* Phenotypic and functional features of human Th17 cells. *J Exp Med* 2007; **204**(8)**:** 1849-1861.

257. Mottet C, Uhlig HH, Powrie F. Cutting edge: cure of colitis by CD4+CD25+ regulatory T cells. *J Immunol* 2003; **170**(8)**:** 3939-3943.

258. Izcue A, Coombes JL, Powrie F. Regulatory lymphocytes and intestinal inflammation. *Annual review of immunology* 2009; **27:** 313-338.

259. Kullberg MC, Jankovic D, Feng CG, Hue S, Gorelick PL, McKenzie BS *et al.* IL-23 plays a key role in Helicobacter hepaticus-induced T cell-dependent colitis. *J Exp Med* 2006; **203**(11)**:** 2485-2494.

260. Chan V, Crocetti G, Grehan M, Zhang L, Danon S, Lee A *et al.* Visualization of Helicobacter species within the murine cecal mucosa using specific fluorescence in situ hybridization. *Helicobacter* 2005; **10**(2)**:** 114-124.

261. Fox JG, Dewhirst FE, Tully JG, Paster BJ, Yan L, Taylor NS *et al.* Helicobacter hepaticus sp. nov., a microaerophilic bacterium isolated from livers and intestinal mucosal scrapings from mice. *Journal of clinical microbiology* 1994; **32**(5)**:** 1238-1245.

262. Kullberg MC, Ward JM, Gorelick PL, Caspar P, Hieny S, Cheever A *et al.* Helicobacter hepaticus triggers colitis in specific-pathogen-free interleukin-10 (IL-10)-deficient mice through an IL-12- and gamma interferon-dependent mechanism. *Infect Immun* 1998; **66**(11)**:** 5157-5166.

263. Kullberg MC, Jankovic D, Gorelick PL, Caspar P, Letterio JJ, Cheever AW *et al.* Bacteria-triggered CD4(+) T regulatory cells suppress Helicobacter hepaticus-induced colitis. *J Exp Med* 2002; **196**(4)**:** 505-515.

264. Read S, Malmstrom V, Powrie F. Cytotoxic T lymphocyte-associated antigen 4 plays an essential role in the function of CD25(+)CD4(+) regulatory cells that control intestinal inflammation. *J Exp Med* 2000; **192**(2)**:** 295-302.

265. Asquith MJ, Boulard O, Powrie F, Maloy KJ. Pathogenic and protective roles of MyD88 in leukocytes and epithelial cells in mouse models of inflammatory bowel disease. *Gastroenterology* 2010; **139**(2)**:** 519-529, 529 e511-512.

266. Andersen-Nissen E, Smith KD, Strobe KL, Barrett SL, Cookson BT, Logan SM *et al.* Evasion of Toll-like receptor 5 by flagellated bacteria. *Proc Natl Acad Sci U S A* 2005; **102**(26)**:** 9247-9252.

267. Maloy KJ, Salaun L, Cahill R, Dougan G, Saunders NJ, Powrie F. CD4+CD25+ T(R) cells suppress innate immune pathology through cytokine-dependent mechanisms. *J Exp Med* 2003; **197**(1)**:** 111-119.

268. Asquith M. Toll-Like Receptors in the Induction and Regulation of Intestinal Inflammation. DPhil thesis, University of Oxford, Oxford, 2010.

269. Boulard O, Kirchberger S, Royston DJ, Maloy KJ, Powrie FM. Identification of a genetic locus controlling bacteria-driven colitis and associated cancer through effects on innate inflammation. *J Exp Med* 2012; **209**(7)**:** 1309-1324.

270. Kirchberger S, Royston DJ, Boulard O, Thornton E, Franchini F, Szabady RL *et al.* Innate lymphoid cells sustain colon cancer through production of interleukin-22 in a mouse model. *J Exp Med* 2013; **210**(5)**:** 917-931.

271. Wirtz S, Neufert C, Weigmann B, Neurath MF. Chemically induced mouse models of intestinal inflammation. *Nat Protoc* 2007; **2**(3)**:** 541-546.

272. Strober W, Fuss IJ, Blumberg RS. The immunology of mucosal models of inflammation. *Annual review of immunology* 2002; **20:** 495-549.

273. Kim TW, Seo JN, Suh YH, Park HJ, Kim JH, Kim JY *et al.* Involvement of lymphocytes in dextran sulfate sodium-induced experimental colitis. *World J Gastroenterol* 2006; **12**(2)**:** 302-305.

274. Araki A, Kanai T, Ishikura T, Makita S, Uraushihara K, Iiyama R *et al.* MyD88-deficient mice develop severe intestinal inflammation in dextran sodium sulfate colitis. *J Gastroenterol* 2005; **40**(1)**:** 16-23.

275. Ivison SM, Himmel ME, Hardenberg G, Wark PA, Kifayet A, Levings MK *et al.* TLR5 is not required for flagellin-mediated exacerbation of DSS colitis. *Inflamm Bowel Dis* 2010; **16**(3)**:** 401-409.

276. Podolsky DK, Gerken G, Eyking A, Cario E. Colitis-associated variant of TLR2 causes impaired mucosal repair because of TFF3 deficiency. *Gastroenterology* 2009; **137**(1)**:** 209-220.

277. Rakoff-Nahoum S, Paglino J, Eslami-Varzaneh F, Edberg S, Medzhitov R. Recognition of commensal microflora by toll-like receptors is required for intestinal homeostasis. *Cell* 2004; **118**(2)**:** 229-241.

278. Cox JH, Kljavin NM, Ota N, Leonard J, Roose-Girma M, Diehl L *et al.* Opposing consequences of IL-23 signaling mediated by innate and adaptive cells in chemically induced colitis in mice. *Mucosal Immunol* 2012; **5**(1)**:** 99-109.

279. Uematsu S, Jang MH, Chevrier N, Guo Z, Kumagai Y, Yamamoto M *et al.* Detection of pathogenic intestinal bacteria by Toll-like receptor 5 on intestinal CD11c+ lamina propria cells. *Nat Immunol* 2006; **7**(8)**:** 868-874.

280. Kamanaka M, Kim ST, Wan YY, Sutterwala FS, Lara-Tejero M, Galan JE *et al.* Expression of interleukin-10 in intestinal lymphocytes detected by an interleukin-10 reporter knockin tiger mouse. *Immunity* 2006; **25**(6)**:** 941-952.

281. Kendal AR, Chen Y, Regateiro FS, Ma J, Adams E, Cobbold SP *et al.* Sustained suppression by Foxp3+ regulatory T cells is vital for infectious transplantation tolerance. *J Exp Med* 2011; **208**(10)**:** 2043-2053.

282. Markel P, Shu P, Ebeling C, Carlson GA, Nagle DL, Smutko JS *et al.* Theoretical and empirical issues for marker-assisted breeding of congenic mouse strains. *Nat Genet* 1997; **17**(3)**:** 280-284.

283. Feng S, Ku K, Hodzic E, Lorenzana E, Freet K, Barthold SW. Differential detection of five mouse-infecting helicobacter species by multiplex PCR. *Clinical and diagnostic laboratory immunology* 2005; **12**(4)**:** 531-536.

284. Fox JG, Dewhirst FE, Shen Z, Feng Y, Taylor NS, Paster BJ *et al.* Hepatic Helicobacter species identified in bile and gallbladder tissue from Chileans with chronic cholecystitis. *Gastroenterology* 1998; **114**(4)**:** 755-763.

285. Ge Z, White DA, Whary MT, Fox JG. Fluorogenic PCR-based quantitative detection of a murine pathogen, Helicobacter hepaticus. *Journal of clinical microbiology* 2001; **39**(7)**:** 2598-2602.

286. Bry L, Brenner MB. Critical role of T cell-dependent serum antibody, but not the gut-associated lymphoid tissue, for surviving acute mucosal infection with Citrobacter rodentium, an attaching and effacing pathogen. *J Immunol* 2004; **172**(1)**:** 433-441.

287. Boulard O, Asquith MJ, Powrie F, Maloy KJ. TLR2-independent induction and regulation of chronic intestinal inflammation. *Eur J Immunol* 2010; **40**(2)**:** 516-524.

288. Reikvam DH, Erofeev A, Sandvik A, Grcic V, Jahnsen FL, Gaustad P *et al.* Depletion of murine intestinal microbiota: effects on gut mucosa and epithelial gene expression. *PLoS One* 2011; **6**(3)**:** e17996.

289. Blackwood CB, Oaks A, Buyer JS. Phylum- and class-specific PCR primers for general microbial community analysis. *Appl Environ Microbiol* 2005; **71**(10)**:** 6193-6198.

290. Jung P, Sato T, Merlos-Suarez A, Barriga FM, Iglesias M, Rossell D *et al.* Isolation and in vitro expansion of human colonic stem cells. *Nat Med* 2011; **17**(10)**:** 1225-1227.

291. Young VB, Knox KA, Pratt JS, Cortez JS, Mansfield LS, Rogers AB *et al.* In vitro and in vivo characterization of Helicobacter hepaticus cytolethal distending toxin mutants. *Infect Immun* 2004; **72**(5)**:** 2521-2527.

292. Ahmed S, Macfarlane GT, Fite A, McBain AJ, Gilbert P, Macfarlane S. Mucosa-associated bacterial diversity in relation to human terminal ileum and colonic biopsy samples. *Appl Environ Microbiol* 2007; **73**(22)**:** 7435-7442.

293. Snyder LA, Loman NJ, Futterer K, Pallen MJ. Bacterial flagellar diversity and evolution: seek simplicity and distrust it? *Trends in microbiology* 2009; **17**(1)**:** 1-5.

294. Franchi L, Munoz-Planillo R, Nunez G. Sensing and reacting to microbes through the inflammasomes. *Nat Immunol* 2012; **13**(4)**:** 325-332.

295. Ceballos-Olvera I, Sahoo M, Miller MA, Del Barrio L, Re F. Inflammasome-dependent pyroptosis and IL-18 protect against Burkholderia pseudomallei lung infection while IL-1beta is deleterious. *PLoS Pathog* 2011; **7**(12)**:** e1002452.

296. Hu B, Elinav E, Huber S, Booth CJ, Strowig T, Jin C *et al.* Inflammation-induced tumorigenesis in the colon is regulated by caspase-1 and NLRC4. *Proc Natl Acad Sci U S A* 2010; **107**(50)**:** 21635-21640.

297. Allen IC, TeKippe EM, Woodford RM, Uronis JM, Holl EK, Rogers AB *et al.* The NLRP3 inflammasome functions as a negative regulator of tumorigenesis during colitis-associated cancer. *J Exp Med*; **207**(5)**:** 1045-1056.

298. Willing BP, Vacharaksa A, Croxen M, Thanachayanont T, Finlay BB. Altering host resistance to infections through microbial transplantation. *PLoS One* 2011; **6**(10)**:** e26988.

299. Maaser C, Housley MP, Iimura M, Smith JR, Vallance BA, Finlay BB *et al.* Clearance of Citrobacter rodentium requires B cells but not secretory immunoglobulin A (IgA) or IgM antibodies. *Infect Immun* 2004; **72**(6)**:** 3315-3324.

300. Borenshtein D, Nambiar PR, Groff EB, Fox JG, Schauer DB. Development of fatal colitis in FVB mice infected with Citrobacter rodentium. *Infect Immun* 2007; **75**(7)**:** 3271-3281.

301. Vallance BA, Deng W, Jacobson K, Finlay BB. Host susceptibility to the attaching and effacing bacterial pathogen Citrobacter rodentium. *Infect Immun* 2003; **71**(6)**:** 3443-3453.

302. Wickham ME, Lupp C, Vazquez A, Mascarenhas M, Coburn B, Coombes BK *et al.* Citrobacter rodentium virulence in mice associates with bacterial load and the type III effector NleE. *Microbes Infect* 2007; **9**(3)**:** 400-407.

303. Sauer JD, Pereyre S, Archer KA, Burke TP, Hanson B, Lauer P *et al.* Listeria monocytogenes engineered to activate the Nlrc4 inflammasome are severely attenuated and are poor inducers of protective immunity. *Proc Natl Acad Sci U S A* 2011; **108**(30)**:** 12419-12424.

304. Witte CE, Archer KA, Rae CS, Sauer JD, Woodward JJ, Portnoy DA. Innate immune pathways triggered by Listeria monocytogenes and their role in the induction of cell-mediated immunity. *Advances in immunology* 2012; **113:** 135-156.

305. Liang SC, Tan XY, Luxenberg DP, Karim R, Dunussi-Joannopoulos K, Collins M *et al.* Interleukin (IL)-22 and IL-17 are coexpressed by Th17 cells and cooperatively enhance expression of antimicrobial peptides. *J Exp Med* 2006; **203**(10)**:** 2271-2279.

306. Cai S, Batra S, Wakamatsu N, Pacher P, Jeyaseelan S. NLRC4 inflammasome-mediated production of IL-1beta modulates mucosal immunity in the lung against gram-negative bacterial infection. *J Immunol* 2012; **188**(11)**:** 5623-5635.

307. Tomalka J, Ganesan S, Azodi E, Patel K, Majmudar P, Hall BA *et al.* A novel role for the NLRC4 inflammasome in mucosal defenses against the fungal pathogen Candida albicans. *PLoS Pathog* 2011; **7**(12)**:** e1002379.

308. Spehlmann ME, Dann SM, Hruz P, Hanson E, McCole DF, Eckmann L. CXCR2-dependent mucosal neutrophil influx protects against colitis-associated diarrhea caused by an attaching/effacing lesion-forming bacterial pathogen. *J Immunol* 2009; **183**(5)**:** 3332-3343.

309. Ferreira RB, Gill N, Willing BP, Antunes LC, Russell SL, Croxen MA *et al.* The intestinal microbiota plays a role in Salmonella-induced colitis independent of pathogen colonization. *PLoS One* 2011; **6**(5)**:** e20338.

310. Wlodarska M, Willing B, Keeney KM, Menendez A, Bergstrom KS, Gill N *et al.* Antibiotic treatment alters the colonic mucus layer and predisposes the host to exacerbated Citrobacter rodentium-induced colitis. *Infect Immun* 2011; **79**(4)**:** 1536-1545.

311. Kamada N, Kim YG, Sham HP, Vallance BA, Puente JL, Martens EC *et al.* Regulated virulence controls the ability of a pathogen to compete with the gut microbiota. *Science* 2012; **336**(6086)**:** 1325-1329.

312. Jarry A, Vallette G, Cassagnau E, Moreau A, Bou-Hanna C, Lemarre P *et al.* Interleukin 1 and interleukin 1beta converting enzyme (caspase 1) expression in the human colonic epithelial barrier. Caspase 1 downregulation in colon cancer. *Gut* 1999; **45**(2)**:** 246-251.

313. Fruchtman S, Simmons JG, Michaylira CZ, Miller ME, Greenhalgh CJ, Ney DM *et al.* Suppressor of cytokine signaling-2 modulates the fibrogenic actions of GH and IGF-I in intestinal mesenchymal cells. *Am J Physiol Gastrointest Liver Physiol* 2005; **289**(2)**:** G342-350.

314. Levy JA. The unexpected pleiotropic activities of RANTES. *J Immunol* 2009; **182**(7)**:** 3945-3946.

315. Cormier SA, Larson KA, Yuan S, Mitchell TL, Lindenberger K, Carrigan P *et al.* Mouse eosinophil-associated ribonucleases: a unique subfamily expressed during hematopoiesis. *Mamm Genome* 2001; **12**(5)**:** 352-361.

316. Roark CL, Simonian PL, Fontenot AP, Born WK, O'Brien RL. gammadelta T cells: an important source of IL-17. *Curr Opin Immunol* 2008; **20**(3)**:** 353-357.

317. Rayamajhi M, Zhang Y, Miao EA. Detection of pyroptosis by measuring released lactate dehydrogenase activity. *Methods Mol Biol* 2013; **1040:** 85-90.

318. Sato T, Clevers H. Growing self-organizing mini-guts from a single intestinal stem cell: mechanism and applications. *Science* 2013; **340**(6137)**:** 1190-1194.

319. Khan MA, Bouzari S, Ma C, Rosenberger CM, Bergstrom KS, Gibson DL *et al.* Flagellin-dependent and -independent inflammatory responses following infection by enteropathogenic Escherichia coli and Citrobacter rodentium. *Infect Immun* 2008; **76**(4)**:** 1410-1422.

320. Gurung P, Malireddi RK, Anand PK, Demon D, Walle LV, Liu Z *et al.* Toll or interleukin-1 receptor (TIR) domain-containing adaptor inducing interferon-beta (TRIF)-mediated caspase-11 protease production integrates Toll-like receptor 4 (TLR4) protein- and Nlrp3 inflammasome-mediated host defense against enteropathogens. *J Biol Chem* 2012; **287**(41)**:** 34474-34483.

321. Wang S, Miura M, Jung YK, Zhu H, Li E, Yuan J. Murine caspase-11, an ICE-interacting protease, is essential for the activation of ICE. *Cell* 1998; **92**(4)**:** 501-509.

322. Kayagaki N, Warming S, Lamkanfi M, Vande Walle L, Louie S, Dong J *et al.* Non-canonical inflammasome activation targets caspase-11. *Nature* 2011; **479**(7371)**:** 117-121.

323. Kang SJ, Popat R, Bragdon C, Odonnell K, Phelan S, Yuan J *et al.* Caspase-11 is not necessary for chemotherapy-induced intestinal mucositis. *DNA and cell biology* 2004; **23**(8)**:** 490-495.

324. Kayagaki N, Wong MT, Stowe IB, Ramani SR, Gonzalez LC, Akashi-Takamura S *et al.* Noncanonical Inflammasome Activation by Intracellular LPS Independent of TLR4. *Science* 2013.

325. Moore KW, de Waal Malefyt R, Coffman RL, O'Garra A. Interleukin-10 and the interleukin-10 receptor. *Annual review of immunology* 2001; **19:** 683-765.

326. Sterzenbach T, Bartonickova L, Behrens W, Brenneke B, Schulze J, Kops F *et al.* Role of the Helicobacter hepaticus flagellar sigma factor FliA in gene regulation and murine colonization. *J Bacteriol* 2008; **190**(19)**:** 6398-6408.

327. Kullberg MC, Andersen JF, Gorelick PL, Caspar P, Suerbaum S, Fox JG *et al.* Induction of colitis by a CD4+ T cell clone specific for a bacterial epitope. *Proc Natl Acad Sci U S A* 2003; **100**(26)**:** 15830-15835.

328. Lightfield KL, Persson J, Brubaker SW, Witte CE, von Moltke J, Dunipace EA *et al.* Critical function for Naip5 in inflammasome activation by a conserved carboxy-terminal domain of flagellin. *Nat Immunol* 2008; **9**(10)**:** 1171-1178.

329. Boutin SR, Shen Z, Rogers AB, Feng Y, Ge Z, Xu S *et al.* Different Helicobacter hepaticus strains with variable genomic content induce various degrees of hepatitis. *Infect Immun* 2005; **73**(12)**:** 8449-8452.

330. Hacker J, Kaper JB. Pathogenicity islands and the evolution of microbes. *Annual review of microbiology* 2000; **54:** 641-679.

331. Chow J, Mazmanian SK. A pathobiont of the microbiota balances host colonization and intestinal inflammation. *Cell Host Microbe* 2010; **7**(4)**:** 265-276.

332. Diez E, Lee SH, Gauthier S, Yaraghi Z, Tremblay M, Vidal S *et al.* Birc1e is the gene within the Lgn1 locus associated with resistance to Legionella pneumophila. *Nat Genet* 2003; **33**(1)**:** 55-60.

333. Fox JG, Li X, Yan L, Cahill RJ, Hurley R, Lewis R *et al.* Chronic proliferative hepatitis in A/JCr mice associated with persistent Helicobacter hepaticus infection: a model of helicobacter-induced carcinogenesis. *Infect Immun* 1996; **64**(5)**:** 1548-1558.

334. Erdman SE, Poutahidis T, Tomczak M, Rogers AB, Cormier K, Plank B *et al.* CD4+ CD25+ regulatory T lymphocytes inhibit microbially induced colon cancer in Rag2-deficient mice. *Am J Pathol* 2003; **162**(2)**:** 691-702.

335. Hitzler I, Sayi A, Kohler E, Engler DB, Koch KN, Hardt WD *et al.* Caspase-1 has both proinflammatory and regulatory properties in Helicobacter infections, which are differentially mediated by its substrates IL-1beta and IL-18. *J Immunol* 2012; **188**(8)**:** 3594-3602.

336. Arnold IC, Zigova Z, Holden M, Lawley TD, Rad R, Dougan G *et al.* Comparative whole genome sequence analysis of the carcinogenic bacterial model pathogen Helicobacter felis. *Genome biology and evolution* 2011; **3:** 302-308.

337. Rogers AB, Fox JG. Inflammation and Cancer. I. Rodent models of infectious gastrointestinal and liver cancer. *Am J Physiol Gastrointest Liver Physiol* 2004; **286**(3)**:** G361-366.

338. Coccia M. The role of IL-1beta in intestinal inflammation. DPhil thesis, University of Oxford, Oxford, 2011.

339. Wirtz S, Becker C, Blumberg R, Galle PR, Neurath MF. Treatment of T cell-dependent experimental colitis in SCID mice by local administration of an adenovirus expressing IL-18 antisense mRNA. *J Immunol* 2002; **168**(1)**:** 411-420.

340. Hu B, Elinav E, Flavell RA. Inflammasome-mediated suppression of inflammation-induced colorectal cancer progression is mediated by direct regulation of epithelial cell proliferation. *Cell cycle* 2011; **10**(12)**:** 1936-1939.

341. Smith KD, Andersen-Nissen E, Hayashi F, Strobe K, Bergman MA, Barrett SL *et al.* Toll-like receptor 5 recognizes a conserved site on flagellin required for protofilament formation and bacterial motility. *Nat Immunol* 2003; **4**(12)**:** 1247-1253.

342. Duck LW, Walter MR, Novak J, Kelly D, Tomasi M, Cong Y *et al.* Isolation of flagellated bacteria implicated in Crohn's disease. *Inflamm Bowel Dis* 2007; **13**(10)**:** 1191-1201.

343. Bambou JC, Giraud A, Menard S, Begue B, Rakotobe S, Heyman M *et al.* In vitro and ex vivo activation of the TLR5 signaling pathway in intestinal epithelial cells by a commensal Escherichia coli strain. *J Biol Chem* 2004; **279**(41)**:** 42984-42992.

344. Ortega-Cava CF, Ishihara S, Rumi MA, Aziz MM, Kazumori H, Yuki T *et al.* Epithelial toll-like receptor 5 is constitutively localized in the mouse cecum and exhibits distinctive down-regulation during experimental colitis. *Clinical and vaccine immunology : CVI* 2006; **13**(1)**:** 132-138.

345. Maaser C, Heidemann J, von Eiff C, Lugering A, Spahn TW, Binion DG *et al.* Human intestinal microvascular endothelial cells express Toll-like receptor 5: a binding partner for bacterial flagellin. *J Immunol* 2004; **172**(8)**:** 5056-5062.

346. Crellin NK, Garcia RV, Hadisfar O, Allan SE, Steiner TS, Levings MK. Human CD4+ T cells express TLR5 and its ligand flagellin enhances the suppressive capacity and expression of FOXP3 in CD4+CD25+ T regulatory cells. *J Immunol* 2005; **175**(12)**:** 8051-8059.

347. Hardenberg G, Yao Y, Piccirillo CA, Levings MK, Steiner TS. Toll-like receptor 5 deficiency protects from wasting disease in a T cell transfer colitis model in T cell receptor-beta-deficient mice. *Inflamm Bowel Dis* 2012; **18**(1)**:** 85-93.

348. Zheng B, Morgan ME, van de Kant HJ, Garssen J, Folkerts G, Kraneveld AD. Transcriptional modulation of pattern recognition receptors in acute colitis in mice. *Biochimica et biophysica acta* 2013; **1832**(12)**:** 2162-2172.

349. Gewirtz AT, Navas TA, Lyons S, Godowski PJ, Madara JL. Cutting edge: bacterial flagellin activates basolaterally expressed TLR5 to induce epithelial proinflammatory gene expression. *J Immunol* 2001; **167**(4)**:** 1882-1885.

350. Cario E, Podolsky DK. Differential alteration in intestinal epithelial cell expression of toll-like receptor 3 (TLR3) and TLR4 in inflammatory bowel disease. *Infect Immun* 2000; **68**(12)**:** 7010-7017.

351. Jarchum I, Liu M, Lipuma L, Pamer EG. Toll-like receptor 5 stimulation protects mice from acute Clostridium difficile colitis. *Infect Immun* 2011; **79**(4)**:** 1498-1503.

352. Vijay-Kumar M, Aitken JD, Kumar A, Neish AS, Uematsu S, Akira S *et al.* Toll-like receptor 5-deficient mice have dysregulated intestinal gene expression and nonspecific resistance to Salmonella-induced typhoid-like disease. *Infect Immun* 2008; **76**(3)**:** 1276-1281.

353. Uematsu S, Fujimoto K, Jang MH, Yang BG, Jung YJ, Nishiyama M *et al.* Regulation of humoral and cellular gut immunity by lamina propria dendritic cells expressing Toll-like receptor 5. *Nat Immunol* 2008; **9**(7)**:** 769-776.

354. Kinnebrew MA, Buffie CG, Diehl GE, Zenewicz LA, Leiner I, Hohl TM *et al.* Interleukin 23 production by intestinal CD103(+)CD11b(+) dendritic cells in response to bacterial flagellin enhances mucosal innate immune defense. *Immunity* 2012; **36**(2)**:** 276-287.

355. Flores-Langarica A, Marshall JL, Hitchcock J, Cook C, Jobanputra J, Bobat S *et al.* Systemic flagellin immunization stimulates mucosal CD103+ dendritic cells and drives Foxp3+ regulatory T cell and IgA responses in the mesenteric lymph node. *J Immunol* 2012; **189**(12)**:** 5745-5754.

356. Vijay-Kumar M, Aitken JD, Carvalho FA, Cullender TC, Mwangi S, Srinivasan S *et al.* Metabolic syndrome and altered gut microbiota in mice lacking Toll-like receptor 5. *Science* 2010; **328**(5975)**:** 228-231.

357. Vijay-Kumar M, Sanders CJ, Taylor RT, Kumar A, Aitken JD, Sitaraman SV *et al.* Deletion of TLR5 results in spontaneous colitis in mice. *J Clin Invest* 2007; **117**(12)**:** 3909-3921.

358. Morrissey PJ, Charrier K, Braddy S, Liggitt D, Watson JD. CD4+ T cells that express high levels of CD45RB induce wasting disease when transferred into congenic severe combined immunodeficient mice. Disease development is prevented by cotransfer of purified CD4+ T cells. *J Exp Med* 1993; **178**(1)**:** 237-244.

359. Zenewicz LA, Yancopoulos GD, Valenzuela DM, Murphy AJ, Stevens S, Flavell RA. Innate and adaptive interleukin-22 protects mice from inflammatory bowel disease. *Immunity* 2008; **29**(6)**:** 947-957.

360. Zeng H, Wu H, Sloane V, Jones R, Yu Y, Lin P *et al.* Flagellin/TLR5 responses in epithelia reveal intertwined activation of inflammatory and apoptotic pathways. *Am J Physiol Gastrointest Liver Physiol* 2006; **290**(1)**:** G96-G108.

361. Ahern P. Dissection of the role of IL-23 in intestinal inflammation. DPhil thesis, University of Oxford, Oxford, 2010.

362. Murai M, Turovskaya O, Kim G, Madan R, Karp CL, Cheroutre H *et al.* Interleukin 10 acts on regulatory T cells to maintain expression of the transcription factor Foxp3 and suppressive function in mice with colitis. *Nat Immunol* 2009; **10**(11)**:** 1178-1184.

363. Coombes JL, Siddiqui KR, Arancibia-Carcamo CV, Hall J, Sun CM, Belkaid Y *et al.* A functionally specialized population of mucosal CD103+ DCs induces Foxp3+ regulatory T cells via a TGF-beta and retinoic acid-dependent mechanism. *J Exp Med* 2007; **204**(8)**:** 1757-1764.

364. Letran SE, Lee SJ, Atif SM, Flores-Langarica A, Uematsu S, Akira S *et al.* TLR5-deficient mice lack basal inflammatory and metabolic defects but exhibit impaired CD4 T cell responses to a flagellated pathogen. *J Immunol* 2011; **186**(9)**:** 5406-5412.

365. Ubeda C, Lipuma L, Gobourne A, Viale A, Leiner I, Equinda M *et al.* Familial transmission rather than defective innate immunity shapes the distinct intestinal microbiota of TLR-deficient mice. *J Exp Med* 2012; **209**(8)**:** 1445-1456.

366. Carvalho FA, Nalbantoglu I, Ortega-Fernandez S, Aitken JD, Su Y, Koren O *et al.* Interleukin-1beta (IL-1beta) promotes susceptibility of Toll-like receptor 5 (TLR5) deficient mice to colitis. *Gut* 2012; **61**(3)**:** 373-384.

367. Solnick JV, Schauer DB. Emergence of diverse Helicobacter species in the pathogenesis of gastric and enterohepatic diseases. *Clinical microbiology reviews* 2001; **14**(1)**:** 59-97.

368. Andrutis KA, Fox JG, Schauer DB, Marini RP, Murphy JC, Yan L *et al.* Inability of an isogenic urease-negative mutant stain of Helicobacter mustelae to colonize the ferret stomach. *Infect Immun* 1995; **63**(9)**:** 3722-3725.

369. Tsuda M, Karita M, Morshed MG, Okita K, Nakazawa T. A urease-negative mutant of Helicobacter pylori constructed by allelic exchange mutagenesis lacks the ability to colonize the nude mouse stomach. *Infect Immun* 1994; **62**(8)**:** 3586-3589.

370. Lefevre M. Role of Helicobacter hepaticus in intestinal inflammation. DPhil thesis, University of Oxford, Oxford, 2008.

371. Ge Z, Feng Y, Whary MT, Nambiar PR, Xu S, Ng V *et al.* Cytolethal distending toxin is essential for Helicobacter hepaticus colonization in outbred Swiss Webster mice. *Infect Immun* 2005; **73**(6)**:** 3559-3567.

372. Liyanage NP, Manthey KC, Dassanayake RP, Kuszynski CA, Oakley GG, Duhamel GE. Helicobacter hepaticus cytolethal distending toxin causes cell death in intestinal epithelial cells via mitochondrial apoptotic pathway. *Helicobacter* 2010; **15**(2)**:** 98-107.

373. Pratt JS, Sachen KL, Wood HD, Eaton KA, Young VB. Modulation of host immune responses by the cytolethal distending toxin of Helicobacter hepaticus. *Infect Immun* 2006; **74**(8)**:** 4496-4504.

374. Bingle LE, Bailey CM, Pallen MJ. Type VI secretion: a beginner's guide. *Current opinion in microbiology* 2008; **11**(1)**:** 3-8.

375. Silverman JM, Brunet YR, Cascales E, Mougous JD. Structure and regulation of the type VI secretion system. *Annual review of microbiology* 2012; **66:** 453-472.

376. Cascales E. The type VI secretion toolkit. *EMBO Rep* 2008; **9**(8)**:** 735-741.

377. Filloux A, Hachani A, Bleves S. The bacterial type VI secretion machine: yet another player for protein transport across membranes. *Microbiology* 2008; **154**(Pt 6)**:** 1570-1583.

378. Jani AJ, Cotter PA. Type VI secretion: not just for pathogenesis anymore. *Cell Host Microbe* 2010; **8**(1)**:** 2-6.

379. Pukatzki S, McAuley SB, Miyata ST. The type VI secretion system: translocation of effectors and effector-domains. *Current opinion in microbiology* 2009; **12**(1)**:** 11-17.

380. Schwarz S, Hood RD, Mougous JD. What is type VI secretion doing in all those bugs? *Trends in microbiology* 2010; **18**(12)**:** 531-537.

381. Pukatzki S, Ma AT, Revel AT, Sturtevant D, Mekalanos JJ. Type VI secretion system translocates a phage tail spike-like protein into target cells where it cross-links actin. *Proc Natl Acad Sci U S A* 2007; **104**(39)**:** 15508-15513.

382. Hood RD, Singh P, Hsu F, Guvener T, Carl MA, Trinidad RR *et al.* A type VI secretion system of Pseudomonas aeruginosa targets a toxin to bacteria. *Cell Host Microbe* 2010; **7**(1)**:** 25-37.

383. Murdoch SL, Trunk K, English G, Fritsch MJ, Pourkarimi E, Coulthurst SJ. The opportunistic pathogen Serratia marcescens utilizes type VI secretion to target bacterial competitors. *J Bacteriol* 2011; **193**(21)**:** 6057-6069.

384. Pukatzki S, Ma AT, Sturtevant D, Krastins B, Sarracino D, Nelson WC *et al.* Identification of a conserved bacterial protein secretion system in Vibrio cholerae using the Dictyostelium host model system. *Proc Natl Acad Sci U S A* 2006; **103**(5)**:** 1528-1533.

385. Blondel CJ, Jimenez JC, Leiva LE, Alvarez SA, Pinto BI, Contreras F *et al.* The type VI secretion system encoded in Salmonella pathogenicity island 19 is required for Salmonella enterica serotype Gallinarum survival within infected macrophages. *Infect Immun* 2013; **81**(4)**:** 1207-1220.

386. Blondel CJ, Yang HJ, Castro B, Chiang S, Toro CS, Zaldivar M *et al.* Contribution of the type VI secretion system encoded in SPI-19 to chicken colonization by Salmonella enterica serotypes Gallinarum and Enteritidis. *PLoS One* 2010; **5**(7)**:** e11724.

387. Liu J, Guo JT, Li YG, Johnston RN, Liu GR, Liu SL. The type VI secretion system gene cluster of Salmonella typhimurium: Required for full virulence in mice. *Journal of basic microbiology* 2013; **53**(7)**:** 600-607.

388. Pezoa D, Yang HJ, Blondel CJ, Santiviago CA, Andrews-Polymenis HL, Contreras I. The type VI secretion system encoded in SPI-6 plays a role in gastrointestinal colonization and systemic spread of Salmonella enterica serovar Typhimurium in the chicken. *PLoS One* 2013; **8**(5)**:** e63917.

389. Suerbaum S, Josenhans C, Sterzenbach T, Drescher B, Brandt P, Bell M *et al.* The complete genome sequence of the carcinogenic bacterium Helicobacter hepaticus. *Proc Natl Acad Sci U S A* 2003; **100**(13)**:** 7901-7906.

390. Ge Z, Sterzenbach T, Whary MT, Rickman BH, Rogers AB, Shen Z *et al.* Helicobacter hepaticus HHGI1 is a pathogenicity island associated with typhlocolitis in B6.129-IL10 tm1Cgn mice. *Microbes Infect* 2008; **10**(7)**:** 726-733.

391. Bartonickova L, Sterzenbach T, Nell S, Kops F, Schulze J, Venzke A *et al.* Hcp and VgrG1 are secreted components of the Helicobacter hepaticus type VI secretion system and VgrG1 increases the bacterial colitogenic potential. *Cell Microbiol* 2013; **15**(6)**:** 992-1011.

392. Elinav E, Henao-Mejia J, Flavell RA. Integrative inflammasome activity in the regulation of intestinal mucosal immune responses. *Mucosal Immunol* 2013; **6**(1)**:** 4-13.

393. Kummer JA, Broekhuizen R, Everett H, Agostini L, Kuijk L, Martinon F *et al.* Inflammasome components NALP 1 and 3 show distinct but separate expression profiles in human tissues suggesting a site-specific role in the inflammatory response. *The journal of histochemistry and cytochemistry : official journal of the Histochemistry Society* 2007; **55**(5)**:** 443-452.

394. Gracie JA, Robertson SE, McInnes IB. Interleukin-18. *J Leukoc Biol* 2003; **73**(2)**:** 213-224.

395. Huber S, Gagliani N, Zenewicz LA, Huber FJ, Bosurgi L, Hu B *et al.* IL-22BP is regulated by the inflammasome and modulates tumorigenesis in the intestine. *Nature* 2012; **491**(7423)**:** 259-263.

396. Watson AJ, Chu S, Sieck L, Gerasimenko O, Bullen T, Campbell F *et al.* Epithelial barrier function in vivo is sustained despite gaps in epithelial layers. *Gastroenterology* 2005; **129**(3)**:** 902-912.

397. Rosenblatt J, Raff MC, Cramer LP. An epithelial cell destined for apoptosis signals its neighbors to extrude it by an actin- and myosin-dependent mechanism. *Curr Biol* 2001; **11**(23)**:** 1847-1857.

398. Bullen TF, Forrest S, Campbell F, Dodson AR, Hershman MJ, Pritchard DM *et al.* Characterization of epithelial cell shedding from human small intestine. *Laboratory investigation; a journal of technical methods and pathology* 2006; **86**(10)**:** 1052-1063.

399. Bergsbaken T, Fink SL, Cookson BT. Pyroptosis: host cell death and inflammation. *Nat Rev Microbiol* 2009; **7**(2)**:** 99-109.

400. Sap KA. *Labeling Methods in Mass Spectrometry Based Quantitative Proteomics, Integrative Proteomics. Dr. Hon-Chiu Leung*: http://www.intechopen.com/books/integrative-proteomics/labeling-methods-in-mass-spectrometry-based-quantitative-proteomics, 2012.

401. Boersema PJ, Aye TT, van Veen TA, Heck AJ, Mohammed S. Triplex protein quantification based on stable isotope labeling by peptide dimethylation applied to cell and tissue lysates. *Proteomics* 2008; **8**(22)**:** 4624-4632.

402. Sauer B. Inducible gene targeting in mice using the Cre/lox system. *Methods* 1998; **14**(4)**:** 381-392.

403. el Marjou F, Janssen KP, Chang BH, Li M, Hindie V, Chan L *et al.* Tissue-specific and inducible Cre-mediated recombination in the gut epithelium. *Genesis* 2004; **39**(3)**:** 186-193.

404. Yi CH, Yuan J. The Jekyll and Hyde functions of caspases. *Developmental cell* 2009; **16**(1)**:** 21-34.

405. Becker C, Watson AJ, Neurath MF. Complex roles of caspases in the pathogenesis of inflammatory bowel disease. *Gastroenterology* 2013; **144**(2)**:** 283-293.

406. Bossaller L, Chiang PI, Schmidt-Lauber C, Ganesan S, Kaiser WJ, Rathinam VA *et al.* Cutting edge: FAS (CD95) mediates noncanonical IL-1beta and IL-18 maturation via caspase-8 in an RIP3-independent manner. *J Immunol* 2012; **189**(12)**:** 5508-5512.

407. Sagulenko V, Thygesen SJ, Sester DP, Idris A, Cridland JA, Vajjhala PR *et al.* AIM2 and NLRP3 inflammasomes activate both apoptotic and pyroptotic death pathways via ASC. *Cell Death Differ* 2013; **20**(9)**:** 1149-1160.

408. Kumar Y, Radha V, Swarup G. Interaction with Sug1 enables Ipaf ubiquitination leading to caspase 8 activation and cell death. *Biochem J* 2010; **427**(1)**:** 91-104.

409. Varfolomeev EE, Schuchmann M, Luria V, Chiannilkulchai N, Beckmann JS, Mett IL *et al.* Targeted disruption of the mouse Caspase 8 gene ablates cell death induction by the TNF receptors, Fas/Apo1, and DR3 and is lethal prenatally. *Immunity* 1998; **9**(2)**:** 267-276.

410. Gunther C, Martini E, Wittkopf N, Amann K, Weigmann B, Neumann H *et al.* Caspase-8 regulates TNF-alpha-induced epithelial necroptosis and terminal ileitis. *Nature* 2011; **477**(7364)**:** 335-339.

411. Welz PS, Wullaert A, Vlantis K, Kondylis V, Fernandez-Majada V, Ermolaeva M *et al.* FADD prevents RIP3-mediated epithelial cell necrosis and chronic intestinal inflammation. *Nature* 2011; **477**(7364)**:** 330-334.

412. Masumoto J, Taniguchi S, Nakayama J, Shiohara M, Hidaka E, Katsuyama T *et al.* Expression of apoptosis-associated speck-like protein containing a caspase recruitment

domain, a pyrin N-terminal homology domain-containing protein, in normal human tissues. *The journal of histochemistry and cytochemistry : official journal of the Histochemistry Society* 2001; **49**(10)**:** 1269-1275.

413. Lupfer C, Kanneganti TD. Unsolved Mysteries in NLR Biology. *Front Immunol* 2013; **4:** 285.

414. Perez-Lopez A, Rosales-Reyes R, Alpuche-Aranda CM, Ortiz-Navarrete V. Salmonella downregulates Nod-like receptor family CARD domain containing protein 4 expression to promote its survival in B cells by preventing inflammasome activation and cell death. *J Immunol* 2013; **190**(3)**:** 1201-1209.

415. Pearson JS, Giogha C, Ong SY, Kennedy CL, Kelly M, Robinson KS *et al.* A type III effector antagonizes death receptor signalling during bacterial gut infection. *Nature* 2013; **501**(7466)**:** 247-251.

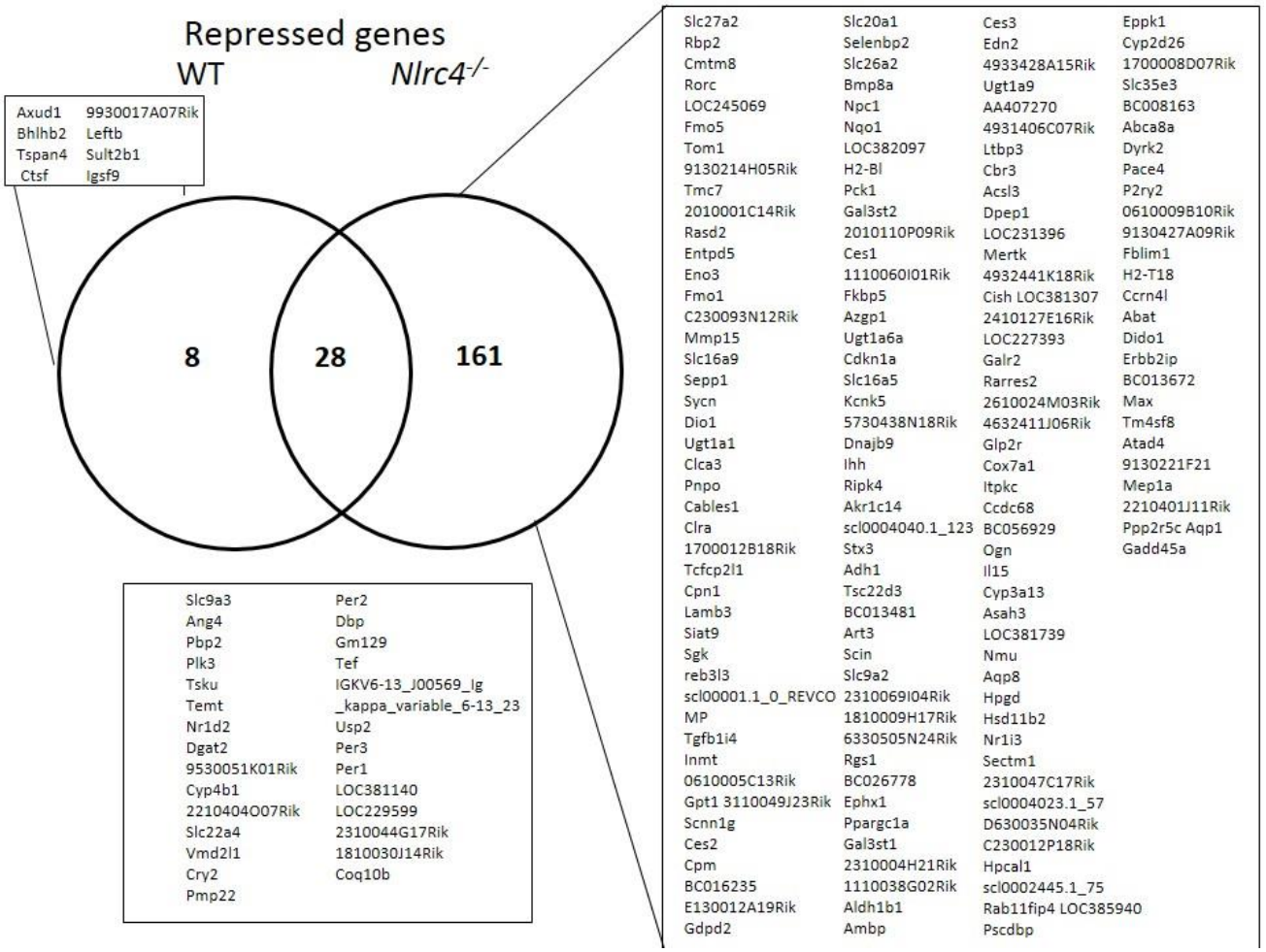
416. LaRock CN, Cookson BT. The Yersinia virulence effector YopM binds caspase-1 to arrest inflammasome assembly and processing. *Cell Host Microbe* 2012; **12**(6)**:** 799-805.

417. Hilbi H, Moss JE, Hersh D, Chen Y, Arondel J, Banerjee S *et al.* Shigella-induced apoptosis is dependent on caspase-1 which binds to IpaB. *J Biol Chem* 1998; **273**(49)**:** 32895-32900.

418. Carvalho FA, Aitken JD, Gewirtz AT, Vijay-Kumar M. TLR5 activation induces secretory interleukin-1 receptor antagonist (sIL-1Ra) and reduces inflammasome-associated tissue damage. *Mucosal Immunol* 2011; **4**(1)**:** 102-111.

419. Pang IK, Ichinohe T, Iwasaki A. IL-1R signaling in dendritic cells replaces pattern-recognition receptors in promoting CD8(+) T cell responses to influenza A virus. *Nat Immunol* 2013; **14**(3)**:** 246-253.

Appendix 1


Repressed genes
WT
Nlrc4-/-
Axud1 9930017A07Rik
Bhlhb2 Leftb
Tspan4 Sult2b1
Ctsf Igsf9
8
28
161
Slc9a3 Per2
Ang4 Dbp
Pbp2 Gm129
Plk3 Tef
Tsku IGKV6-13_J00569_Ig
Temt _kappa_variable_6-13_23
Nr1d2 Usp2
Dgat2 Per3
9530051K01Rik Per1
Cyp4b1 LOC381140
2210404O07Rik LOC229599
Slc22a4 2310044G17Rik
Vmd2l1 1810030J14Rik
Cry2 Coq10b
Pmp22
Slc27a2 Slc20a1 Ces3 Eppk1
Rbp2 Selenbp2 Edn2 Cyp2d26
Cmtm8 Slc26a2 4933428A15Rik 1700008D07Rik
Rorc Bmp8a Ugt1a9 Slc35e3
LOC245069 Npc1 AA407270 BC008163
Fmo5 Nqo1 4931406C07Rik Abca8a
Tom1 LOC382097 Ltbp3 Dyrk2
9130214H05Rik H2-Bl Cbr3 Pace4
Tmc7 Pck1 Acsl3 P2ry2
2010001C14Rik Gal3st2 Dpep1 0610009B10Rik
Rasd2 2010110P09Rik LOC231396 9130427A09Rik
Entpd5 Ces1 Mertk Fblim1
Eno3 1110060I01Rik 4932441K18Rik H2-T18
Fmo1 Fkbp5 Cish LOC381307 Ccrn4l
C230093N12Rik Azgp1 2410127E16Rik Abat
Mmp15 Ugt1a6a LOC227393 Dido1
Slc16a9 Cdkn1a Galr2 Erbb2ip
Sepp1 Slc16a5 Rarres2 BC013672
Sycn Kcnk5 2610024M03Rik Max
Dio1 5730438N18Rik 4632411J06Rik Tm4sf8
Ugt1a1 Dnajb9 Glp2r Atad4
Clca3 Ihh Cox7a1 9130221F21
Pnpo Ripk4 Itpkc Mep1a
Cables1 Akr1c14 Ccdc68 2210401J11Rik
Clra scl0004040.1_123 BC056929 Ppp2r5c Aqp1
1700012B18Rik Stx3 Ogn Gadd45a
Tcfcp2l1 Adh1 Il15
Cpn1 Tsc22d3 Cyp3a13
Lamb3 BC013481 Asah3
Siat9 Art3 LOC381739
Sgk Scin Nmu
reb3l3 Slc9a2 Aqp8
scl00001.1_0_REVCO 2310069I04Rik Hpgd
MP 1810009H17Rik Hsd11b2
Tgfb1i4 6330505N24Rik Nr1i3
Inmt Rgs1 Sectm1
0610005C13Rik BC026778 2310047C17Rik
Gpt1 3110049J23Rik Ephx1 scl0004023.1_57
Scnn1g Ppargc1a D630035N04Rik
Ces2 Gal3st1 C230012P18Rik
Cpm 2310004H21Rik Hpcal1
BC016235 1110038G02Rik scl0002445.1_75
E130012A19Rik Aldh1b1 Rab11fip4 LOC385940
Gdpd2 Ambp Pscdbp